MOUSE MODELS OF PROSTATE CANCER

Hanneke Korsten

The studies in this thesis were financially supported by the Dutch Cancer Society (KWF).

Printing of this thesis is financially supported by:
Astellas Pharma B.V.
Department of Pathology of the ErasmusMC Rotterdam
Dutch Cancer Society (KWF)
Erasmus University Rotterdam
Stichting Urologisch Wetenschappelijk Onderzoek (SUWO)

Lay-out by: Legatron Electronic Publishing, Rotterdam
Printed by: Ipskamp Drukkers BV, Enschede

© H. Korsten, 2012

All rights reserved. No part of the material protected by this copyright notice may be reproduced or utilized in any form or by any electronic, mechanical, or other means, now known or hereafter invented, including photocopying and recording, or in any information storage and retrieval system without prior written permission of the author.

MOUSE MODELS OF PROSTATE CANCER

Muismodellen voor prostaatkanker

Proefschrift

ter verkrijging van de graad van doctor aan de
Erasmus Universiteit Rotterdam
op gezag van de
rector magnificus

prof.dr. H.G. Schmidt

en volgens besluit van het College voor Promoties.
De openbare verdediging zal plaatsvinden op

woensdag 3 oktober 2012 om 13.30 uur

door

Hanneke Korsten
geboren te Nijmegen

ERASMUS UNIVERSITEIT ROTTERDAM

Promotiecommissie

Promotor:	Prof.dr.ir. J. Trapman
Overige leden:	Prof.dr.ir. G.W. Jenster
	Prof.dr. R. Fodde
	Dr. G. van der Pluijm

Contents

CHAPTER 1 General introduction 9

1 Genetics of prostate cancer 10

1.1 The *TMPRSS2-ERG* fusion gene 12

1.2 The *PTEN* tumor suppressor gene 13

1.2.1 PTEN function 13

1.2.2 PTEN alterations in prostate cancer 14

1.3 The *TP53* tumor suppressor gene 15

2 Mouse models of prostate cancer 16

2.1 Conventional and conditional genetically engineered mouse models of prostate cancer 18

2.2 First generation mouse prostate cancer models 20

2.3 Single gene overexpression mouse prostate cancer models 21

2.3.1 Mouse prostate cancer models with overexpression of *ERG* and *ETV1* 21

2.3.2 The PB-Myc model 22

2.3.3 The PB-Akt model 22

2.3.4 The androgen receptor mouse models of prostate cancer 22

2.4 Single gene loss of function mouse prostate cancer models 23

2.4.1 The *Nkx3.1* knockout mouse model 23

2.4.2 The *Pten* knockout mouse models 24

2.4.3 *Trp53* knockout and mutant *Trp53* mouse models 26

2.5 Double genetically engineered mouse models for prostate cancer 27

2.5.1 The effect of a second event in conventional *Pten+/-* knockout mice 27

2.5.2 The effect of a second genetic event in conditional *Pten* knockout mice 29

3 Scope of this thesis 31

4 References 32

Chapter 2 **Accumulating Progenitor Cells in the Luminal Epithelial Cell Layer are Candidate Tumor Initiating Cells in a *Pten* Knockout Mouse Prostate Cancer Model** **39**

Chapter 3 **Characterization of heterogeneous prostate tumors in targeted *Pten* knockout mice** **75**

Chapter 4 **Metastatic, chromosomal instable prostate cancer by *Trp53* inactivation in a targeted *Pten* knockout mouse prostate cancer model** **103**

Chapter 5 **Identification of *TDRD1* as a direct target gene of *ERG* in primary prostate cancer** **143**

Chapter 6 **General discussion** **181**

Summary 195
Samenvatting 197
Curriculum vitae 199
List of publications 201
Dankwoord 203
PhD Portfolio 205

Abbreviations

aCGH	Array-based comparative genomic hybridization
Agr2	Anterior gradient 2
Adam12	A disintegrin and metalloprotease 12
APC	Anaphase-promoting- complex
AR	Androgen receptor
ARHGDIB	Rho GDP dissociation inhibitor, beta
BAD	BCL2-associated agonist of cell-death
BrdU	Bromodeoxyuridine
CARN	Castrate resistant Nkx3.1-expressing cells
CENP-C1	Centromere C1
CK	Cytokeratin
Clu	Clusterin
CRPC	Castration-resistance prostate cancer
Cpn1	Carboxypeptidase N
DSB	Double-strand break
ECM	Extracellular matrix
E.d.	Embryonal day
ERG	V-ets erythroblastosis virus E26 oncogene homolog
EMT	Epithelial mesenchymal transition
ES	Embryonal stem
ETS	E26 transformation-specific
FGFR1	Fibroblast growth factor receptor-1
GEMM	Genetically engineered mouse model
GF	Growth factor
GHR	Growth hormone receptor
Gja1	Gap junction protein, alpha 1
GSK3	Glycogen synthase kinase 3
JNK	Jun N-terminal Kinase
HDAC1	Histone deacetylase 1
HIF1α	Hypoxia inducible factor 1α
HMBS	Hydroxymethylbilane synthase
HP	Hyperplastic prostate
HPRT	Hypoxanthine guanine phosphoribosyl transferase 1
HPGD	Hydroxyprostaglandin dehydrogenase 15-(NAD)
IDC	Intraductal carcinoma
IGHA	Immunoglobulin heavy constant alpha 1
IHC	Immunohistochemistry
JNK	Jun N-terminal Kinase
Luc	Luciferase
Ly6a	Lymphocyte antigen 6a
MAPK	Mitogen-activated protein kinase
MMTV	Mouse mammary tumor virus
MWU	Mann Whitney U
miRNA	MicroRNA
mTOR	Mammalian target of rapamycin
NAP	Normal adjacent prostate
NKX3.1	NK3 homeobox 1
NP	Normal prostate
pAkt	Phospho-Akt
PB	Probasin
PCA	Principal component analysis
P.d.	Postnatal day
PIN	Prostatic intraepithelial neoplasia

PI3K	Phosphoinositide-3-kinase
PIP2	Phosphatidylinositol (4,5)-phosphate
PIP3	Phosphatidylinositol (3,4,5)-phosphate
PLA2G7	Phospholipase A2, Group VII
Pou5f1	Pou-domain, class 5 transcription factor 1
PSA	Prostate specific antigen
PSCA	Prostate stem cell antigen
PTEN	Phosphatase and tensin homologue
RB1	Retinoblastoma 1
RTK	Receptor tyrosine kinase
SAM	Significance Analysis of Microarrays
SCID	Severe combined immunodeficiency
SLC45A3	Solute carrier family 45 member 3
SPSS	Statistical Package for Social Sciences
Sox2	SRY-box containing gene
Star	Steroidogenic acute regulatory protein
SYP	Synaptophysin
TC	Tumor class
TDRD1	Tudor domain containing 1
TFF3	Trefoil factor 3
TH	Tyrosine hydroxylase
TMPRSS2	Transmembrane protease, serine 2
TNF	Tumor necrosis factor
TRAMP	Transgenic adenocarcinoma mouse prostate model
TSC2	mTOR activity regulator tuberous sclerosis 2
TURP	Transurethral resection of the prostate
QPCR	Quantitative PCR
Q-RT-PCR	Quantitative reverse transcription-PCR

CHAPTER 1

General introduction

Prostate cancer is the most frequently diagnosed type of cancer in men in countries with a Western lifestyle [1]. Yearly, in the Netherlands approximately 9,000 men are diagnosed with prostate cancer, of which 25 percent dies as a result of the disease (KWF Cancer Foundation). Clinically localized prostate cancer can be treated by surgery or radiotherapy [2, 3]. A third treatment option is active surveillance, where the patient is not treated initially but closely monitored. If the prostate tumor is metastasized, androgen deprivation therapy by orchiectomy or gonadotropin-releasing hormone agonists or antagonists is standard therapy [4]. Although most tumors show an initial good response, unfortunately, the majority of the patients eventually develop castration-resistance prostate cancer (CRPC) within 1-3 years. In CRPC aberrant activation of the androgen receptor (AR), by amplification of the *AR* locus at Xq12, resulting in AR overexpression, *AR* mutation, aberrant cofactor expression and function, ligand-independent AR activation and intratumoral androgen synthesis, is common [5-10]. Following failure of endocrine therapy, CRPC patients can be treated with docetaxel that has been shown to prolong survival for a few months [11]. Until recently, CRPC patients had limited treatment options after docetaxel chemotherapy, however, novel therapies emerged, like vaccines-based immunotherapy, administration of the novel AR antagonist MDV3100 or the inhibitor of cytochrome p450 c17 abiraterone acetate, which inhibits androgen synthesis in the adrenal gland [7, 11]. Overall, CRPC patients have a poor prognosis with an average survival of 9-13 months [12].

1. GENETICS OF PROSTATE CANCER

During recent years our knowledge of mechanisms of prostate tumorigenesis and the role of individual genes in this process has rapidly increased, but there are still many questions to be addressed. To offer prostate cancer patients a better and more efficient treatment, it is crucial to increase our knowledge of the process of tumor development. Prostatic intraepithelial neoplasia (PIN) is generally accepted as the precursor of prostate cancer [13]. PIN is characterized by cell proliferation within prostate ducts, with nuclear and nucleolar enlargement similar to prostate cancer. Unlike cancer, PIN retains a basal epithelial cell layer.

Like other tumors, prostate cancer development and progressive growth is driven by the accumulation of genetic and epigenetic changes [14]. Screening of the genome for chromosomal losses or gains has been instrumental in the identification of potential tumor suppressor genes or oncogenes, respectively.

In PIN lesions early genetic events, including a gene fusion between *transmembrane protease, serine 2* (*TMPRSS2)* and the oncogene *V-ets erythroblastosis virus E26 oncogene homolog (ERG)* and mono-allelic loss of the tumor suppressor gene *Phosphatase and tensin homologue (PTEN)* are detected [15, 16]. The TMPRSS2-ERG fusion gene, published in 2005, occurs in 40-60% of

all prostate cancer patients [17-19]. A 21q22 interstitial deletion spanning *TMPRSS2* and *ERG* is frequently detected in prostate cancer [10, 19]. Another common early event is loss of one allele of the tumor suppressor gene *PTEN*. Loss of 10q23, the *PTEN* locus, is detected in more than half of the patients with localized disease [20-22].

In primary, localized prostate cancer chromosomal alterations like gain of parts of chromosome 8q and 7 and loss of regions on 6q, 8p, 13q and 16q are frequently observed. Less frequently observed regions of gain are 3q, 17q and Xq and loss of regions on 2q, 5q, 10q, 17p and 18q [10, 23, 24]. In most of these regions a tumor suppressor gene or oncogene has not been identified. For example, no classical oncogene has been identified in the regions of amplified DNA at chromosome 7q [10, 23]. Another frequent alteration in the prostate oncogenome is loss of chromosome 8p, a large region that harbours the homeobox gene *NKX3.1*, a gene with a role in prostate development and differentiation [9, 10, 21, 25, 26]. Loss of the short arm of chromosome 8 is found in 50-85% of all prostate cancer patients [9, 21]. So far, it is unclear which gene or genes located in this region is/are involved in prostate tumor. In contrast to loss or gain of large chromosomal regions, some focal alterations are observed in prostate cancer pointing to specific genes. Amplification of 8q24 in 20-40% of the prostate cancer patients points to the oncogenic role of *c-MYC* in prostate cancer. *C-MYC* amplification is most frequent in prostate tumors with a more advanced phenotype [9, 10, 21]. Furthermore, focal losses of 10q23, 13q14 and 17p13 point to inactivation of established tumor suppressor genes. *PTEN,* located at 10q23, is the most frequently inactivated tumor suppressor gene in prostate. In primary prostate cancer 30-60% of the patients harbour loss of one *PTEN* allele [16, 22, 27]. The tumor suppressor gene *Retinoblastoma 1* (*RB1*) is located at chromosome 13q14. Loss of the *RB1* locus occurs in at least 30% of the prostate cancer patients of which 10% showed bi-allelic loss [21, 28]. Mono-allelic loss of the *TP53* locus at 17p13 was detected in 30% of prostatectomy and biopsy samples [20]. In general *TP53* alterations are associated with advanced stages of prostate cancer, like CRPC [10, 20].

A schematic representation of the process of prostate tumorigenesis is given in Figure 1. The presence of genetic alterations, like *TMPRSS2-ERG* fusion gene, *PTEN* inactivation, *TP53* inactivation and *AR* activation per tumor stage are indicated.

New techniques like whole genome sequencing, especially whole exome sequencing, and RNA sequencing, will help to understand further the prostate cancer genome [29]. In addition to the genetic alterations in prostate cancer, epigenetic modifications, like promoter methylation, histone modifications and modified expression of microRNA (miRNA), can alter gene expression in prostate cancer. Currently, epigenetic modifications are increasingly recognized to have important roles in prostate tumorigenesis [30, 31]. In this thesis we will mainly focus on the role of genetic events in prostate cancer. Combining data from both analyses of genetic and epigenetic

events in prostate cancer will create a complete picture of alterations in tumors. Ultimately this will lead to improved targeted therapies of cancer patients.

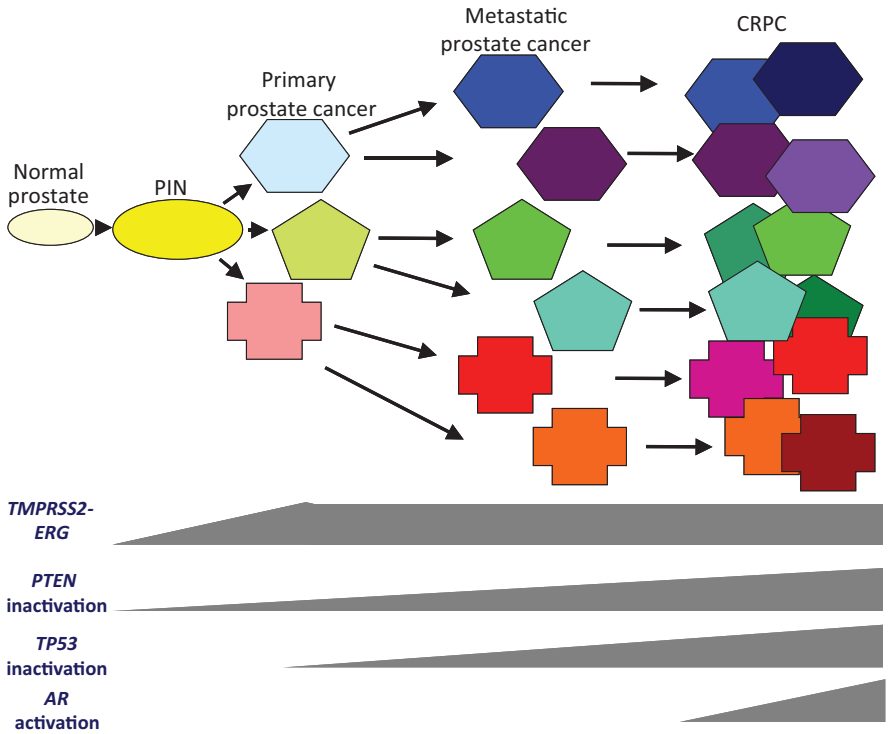

Figure 1. Schematic representation of the process of prostate tumorigenesis. The presence of genetic alterations, like *TMPRSS2-ERG* fusion gene, *PTEN* inactivation, *TP53* inactivation and *AR* activation per tumor stage are indicated by grey bars.

1.1 The *TMPRSS2-ERG* fusion gene

Until recently, fusion genes were thought to be exclusively the oncogenic mechanism of haematological malignancies and sarcomas [32]. In 2005, a fusion between the prostate specific, androgen regulated gene *TMPRSS2* and the oncogene *ERG* was found in prostate cancer patients [19]. This fusion gene occurs in 40-60% of the clinical prostate cancers [17, 18]. ERG is a E26 transformation-specific (ETS) transcription factor family member found overexpressed in sarcomas, acute myeloid leukemias and prostate cancers. In prostate cancer the generation of the *TMPRSS2-ERG* fusion gene leads to *ERG* overexpression. Currently, much effort is focused on the identification of candidate target genes of the *ERG* transcription factor and determining its oncogenic role [17, 32, 33]. So far, the prognostic role of *ERG* alterations in prostate cancer is unclear [33].

In addition to *TMPRSS2-ERG*, other gene fusions were discovered between the regulatory sequences and first exons of androgen-induced genes, such as *TMPRSS2, NDRG1*, *SLC45A3* and *C15orf21* and members of the ETS gene family, like *ETV1*, *ETV4* and *ETV5* [21, 32-37]. All these fusion genes occur at much lower frequency in prostate cancer than *TMPRSS2-ERG* fusion genes. In addition to the fusion genes discussed here, it is known that full-length *ETV1* can be translocated and overexpressed [38, 39].

New techniques as discussed above, like whole genome sequencing and RNA sequencing, recently lead to the identifications of new less frequent genomic rearrangements in prostate cancer [40-42]. The data presented above indicate that chromosomal rearrangements are common in human prostate cancer, however, the roles of these newly identified alterations for prostate cancer growth and progression are unclear.

1.2 The *PTEN* tumor suppressor gene

1.2.1 PTEN function

PTEN is a phosphatase, that counteracts phosphoinositide-3-kinase (PI3K) signaling by balancing phosphatidylinositol (4,5)-phosphate (PIP2) and phosphatidylinositol (3,4,5)-phosphate (PIP3) levels in the cell [22, 27, 43]. Activation of the PI3K pathway by binding of growth factors to receptor tyrosine kinases induces PIP3 accumulation. This results in the recruitment of PDK1 and the AKT isoforms (AKT1, AKT2 and AKT3) to the membrane, where AKT isoforms are activated by phosphorylation [27]. Phosphorylated, activated AKT (pAKT) regulates different cellular processes by phosphorylating downstream substrates, including glycogen synthase kinase 3 (GSK3), BCL2-associated agonist of cell-death (BAD), p21 (encoded by *CDKN1A*), p27 (encoded by *CDKN1B*), members of the forkhead transcription factor family (FOXO1, FOXO3 and FOXO4) and mTOR activity regulator tuberous sclerosis 2 (TSC2) [22, 27, 44, 45] (Figure 2). Phosphorylation of TSC2 can impair the ability of the TSC1/2 complex to inhibit the mTORC1 complex, which ultimately leads to its activation [46]. This complex is also directly activated by pAKT, which leads to enhanced translation of mRNA into protein, a hallmark of many cancers [22, 27, 45, 46]. Recently, it was discovered that loss or inactivation of the TSC1/2 complex not only leads to activation of the mTORC1 complex, but also results in upregulation of PTEN [47, 48]. This feedback mechanism prevents overactivation of the mTORC1 complex via inhibition of AKT phosphorylation by PTEN (Figure 2). Changes in phosphorylation of AKT downsteam targets alter the activity and/or localization of these proteins within the cell, which in turn affects processes such as proliferation, apoptosis, cell size, polarity, metabolism, adhesion, migration and angiogenesis [27, 43, 49-51] (Figure 2).

Although regulation of the AKT pathway seems to be a major function of PTEN, PTEN can have some functions independent of the AKT pathway. For example, the JNK signaling pathway was identified as a functional target of PTEN [52]. Furthermore, some new functions of PTEN

were proposed independent of the lipid phosphate activity of PTEN, which is thought to occur mostly at the cell membrane [45]. For example, the binding of PTEN to centromere C1 (CENP-C1) is required for centrosome stability, and its nuclear localization may be required for DNA double-strand break (DSB) repair mediated by DNA repair protein RAD51 [53]. This mechanism was proposed to play a role in the protection against chromosomal instability. In addition, regulation of the tumor suppressor function of anaphase-promoting- complex (APC) and its regulator E-Cadherin (encoded by *CDH1*) in the nucleus, independently of the lipid phosphatase activity, is mentioned as a new function of PTEN [54]. Finally, increasing evidence suggests that PTEN controls stem cell self-renewal [55, 56].

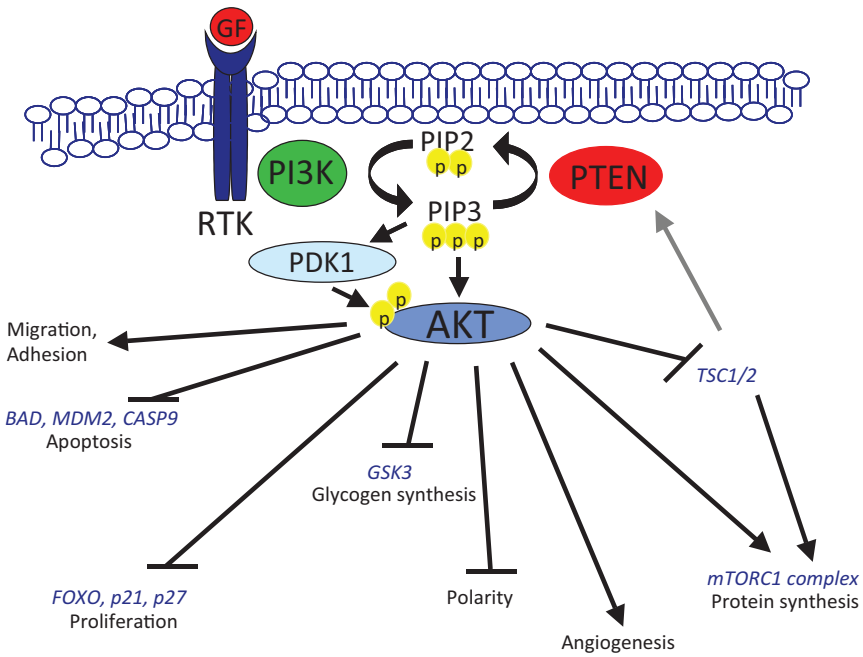

Figure 2. An overview of AKT-dependent targets of PTEN and the biological processes regulated by PTEN. In blue: AKT/PTEN targets, In black: biological processes. GF: growth factor, RTK: receptor tyrosine kinase. The grey arrow indicates the new feedback loop recently identified [47, 48].

1.2.2 PTEN alterations in prostate cancer

The tumor suppressor gene *PTEN* is the most frequently inactivated gene in prostate cancer. Somatic alterations of *PTEN* are not only common in prostate cancer, but also in glioblastomas and endometrial cancers [22]. Germ line mutations of *PTEN* are the cause of the cancer susceptibility

syndromes Cowden disease, Lhermitte-Duclos disease, Bannayana-Riley-Ruvalcaba syndrome, and Proteus-like syndrome [22, 27]. Patients suffering these syndromes show developmental disorders, develop hamartomas and are prone to develop cancer, especially breast, thyroid and endometrium cancer. This confirms that *PTEN* is a gene with crucial functions in development and tumor suppression.

In the prostate, mono-allelic loss of *PTEN* is detected in approximately 25% of the PIN lesions, whereas in clinically localized tumors loss one copy of 10q23 is observed in 30-60% of the patients [16, 22, 27]. In metastatic prostate cancer somatic *PTEN* alterations, including bi-allelic deletions, are detected most frequently [22]. Complete deletion of *PTEN* can occur in up to 50% of the metastatic prostate tumors and less frequently in primary prostate tumors, in ~15% of the cases [22]. Next to inactivation by loss, *PTEN* can also be inactivated by mutation [22, 27]. Mutated *PTEN* is detected in approximately 15% of the primary prostate cancers [22]. In prostate cancer *PTEN* inactivation is associated with an unfavorable prognosis [22, 57-59].

1.3 The *TP53* tumor suppressor gene

TP53 is a DNA-binding protein containing transcription activation, DNA-binding, and oligomerization domains. It binds to p53-binding sites and activates expression of downstream genes, like CDKN1A encoding P21, BAX and BCL2, which inhibit tumor growth and/or invasion [60, 61]. The transcription factor TP53 responds to diverse cellular stresses to regulate target genes that induce processes, including cell cycle arrest, apoptosis, senescence, DNA repair, or changes in metabolism. In human tumors *TP53* is frequently inactivated. Alteration of *TP53* expression by genomic loss or alteration of its properties by point mutation can affect all processes described above [60-62]. Recently, new functions of TP53 were proposed, like inhibition of the inflammatory response, inhibition of stem cell renewal and micro-RNA (mi-RNA) regulation [63-66].

Germ-line mutations of *TP53* are the cause of Li-Fraumeni syndrome, which predisposes to develop of a variety of tumors, including sarcomas, breast tumors, brain tumors and adrenocortical tumors, during childhood and in adult life [60, 67, 68]. In human tumors *TP53* is most frequently altered by genomic loss or mutation, whereas *TP53* can also be inactivated by gene amplification of key negative regulators of TP53, such as *MDM2* and *MDM4* [60, 61]. Loss of properly functioning of TP53 is associated with an unfavorable prognosis in various types of cancer [20, 69].

As discussed, loss of one TP53 allele is observed in ~30% of the prostatectomy and biopsy samples, however loss of the *TP53* locus at 17p13 occurs most frequently in advanced prostate cancer [10, 20]. In addition to loss of heterozygozity, *TP53* mutations occur in prostate [70, 71]. Inactivation of *TP53* can also be caused by overexpression of *MDM2* and *MDM4* [60, 61]. In contrast to high expression of *MDM2* in advanced prostate cancer associated with distant metastasis and poor prognosis, overexpression of *MDM4* is not reported [72, 73].

2. MOUSE MODELS OF PROSTATE CANCER

To increase insight into mechanisms of prostate tumorigenesis and the role of individual genes in this process, *in vivo* models for prostate cancer are needed. Although *in vitro* growing prostate cancer cell lines have their advantages, they also have their limitations. To obtain more knowledge of the complex three-dimensional growth of prostate tumors in humans, *in vivo* experimental systems, like mouse models, have to be used. Transplantation experiments on immuno-deficient mice and the use of genetically engineered mouse models (GEMMs) that mimic human disease are crucial for validating the importance of genetic events in prostate cancer [74, 75]. In *in vivo* model systems the interaction between different cell types can be studied. Ultimately, these models can provide a platform for preclinical testing of novel therapies for prostate cancer patients. Here mouse models of prostate cancer are discussed with a special focus on GEMMs.

The first *in vivo* models of prostate cancer were rats, which developed spontaneous prostate tumors, in contrast to mice [76, 77]. The best-defined rat model is the Dunning model, characterized by development of well-differentiated, non-metastatic and slow-growing tumors.

Despite the difference in prostate anatomy between humans and mice, much effort has been put in manipulating mice in such a way that they develop prostate cancer that recapitulates human disease. The mouse prostate has a lobular structure with four lobes, the anterior, ventral, dorsal and lateral lobe (Figure 3A, left), whereas the human prostate is divided in three zones; the peripheral zone, the central zone and the transitional zone (Figure 3A, right). Based on gene expression data, it was proposed that the dorsal and lateral mouse prostate lobes most closely resemble the peripheral zone of the human prostate, where most prostate tumors develop [78, 79]. However, a consensus was reached by experts that no direct relationship exists between any of the mouse prostate lobes and zones of the human prostate [76]. Furthermore, the process of tumorigenesis and the histopathology is different in mice as compared to humans [76]. Despite all concerns, the mouse is one of the best animals to model cancer, including prostate cancer, because the sequence of genomes of mouse strains is largely known. Another advantage of mouse models is that mice are relatively easy to genetically modify and because of the size and the short gestation time, it is practical and affordable to house and breed mice for scientific research.

Both the human and mouse prostate consists of ducts lined by three different types of epithelial cells: luminal epithelial cells, basal epithelial cells and neuroendocrine cells (Figure 3B). At the apical side, prostate ducts are lined by a single layer of luminal epithelial cells which are dependent on androgens for their function and survival and produce prostatic fluid. The basal epithelial cell layer is located beneath the layer of luminal epithelial cells. Neuroendocrine cells are very rare epithelial cells, interspersed between other epithelial cell types.

These subtypes of epithelial cell types differentially express cell-type specific markers. For example, luminal epithelial cells express Cytokeratin 8 and 18, Cytokeratin 5 and 14 and P63 are expressed by basal epithelial cells and neuroendocrine cells express Chromogranin A and Synaptophysin. In contrast to the high AR expression levels in luminal epithelial cells and the low to negative AR staining in basal epithelial cells, neuroendocrine cells do not express AR.

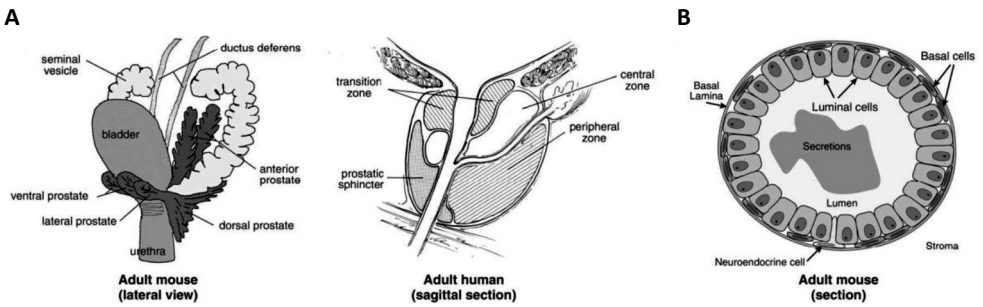

Figure 3. Schematic overview of the prostate anatomy. (**A**) Schematic comparison of mouse (left) and human (right) anatomy. (**B**) Schematic depiction of the cell types within a cross-section of a prostate duct. This figure is adapted from [80].

In the 1980s the first generation GEMMs was generated through zygote pronuclear injection methods that allowed the addition of any cloned gene to the germ line to determine effects of expression of a particular gene on the phenotype [81]. After injection of DNA containing the transgene in a pronucleus of a fertilized zygote, an oocyte, two-cell stage embryos are reimplanted into the oviducts of pseudopregnant foster mothers. A disadvantage of this method to generate transgenic models is that the transgene will be randomly integrated in the mouse genome [82, 83].

An alternative method frequently applied to generate a GEMM involves the use embryonic stem (ES) cells and constructs designed to homogonously recombine into the genome. ES cells are derived from the inner cell mass of a mouse blastocyst. These cells can be transfected or injected with DNA constructs designed to undergo homologous recombination with regions of identical sequence in the genome. In contrast to microinjection of oocytes, this procedure allows the modification of a specific gene in the genome. Genetically modified ES cells are implanted in blastocysts, which will be implanted in the uterus of a pseudopregnant foster mother [82, 83]. Recent progress in mouse genetic engineering technology has led to generation of a new series of mouse models for cancer research [84]. Several new technique are used, including generating

models with inducible mutations or entire human loci, to generate novel mouse models of prostate cancer [85, 86].

2.1 Conventional and conditional genetically engineered mouse models of prostate cancer

Two types of GEMMs can be discriminated, conventional and conditional models. In conventional mouse models the genetic alteration is present in all cells and tissues of the mouse and might be expressed at all developmental stages. In conditional mouse models the alteration of the gene of interest can be induced by, for example, the use of a specific promoter or virus infection. Then, the modification takes place in specific cells and tissues and/or at a specific time point. Conditional mouse models are useful to circumvent embryonic lethality of a genetic alteration or to study the effect of an alteration in a specific cell population. The DNA recombination technique most frequently used for conditional inactivation or activation of a gene is the bacterial Cre-loxP system [77]. In mouse models using the Cre-loxP system, a specific promoter drives the expression of the sequence specific DNA recombinase Cre, which mediates intramolecular recombination and deletion of DNA between the 34bp loxP sequences.

It is also possible to regulate DNA recombination in conditional models by, for example, using inducible variants of Cre, like the tamoxifen-inducible variant (CreERTM) [87]. Here, a fusion gene is created between Cre and a mutant form of the ligand-binding domain of the estrogen receptor (ERTM). This mutant prevents binding of the natural ligand (17β-estradiol) at normal physiological concentrations, but renders the ERTM domain responsive for tamoxifen, a drug normally functioning as an antagonist of the estrogen receptor. Upon addition of tamoxifen, Cre can be expressed and DNA recombination takes place.

For the generation of conditional mouse models for prostate cancer either the prostate specific, androgen regulated rat probasin (PB) or the human prostate specific antigen (PSA) promoter is most frequently used. In these models, the PB or PSA promoter drives the expression or inactivation of a gene specifically in the mouse prostate. Recently *Nkx3.1-CreERT2* mice were added to the transgenic prostate specific mouse lines [88]. In conditional prostate cancer models, several versions of the PB promoter can be used [77, 89]. Next to the short PB promoter (-426/+28 bp), a longer (12kb) fragment of the PB promoter can be used, which elicits a higher expression level than the short version. To generate a PB promoter efficient in directing high expression levels specifically in the prostate, the composite ARR2PB promoter was created. In this promoter two androgen responsive elements regions (ARR) were linked to the PB promoter. The PSA promoter used for prostate specific transgene expression was a 6 kb fragment, which mimics the prostate specific and androgen regulated expression of the endogenous *PSA* gene in humans [90]. As mentioned, in addition to the prostate specific PB and PSA promoter, the Nkx3.1 promoter was used in conditional mouse models of prostate cancer [88]. Furthermore, models were generated using other promoters proposed to be prostate specific, like the C3, PSP94 and

MMTV promoter [77, 89]. Mouse models driven by these promoters show no alterations specific to the prostate and histological abnormalities were detected in a broader range of tissues. An overview of the conditional mouse prostate cancer models driven by the PB, PSA or Nkx3.1 promoter is given in Table 1. A selected number of mouse models of prostate cancer will be discussed below.

Table 1. Overview of prostate specific conditional mouse models for prostate cancer.

Mouse model	Genetic background	Phenotype	Reference
PB-targeted			
PB-AR	FVB/N	PIN	[91]
PB-AR	FVB/N	No phenotype	[92]
PB-AR T857A	FVB/N	No phenotype	[92]
PB-AR E231G	FVB/N	Metastatic prostate carcinoma	[92]
PB-Cre;AR-loxP/loxP	C57BL/6	Dedifferentiation of prostate epithelium	[93]
PB-AKT1	FVB/N	PIN	[94]
PB-Cre;APC-loxP/loxP	Mixed	Invasive prostate carcinoma	[95]
PB-Bcl2	C57BL/6	No phenotype	[96]
PB-Cre;Brca2-loxP/loxP	Mixed	PIN	[97]
PB-Cre;Catnb-+/loxP	C57BL/6	Invasive prostate carcinoma	[98]
PB-Erbb2	FVB/N	PIN	[99]
PB-EcoR1	FVB/N	Invasive prostate carcinoma	[100]
PB-ERG	FVB/N	PIN	[101]
PB-ERG	129	PIN	[102]
PB-ETV1	FVB/N	PIN	[38]
PB-ETV1	Mixed	Prostate hyperplasia/PIN	[103]
PB-ETV1	Mixed	PIN	[103]
PB-FGF2	Mixed	Prostate hyperplasia	[104]
PB-FGF7	C57BL/6	Prostate hyperplasia	[105]
PB-FGFR2iiib	C57BL/6	Prostate hyperplasia	[105]
PB-FGF8b	Mixed	PIN	[106]
PB-iFGFR1	FVB/N	Metastatic sarcoma, invasive prostate carcinoma	[107]
PB-FGFR1 K656E	FVB/N	PIN	[108]
PB-Fos	FVB/N	No phenotype	[100]
PB-Hepsin	C57BL/6	Disorganization basement membrane	[109]
PB-IGF1	Mixed	No phenotype	[110]
PB-IGF1des	FVB/N	Prostate hyperplasia	[111]
PB-Cre;K-ras+/V12	C57BL/6	Invasive prostate carcinoma	[98]

Mouse model *(Continued)*	Genetic background	Phenotype	Reference
PB-targeted			
PB-15-LO-1	C57BL/6	PIN	[112]
PB-Myc-low	FVB/N	Invasive prostate carcinoma	[113]
PB-Myc-High	FVB/N	Invasive prostate carcinoma	[113]
PB-Cre;Z-Myc	Mixed	PIN	[114]
PB-Neu	C57BL/6	Invasive prostate carcinoma	[115]
PB-Cre;Pten-loxP/loxP	Mixed	Metastatic prostate carcinoma	[116]
PB-Cre;Pten-loxP/loxP	Mixed	Invasive prostate carcinoma	[117]
PB-CreERTM;Pten-loxP/loxP	Mixed	Invasive prostate carcinoma	[118]
PB-rPRL	Mixed	Prostate hyperplasia	[119]
PB-p110ß	FVB/N	PIN	[120]
PB-Cre;p44/WDR44-loxP/loxP	C57BL/6/J	PIN	[121]
PB-HRAS	Mixed	PIN	[122]
PB-Cre;RB1-loxP/loxP	C57BL/6	PIN	[123]
PB-SKP2	CD1	PIN	[124]
PB-SV40 large T antigen	B6D2F1	Invasive prostate carcinoma	[125]
PB-SV40 largeT/smallT (TRAMP)	C57BL/6	Metastatic prostate carcinoma	[126]
PB-SV40 LargeT, line 12T-7f (Lady model)	CD1	Invasive prostate carcinoma	[127]
PB-SV40 LargeT, line 12T-10 (Lady model)	CD1	Metastatic prostate carcinoma	[128]
PB-Trp53/His273	B6SJLF2	PIN	[129]
PB-Cre;Trp53-loxP/loxP	Mixed	PIN	[130]
PB-Cre;Trp53-loxP/loxP	Mixed	No phenotype	[131]
PSA-targeted			
PSA-Cre;Nkx3.1-loxP/loxP	C57BL/6	PIN	[132]
PSA-Cre-ERTM;Pten-loxP/loxP	Mixed	Invasive prostate carcinoma	[133]
PSA-Cre;Pten-loxP/loxP	Mixed	Metastatic prostate carcinoma	[134]
Nkx3.1-targeted			
Nkx3.1-CreERT2;Pten-loxP/loxP	Mixed	PIN and microinvasive carcinoma	[88]

PIN: Prostate intraepithelial neoplasia

2.2 First generation mouse prostate cancer models

The first prostate cancer model was the transgenic adenocarcinoma mouse prostate model (TRAMP) [126]. In this model overexpression of the SV40 small and large T antigen in prostate epithelium is driven by the short PB promoter. TRAMP mice develop lesions resembling PIN by 10 weeks of age in the ventral and dorsolateral lobe of the prostate and invasive adenocarcinoma was observed at 12 weeks. Elevated levels of nuclear P53 and a heterogeneous staining pattern of the AR was observed in prostate tumors of these mice. In older TRAMP mice (18-24 weeks)

distant prostate cancer metastases were observed [135]. Metastatic prostate cancer cells were found in lymph nodes, lung, kidney, adrenal glands and bone.

In the LADY model the large version of the PB promoter was used to drive the expression of the SV40 Large T antigen [80]. The disease progression in this prostate cancer model is less aggressive than in TRAMP mice. All mice develop prostate tumors without metastases at older age (12-20 weeks). Remarkably, prostate tumors of both TRAMP and LADY mice expressed neuroendocrine markers, like synaptophysin. Neuroendocrine transdifferentiation in human prostate cancer is associated with prostate cancer progression and worse prognosis [136].

2.3 Single gene overexpression mouse prostate cancer models

2.3.1 Mouse prostate cancer models with overexpression of *ERG* and *ETV1*

As discussed in paragraph 1, fusion genes involving ETS transcription factors are genomic alterations already detected in PIN lesion and most prominent in localized primary prostate cancer. Mouse models can be used to unravel to the function of individual ETS gene family members [137, 138]. For example, homozygous conventional *Etv1* knockout mice exhibited postnatal lethality by 5 weeks of age, probably caused by neural defects.

To unravel the function of overexpression of two ETS transcription factors frequently involved in fusion genes in prostate cancer, *ERG* and *ETV1*, and its truncated variants, targeted mouse prostate cancer models were generated. *ARR2PB;ERG* mice with targeted expression of the most commonly expressed variant of human truncated *ERG* (exon 4-11) [101, 102] were generated, whereas in other studies *ARR2PB;TMPRSS2(exon1)-ERG(exon4-11)* mice were characterized [139] (Korsten *et al.*, unpublished results). The reported prostate phenotypes in these mouse models with ERG overexpression varied from PIN with nuclear atypia, hyperchromasia and macronucleoli to a normal prostate histology [101, 102, 139, 140] (Korsten *et al*., unpublished results). *In ARR2PB-ERG* mice which developed PIN lesions, loss of basal epithelial cell markers and smooth muscle actin staining was observed [101, 102]. None of the transgenic mice with *ERG* overexpression developed prostate cancer, suggesting that additional events are required for tumor formation.

The group of Tomlins and colleagues characterized a mouse model with overexpression of an *ETV1* isoform (exon 5-12) driven by the ARR2PB promoter [38]. After 3 months, PIN lesions were detected in ~75% of the prostates of these transgenic mice. None of these mice developed prostate tumors at older age. In prostate cancer patients both overexpression of truncated and full-length *ETV1* can be observed [38, 39]. To compare the effect of targeted overexpression of full-length and truncated *ETV1*, both *ARR2PB-ETV1* and *ARR2PB-ETV1(exon 6-12)* mice, expressing the most common *ETV1* variant, were generated and characterized [103]. Mice overexpressing full-length *ETV1* developed PIN lesions at older age (>12 months), whereas in prostates of *ARR2PB-ETV1(exon6-12)* mice both prostate hyperplasia and PIN lesions were observed after 6

months. Like the mouse models overexpressing (truncated) *ERG*, overexpression of full-length or truncated *ETV1* seems not to be sufficient for tumor formation.

2.3.2 The PB-Myc model

Amplification of the *c-MYC* locus at 8q24 is observed in a considerable part of the prostate cancer patients (Paragraph 1). Two related mouse models were generated with prostate specific overexpression of human *c-MYC* [113]. In both models *c-MYC* expression is driven by the PB promoter, however the strength of the promoters used was different. In the *Lo-Myc* model the transgene expression was driven by the short PB promoter, whereas in the *Hi-Myc* model the modified ARR2PB promoter was used. *Hi-Myc* mice develop PIN lesions at 2 weeks of age and at 3-6 months the mice develop invasive adenocarcinoma. In prostates of *Lo-Myc* mice the prostate tumor development is slower and starts at 10-12 months. These data show that *MYC* overexpression in the prostate is sufficient to induce tumorigenesis and that the gene dosage affects the rate of disease progression. Recently, in a new mouse model of prostate cancer induced by *c-MYC* overexpression, loss of *Pten* and *Trp53* was observed in early stages of prostate tumorigenesis [141].

2.3.3 The PB-Akt model

Cell signaling mediated by activated AKT occurs frequent in tumors, including prostate tumors. As discussed in paragraph 1.2 in prostate tumors AKT is activated by inactivation of *PTEN*. To investigate whether AKT activation in normal epithelial cells is sufficient for transformation, transgenic mice were generated with activated human AKT expression in luminal epithelial cells driven by the short version of the PB promoter (PAKT mice) [94]. In this mouse model, downstream targets of AKT, such as GSK3 and P70S6K, were phosphorylated, indicating that the activated AKT was functional. PAKT mice did not develop prostate carcinoma, but PIN lesions were observed in prostates of these mice. Expression profiling showed that markers for neovascularization were higher expressed in prostates of PAKT mice as compared to prostates of control littermates. This model shows that phosphorylated, activated AKT regulates biological processes, but is insufficient for tumor formation.

2.3.4 The androgen receptor mouse models of prostate cancer

As mentioned before, in CRPC aberrant activation of the AR pathway is frequently observed [5-9]. To study the effect of alteration of the AR in prostate cancer, mouse models with prostate specific overexpression of mutant or wild type AR driven by the short PB promoter were generated [89, 91, 92]. AR overexpression caused prostate dysplasia resembling PIN lesions in humans in 45% of the older mice (>12 months) [89, 91]. These mice never developed prostate carcinoma, indicating that sole AR overexpression in luminal cells is insufficient to induce prostate cancer.

In addition to these mice, mouse models were generated with targeted expression of two types of mutant AR, the AR-T857A (mouse AR equivalent to human T877A AR mutant) and the AR-E231G mutation [92]. Mice expressing the AR-T857A mutation were used to study the AR ligand binding response, whereas expression of an AR-E231G mutation leads to an altered AR function. Interestingly, mice with targeted overexpression of wild type AR or the T857A AR mutant show no aberrant prostate histology up to 12 months, whereas mice with targeted expression of the E231G AR mutant develop PIN lesions at 12 weeks, which developed into metastatic prostate cancer at 12 months of age. These data demonstrate that in contrast to a mutation in the ligand binding domain (LBD) of the AR (the T857A mutation), a mutation in the N-terminal domain (NTD) (E231G mutation), which leads to increased AR sensitivity, can initiate cancer.

In addition to studies on the effect of overexpression of wild type and mutant *AR* in the mouse prostate, the effect of targeted *AR* inactivation was investigated [93]. ARR2PB-Cre driven inactivation of the *AR* in prostate epithelial cells induced loss of differentiation, cell death of CK8/18+ luminal epithelial cells and proliferation of the remaining epithelium, especially the CK5+ basal epithelial cells. In older AR knockout mice (24 weeks), nearly all prostate ducts contained a dedifferentiated epithelium with lack of glandular infolding. In line with these data decreased expression of androgen regulated genes, like *Probasin*, *Psp94* and *Nkx3.1*, was detected in prostates of these targeted *AR* knockout mice. Restoration of AR function via knockin of the constitutively activated T857A *AR* mutant rescued the phenotype observed in prostates of targeted *AR* knockout mice.

2.4 Single gene loss of function mouse prostate cancer models

2.4.1 The *Nkx3.1* knockout mouse model

Loss of chromosome 8p harbouring the homeobox gene *NKX3.1* is detected in more than half of the prostate cancer patients (Paragraph 1). Although specific *NKX3.1* inactivation by homozygous deletion or mutation is not detected in prostate cancer, this gene is subject of investigations, since *NKX3.1* is involved in important processes in the prostate, like prostate development and differentiation [25, 26]. To investigate the effect of inactivation of *Nkx3.1* in the mouse prostate, *Nkx3.1* knockout mouse models were generated. Complete inactivation of *Nkx3.1* in mice results in developmental effects of the prostate gland, including defects in ductal branching morphogenesis, reduced production of prostatic secretions and induced hyperplasia and dysplasia of epithelial cells. This phenotype was observed both in mono-allelic as well as in bi-allelic *Nkx3.1* knockout mice [142]. At older age (>1 year) homozygous *Nkx3.1* knockout mice develop PIN lesions, which never progressed to invasive cancer [143].

PSA-Cre driven inactivation of one or two floxed copies of *Nkx3.1* specifically in the mouse prostate also resulted in the development of PIN [132]. Epithelial cells within PIN foci in prostates of heterozygous *Nkx3.1* knockout mice had lost the wild type *Nkx3.1* allele. Interestingly, in

both conventional and conditional *Nkx3.1* knockout mice the differentiation status of luminal epithelial cells within PIN lesions was disturbed. This suggests that *Nkx3.1* is an important gene to establish and maintain the terminal differentiation of luminal epithelial cells in the prostate.

2.4.2 The *Pten* knockout mouse models

The most intensively studied tumor suppressor gene in mouse cancer models is *Pten*. Conventional *Pten-/-* mice have developmental defects and are embryonic lethal. Heterozygous *Pten* knockout mice are viable and are susceptible for tumor development [144, 145]. These mice develop a broad range of tumors, including germ cell, gonadostromal, thyroid and colon tumors. Prostates of *Pten+/-* mice contained foci of hyperplastic and dysplastic cells. These histological changes resembled those observed in patients suffering the cancer predisposition syndrome Cowden disease caused by germline mutations in *PTEN* [146]. Recently, in addition to conventional *Pten+/-* knockout mice, transgenic mice were generated carrying *PTEN* mutations identified in patients with Cowden disease, the C124R and G129E *PTEN* mutations [84]. During development similar abnormalities were observed in these mutant *Pten* mice, however the frequency and severity of proliferative lesions/tumors at older age (9 months) was different. This allele-specific tumor spectrum may explain differences in cancer susceptibility between patients suffering Cowden disease.

To study the effect of complete *Pten* inactivation in the prostate, conditional mouse prostate cancer models were generated based on *Pten* inactivation driven by the prostate specific, androgen dependent PB, PSA and Nkx3.1 promoter [88, 116, 117, 134]. In these models, embryonic lethality caused by complete *Pten* inactivation in conventional mouse models was circumvented. Bi-allelic PB-Cre targeted *Pten* knockout mice developed prostate hyperplasia by 4 weeks of age, PIN lesions at 6 weeks and ultimately invasive prostate tumors were observed at full penetrance (>9 weeks) [116]. Lymphovascular invasion resulting in prostate cancer metastases in lymph nodes and pulmonary alveolar spaces was detected in ~50% of the homozygous *Pten* knockout mice at older age (>12 weeks). To test the androgen responsibility of *Pten* negative tumor cells, targeted *PB-Cre;Pten-loxP/loxP* knockout mice were castrated at 16 weeks, when invasive tumor had already formed. Despite the induced apoptotic response at 3 days post-castration after castration in these mice, 2.5 months after castration a considerable amount of residual tumor cells was detected. These data indicate that the majority of cancer cells in this model are androgen dependent and do not survive androgen ablation therapy, in contrast to a subpopulation of cancer cells which does not depend on androgens. Expression profiling revealed similarities between *Pten* negative prostate tumors and human prostate cancer. For example, genes associated with prostate cancer metastases, like *Col1a1*, *Col1a2* and *Myh11*, were differentially expressed in this mouse model.

Like observed in *PB-Cre;Pten* knockout mice, *PSA-Cre;Pten* knockout mice also developed invasive prostate cancer [134]. Prostate cancer metastases were rare in this mouse model. Mono-allelic *Pten* knockout mice developed hyperplastic foci at older age (>10 months), which never progressed into prostate cancer. A major difference between PB-Cre and the PSA-Cre models is the latency time for prostate tumor development. Complete *Pten* inactivation in PB-Cre mice results in tumor development after 2.5 months, whereas in PSA-Cre driven *Pten* knockout mice tumors are observed at 10 months of age or older. Because of the slower process of prostate tumorigenesis in the PSA-Cre driven model, the process of tumor formation can be studied very accurately. Like the PB-Cre and PSA-Cre targeted model *Pten* knockout model, NKX3.1-CreERT2 targeted *Pten* knockout mice can developed PIN with microinvasive cancer [88].

In contrast to the TRAMP and LADY mouse model, targeted *Pten* knockout prostate cancer models develop prostate tumors composed of cells with characteristics of luminal epithelial cells. Here, most tumor cells expressed Cytokeratin 8 and AR, whereas expression of neuroendocrine markers in these cells was rare, like in human tumors. Although tumor cells in both the *PB-Cre;Pten* and *PSA-Cre;Pten* knockout models shared many characteristic and showed large overlap in expression profile, different candidate tumor initiating cells were identified. In our *PSA-Cre* targeted *Pten* knockout model *Clu+Tacstd2+Sca-1+* cells in the luminal epithelial layer were proposed as tumor initiating cells [147], whereas in *Pten* knockout mice targeted by PB-Cre candidate tumor initiating cells located in the P63+ basal epithelial cell layer were identified [148, 149].

In addition to prostate specific *Pten* knockout mouse models, *Pten* knockout mice driven by the mouse mammary tumor virus (MMTV) promoter developed prostate cancer [150]. In these mice, *Pten* inactivation was detected in mammary epithelial cells, epidermis, prostate and thymus, resulting in epidermal hyperplasia, invasive prostate carcinoma and thymic lymphomas. *MMTV-Cre;Pten-loxP/loxP* mice died of lymphoid malignancy at 3 months, making it impossible to study the progression and metastasis of prostate tumors. Analysis of lesions in the epidermis and the prostate suggested that in this mouse model neoplasia results from expansion of the basal epithelial cell population.

Analysis of *Pten* knockout mice increased our knowledge of *Pten*, its function in tumor development and the use of GEMM as models for human cancer. It was shown that Pten is haploinsufficient in tumor suppression and that even a small variation in *Pten* expression level influences the phenotype observed in the mice [117]. Furthermore, Trotman and colleagues showed that the choice of the promoter determines the rate of prostate tumor development in these conditional *Pten* knockout mice due to differences in the strength of the promoter. The tumor development was faster in ARR2PB driven *Pten* knockout mice than in a mouse model driven by the short PB promoter. This effect was also observed in Myc transgenic mice (paragraph 2.3.2). In addition, controlled ablation of *Pten* in Tamoxifen-inducible *ARR2PB-CreER(T2);Pten-*

loxP/loxP and *PSA-CreER(T2);Pten-loxP/loxP* mice demonstrated that timing of *Pten* inactivation is crucial for the rate of prostate tumor development [118, 133].

Studies of *Pten* knockout mice also increased our knowledge about signaling pathways and cellular processes controlled by Pten. For example, *Pten* knockout models showed that next to the Akt pathway, also the Erk pathway can be activation upon *Pten* inactivation [151]. The activation of these pathways and possibly yet unknown mechanisms will lead to alterations in cellular processes. Pten appeared to be essential for processes like proliferation, differentiation, regulation of cell size and stem/progenitor cell renewal [134, 147, 148, 152]. Furthermore, it was shown that *Pten* inactivation in PB-Cre targeted mice induces the expression of cellular senescence markers in the prostate [131].

2.4.3 *Trp53* knockout and mutant *Trp53* mouse models

In the last 20 years the molecular and biological significance of *TP53* mutations and inactivation of *Trp53* was studied in genetically engineered mice [153]. In 1989, the first conventional transgenic mice carrying mutant *Trp53* were described and three years later the first conventional *Trp53* knockout mice were characterized [154, 155]. Remarkably, both mice carrying the activating *Trp53* mutation and *Trp53* knockout mice were viable and developed normally. This corresponds with a role for the tumor suppressor gene *TP53* as responder to DNA damage and oncogenic stress, so, not surprisingly, both mouse models are prone to develop tumors. In these models the function of Trp53 could be studied and insight into mechanisms of Trp53 protein stabilization in tumor tissue was provided by mutant *Trp53* mouse models. Furthermore, analysis of the tumor spectrum of mutant *Trp53* transgenic mice led to the discovery of germline *Trp53* mutations as the cause of most cases of Li-Fraumeni syndrome, a hereditary disorder with predisposition to develop cancer [68]. Interestingly, next to the enhanced tumor susceptibility caused by loss of *Trp53* function, reduced longevity was observed in these mice [156].

Restoration of the Trp53 function in *Trp53* knockout mice leads to regression of the tumor, however the mechanism of tumor suppression appeared to depend on the tissue type [153, 157, 158]. In lymphomas restoration of Trp53 function induces apoptosis, whereas in sarcomas and liver tumors a cellular senescence response was observed. Interestingly, transgenic mice with an extra copy of *Trp53* (Super p53 mice) confirmed that *Trp53* is an important tumor suppressor gene [153, 159]. These mice are resistant to tumor formation and show no premature aging.

The phenotype observed in mutant *Trp53* mice depends on the type of *Trp53* mutation, which is introduced [153]. For example, mice carrying the R172H mutation developed spontaneous, metastatic tumors, whereas mice carrying the S389A mutation only showed skin tumor development after ultraviolet induction. Remarkably, even the tumor spectrum between conventional *Trp53+/-* and *Trp53-/-* mice was slightly different [153]. Bi-allelic knockout *Trp53-/-*

mice developed mainly lymphomas and some soft tissue sarcomas, whereas *Trp53+/-* knockout mice developed lymphomas, soft tissue sarcomas and osteosarcomas in equal amounts.

So far, three prostate specific ARR2PB-Cre driven *Trp53* knockout mouse models are described [130, 131, 160]. In one of these models dysplastic foci were observed in prostates of old *Trp53* knockout mice [130], whereas the other prostate specific *Trp53* knockout mouse model showed no aberrant prostate histology [131]. In our laboratory *PSA-Cre;Trp53-loxP/loxP* knockout mice were generated (Korsten *et al*., to be published). The characterization of these mice is described in Chapter 4. Furthermore, the effect of prostate specific expression of mutant *TP53* with a mutation at amino acid 273 was investigated [129]. These mice developed PIN lesions containing cells with nuclear atypia. In prostates of these mice, expressing mutant *TP53,* the apoptotic response was inhibited by castration.

2.5 Double genetically engineered mouse models for prostate cancer

In addition to single genetically modified mouse models for prostate cancer, double genetically engineered mouse models can be generated to address the question whether synergism can be detected between pathways. These bigenic models are generated by crossing two different genetically modified mouse lines. They recapitulate better the complex human situation, because in prostate tumors multiple genetic alterations are found within one tumor. Because for prostate cancer the number of double transgenic mouse models is very large, here as an example mouse models involving the most frequently inactivated tumor suppressor gene in prostate cancer *Pten* are discussed. The effect of secondary events in both conventional and conditional *Pten* knockout mouse models is discussed in paragraph 2.5.1. and 2.5.2. respectively.

2.5.1 The effect of a second event in conventional *Pten+/-* knockout mice

As described previously, conventional *Pten+/-* knockout mice develop PIN lesions at older age [144]. In contrast to the mono-allelic *Pten* knockout mouse model, in combination with other genetic alterations the prostates in these double genetically engineered mice are more severely affected. For example, conventional *Nkx3.1* knockout mice developed hyperplasia and dysplasia of the prostate epithelial cells [142]. Inactivation of *Nkx3.1* in *Pten+/-* mice (*Nkx3.1-/-Pten+/-* and *Nkx3.1+/-Pten+/-* mice*)* resulted in the development of PIN lesions containing poorly differentiated cells with prominent nucleoli and frequent mitotic figures in most prostate lobes at 12 months of age [143, 161]. Correspondingly, in these prostate parts of *Nkx3.1-/-Pten+/-* knockout mice relatively more clusters of cells overexpressing pAkt were detected and the wild type *Pten* allele was frequently lost. Examination of the prostate histology showed lesions resembling adenocarcinoma in the dorsal-lateral lobes of *Nkx3.1/Pten* knockout mice at older age (>12 months) [161]. Part of these tumors (25%) metastasized to lymph nodes. Recent work demonstrated that a subpopulation of prostate epithelial cells in *Nkx3.1/Pten* knockout mice are

androgen independent for their growth [162]. It was proposed that activation of the Akt and Erk signaling in this mouse model promotes androgen-independent growth of prostate cells [162].

Another tumor suppressor gene that can be inactivated in advanced prostate cancer is *CDKN1B,* encoding p27 [163]. Conventional *Cdkn1b-/-* mice develop prostate hyperplasia at older age which never progressed to prostate tumors [164]. Inactivation of this gene in conventional *Pten* knockout mice promoted prostate tumor development and had a negative effect on the survival rate due to tumor formation in multiple organs, including the prostate. The proliferation rate in prostates of *Cdkn1b-/-Pten+/-* knockout mice was higher than in prostates of single knockout mice. Essentially similar data were described in a study where the *INK4a/ARF* gene, a negative regulator of the cell cyclus, was inactivated in Pten+/- mice. These mice also developed prostate cancer at older age, in contrast to the single knockout mouse models [165].

As discussed in Chapter 1, *PTEN* inactivation results in activation of the AKT pathway, so it is interesting to investigate whether it is possible to inhibit the process of PIN/tumor development in *Pten* knockout mice by inactivation of *Akt1* [166]. Complete inactivation of *Akt1* in *Pten+/-* mice significantly inhibited the formation of PIN/tumorigenesis in several organs. The most profound effects were detected in the prostate, endometrium and the small intestine. In these organs even heterozygous loss of *Akt1* had a negative effect on PIN/tumor development. In line with these results, the expression levels of phosphorylated S6 (pS6) ribosomal protein, a marker for of the mTOR pathway activity, was lower in prostates of *Pten+/-Akt1-/-* knockout mice. These data confirm that downstream targets of Akt1 are indeed affected in these mice.

The effect of inactivation of an Akt downstream target, *Tuberous scleroses (TSC) 2*, in *Pten+/-* mice was also studied [134]. *TSC2* inhibits the activation of the mTOR pathway. In contrast to *Pten+/-* mice, *Pten+/-Tsc2+/-* mice had a shorter survival time and developed prostate cancer in 75% of the mice at 8 months of age. In prostates of these mice the expression of Phospho-mTOR and its downstream target Phospho-p70S6 was increased as compared to single knockout mice. These data underscore the relevance of mTOR pathway activation for prostate tumorigenesis.

In addition to *Pten* inactivation in combination with loss of function of genes, the effect of oncogenic events was investigated in *Pten+/-* mice. As described prostate specific overexpression of truncated ERG in the mouse prostate did not result in a significant phenotype and is insufficient for prostate cancer development. Recently, mono-allelic loss of *Pten* in combination with targeted overexpression of the most common ERG isoform was twice reported to promote prostate cancer development [139, 140]. Analysis of the prostate histology resulted in conflicting data. In one model at the age of 6 months all *PB-ERG;Pten+/-* mice developed prostatic adenocarcinoma in contrast to PIN lesions observed in *Pten+/-* mice, whereas in another model overexpression of truncated ERG in combination with mono-allelic *Pten* inactivation only PIN lesions were observed. Targeted overexpression of the *TMPRSS2-ERG* fusion gene in *PB-AKT* transgenic mice resulted in more severe PIN lesions than observed in single AKT transgenic mice, but no tumors

was observed [139]. Remarkably, in prostates of *PB-Cre;TMPRSS2-ERG;Myc* mice no synergistic effect of *TMPRSS2-ERG* and *Myc* overexpression was observed [139].

Mono-allelic loss of *Pten* in *PB-Erbb2* mice resulted in the development of adenocarcinomas [167]. The proliferation markers *CyclinD1* and *Pcna* were high expressed in these tumors. Essentially identical data were observed after overexpression of *FGF8b* in *Pten+/-* mice [168]. PB-Cre driven *FGF8b* mice develop PIN lesions at older age. Mono-allelic loss of *Pten* in this model triggers the development of metastatic adenocarcinomas at an age of 9 months or older.

Finally, *Pten+/-* mice were also crossed with TRAMP mice, which were known to develop prostate tumors (paragraph 2.2). In TRAMP mice haploinsufficiency of the *Pten* gene promotes the progression of prostate cancer [169]. *Pten+/-TRAMP* mice developed larger prostate tumors at a faster rate than observed in *Pten+/-* or *TRAMP* mice. Interestingly, in 68% of the prostate tumors of *Pten+/-TRAMP* mice loss of the wild type *Pten* allele was found. The survival rate of these mice was inversely correlated to the dose of *Pten*.

In conclusion, these data show that mono-allelic loss of *Pten* can have profound effects on the observed phenotype and the prostate characteristics in GEMMs. The effects observed depend on the mouse model used to test the effect of *Pten* inactivation.

2.5.2 The effect of a second genetic event in conditional *Pten* knockout mice

Next to the effect of secondary events in conventional *Pten+/-* knockout mice, the impact of two genetic alterations was also studied in conditional *Pten* knockout mice. *TP53* is frequently inactivated in advanced prostate tumors (Paragraph 1). Combined PB-Cre driven inactivation of both *Pten* and *Trp53*, resulted in an acceleration of the prostate tumor development compared to the cancer development in targeted *Pten* knockout [131, 160]. Targeted *Pten/Trp53* knockout mice start to develop prostate tumors as early as 2 months of age. These tumors were 32-times bigger as compared to tumors in PB-Cre driven *Pten* knockout mice. A proposed mechanism important for this observed effect was the inhibition of TP53 dependent cellular senescence in *Pten/Trp53* knockout mice. The analysis of prostate tumor development and progression in *PSA-Cre;Pten;Trp53* double knockout mice is described in Chapter 4.

Another frequent event in prostate cancer is the overexpression of *MYC* (Paragraph 1). Loss of one *Pten* allele in a mouse model with targeted *Myc* overexpression induced cancer in ~20 percent of the mice [114]. In this mouse model *Pten* loss induced activation of the c-jun N-terminal kinase (JNK) pathway, which appeared to be an anti-apoptotic pathway. Remarkably, the p53-dependent cellular senescence response in *Pten* knockout mice was switched to an apoptotic response by repression of *P21* by *c-Myc*. In addition to this model, the effect of RAS pathway activation was also assessed in conditional *Pten* knockout mice [170]. Although sole *RAS* activation was not sufficient for prostate cancer initiation, in combination with *Pten* inactivation

the prostate cancer progression was accelerated associated with epithelial-mesenchymal transition and macrometastases in all mice.

Recently, activation of the TGFβ/BMP-SMAD signaling was detected in prostate tumors of *Pten* negative mice [171]. Genetic co-deletion of *Smad4* in PB-Cre targeted *Pten* knockout mice resulted in full penetrance of invasive, metastatic and letal prostate tumors. This suggests that SMAD4 can function as a suppressor of tumor progression.

These data again show that *Pten* loss can have profound effects on the characteristics of prostate lesions in GEMMs. Studies in these double genetically engineered mouse models will provide insight into the working mechanisms of PTEN.

3. SCOPE OF THIS THESIS

The investigations described in this thesis are mainly focused on analysis of prostate tumorigenesis in mouse models of prostate cancer induced by targeted inactivation of *Pten*, the most frequently inactivated tumor suppressor gene in clinical prostate cancer. The characterization of the mouse models increases our general knowledge of initiation and progression of prostate tumor development. Although mice are not identical to men, aspects of the mouse model will be of importance for human prostate cancer. In **Chapter 2** we addressed the question what the characteristics are of tumor initiating cells from which prostate hyperplasia/tumors developed in *PSA-Cre;Pten-loxP/loxP* knockout mice. The mechanism of hyperplasia development in *PSA-Cre;Pten-loxP/loxP* knockout mice was studied and candidate tumor initiating cells were identified. In contrast to previous studies in different models, the results showed that epithelial progenitor cells in the luminal epithelial cell layer can function as tumor initiating cells. The later stages of prostate tumorigenesis in targeted *Pten* knockout mice are described in **Chapter 3**. Characterization of prostate tumors of *Pten* knockout mice showed histological heterogeneity. Furthermore, biological processes associated with tumorigenesis were identified. Heterogeneity was also detected between *in vitro* growing prostate cancer cell lines derived from the targeted *Pten* knockout mice. As mentioned in Chapter 1, *TP53* is frequently inactivated in late stage clinical prostate cancer. The effect of *Trp53* inactivation in *Pten* knockout mice is described in **Chapter 4.** Here also, the morphological, biological and molecular aspects of different stages of tumor development were investigated and tumors were characterized. Cell lines derived from prostate cancers of either targeted *Pten* and *Pten;Trp53* knockout mice were also used to investigate the effect of *Trp53* inactivation in tumor cells. In addition to the characterization of mouse models as described in Chapter 2-4, gene expression array data of human prostate cancer samples were analyzed in an attempt to identify target genes of the *ERG* oncogene **(Chapter 5).** Here a new direct target gene of ERG was identified. *TMPRSS2-ERG* gene fusion causing ERG overexpression is a common event in prostate cancer. Our data will help elucidating the role of *ERG* in prostate cancer. Finally, in **Chapter 6** the results described in this thesis are discussed and suggestions for further research are proposed.

4. REFERENCES

1. Jemal, A., et al., *Global cancer statistics.* CA Cancer J Clin, 2011. **61**(2): p. 69-90.
2. Kollmeier, M.A. and M.J. Zelefsky, *Brachytherapy for clinically localized prostate cancer: optimal patient selection.* Arch Esp Urol, 2011. **64**(8): p. 847-57.
3. Bianco, F.J., *Robotic radical prostatectomy: present and future.* Arch Esp Urol, 2011. **64**(8): p. 839-46.
4. Ginzburg, S. and P.C. Albertsen, *The timing and extent of androgen deprivation therapy for prostate cancer: weighing the clinical evidence.* Endocrinol Metab Clin North Am, 2011. **40**(3): p. 615-23, ix.
5. Feldman, B.J. and D. Feldman, *The development of androgen-independent prostate cancer.* Nat Rev Cancer, 2001. **1**(1): p. 34-45.
6. Culig, Z. and G. Bartsch, *Androgen axis in prostate cancer.* J Cell Biochem, 2006. **99**(2): p. 373-81.
7. Ryan, C.J. and D.J. Tindall, *Androgen receptor rediscovered: the new biology and targeting the androgen receptor therapeutically.* J Clin Oncol, 2011. **29**(27): p. 3651-8.
8. Dutt, S.S. and A.C. Gao, *Molecular mechanisms of castration-resistant prostate cancer progression.* Future Oncol, 2009. **5**(9): p. 1403-13.
9. Dong, J.T., *Prevalent mutations in prostate cancer.* J Cell Biochem, 2006. **97**(3): p. 433-47.
10. Taylor, B.S., et al., *Integrative genomic profiling of human prostate cancer.* Cancer Cell, 2010. **18**(1): p. 11-22.
11. Amaral, T.M., et al., *Castration-resistant prostate cancer: mechanisms, targets, and treatment.* Prostate Cancer, 2012. **2012**: p. 327253.
12. Kirby, M., C. Hirst, and E.D. Crawford, *Characterising the castration-resistant prostate cancer population: a systematic review.* Int J Clin Pract, 2011. **65**(11): p. 1180-92.
13. Montironi, R., et al., *Prostatic intraepithelial neoplasia: its morphological and molecular diagnosis and clinical significance.* BJU Int, 2011. **108**(9): p. 1394-401.
14. Hanahan, D. and R.A. Weinberg, *Hallmarks of cancer: the next generation.* Cell, 2011. **144**(5): p. 646-74.
15. Zhang, S., et al., *Detection of TMPRSS2 gene deletions and translocations in carcinoma, intraepithelial neoplasia, and normal epithelium of the prostate by direct fluorescence in situ hybridization.* Diagn Mol Pathol, 2010. **19**(3): p. 151-6.
16. Yoshimoto, M., et al., *Interphase FISH analysis of PTEN in histologic sections shows genomic deletions in 68% of primary prostate cancer and 23% of high-grade prostatic intra-epithelial neoplasias.* Cancer Genet Cytogenet, 2006. **169**(2): p. 128-37.
17. Clark, J.P. and C.S. Cooper, *ETS gene fusions in prostate cancer.* Nat Rev Urol, 2009. **6**(8): p. 429-39.
18. Tu, J.J., et al., *Gene fusions between TMPRSS2 and ETS family genes in prostate cancer: frequency and transcript variant analysis by RT-PCR and FISH on paraffin-embedded tissues.* Mod Pathol, 2007. **20**(9): p. 921-8.
19. Tomlins, S.A., et al., *Recurrent fusion of TMPRSS2 and ETS transcription factor genes in prostate cancer.* Science, 2005. **310**(5748): p. 644-8.
20. Ribeiro, F.R., et al., *Comparison of chromosomal and array-based comparative genomic hybridization for the detection of genomic imbalances in primary prostate carcinomas.* Mol Cancer, 2006. **5**: p. 33.
21. Joshua, A.M., et al., *Prostatic preneoplasia and beyond.* Biochim Biophys Acta, 2008. **1785**(2): p. 156-81.
22. Majumder, P.K. and W.R. Sellers, *Akt-regulated pathways in prostate cancer.* Oncogene, 2005. **24**(50): p. 7465-74.
23. Sun, J., et al., *DNA copy number alterations in prostate cancers: a combined analysis of published CGH studies.* Prostate, 2007. **67**(7): p. 692-700.
24. Saramaki, O.R., et al., *Genetic aberrations in prostate cancer by microarray analysis.* Int J Cancer, 2006. **119**(6): p. 1322-9.
25. Abate-Shen, C., M.M. Shen, and E. Gelmann, *Integrating differentiation and cancer: the Nkx3.1 homeobox gene in prostate organogenesis and carcinogenesis.* Differentiation, 2008. **76**(6): p. 717-27.
26. Abdulkadir, S.A., *Mechanisms of prostate tumorigenesis: roles for transcription factors Nkx3.1 and Egr1.* Ann N Y Acad Sci, 2005. **1059**: p. 33-40.

27. Salmena, L., A. Carracedo, and P.P. Pandolfi, *Tenets of PTEN tumor suppression.* Cell, 2008. **133**(3): p. 403-14.
28. MacGrogan, D. and R. Bookstein, *Tumour suppressor genes in prostate cancer.* Semin Cancer Biol, 1997. **8**(1): p. 11-9.
29. Barbieri, C.E., F. Demichelis, and M.A. Rubin, *Molecular genetics of prostate cancer: emerging appreciation of genetic complexity.* Histopathology, 2012. **60**(1): p. 187-98.
30. Jeronimo, C., et al., *Epigenetics in prostate cancer: biologic and clinical relevance.* Eur Urol, 2011. **60**(4): p. 753-66.
31. Nelson, W.G., A.M. De Marzo, and S. Yegnasubramanian, *Epigenetic alterations in human prostate cancers.* Endocrinology, 2009. **150**(9): p. 3991-4002.
32. Kumar-Sinha, C., S.A. Tomlins, and A.M. Chinnaiyan, *Recurrent gene fusions in prostate cancer.* Nat Rev Cancer, 2008. **8**(7): p. 497-511.
33. Rosen, P., et al., *Clinical potential of the ERG oncoprotein in prostate cancer.* Nat Rev Urol, 2012. **9**(3): p. 131-7.
34. Hermans, K.G., et al., *Truncated ETV1, fused to novel tissue-specific genes, and full-length ETV1 in prostate cancer.* Cancer Res, 2008. **68**(18): p. 7541-9.
35. Helgeson, B.E., et al., *Characterization of TMPRSS2:ETV5 and SLC45A3:ETV5 gene fusions in prostate cancer.* Cancer Res, 2008. **68**(1): p. 73-80.
36. Han, B., et al., *A fluorescence in situ hybridization screen for E26 transformation-specific aberrations: identification of DDX5-ETV4 fusion protein in prostate cancer.* Cancer Res, 2008. **68**(18): p. 7629-37.
37. Pflueger, D., et al., *N-myc downstream regulated gene 1 (NDRG1) is fused to ERG in prostate cancer.* Neoplasia, 2009. **11**(8): p. 804-11.
38. Tomlins, S.A., et al., *Integrative molecular concept modeling of prostate cancer progression.* Nat Genet, 2007. **39**(1): p. 41-51.
39. Gasi, D., et al., *Overexpression of full-length ETV1 transcripts in clinical prostate cancer due to gene translocation.* PLoS One, 2011. **6**(1): p. e16332.
40. Palanisamy, N., et al., *Rearrangements of the RAF kinase pathway in prostate cancer, gastric cancer and melanoma.* Nat Med, 2010. **16**(7): p. 793-8.
41. Berger, M.F., et al., *The genomic complexity of primary human prostate cancer.* Nature, 2011. **470**(7333): p. 214-20.
42. Maher, C.A., et al., *Transcriptome sequencing to detect gene fusions in cancer.* Nature, 2009. **458**(7234): p. 97-101.
43. Leslie, N.R. and C.P. Downes, *PTEN function: how normal cells control it and tumour cells lose it.* Biochem J, 2004. **382**(Pt 1): p. 1-11.
44. Sansal, I. and W.R. Sellers, *The biology and clinical relevance of the PTEN tumor suppressor pathway.* J Clin Oncol, 2004. **22**(14): p. 2954-63.
45. Hollander, M.C., G.M. Blumenthal, and P.A. Dennis, *PTEN loss in the continuum of common cancers, rare syndromes and mouse models.* Nat Rev Cancer, 2011. **11**(4): p. 289-301.
46. Huang, J. and B.D. Manning, *A complex interplay between Akt, TSC2 and the two mTOR complexes.* Biochem Soc Trans, 2009. **37**(Pt 1): p. 217-22.
47. Zha, X., et al., *TSC1/TSC2 inactivation inhibits AKT through mTORC1-dependent up-regulation of STAT3-PTEN cascade.* Cancer Lett, 2011. **313**(2): p. 211-7.
48. Das, F., et al., *Unrestrained mammalian target of rapamycin complexes 1 and 2 increase expression of phosphatase and tensin homolog deleted on chromosome 10 to regulate phosphorylation of Akt kinase.* J Biol Chem, 2012. **287**(6): p. 3808-22.
49. Hamada, K., et al., *The PTEN/PI3K pathway governs normal vascular development and tumor angiogenesis.* Genes Dev, 2005. **19**(17): p. 2054-65.
50. Restuccia, D.F. and B.A. Hemmings, *From man to mouse and back again: advances in defining tumor AKTivities in vivo.* Dis Model Mech, 2010. **3**(11-12): p. 705-20.
51. Carnero, A., *The PKB/AKT pathway in cancer.* Curr Pharm Des, 2010. **16**(1): p. 34-44.

52. Vivanco, I., et al., *Identification of the JNK signaling pathway as a functional target of the tumor suppressor PTEN.* Cancer Cell, 2007. **11**(6): p. 555-69.
53. Shen, W.H., et al., *Essential role for nuclear PTEN in maintaining chromosomal integrity.* Cell, 2007. **128**(1): p. 157-70.
54. Song, M.S., et al., *Nuclear PTEN regulates the APC-CDH1 tumor-suppressive complex in a phosphatase-independent manner.* Cell, 2011. **144**(2): p. 187-99.
55. Akala, O.O. and M.F. Clarke, *Hematopoietic stem cell self-renewal.* Curr Opin Genet Dev, 2006. **16**(5): p. 496-501.
56. Rossi, D.J. and I.L. Weissman, *Pten, tumorigenesis, and stem cell self-renewal.* Cell, 2006. **125**(2): p. 229-31.
57. Bertram, J., et al., *Loss of PTEN is associated with progression to androgen independence.* Prostate, 2006. **66**(9): p. 895-902.
58. Koksal, I.T., et al., *The assessment of PTEN tumor suppressor gene in combination with Gleason scoring and serum PSA to evaluate progression of prostate carcinoma.* Urol Oncol, 2004. **22**(4): p. 307-12.
59. Yoshimoto, M., et al., *FISH analysis of 107 prostate cancers shows that PTEN genomic deletion is associated with poor clinical outcome.* Br J Cancer, 2007. **97**(5): p. 678-85.
60. Whibley, C., P.D. Pharoah, and M. Hollstein, *p53 polymorphisms: cancer implications.* Nat Rev Cancer, 2009. **9**(2): p. 95-107.
61. Vogelstein, B., D. Lane, and A.J. Levine, *Surfing the p53 network.* Nature, 2000. **408**(6810): p. 307-10.
62. Junttila, M.R. and G.I. Evan, *p53--a Jack of all trades but master of none.* Nat Rev Cancer, 2009. **9**(11): p. 821-9.
63. Krizhanovsky, V. and S.W. Lowe, *Stem cells: The promises and perils of p53.* Nature, 2009. **460**(7259): p. 1085-6.
64. Komarova, E.A., et al., *p53 is a suppressor of inflammatory response in mice.* Faseb J, 2005. **19**(8): p. 1030-2.
65. Aparicio, S. and C.J. Eaves, *p53: a new kingpin in the stem cell arena.* Cell, 2009. **138**(6): p. 1060-2.
66. Aylon, Y. and M. Oren, *New plays in the p53 theater.* Curr Opin Genet Dev, 2011. **21**(1): p. 86-92.
67. Birch, J.M., *The Li-Fraumeni cancer family syndrome.* J Pathol, 1990. **161**(1): p. 1-2.
68. Malkin, D., et al., *Germ line p53 mutations in a familial syndrome of breast cancer, sarcomas, and other neoplasms.* Science, 1990. **250**(4985): p. 1233-8.
69. Qian, J., et al., *Loss of p53 and c-myc overrepresentation in stage T(2-3)N(1-3)M(0) prostate cancer are potential markers for cancer progression.* Mod Pathol, 2002. **15**(1): p. 35-44.
70. Vinall, R.L., et al., *Evidence for an alternate molecular progression in prostate cancer.* Dis Model Mech, 2012.
71. Heidenberg, H.B., et al., *Alteration of the tumor suppressor gene p53 in a high fraction of hormone refractory prostate cancer.* J Urol, 1995. **154**(2 Pt 1): p. 414-21.
72. Leite, K.R., et al., *Abnormal expression of MDM2 in prostate carcinoma.* Mod Pathol, 2001. **14**(5): p. 428-36.
73. Khor, L.Y., et al., *MDM2 and Ki-67 predict for distant metastasis and mortality in men treated with radiotherapy and androgen deprivation for prostate cancer: RTOG 92-02.* J Clin Oncol, 2009. **27**(19): p. 3177-84.
74. van Weerden, W.M., et al., *Development of seven new human prostate tumor xenograft models and their histopathological characterization.* Am J Pathol, 1996. **149**(3): p. 1055-62.
75. Valkenburg, K.C. and B.O. Williams, *Mouse models of prostate cancer.* Prostate Cancer, 2011. **2011**: p. 895238.
76. Shappell, S.B., et al., *Prostate pathology of genetically engineered mice: definitions and classification. The consensus report from the Bar Harbor meeting of the Mouse Models of Human Cancer Consortium Prostate Pathology Committee.* Cancer Res, 2004. **64**(6): p. 2270-305.
77. Ahmad, I., O.J. Sansom, and H.Y. Leung, *Advances in mouse models of prostate cancer.* Expert Rev Mol Med, 2008. **10**: p. e16.

78. Thielen, J.L., et al., *Markers of prostate region-specific epithelial identity define anatomical locations in the mouse prostate that are molecularly similar to human prostate cancers.* Differentiation, 2007. **75**(1): p. 49-61.
79. Berquin, I.M., et al., *Expression signature of the mouse prostate.* J Biol Chem, 2005. **280**(43): p. 36442-51.
80. Abate-Shen, C. and M.M. Shen, *Mouse models of prostate carcinogenesis.* Trends Genet, 2002. **18**(5): p. S1-5.
81. Ghebranious, N. and L.A. Donehower, *Mouse models in tumor suppression.* Oncogene, 1998. **17**(25): p. 3385-400.
82. Sigmund, C.D., *Major approaches for generating and analyzing transgenic mice. An overview.* Hypertension, 1993. **22**(4): p. 599-607.
83. Kasper, S. and J.A. Smith, Jr., *Genetically modified mice and their use in developing therapeutic strategies for prostate cancer.* J Urol, 2004. **172**(1): p. 12-9.
84. Wang, F., *Modeling human prostate cancer in genetically engineered mice.* Prog Mol Biol Transl Sci, 2011. **100**: p. 1-49.
85. Hensley, P.J. and N. Kyprianou, *Modeling prostate cancer in mice: limitations and opportunities.* J Androl, 2011. **33**(2): p. 133-44.
86. Devoy, A., et al., *Genomically humanized mice: technologies and promises.* Nat Rev Genet, 2011. **13**(1): p. 14-20.
87. Hayashi, S. and A.P. McMahon, *Efficient recombination in diverse tissues by a tamoxifen-inducible form of Cre: a tool for temporally regulated gene activation/inactivation in the mouse.* Dev Biol, 2002. **244**(2): p. 305-18.
88. Wang, X., et al., *A luminal epithelial stem cell that is a cell of origin for prostate cancer.* Nature, 2009. **461**(7263): p. 495-500.
89. Kasper, S., *Survey of genetically engineered mouse models for prostate cancer: analyzing the molecular basis of prostate cancer development, progression, and metastasis.* J Cell Biochem, 2005. **94**(2): p. 279-97.
90. Cleutjens, K.B., et al., *A 6-kb promoter fragment mimics in transgenic mice the prostate-specific and androgen-regulated expression of the endogenous prostate-specific antigen gene in humans.* Mol Endocrinol, 1997. **11**(9): p. 1256-65.
91. Stanbrough, M., et al., *Prostatic intraepithelial neoplasia in mice expressing an androgen receptor transgene in prostate epithelium.* Proc Natl Acad Sci U S A, 2001. **98**(19): p. 10823-8.
92. Han, G., et al., *Mutation of the androgen receptor causes oncogenic transformation of the prostate.* Proc Natl Acad Sci U S A, 2005. **102**(4): p. 1151-6.
93. Wu, C.T., et al., *Increased prostate cell proliferation and loss of cell differentiation in mice lacking prostate epithelial androgen receptor.* Proc Natl Acad Sci U S A, 2007. **104**(31): p. 12679-84.
94. Majumder, P.K., et al., *Prostate intraepithelial neoplasia induced by prostate restricted Akt activation: the MPAKT model.* Proc Natl Acad Sci U S A, 2003. **100**(13): p. 7841-6.
95. Bruxvoort, K.J., et al., *Inactivation of Apc in the mouse prostate causes prostate carcinoma.* Cancer Res, 2007. **67**(6): p. 2490-6.
96. Bruckheimer, E.M., et al., *Bcl-2 accelerates multistep prostate carcinogenesis in vivo.* Oncogene, 2000. **19**(46): p. 5251-8.
97. Francis, J.C., et al., *Brca2 and Trp53 deficiency cooperate in the progression of mouse prostate tumourigenesis.* PLoS Genet, 2010. **6**(6): p. e1000995.
98. Pearson, H.B., T.J. Phesse, and A.R. Clarke, *K-ras and Wnt signaling synergize to accelerate prostate tumorigenesis in the mouse.* Cancer Res, 2009. **69**(1): p. 94-101.
99. Casimiro, M., et al., *ErbB-2 induces the cyclin D1 gene in prostate epithelial cells in vitro and in vivo.* Cancer Res, 2007. **67**(9): p. 4364-72.
100. Voelkel-Johnson, C., et al., *Genomic instability-based transgenic models of prostate cancer.* Carcinogenesis, 2000. **21**(8): p. 1623-7.

101. Tomlins, S.A., et al., *Role of the TMPRSS2-ERG gene fusion in prostate cancer.* Neoplasia, 2008. **10**(2): p. 177-88.
102. Klezovitch, O., et al., *A causal role for ERG in neoplastic transformation of prostate epithelium.* Proc Natl Acad Sci U S A, 2008. **105**(6): p. 2105-10.
103. Shin, S., et al., *Induction of Prostatic Intraepithelial Neoplasia and Modulation of Androgen Receptor by ETS Variant 1/ETS-Related Protein 81.* Cancer Res, 2009.
104. Konno-Takahashi, N., et al., *Engineered FGF-2 expression induces glandular epithelial hyperplasia in the murine prostatic dorsal lobe.* Eur Urol, 2004. **46**(1): p. 126-32.
105. Foster, B.A., et al., *Enforced expression of FGF-7 promotes epithelial hyperplasia whereas a dominant negative FGFR2iiib promotes the emergence of neuroendocrine phenotype in prostate glands of transgenic mice.* Differentiation, 2002. **70**(9-10): p. 624-32.
106. Song, Z., et al., *Fibroblast growth factor 8 isoform B overexpression in prostate epithelium: a new mouse model for prostatic intraepithelial neoplasia.* Cancer Res, 2002. **62**(17): p. 5096-105.
107. Freeman, K.W., et al., *Conditional activation of fibroblast growth factor receptor (FGFR) 1, but not FGFR2, in prostate cancer cells leads to increased osteopontin induction, extracellular signal-regulated kinase activation, and in vivo proliferation.* Cancer Res, 2003. **63**(19): p. 6237-43.
108. Wang, F., et al., *Chronic activity of ectopic type 1 fibroblast growth factor receptor tyrosine kinase in prostate epithelium results in hyperplasia accompanied by intraepithelial neoplasia.* Prostate, 2004. **58**(1): p. 1-12.
109. Klezovitch, O., et al., *Hepsin promotes prostate cancer progression and metastasis.* Cancer Cell, 2004. **6**(2): p. 185-95.
110. Konno-Takahashi, N., et al., *Engineered IGF-I expression induces glandular enlargement in the murine prostate.* J Endocrinol, 2003. **177**(3): p. 389-98.
111. Kaplan-Lefko, P.J., et al., *Enforced epithelial expression of IGF-1 causes hyperplastic prostate growth while negative selection is requisite for spontaneous metastogenesis.* Oncogene, 2008. **27**(20): p. 2868-76.
112. Kelavkar, U.P., et al., *Conditional expression of human 15-lipoxygenase-1 in mouse prostate induces prostatic intraepithelial neoplasia: the FLiMP mouse model.* Neoplasia, 2006. **8**(6): p. 510-22.
113. Ellwood-Yen, K., et al., *Myc-driven murine prostate cancer shares molecular features with human prostate tumors.* Cancer Cell, 2003. **4**(3): p. 223-38.
114. Kim, J., et al., *Interactions between cells with distinct mutations in c-MYC and Pten in prostate cancer.* PLoS Genet, 2009. **5**(7): p. e1000542.
115. Li, Z., et al., *Prostatic intraepithelial neoplasia and adenocarcinoma in mice expressing a probasin-Neu oncogenic transgene.* Carcinogenesis, 2006. **27**(5): p. 1054-67.
116. Wang, S., et al., *Prostate-specific deletion of the murine Pten tumor suppressor gene leads to metastatic prostate cancer.* Cancer Cell, 2003. **4**(3): p. 209-21.
117. Trotman, L.C., et al., *Pten dose dictates cancer progression in the prostate.* PLoS Biol, 2003. **1**(3): p. E59.
118. Luchman, H.A., et al., *The pace of prostatic intraepithelial neoplasia development is determined by the timing of Pten tumor suppressor gene excision.* PLoS One, 2008. **3**(12): p. e3940.
119. Kindblom, J., et al., *Prostate hyperplasia in a transgenic mouse with prostate-specific expression of prolactin.* Endocrinology, 2003. **144**(6): p. 2269-78.
120. Lee, S.H., et al., *A constitutively activated form of the p110beta isoform of PI3-kinase induces prostatic intraepithelial neoplasia in mice.* Proc Natl Acad Sci U S A, 2010. **107**(24): p. 11002-7.
121. Gao, S., et al., *Altered differentiation and proliferation of prostate epithelium in mice lacking the androgen receptor cofactor p44/WDR77.* Endocrinology, 2010. **151**(8): p. 3941-53.
122. Scherl, A., et al., *Prostatic intraepithelial neoplasia and intestinal metaplasia in prostates of probasin-RAS transgenic mice.* Prostate, 2004. **59**(4): p. 448-59.
123. Maddison, L.A., et al., *Conditional deletion of Rb causes early stage prostate cancer.* Cancer Res, 2004. **64**(17): p. 6018-25.
124. Shim, E.H., et al., *Expression of the F-box protein SKP2 induces hyperplasia, dysplasia, and low-grade carcinoma in the mouse prostate.* Cancer Res, 2003. **63**(7): p. 1583-8.

125. Hill, R., et al., *Heterogeneous tumor evolution initiated by loss of pRb function in a preclinical prostate cancer model.* Cancer Res, 2005. **65**(22): p. 10243-54.
126. Greenberg, N.M., et al., *Prostate cancer in a transgenic mouse.* Proc Natl Acad Sci U S A, 1995. **92**(8): p. 3439-43.
127. Kasper, S., et al., *Development, progression, and androgen-dependence of prostate tumors in probasin-large T antigen transgenic mice: a model for prostate cancer.* Lab Invest, 1998. **78**(3): p. 319-33.
128. Masumori, N., et al., *A probasin-large T antigen transgenic mouse line develops prostate adenocarcinoma and neuroendocrine carcinoma with metastatic potential.* Cancer Res, 2001. **61**(5): p. 2239-49.
129. Elgavish, A., et al., *Transgenic mouse with human mutant p53 expression in the prostate epithelium.* Prostate, 2004. **61**(1): p. 26-34.
130. Zhou, Z., et al., *Synergy of p53 and Rb deficiency in a conditional mouse model for metastatic prostate cancer.* Cancer Res, 2006. **66**(16): p. 7889-98.
131. Chen, Z., et al., *Crucial role of p53-dependent cellular senescence in suppression of Pten-deficient tumorigenesis.* Nature, 2005. **436**(7051): p. 725-30.
132. Abdulkadir, S.A., et al., *Conditional loss of Nkx3.1 in adult mice induces prostatic intraepithelial neoplasia.* Mol Cell Biol, 2002. **22**(5): p. 1495-503.
133. Ratnacaram, C.K., et al., *Temporally controlled ablation of PTEN in adult mouse prostate epithelium generates a model of invasive prostatic adenocarcinoma.* Proc Natl Acad Sci U S A, 2008. **105**(7): p. 2521-6.
134. Ma, X., et al., *Targeted biallelic inactivation of Pten in the mouse prostate leads to prostate cancer accompanied by increased epithelial cell proliferation but not by reduced apoptosis.* Cancer Res, 2005. **65**(13): p. 5730-9.
135. Gingrich, J.R., et al., *Metastatic prostate cancer in a transgenic mouse.* Cancer Res, 1996. **56**(18): p. 4096-102.
136. Komiya, A., et al., *Neuroendocrine differentiation in the progression of prostate cancer.* Int J Urol, 2009. **16**(1): p. 37-44.
137. Bartel, F.O., T. Higuchi, and D.D. Spyropoulos, *Mouse models in the study of the Ets family of transcription factors.* Oncogene, 2000. **19**(55): p. 6443-54.
138. Netzer, S., et al., *Ectopic expression of the ets transcription factor ER81 in transgenic mouse mammary gland enhances both urokinase plasminogen activator and stromelysin-1 transcription.* Transgenic Res, 2002. **11**(2): p. 123-31.
139. King, J.C., et al., *Cooperativity of TMPRSS2-ERG with PI3-kinase pathway activation in prostate oncogenesis.* Nat Genet, 2009. **41**(5): p. 524-6.
140. Carver, B.S., et al., *Aberrant ERG expression cooperates with loss of PTEN to promote cancer progression in the prostate.* Nat Genet, 2009. **41**(5): p. 619-24.
141. Kim, J., et al., *A mouse model of heterogeneous, c-MYC-initiated prostate cancer with loss of Pten and p53.* Oncogene, 2012. **31**(3): p. 322-32.
142. Bhatia-Gaur, R., et al., *Roles for Nkx3.1 in prostate development and cancer.* Genes Dev, 1999. **13**(8): p. 966-77.
143. Kim, M.J., et al., *Nkx3.1 mutant mice recapitulate early stages of prostate carcinogenesis.* Cancer Res, 2002. **62**(11): p. 2999-3004.
144. Di Cristofano, A., et al., *Pten is essential for embryonic development and tumour suppression.* Nat Genet, 1998. **19**(4): p. 348-55.
145. Suzuki, A., et al., *High cancer susceptibility and embryonic lethality associated with mutation of the PTEN tumor suppressor gene in mice.* Curr Biol, 1998. **8**(21): p. 1169-78.
146. Gustafson, S., et al., *Cowden syndrome.* Semin Oncol, 2007. **34**(5): p. 428-34.
147. Korsten, H., et al., *Accumulating progenitor cells in the luminal epithelial cell layer are candidate tumor initiating cells in a Pten knockout mouse prostate cancer model.* PLoS One, 2009. **4**(5): p. e5662.
148. Wang, S., et al., *Pten deletion leads to the expansion of a prostatic stem/progenitor cell subpopulation and tumor initiation.* Proc Natl Acad Sci U S A, 2006. **103**(5): p. 1480-5.

149. Mulholland, D.J., et al., *Lin-Sca-1+CD49fhigh stem/progenitors are tumor-initiating cells in the Pten-null prostate cancer model.* Cancer Res, 2009. **69**(22): p. 8555-62.
150. Backman, S.A., et al., *Early onset of neoplasia in the prostate and skin of mice with tissue-specific deletion of Pten.* Proc Natl Acad Sci U S A, 2004. **101**(6): p. 1725-30.
151. Suzuki, A., et al., *Portrait of PTEN: messages from mutant mice.* Cancer Sci, 2008. **99**(2): p. 209-13.
152. Mulholland, D.J., J. Jiao, and H. Wu, *Hormone refractory prostate cancer: Lessons learned from the PTEN prostate cancer model.* Adv Exp Med Biol, 2008. **617**: p. 87-95.
153. Donehower, L.A. and G. Lozano, *20 years studying p53 functions in genetically engineered mice.* Nat Rev Cancer, 2009. **9**(11): p. 831-41.
154. Lavigueur, A., et al., *High incidence of lung, bone, and lymphoid tumors in transgenic mice overexpressing mutant alleles of the p53 oncogene.* Mol Cell Biol, 1989. **9**(9): p. 3982-91.
155. Donehower, L.A., et al., *Mice deficient for p53 are developmentally normal but susceptible to spontaneous tumours.* Nature, 1992. **356**(6366): p. 215-21.
156. Dumble, M., et al., *Insights into aging obtained from p53 mutant mouse models.* Ann N Y Acad Sci, 2004. **1019**: p. 171-7.
157. Ventura, A., et al., *Restoration of p53 function leads to tumour regression in vivo.* Nature, 2007. **445**(7128): p. 661-5.
158. Xue, W., et al., *Senescence and tumour clearance is triggered by p53 restoration in murine liver carcinomas.* Nature, 2007. **445**(7128): p. 656-60.
159. Garcia-Cao, I., et al., *"Super p53" mice exhibit enhanced DNA damage response, are tumor resistant and age normally.* Embo J, 2002. **21**(22): p. 6225-35.
160. Martin, P., et al., *Prostate epithelial Pten/TP53 loss leads to transformation of multipotential progenitors and epithelial to mesenchymal transition.* Am J Pathol, 2011. **179**(1): p. 422-35.
161. Abate-Shen, C., et al., *Nkx3.1; Pten mutant mice develop invasive prostate adenocarcinoma and lymph node metastases.* Cancer Res, 2003. **63**(14): p. 3886-90.
162. Gao, H., et al., *Emergence of androgen independence at early stages of prostate cancer progression in Nkx3.1; Pten mice.* Cancer Res, 2006. **66**(16): p. 7929-33.
163. Di Cristofano, A., et al., *Pten and p27KIP1 cooperate in prostate cancer tumor suppression in the mouse.* Nat Genet, 2001. **27**(2): p. 222-4.
164. Cordon-Cardo, C., et al., *Distinct altered patterns of p27KIP1 gene expression in benign prostatic hyperplasia and prostatic carcinoma.* J Natl Cancer Inst, 1998. **90**(17): p. 1284-91.
165. You, M.J., et al., *Genetic analysis of Pten and Ink4a/Arf interactions in the suppression of tumorigenesis in mice.* Proc Natl Acad Sci U S A, 2002. **99**(3): p. 1455-60.
166. Chen, M.L., et al., *The deficiency of Akt1 is sufficient to suppress tumor development in Pten+/- mice.* Genes Dev, 2006. **20**(12): p. 1569-74.
167. Rodriguez, O.C., et al., *A reduction in Pten tumor suppressor activity promotes ErbB-2-induced mouse prostate adenocarcinoma formation through the activation of signaling cascades downstream of PDK1.* Am J Pathol, 2009. **174**(6): p. 2051-60.
168. Zhong, C., et al., *Cooperation between FGF8b overexpression and PTEN deficiency in prostate tumorigenesis.* Cancer Res, 2006. **66**(4): p. 2188-94.
169. Kwabi-Addo, B., et al., *Haploinsufficiency of the Pten tumor suppressor gene promotes prostate cancer progression.* Proc Natl Acad Sci U S A, 2001. **98**(20): p. 11563-8.
170. Mulholland, D.J., et al., *Pten Loss and RAS/MAPK Activation Cooperate to Promote EMT and Metastasis Initiated from Prostate Cancer Stem/Progenitor Cells.* Cancer Res, 2012. **72**(7): p. 1878-89.
171. Ding, Z., et al., *SMAD4-dependent barrier constrains prostate cancer growth and metastatic progression.* Nature, 2011. **470**(7333): p. 269-73.

CHAPTER 2

Accumulating Progenitor Cells in the Luminal Epithelial Cell Layer are Candidate Tumor Initiating Cells in a *Pten* Knockout Mouse Prostate Cancer Model

Hanneke Korsten, Angelique Ziel-van der Made, Xiaoqian Ma, Theo van der Kwast, Jan Trapman

Department of Pathology, Josephine Nefkens Institute, Erasmus MC, 3000 CA Rotterdam, The Netherlands

PLoS One. 2009 May 22;4(5):e5662.

ABSTRACT

The *PSA-Cre;Pten-loxP/loxP* mouse prostate cancer model displays clearly defined stages of hyperplasia and cancer. Here, the initial stages of hyperplasia development are studied. Immunohistochemical staining showed that accumulated $pAkt^+$ hyperplastic cells overexpress luminal epithelial cell marker CK8, and progenitor cell markers CK19 and Sca-1, but not basal epithelial cell markers. By expression profiling we identified novel hyperplastic cell markers, including Tacstd2 and Clu. Further we showed that at young age prostates of targeted *Pten* knockout mice contained in the luminal epithelial cell layer single $pAkt^+$ cells, which overexpressed CK8, Sca-1, Tacstd2 and Clu; basal epithelial cells were always $pAkt^-$. Importantly, in the luminal epithelial cell layer of normal prostates we detected rare $Clu^+Tacstd2^+Sca\text{-}1^+$ progenitor cells. These novel cells are candidate tumor initiating cells in *Pten* knockout mice. Remarkably, all luminal epithelial cells in the proximal region of normal prostates were $Clu^+Tacstd2^+Sca\text{-}1^+$. However, in *PSA-Cre;Pten-loxP/loxP* mice, the proximal prostate does not contain hyperplastic foci. Small hyperplastic foci in prostates of *PSA-Cre;Pten-loxP/+* mice found at old age, showed complete *Pten* inactivation and a progenitor marker profile. Finally, we present a novel model of prostate development and renewal, including lineage-specific luminal epithelial progenitor cells. It is proposed that *Pten* deficiency induces a shift in the balance of differentiation to proliferation in these cells.

INTRODUCTION

Prostate cancer is the most common tumor in men in countries with a western lifestyle, and a major cause of cancer-related mortality [1]. Complete *PTEN* inactivation is found in ~20% of primary prostate tumors and in up to 60% of prostate cancer metastases [2]. Inactivation of one *PTEN* allele is even more common. High frequency of *PTEN* inactivation is found also in endometrium cancer and in glioblastoma [3]. Germ line mutations of *PTEN* are the cause of Cowden disease and Bannayan-Zonana syndrome, which are characterized by hamartomas and predisposition to breast and thyroid tumors [2, 3].

PTEN counteracts phosphoinositide-3-kinase (PI3K) signaling by balancing phosphatidylinositol (4,5)-phosphate (PIP2) and phosphatidylinositol (3,4,5)-phosphate (PIP3) levels in the cell [2-4]. PIP3 accumulation leads to phosphorylation of downstream targets, including AKT. As a consequence the activities of further downstream effectors are modulated and cell biological functions, including proliferation, apoptosis, cell size, polarity, metabolism, adhesion, migration and angiogenesis are changed [3-6]. Nuclear PTEN might play a role in maintaining genomic stability [7]. Moreover, it has recently been described that PTEN can control stem cell self-renewal [6, 8, 9].

Complete *Pten* inactivation in mice is embryonic lethal. *Pten+/-* mice are viable but develop several hyperplastic and dysplastic lesions in different organs [10, 11]. Conditional *Pten* knockout mouse models confirmed that *Pten* inactivation plays an important role in cancer development and tumor progression. Mice with prostate-specific *Pten* inactivation develop hyperplasia, mPIN and ultimately prostate cancer [12-15].

As first identified for hematopoietic cells, it is now generally accepted that all tissues contain rare tissue-specific stem cells that are capable of self-renewal and of differentiation through asymmetrical cell division [16, 17]. These cells are not only essential for organogenesis during development, but also for tissue renewal in the adult species. As clearly shown in different types of leukemia, tumors might develop by modification of hematopoietic stem cells or, alternatively, from multipotent or lineage-specific progenitor cells that have acquired stem cell-like characteristics [18]. Although less clear, the same mechanism has been proposed for the development of solid tumors, including prostate cancer. According to the stem cell model, each tumor contains a small number of cells with properties related to normal stem cells, that are essential for tumor maintenance [16, 19-21]. Complementary to the tumor stem cell theory, the clonal evolution model proposes that tumors can develop by expansion of dominant clones [22-24].

Study of tumor development in mouse prostate cancer models can be instrumental in understanding human prostate cancer. In the normal human and mouse prostate, stem cells and progenitor cells, or transit-amplifying cells, are proposed to be present in the basal epithelial

cell layer [21, 25-27]. In addition, in mice, the proximal region of the prostate has been indicated as a putative stem/progenitor cell niche [28-30]. So far, our knowledge of initial steps in tumor development in mouse models of prostate cancer is limited. In the *Probasin(PB)-Cre* induced *Pten* knockout model, *Pten* inactivation in a $p63^+$ stem/progenitor cell population in the basal epithelial cell layer has been postulated [31]. In a prostate-specific *Trp53/Rb* knockout model, luminal/neuroendocrine progenitor cells in the proximal prostate have been indicated as potential tumor initiating cells [32].

In the present study we investigated early steps in prostate tumor development in a different targeted *Pten* inactivation model, based on *PSA-Cre* expression. Previously, we described that in this model clearly defined stages of prostate hyperplasia and cancer can be discriminated [13]. Here we showed that hyperplastic cells in *Pten* knockout mice have a phenotype of luminal epithelial progenitor cells, including overexpression of CK8, CK19 and Sca-1. By expression profiling novel hyperplastic cell markers were identified. The first hyperplastic $pAkt^+$ cells in prostates of young *Pten* knockout mice were found in the luminal epithelial cell layer. Importantly, we also identified at low frequency novel lineage-specific progenitor cells in the luminal epithelial cell layer of normal prostates. Our findings indicate that *Pten* inactivation in this mouse model leads to accumulation of the novel identified luminal epithelial progenitor cells by a drastic change of the differentiation/proliferation balance of these cells. Although all cells in the luminal epithelial cell layer in the proximal prostate showed expression of the novel lineage-specific markers, hyperplastic foci did not develop from this region of the prostate.

RESULTS

Hyperplastic cells in prostates of *PSA-Cre;Pten-loxP/loxP* mice have a phenotype of luminal epithelial cells and express epithelial progenitor cell markers

Previously, we described prostate cancer development in *PSA-Cre;Pten-loxP/loxP* mice [13]. In prostates of 4-5 months (4-5m) old *PSA-Cre;Pten-loxP/loxP* mice hyperplastic epithelial cells overexpress Phospho-Akt (pAkt) and the luminal epithelial markers Cytokeratins 8/18 (CK8/18). Hyperplastic cells were negative for the basal epithelial markers Cytokeratins 5/14 (CK5/14). The androgen receptor (AR) was expressed at equal levels in normal and hyperplastic prostates [13].

In the present study we characterized by QPCR and immunohistochemistry hyperplastic prostate cells of *PSA-Cre;Pten-loxP/loxP* mice. First, the expression of additional progenitor, basal and luminal epithelial cell markers was analyzed at 2m and at 4-5m. At these ages prostates of *PSA-Cre;Pten-loxP/loxP* mice are for ~70% and >90% hyperplastic, respectively (Figure S1A). Expression of *Probasin* and *Nkx3.1*, markers of differentiated luminal cells, was much lower in hyperplastic prostates, but *CK8* was higher expressed in these tissues. Low expression of the

basal epithelial cell markers *CK5* and *p63* was detected. Interestingly, expression of the epithelial progenitor cell marker *CK19* [33, 34] was high in hyperplastic prostates. *Nkx3.1*, *CK8*, *CK19* and *p63* mRNA expression data were confirmed by immunohistochemistry of normal and hyperplastic prostates (4-5m) (Figure S1B-S1I). Nuclear Nkx3.1 staining was seen in luminal epithelial cells of normal prostates, but nuclei of hyperplastic cells were hardly positive (Figure S1B-S1C). A faint CK8 staining was observed at the apical side of luminal epithelial cells in normal prostates, whereas in hyperplastic prostates of *PSA-Cre;Pten-loxP/loxP* mice CK8 was overexpressed (Figure S1D-S1E). Importantly, CK19 was clearly higher expressed in hyperplastic cells than in normal prostate epithelial cells (Figure S1F-S1G). Hyperplastic cells were negative for the basal epithelial cell marker p63, but an apparent normal $p63^{+}$ basal epithelial cell layer was present below a multilayer of hyperplastic cells (Figure S1H-S1I). From these data we conclude that *Pten* inactivation in prostates of *PSA-Cre;Pten-loxP/loxP* mice results in the accumulation of hyperplastic cells with luminal progenitor cell characteristics ($Nkx3.1^{+/-}CK8^{+}CK19^{+}p63^{-}$).

Expression profiling identifies novel genes with high expression in hyperplastic prostate epithelium

Expression profiling was performed to identify novel genes differentially expressed in hyperplastic prostates of *PSA-Cre;Pten-loxP/loxP* mice (4-5m). Principal Component Analysis (PCA) and unsupervised hierarchical clustering (Figure 1A and 1B) of the cDNA array data showed a clear differential gene expression profile between hyperplastic prostates and normal prostates.

To identify genes preferentially expressed in hyperplastic prostate cells, differences in mean expression levels were calculated. The mouse progenitor/stem cell marker *Sca-1* was one of the top twenty genes with the highest expression in hyperplastic prostates (Figure 1C); *CK19* was in the top fifty differentially expressed genes (data not shown). Genes that showed high expression in hyperplastic prostates by calculation of differences in mean expression level (Figure 1C), like *Expi, Wfdc2, Tacstd2 (Trop2), Clu, Ppp1r1b*, *Sca-1* and *CK19*, were also found overexpressed by Significance Analysis of Microarray (SAM) (Figure 1D). Full names of the top twenty overexpressed genes are listed in Table S1. A more extensive list of all significantly upregulated or downregulated genes identified by SAM analysis is provided in Table S2. Note that *CK19* is in the top twenty of upregulated genes.

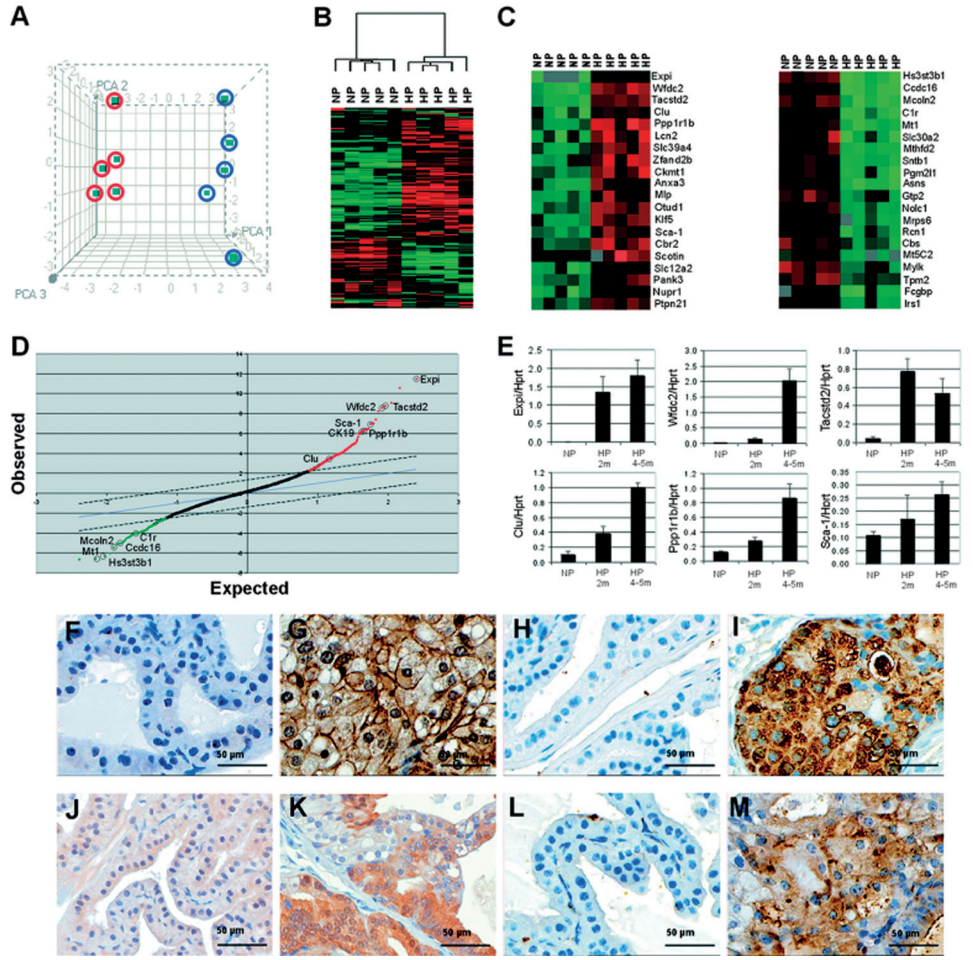

Figure 1. Identification of new hyperplastic cell markers in prostates of *PSA-Cre;Pten-loxP/loxP* mice. (**A**) Principal component analysis (PCA) of gene expression in normal prostates (blue circles) and hyperplastic prostates of *PSA-Cre;Pten-loxP/loxP* mice (red circles) at 4-5m. (**B**) Unsupervised hierarchical clustering of the gene expression profiles of five normal prostates (NP) and five hyperplastic prostates (HP). Green indicates lower gene expression and red indicates higher expression. (**C**) The twenty genes with the largest differential expression in HP as compared to NP as determined by calculation of the difference in mean expression level. (**D**) Significance Analysis of Microarrays (SAM) of the same samples as shown in C. Note that by SAM analysis essentially identical genes were identified as by calculation of the difference in mean expression level. (**E**) QPCR analysis of the five genes with the highest expression in HP as compared to NP and of *Sca-1*. Each subgroup was composed of five prostate samples. The expression levels in hyperplastic prostates of 2m and 4-5m old mice and in prostates of control littermates are shown as average expression level +/- SE relative to *Hprt* expression. (F-M) Immunohistochemical analysis of new hyperplastic cell markers in NP and HP of *PSA-Cre;Pten-loxP/loxP* mice (4-5m). (**F**) Tacstd2 NP, (**G**) Tacstd2 HP, (**H**) Clu NP, (**I**) Clu HP, (**J**) Ppp1r1b NP, (**K**) Ppp1r1b HP, (**L**) Sca-1 NP and (**M**) Sca-1 HP.

The expression profiles of the five genes with the highest overexpression in hyperplastic prostates of targeted *Pten* knockout mice, *Expi, Wfdc2, Tacstd2, Clu* and *Ppp1r1b* (Figure 1C), and of *Sca-1*, were verified by QPCR in prostates of *Pten* knockout mice and in normal prostates at 2m and at 4-5m (Figure 1E). QPCR showed that the expression of *Expi* and *Tacstd2* in *PSA-Cre;Pten-loxP/loxP* mice was already high at 2m; *Clu* and *Sca-1* showed a gradually increasing expression level. However, for *Wfdc2* and *Ppp1r1b* the sharpest raise in expression was observed in completely hyperplastic prostates (4-5m).

Next, expression of markers for which appropriate antibodies were available, Tacstd2, Clu, Ppp1r1b and Sca-1, was studied by immunohistochemistry in normal and hyperplastic prostates (Figure 1F-1M). Tacstd2 immunohistochemistry showed membrane staining in hyperplastic tissues, in agreement with its known location as a transmembrane protein [35]. Clu was mainly present in the cytoplasm of hyperplastic cells. As predicted from the QPCR data, the expression pattern of Ppp1r1b in hyperplastic cells was more heterogeneous. In agreement with the CK19 staining (Figure S1), Sca-1 staining indicated that hyperplastic cells have a progenitor cell phenotype.

Genes with lower expression in hyperplastic prostates of *PSA-Cre;Pten-loxP/loxP* mice were also identified both by calculation of the difference in mean expression level and by SAM (Figure 1C and 1D). The expression profiles of genes with the lowest expression in hyperplastic prostates, *Hs3st3b1, Ccdc16, Mcoln2, C1r* and *Mt1* (Figure 1C), were confirmed by QPCR (Figure S2). Expression of all genes was already low in hyperplastic prostates at 2m in *PSA-Cre;Pten-loxP/loxP* mice.

Initial pAkt$^+$ hyperplastic cells in the luminal epithelial cell layer in prostates of *PSA-Cre;Pten-loxP/loxP* mice express Clu, Tacstd2 and Sca-1

To collect information of candidate tumor initiating cells, we examined in detail the early development of hyperplasia in prostates of *PSA-Cre;Pten-loxP/loxP* mice, which starts at 4-5 weeks (4-5w). Prostates of wild type mice at 4-5w were half the size of those of adult mice (2m and 4-5m) (Figure 2A). In contrast to prostate weights of older mice (2m and 4-5m), prostate weights of young *PSA-Cre;Pten-loxP/loxP* mice (4-5w) were not different from control littermates (Figure 2A). At 4-5m the prostate weights of *PSA-Cre;Pten-loxP/loxP* mice were ~3-fold higher than those of controls, caused by the increased number and size of hyperplastic cells.

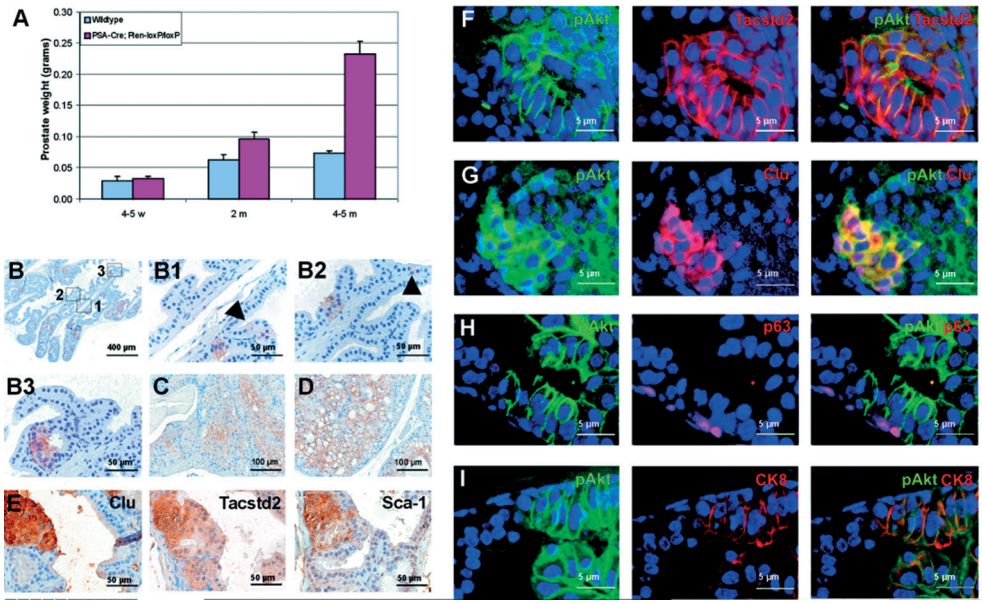

Figure 2. Single pAkt+ luminal epithelial cells in prostates of young *PSA-Cre;Pten-loxP/loxP* mice (4-5w) are Clu$^+$Tacstd2$^+$Sca-1$^+$. (**A**) Prostate weights (average +/- SE) of wild type mice and *PSA-Cre;Pten-loxP/loxP* mice at 4-5w, 2m and 4-5m. (**B**) pAkt staining of hyperplastic foci/cells in the luminal epithelial cell layer of a prostate of a 4-5w old *PSA-Cre;Pten-loxP/loxP* mouse. Magnifications of three indicated regions are shown in B1, B2 and B3. Arrow heads in B1 and B2 indicate single pAkt$^+$ cells. Phospho-Akt staining of prostates of 2m (**C**) and 4-5m (**D**) old *PSA-Cre;Pten-loxP/loxP* mice shows that respectively ~70% and 100% of the luminal epithelial cells were pAkt$^+$. (**E**) Consecutive slides of a prostate of a 4-5w old *PSA-Cre;Pten-loxP/loxP* mouse stained for Clu, Tacstd2 and Sca-1 shows coexpression of these markers in a small hyperplastic focus. Immunofluorescent double stainings confirmed co-localization of (**F**) Tacstd2 and pAkt, (**G**) Clu and pAkt and (**I**) CK8 and pAkt. (**H**) pAkt$^+$ cells were not observed in the p63$^+$ basal epithelial cell layer.

Phospho-Akt expression was used as marker of *Pten* inactivation to visualize the first Pten negative cells. At 4-5w, scattered throughout all prostate lobes, single pAkt$^+$ hyperplastic cells and small pAkt$^+$ foci were detected (Figure 2B). Importantly, all pAkt$^+$ cells were exclusively present in the luminal epithelial cell layer and not in the basal epithelial cell layer. At 2m and at 4-5m ~70% and almost 100% of the luminal epithelial cells showed pAkt membrane staining, respectively (Figure 2C and 2D). Basal epithelial cells remained pAkt negative. Sca-1 and the new hyperplastic cell markers Clu and Tacstd2 were also expressed in the initial hyperplastic foci (Figure 2E), but Ppp1r1b expression could not yet be detected in hyperplastic cells at 4-5w (data not shown).

To allow accurate characterization of initial hyperplastic pAkt$^+$ cells, immunofluorescent double staining was carried out (Figure 2F-2I). Importantly, all pAkt$^+$ cells showed expression of Clu and Tacstd2. Moreover, all pAkt$^+$ cells overexpressed CK8 and were negative for the basal

epithelial cell marker p63. This finding strongly suggests that the first pAkt$^+$ cells, which were exclusively observed in the luminal epithelial layer, are identical to the majority of accumulating hyperplastic cells with an epithelial progenitor cell phenotype at 4-5m.

PSA-Cre;Pten-loxP/+ mice develop hyperplastic foci with the same marker profile as hyperplastic foci in prostates of *PSA-Cre;Pten-loxP/loxP* mice

Previously, we reported that heterozygous *PSA-Cre;Pten-loxP/+* mice do not develop prostate tumors, but that they can develop hyperplastic foci at older age [13]. The availability of novel hyperplastic cell markers allowed a more accurate study of hyperplasia development in these mice. Clu staining of prostates of *PSA-Cre;Pten-loxP/+* mice showed that already at 4-5m a few small hyperplastic foci could be detected (Figure S3). At 7-8m the number of hyperplastic foci was still very low, but a clear increase of hyperplastic foci was detected in older mice (>11m). Clu$^+$ hyperplastic foci were not observed in prostates of control littermates (data not shown).

Interestingly, like in prostates of young *PSA-Cre;Pten-loxP/loxP* mice hyperplastic Clu$^+$ foci of *PSA-Cre;Pten-loxP/+* mice (Figure 3A) showed pAkt overexpression (Figure 3B). In line with this observation Pten staining was negative in these foci (data not shown), indicating that the second *Pten* allele was inactivated in the pAkt$^+$ hyperplastic cells. Hyperplastic cells in *PSA-Cre;Pten-loxP/+* mice were also Tacstd2 and Sca-1 positive (Figure 3C and 3D). So, hyperplastic cells in prostates of *PSA-Cre;Pten-loxP/+* mice had an identical expression profile as hyperplastic foci in young *PSA-Cre;Pten-loxP/loxP* mice.

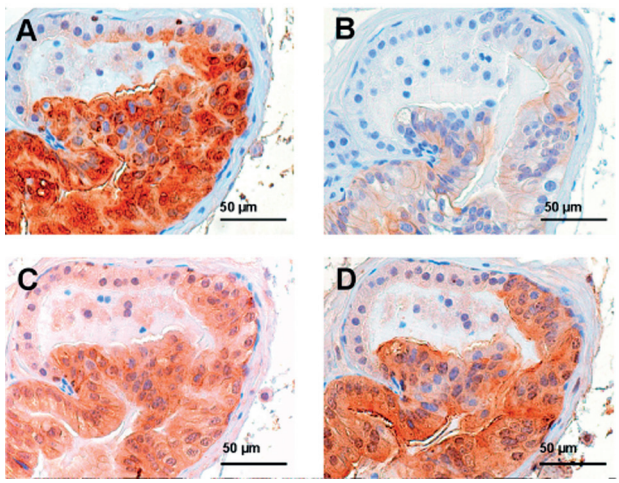

Figure 3. Hyperplastic cells in prostates of *PSA-Cre;Pten-loxP/+* mice and *PSA-Cre;Pten-loxP/loxP* mice express identical markers. Consecutive sections of a hyperplastic focus in the prostate of a *PSA-Cre;Pten-loxP/+* mouse were stained for (**B**) pAkt and the hyperplastic cell markers (**A**) Clu, (**C**) Tacstd2 and (**D**) Sca-1 by immunohistochemistry.

Single Clu$^+$Tacstd2$^+$Sca-1$^+$ epithelial progenitor cells are present in the luminal epithelial cell layer of normal prostates

Next, we investigated whether hyperplastic cell markers were expressed in normal prostates at different ages. Interestingly, at 4-5w single Clu$^+$Tacstd2$^+$Sca-1$^+$ cells were detected in the luminal epithelial cell layer of normal prostates (Figure 4A-4C). Some basal epithelial cells stained positive for Tacstd2 and Sca-1, however, Clu$^+$ cells were never observed in the basal epithelial layer. The presence of Clu$^+$Tacstd2$^+$Sca-1$^+$ cells in the luminal epithelial cell layer of normal mouse prostates suggests that these cells are previously not yet identified lineage-specific progenitor cells of the luminal epithelial cells. It is tempting to speculate that in *Pten* knockout mice hyperplastic prostate cells with similar characteristics as these progenitor cells originate from these cells. This hypothesis is in line with the observation that pAkt$^+$ hyperplastic cells were exclusively found in the luminal epithelial cell layer (Figure 2B, 2H, and 2I).

To estimate the frequency of Clu$^+$Tacstd2$^+$Sca-1$^+$ epithelial progenitor cells at different ages, prostates from developing (4-5w) and from adult (4-5m) mice were stained for Clu expression. At 4-5w 1/250, and at 4-5m 1/25.000 luminal epithelial cells were Clu$^+$, respectively (Figure 4A and 4D), indicating that in developing prostates the number of lineage-specific progenitor cells is much higher than in fully mature prostates. The presence of Clu$^+$Tacstd2$^+$Sca-1$^+$ luminal progenitor cells in normal adult prostates makes these cells candidates from which hyperplastic foci develop in *PSA-Cre;Pten-loxP/+* mice, due to inactivation of the second *Pten* allele.

Clu$^+$Tacstd2$^+$ luminal epithelial progenitor cells in young normal prostates (4-5w) were further characterized by co-localization studies. pAkt overexpression in Clu$^+$Tacstd2$^+$ cells in the luminal epithelial cell layer of normal prostates was never observed (Figure 4E-4F). However, like hyperplastic cells in *PSA-Cre;Pten-loxP/loxP* mice, Clu$^+$Tacstd2$^+$ cells in the luminal epithelial cell layer of normal prostates overexpressed CK8 (Figure 4G-4H). Clu$^+$ cells were exclusively found in the luminal epithelial cell layer, whereas Tacstd2$^+$ cells were present in both the luminal and the basal epithelial cell layer (Figure 4G-4J, and Figure S4). Recently, high expression of Tacstd2 has been identified in basal epithelial cells of the proximal prostate, but not in basal epithelial cells in the more distal prostate [36].

Hyperplastic foci do not develop from epithelial cells in the proximal prostate

The proximal region of the mouse prostate has been proposed as a stem/progenitor cell niche [28-30]. A schematic view of the proximal and distal parts of a mouse prostate lobe is shown in Figure 5A. We studied the properties of the epithelial cells in the proximal prostate in more detail in *PSA-Cre;Pten-loxP/loxP* mice and in normal littermates.

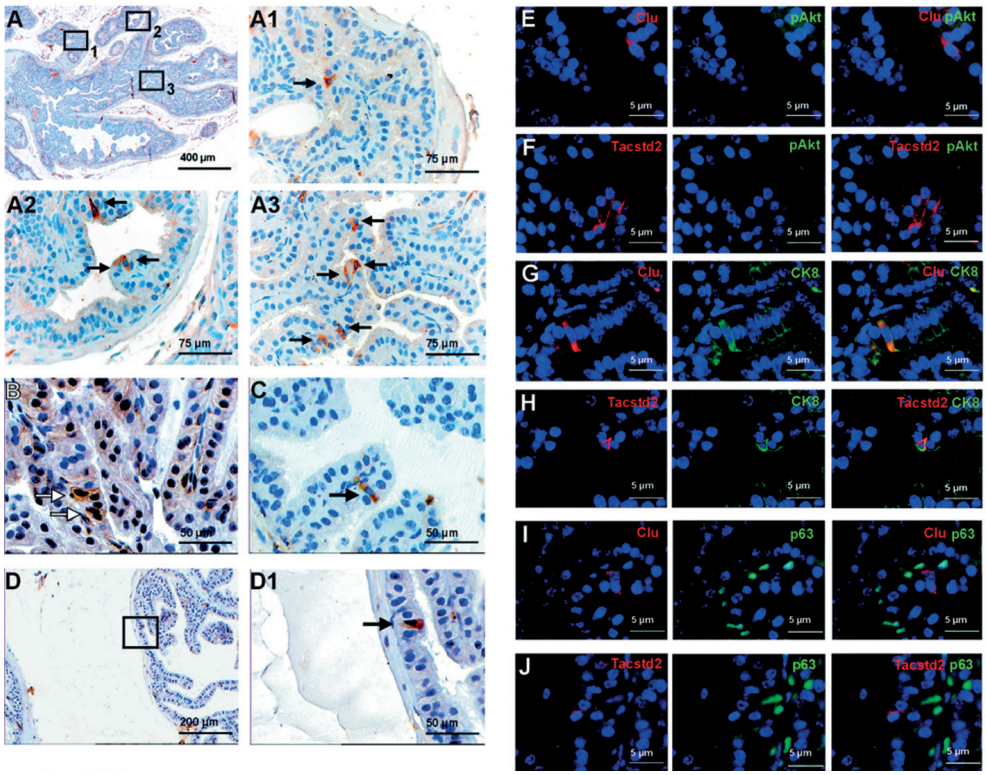

Figure 4. Single Clu$^+$Tacstd2$^+$Sca-1$^+$ cells are present in the luminal epithelial cell layer of the normal prostate. (**A**) Clu staining of a normal prostate of a 4-5w old mouse. Scattered throughout the prostate lobe, single Clu$^+$ cells in the luminal epithelial cell layer were observed. An overview of a whole prostate lobe and higher magnifications of three indicated regions are shown. Arrows indicate positive cells. (**B**) Tacstd2$^+$ and (**C**) Sca-1$^+$ cells in the luminal epithelial cell layer of the developing prostate (4-5w). (**D**) Clu staining of an adult normal prostate (4-5m) showed rare Clu$^+$ cells in the luminal epithelial cell layer. (D1) Higher magnification of the indicated region in (D). (**E-J**) Immunofluorescent double staining of Clu$^+$ and Tacstd2$^+$ cells in the luminal epithelial cell layer of the normal prostate. In normal prostates Clu$^+$ and Tacstd2$^+$ cells were negative for pAkt (**E,F**), overexpressed CK8 (**G,H**) and did not express p63 (**I,J**).

As visualized in longitudinal sections of normal prostate lobes, luminal epithelial cells in the proximal prostate are more compact with less cytoplasm than luminal cells in distal parts of the prostate (Figure 5B). Like in the distal prostate, in the proximal prostate a p63$^+$ basal epithelial cell layer was present below the luminal epithelial cells (Figure 5C). Interestingly, all luminal epithelial cells in the proximal prostate overexpressed CK8 (Figure 5D), like observed in rare lineage-specific luminal progenitor cells in the distal prostate and in hyperplastic cells in *PSA-*

Cre;Pten-loxP/loxP mice. Sca-1 was also high expressed in proximal cells (Figure 5E), confirming that luminal epithelial cells in the proximal prostate have a luminal progenitor phenotype. As indicated by the interrupted line (Figure 5C-5E), there is an abrupt transition from epithelial cells with proximal characteristics to cells with properties of more distal luminal epithelial cells.

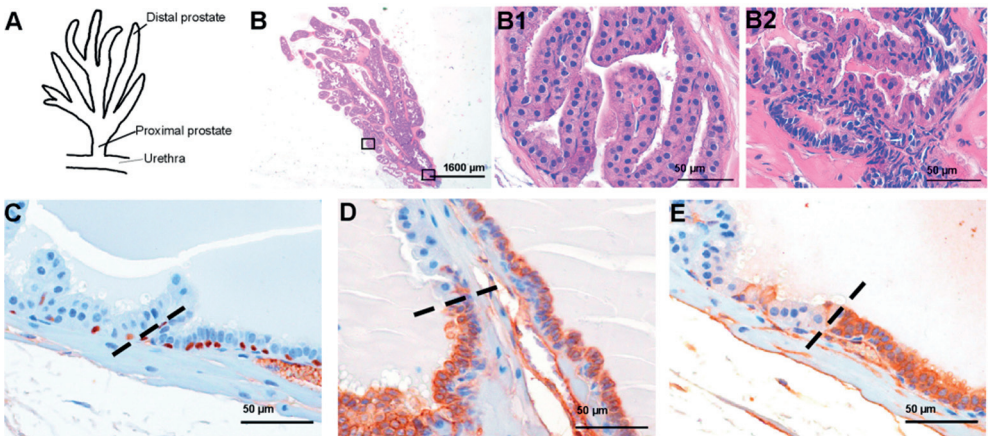

Figure 5. All luminal epithelial cells in the proximal prostate express luminal epithelial progenitor cell markers. (**A**) Schematic picture of a mouse prostate lobe indicating the urethra, the proximal and the distal prostate region. (**B**) Heamatoxylin eosin staining of a longitudinal positioned mouse prostate lobe. Magnifications of the distal (B1) and the proximal (B2) prostate, as indicated in B, showed a difference in morphology of the luminal epithelial cells in the proximal and the distal prostate. (**C-E**) Immunohistochemical analysis of luminal epithelial cells in the proximal region of a normal mouse prostate. (**C**) p63; (**D**) CK8 and (**E**) Sca-1 staining. Dashed lines indicate the abrupt transition of epithelium of the proximal to the distal prostate.

Next, expression profiling of proximal and distal regions of normal adult prostates was performed (Figure 6A). Strikingly, *Ppp1r1b*, *Clu*, *Wfdc2* and *Tacstd2* were among the genes with the highest expression in the proximal prostate. Expression array data were confirmed by QPCR (Figure 6B). As described above, these markers were also overexpressed in accumulated hyperplastic prostate cells of *PSA-Cre;Pten-loxP/loxP* mice (Figure 1) and in rare luminal progenitor cells in the distal prostate (Figure 4). Immunohistochemistry showed high Clu, Tacstd2 and Ppp1r1b expression in the luminal epithelial cells of the proximal prostate (Figure 6C-6E). The cDNA array data confirmed high expression of the luminal progenitor cell markers CK8 and Sca-1 in the proximal prostate (data not shown). In conclusion, a correlation was detected between the marker profile in hyperplastic prostates of *PSA-Cre;Pten-loxP/loxP* mice, rare lineage-specific progenitor cells in the distal prostate and the proximal luminal epithelial cells.

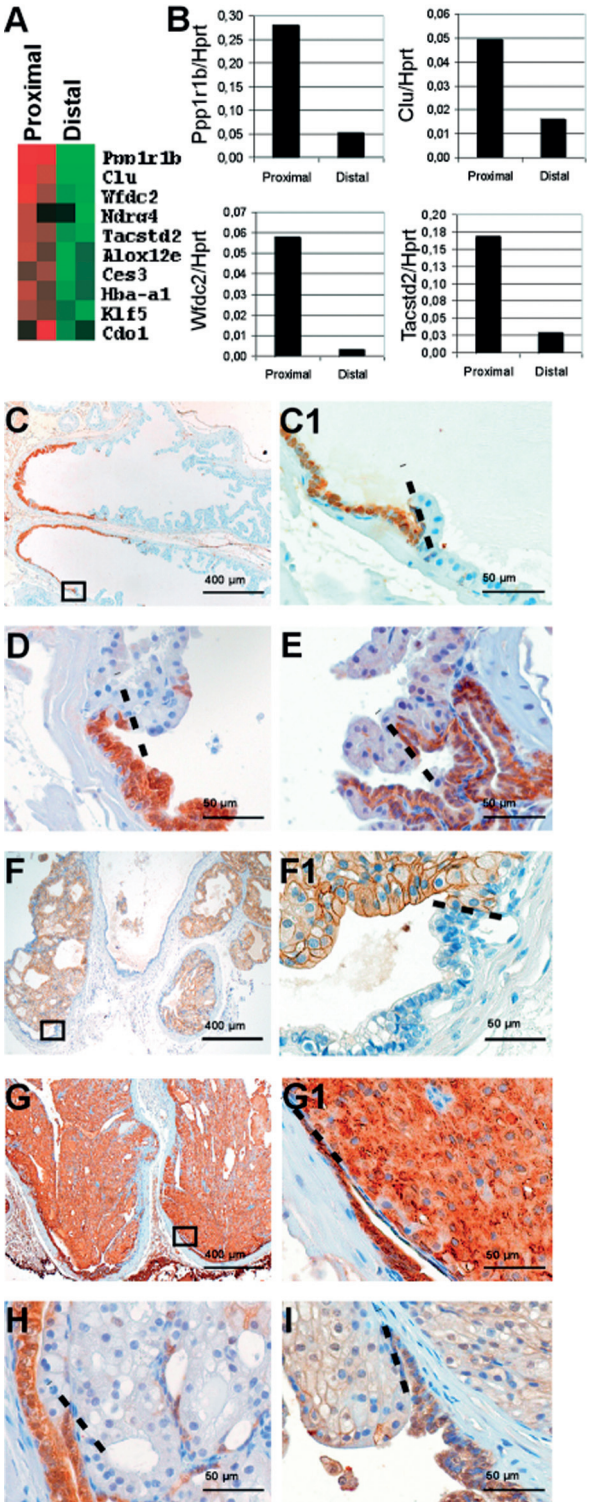

Figure 6. Hyperplastic prostates of *PSA-Cre;Pten-loxP/loxP* mice and luminal epithelial cells in the proximal prostate overexpress identical genes. (**A**) Expression profiling of the proximal and distal prostate region of a normal mouse prostate (4-5m) shows that genes high expressed in hyperplastic prostates of *PSA-Cre;Pten-loxP/loxP* mice are among the ten genes with the highest expression in two proximal prostates as compared to two distal prostates. (**B**) QPCR analysis of hyperplasia markers with high expression in the proximal prostate. (**C-E**) Immunohistochemical analysis confirms high expression of hyperplastic cell markers in the luminal epithelial cell layer of the proximal region of the normal prostate. (**C**) Clu staining of a normal prostate lobe, (C1) magnification of the transition of the proximal to the distal region as indicated in C. Staining for (**D**) Ppp1r1b and (**E**) Tacstd2. Hyperplasia development did not occur in the proximal prostate of *PSA-Cre;Pten-loxP/loxP* mice (4-5m). Proximal luminal epithelial cells of the hyperplastic prostates were negative for pAkt (**F**, magnification of transition proximal/distal prostate in F1), although these cells overexpressed (**G**, **G1**) Clu, (**H**) Ppp1r1b and (**I**) Tacstd2.

We investigated in *PSA-Cre;Pten-loxP/loxP* mice (4-5m) whether hyperplastic foci developed from luminal epithelial cells in the proximal prostate. Longitudinal sections of prostates showed that, although the distal prostate was completely hyperplastic, the epithelium in the proximal prostate was unaffected (Figure 6F-6I). Immunohistochemistry showed that, in contrast to the distal prostate, pAkt was not overexpressed in the proximal prostate (Figure 6F), indicating that *Pten* is not inactivated in this region of the prostate.

Further, we determined the marker profile of epithelial cells in urethral epithelium adjacent to the proximal prostate. In the superficial differentiated layer of the urothelium, the umbrella cells, high CK8 expression was observed. The highest expression of p63, Clu, Tacstd2, and Sca-1 was found in the intermediate/basal epithelial cell layers (Figure S5). The urethra data extend the prostate expression data indicating that Clu, Tacstd2 and Sca-1 show high expression in less differentiated epithelium.

DISCUSSION

In this study we defined the early stages of hyperplasia development in the *PSA-Cre;Pten-loxP/loxP* mouse prostate cancer model. Important aspects of early hyperplasia development and normal prostate development were sequentially addressed. We showed that: (i) Accumulating hyperplastic pAkt$^+$ cells in prostates of *PSA-Cre;Pten-loxP/loxP* mice have a luminal epithelial cell phenotype with expression of known and novel identified markers of epithelial progenitor cells. (ii) The earliest single pAkt$^+$ (Pten$^-$) hyperplastic cells in the prostates of young targeted *Pten* knockout mice are exclusively present in the luminal epithelial cell layer. (iii) At low frequency, in the normal prostate, similar cells, but without pAkt overexpression, could be identified. (iv) Our data indicate further that *Pten* inactivation inhibits differentiation of luminal epithelial progenitor cells to mature cells. (v) We observed that the luminal epithelial cell layer of the proximal prostate is composed of cells that express the same markers as rare progenitor cells in more distal prostate regions. However, hyperplastic foci did not develop from the proximal prostate. (vi) Finally, we showed that at older age *PSA-Cre;Pten-loxP/+* mice developed in the prostate pAkt$^+$ hyperplastic foci with an identical marker profile as in young *PSA-Cre;Pten-loxP/loxP* mice.

Our data accumulate into a hierarchical model of prostate renewal in which we define novel Clu$^+$Tacstd2$^+$Sca-1$^+$ lineage-specific progenitor cells in the luminal epithelial layer of the normal prostate (Figure 7). According to previous findings, prostate stem/multi-potent progenitor cells are situated in the basal epithelial cell layer [21, 25-27]. This cell layer might also contain lineage-specific progenitor cells of the basal epithelial cells. CK19 and Sca-1 positive cells are present both in the luminal and basal epithelial cell layer of the prostate [33, 34], but the expression of

other epithelial cell markers differs in these cell populations. In contrast to previous papers on tumor initiating cells in mouse prostate cancer models [31, 32], our data show that lineage-specific progenitor cells in the luminal epithelial cell layer can function as candidate tumor initiating cells.

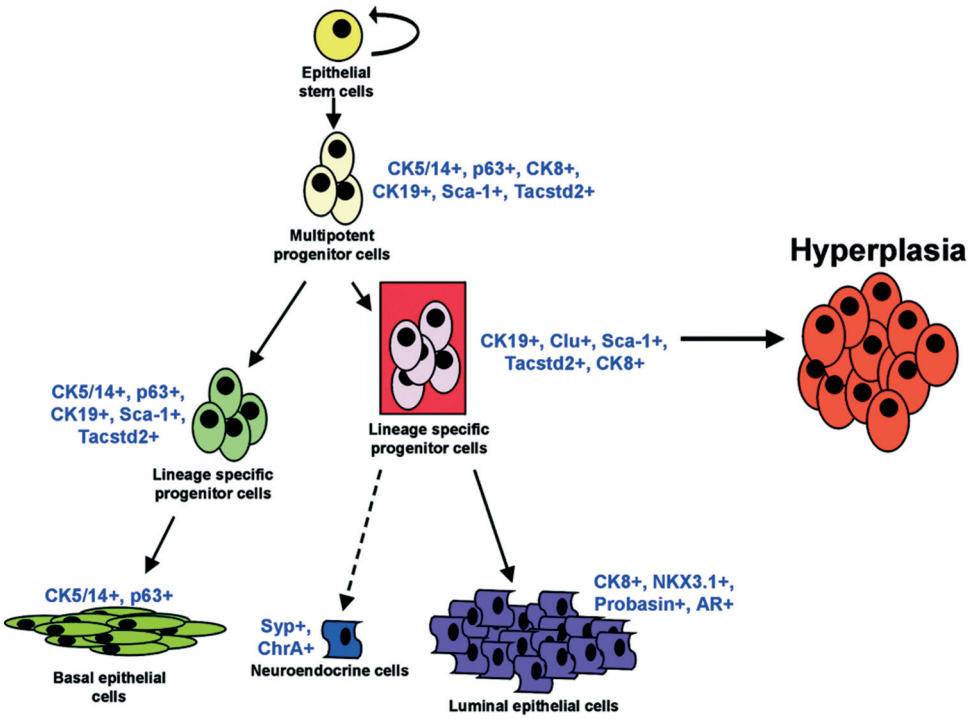

Figure 7. Model for hyperplasia development in *PSA-Cre;Pten-loxP/loxP* mice. The model shows novel identified lineage-specific luminal epithelial progenitor cells in the luminal epithelial cell layer as candidate tumor initiating cells in the prostate cancer mouse model, as indicated by a red background.

It is well-established that complete *Pten* inactivation in *Pten-/-* mice is embryonic lethal. These mice die at embryonic days 7-9, indicative for an important role of Pten in development. *Pten+/-* mice are viable, but develop during aging several tumor types, mostly T-cell lymphomas [10, 11]. During recent years, several mouse prostate cancer models based on *Pten* inactivation have been generated. In essentially all models, mice with prostate-specific *Pten* inactivation showed development of hyperplasia, mPIN lesions and ultimately prostate cancer [12-15]. Prostate hyperplasia in *Pten* knockout mice is characterized by cell enlargement, in line with the properties of Pten as regulator of cell size and protein synthesis [6, 37]. Accumulation of enlarged hyperplastic cells is unique for *Pten* inactivation in the prostate, and has not been seen in mouse prostate cancer models based on different genetic alterations [38-43].

Most studies in targeted *Pten* knockout prostate cancer models use mice with *Pten* inactivation by *PB-Cre* [14, 15, 31]. These mice develop hyperplasia early during prostate development, rapidly progressing to invasive tumors, accompanied by metastases [15, 31]. In our *Pten* knockout prostate cancer model, the PSA promoter is used to inactivate *Pten*. Previously, the PSA promoter has been proven to target transgene expression to the luminal epithelial cells [44]. In contrast to PB-targeted mouse models, PSA-driven *Pten* inactivation induces clearly separate stages of hyperplasia and cancer progression at a slow rate [13]. This makes this model suitable to study the first altered cells.

Although hyperplastic Pten negative cells express AR [13], they are blocked in differentiation to mature cells, as deduced from the low expression of *Nkx3.1* and *Probasin* (Figure S1). So far, a role of Pten in differentiation of prostate luminal epithelial cells was unknown. Available data on the effect of *Pten* on differentiation in other systems is incomplete and conflicting. *Pten* deficiency was shown to stimulate neural stem cell proliferation without affecting differentiation [45, 46]. Mice with *Pten* inactivation in osteoblasts showed enhanced differentiation [47]. Based on the stimulation of cell proliferation by *PTEN* deficiency in many systems, it might be assumed that *Pten* inactivation stimulates proliferation of the accumulating progenitor cells, however, a high proliferation rate might also be an intrinsic property of these cells [13].

None of the genes with clear differential expression in hyperplastic prostates compared to normal prostates (Figure 1 and Figure S1) could be directly correlated to Pten signaling. Expression of known FOXO targets, one of the best studied downstream effectors of pAkt, were not clearly detected amongst the differentially expressed genes in hyperplastic prostates [48]. So, the differentially expressed genes are markers of the cell population enriched in hyperplastic prostates, indirectly induced by *Pten* inactivation.

The gene expression profile of the hyperplastic prostate presented in this study showed overlap with the gene expression profiles of prostate tumors of *PB-Cre;Pten-loxP/loxP* mice [15] and tumors from *PSA-Cre;Pten-loxP/loxP* mice (H. Korsten, unpublished). Out of the 50 genes with the highest expression in prostate tumors of *PB-Cre;Pten* knockout mice, 22 genes were present on our expression arrays. Almost all these genes showed higher expression in hyperplastic prostates of *PSA-Cre;Pten-loxP/loxP* mice. Five genes, *Expi, Clu, Anxa3, Tacstd2* and *Cbr2*, were among the top 20 genes with the highest expression in hyperplastic prostates (Figure 1C). Overexpression of genes in both hyperplasia and tumor indicates that altered expression of these specific genes is not sufficient for development of invasive tumors. A limited number of genes, including *Col3a1*, seems preferentially overexpressed in tumors [15]. These genes are candidate prostate tumor markers.

An important issue addressed in this study concerns the properties of the first altered cells. We scanned thoroughly prostates at 4-5w for cells overexpressing pAkt, as very sensitive marker for *Pten* inactivation. We never observed $pAkt^+$ cells in the basal epithelial cell layer, although

in the luminal epithelial cell layer single pAkt$^+$ cells and small foci of pAkt$^+$ cells were easily detected. High expression of hyperplasia markers Clu, Tacstd2 and Sca-1 was also found in the first hyperplastic cells in the luminal epithelial cell layer at 4–5w. Importantly, the Clu$^+$Tacstd2$^+$Sca-1$^+$ cells, which also overexpress CK8, are at low frequency detectable in the luminal epithelial cell layer of normal prostates. Hence, we propose that these lineage-specific progenitor cells, as first identified in this study, are the target cells for *Pten* inactivation in the prostate cancer model (Figure 7). This would be in line with the properties of the PSA promoter/enhancer used to drive *Cre* expression, which is active in luminal epithelial cells of the mouse prostate [44] and in the more differentiated luminal epithelial cells in the human prostate. Our data indicate expansion of a rather homogeneous hyperplastic progenitor cell population induced by *Pten* inactivation as the first step in tumorigenesis. Follow-up studies, including orthotopic transplantation of hyperplastic cells in syngenic mice with a homogeneous genetic background should reveal further information on the mechanism of tumor development.

The newly identified lineage-specific Clu$^+$Tacstd2$^+$Sca-1$^+$ progenitor cells in the luminal epithelial cell layer share characteristics with late luminal transient-amplifying/intermediate cells (CK8$^+$CK19$^+$CK5/14$^-$) described earlier [33, 34, 49, 50]. Early transient-amplifying/intermediate cells co-express basal epithelial cell and luminal epithelial cell markers, whereas the more differentiated transient-amplifying/intermediate cells in the luminal epithelial cell layer are negative for basal epithelial cell markers [33, 34]. It was postulated that cell of origin for prostate cancer is an early transient-amplifying/intermediate cell in the basal epithelial cell layer [49, 50]. Now, we show that cells with characteristics of late transient-amplifying/intermediate cells in the luminal epithelial cell layer can also function as tumor initiating cells in prostate cancer (Figure 7).

Our findings are substantially different from the *PB-Cre;Pten* knockout mouse model [31]. In these mice it was proposed that *Pten* inactivation in stem/multipotent progenitor cells in the basal epithelial cell layer is the initial event in prostate tumor development. In contrast to the *PSA-Cre;Pten* knockout mouse model, in this model proliferation of p63$^+$ basal epithelial cells was observed. Hence, the modified *Probasin* promoter seems already active in early multipotent progenitor cells, whereas the *PSA* promoter/enhancer is active in lineage-specific luminal progenitor cells (Figure 7). Although comparison with human prostate cancer has its limitations, it should be noted that human prostate tumors do not show an increase in p63$^+$ cells. In fact, negative staining for p63 is considered as indication of prostate cancer [51].

Although preliminary data are available [30, 52-54], further identification and characterization of candidate prostate stem cells and different types of progenitor cells is essential for unraveling prostate development and tumor initiation in mouse models. In normal mouse prostates a Sca-1$^+$Integrinα6$^+$ (CD49f) enriched cell population in the basal epithelial cell layer was reported to possess stem cell characteristics [36, 54]. Preliminary QPCR analysis of hyperplastic prostates of *PSA-Cre;Pten-loxP/loxP* mice indicated that integrina6 (*CD49f*) mRNA expression was not

substantially altered (H. Korsten, unpublished). However, we did find higher expression in hyperplastic prostates of the cell surface marker *integrin*a*2 (CD49a)* (H. Korsten, unpublished), known to be overexpressed in human and possibly in mouse prostate stem/progenitor cells [30, 55, 56]. Recently, another stem cell population was defined by a Sca-1$^+$CD133$^+$CD44$^+$CD117$^+$ phenotype [30]. Sca-1, CD44 and CD117 are expressed in both basal as luminal epithelial progenitor cells, whereas CD133 is exclusively expressed in basal epithelial cells [30, 57]. QPCR analysis showed a lowered CD133 expression in prostates of *PSA-Cre;Pten-loxP/loxP* mice, whereas the expression of Sca-1, CD44 and CD117 was increased (H. Korsten, unpublished). These data suggest that the CD49f$^+$ and the Sca-1$^+$CD133$^+$CD44$^+$CD117$^+$ cells share more characteristics with multipotent progenitor cells than with the lineage-specific luminal progenitor cells identified in this study (Figure 7). The latter findings can form the basis for further isolation and functional characterization of hyperplastic cells from prostates of *PSA-Cre;Pten-loxP/loxP* mice, and of luminal epithelial progenitor cells from the more distal region of the normal prostate.

The proximal region of the prostate has been proposed as a stem/progenitor cell niche [28-30]. As shown here, the more compact Sca-1$^+$ cells in the luminal epithelial cell layer in the proximal prostate express many markers of hyperplastic prostate cells and of progenitors of luminal epithelial cells in the more distal prostate (Figure 5 and 6). High expression of *integrinα2 (CD49a)* and *CD44* was observed in the proximal prostate (H. Korsten, unpublished) [30].

Despite a similar gene expression profile, hyperplasia in *Pten* knockout mice did not develop from luminal epithelial cells in the proximal prostate. In contrast to the distal cells, we did not observe pAkt overexpression in the proximal cells, suggesting that *Pten* is not inactivated in the proximal prostate. At present, it is unknown whether this is due to low Cre expression or limited susceptibility of the *Pten* locus to recombination in this specific part of the prostate. Alternatively, *Pten* is inactivated, but PI3K/PTEN signaling in these cells is not induced. It should be noted that in *PB-Cre;Trp53/Rb* knockout mice tumors arise from the proximal prostate, indicating that proximal cells can function as tumor initiating cells in cancer models [32].

Recently, fusions between genes encoding ETS transcription factors and genes encoding prostate-specific genes, mostly *TMPRSS2-ERG*, have been reported as most frequent genetic alteration in early stages of human prostate cancer [58]. Interestingly, *Tmprss2* expression is induced late during mouse prostate development [59]. We also found a fusion between the *KLK2* gene and the ETS gene *ETV4* in clinical prostate cancer [60]. *KLK2* is highly homologous to the *PSA (KLK3)* gene used in our mouse prostate cancer model for *Cre* expression. Although it is unknown in which cell type the gene fusions occur, because of the high prostate-specificity of most genes that are coupled to ETS genes it is tempting to speculate that the genetic alterations occur and/or become manifest in progenitors of luminal epithelial cells and not in tissue stem cells or multipotent progenitor cells. These findings clearly indicate the high importance of identification of progenitor cells of luminal epithelial cells in the human prostate and further characterization of the mouse progenitors.

MATERIALS AND METHODS

Generation of Prostate Targeted Pten Knockout Mice

The generation of *PSA-Cre* mice (strain FVB), mice carrying the *Pten-loxP* allele (strain 129Ola), and bi-allelic and mono-allelic prostate *Pten* knockout mice have been described previously [13, 61]. Mice were housed according to guidelines of the Erasmus Medical Center, and procedures were carried out in compliance with standards for use of laboratory animals. Animal experiments performed in this manuscript have been approved by the animal experimental committee of the Erasmus Medical Center (DEC-consult).

RNA extraction, cDNA preparation and QPCR analysis

RNA was isolated from frozen mouse prostates using the Qiagen RNeasy RNA extraction Kit (Qiagen, Hilden, Germany) according to the manufacturer's guidelines, including an on column DNAseI digestion. RNA quality was checked by agarose gel electrophoresis. For RNA extraction from normal and hyperplastic prostates at 2m and 4-5m a pool of prostate lobes of one mouse was used. Pools of prostates from five mice were used for each RNA sample from proximal and distal prostate regions of control littermates (4-5m).

The methods for cDNA preparation and QPCR analysis were described previously [60]. Primer sequences are given in Table S3. The expression level of target genes was determined relative to the endogenous reference *Hypoxanthine-guanine Phosphoribosyltransferase (Hprt).*

Immunohistochemistry and Immunofluorescent double staining

Tissues were fixed in buffered 4% formalin for ~16h at room temperature, dehydrated, embedded in paraffin and sections were cut at 4 mm. Antibodies used for immunohistochemistry and immunofluorescence are listed in Table S4. The Nkx3.1 antibody was a kind gift from Dr. Cory Abate-Shen. Microwave treatment was applied for antigen retrieval by boiling in 10 mM sodium citrate (pH 6.0) for 15 min. For CK19 staining, tissue sections were pepsine (0.5%) treated for 30 min at 37°C. Primary antibodies incubation was overnight at 4°C. For immunohistochemistry, tissue sections were incubated with biotin labeled secondary antibody for 1h at room temperature. Immunoreactivity was visualized by streptavidin-peroxidase incubation (HK320-UK, 1:50, BioGenex, San Ramon, CA). For immunofluorescent pAkt, CK8 and p63 staining, tissue sections were incubated with FITC/TRITC labeled secondary antibodies (Table S4). The signals for Clu and Tacstd2 were visualized by incubation with Rabbit Anti-Goat biotin followed by Streptavidin-TRITC. Anti-fading fluorescent mounting medium (H-1000, Vector laboratories, Burlingame, CA) containing DAPI (1:2000, Sigma Chemical, St.Louis, MO) was used to cover the slide. Immunofluorescent stained slides were analyzed with a DMRXA microscope (Leica, Wetzlar, Germany).

To estimate the number of progenitor cells in the luminal epithelial cell layer of normal prostates at 4-5w and at 4-5m, slices of the mouse anterior lobe were stained for Clu. By counting the total cell number and the number of Clu^+ cells in a prostate lobe, an estimation of the frequency of Clu^+ cells could be made.

cDNA microarray hybridization and analysis

The cDNA microarrays were hybridized and normalized as described previously [62, 63]. The common reference, a mixture of RNAs isolated from mouse adult testis and prostate, was in all experiments Cy5-labeled. The cDNA microarrays were manufactured at the Central Microarray Facility at the Netherlands Cancer Institute (NKI, Amsterdam, The Netherlands) and contained 16,416 spots.

Principal component analysis was performed using the Spotfire software package (Spotfire, Inc., Sommerville, MA; spotfire decision site V8.1). For unsupervised hierarchical clustering and visualization of differentially expressed genes the programs Cluster and Treeview were used [64]. After setting criteria for unsupervised hierarchical clustering of normal and hyperplastic prostates (100% signal and at least 2 observations of |0.8|) 528 genes were selected. Within Treeview, the image contrast and mask value settings were 1.5 and 0.2 respectively for all figures.

The difference in mean mRNA expression level of a gene was calculated by substracting the log2 transformed average expression level in normal prostates from the average expression level in hyperplastic prostates. Genes were ranked based on gene expression level difference. Figure 1 shows the mean expression level differences of known genes, which gave a signal in at least two experiments in one group. In addition, by performing Significance Analysis of Microarrays (SAM) (Version 1.21) [65] gene expression levels differences relative to the standard deviation of these expression levels within one group was calculated. By SAM genes with an at least 2 fold change in ratio were identified. The q-value (false discovery rate) for genes identified by SAM analysis was 0.15%.

Microarray data have been submitted to the ArrayExpress public database (Accession E-MEXP-2029).

ACKNOWLEDGMENTS

The authors thank Cory Abate-Shen for providing the Nkx3.1 antibody.

REFERENCES

1. Jemal, A., et al., *Cancer statistics, 2008.* CA Cancer J Clin, 2008. **58**(2): p. 71-96.
2. Majumder, P.K. and W.R. Sellers, *Akt-regulated pathways in prostate cancer.* Oncogene, 2005. **24**(50): p. 7465-74.
3. Salmena, L., A. Carracedo, and P.P. Pandolfi, *Tenets of PTEN tumor suppression.* Cell, 2008. **133**(3): p. 403-14.
4. Leslie, N.R. and C.P. Downes, *PTEN function: how normal cells control it and tumour cells lose it.* Biochem J, 2004. **382**(Pt 1): p. 1-11.
5. Hamada, K., et al., *The PTEN/PI3K pathway governs normal vascular development and tumor angiogenesis.* Genes Dev, 2005. **19**(17): p. 2054-65.
6. Stiles, B., et al., *PTENless means more.* Dev Biol, 2004. **273**(2): p. 175-84.
7. Shen, W.H., et al., *Essential role for nuclear PTEN in maintaining chromosomal integrity.* Cell, 2007. **128**(1): p. 157-70.
8. Akala, O.O. and M.F. Clarke, *Hematopoietic stem cell self-renewal.* Curr Opin Genet Dev, 2006.
9. Rossi, D.J. and I.L. Weissman, *Pten, tumorigenesis, and stem cell self-renewal.* Cell, 2006. **125**(2): p. 229-31.
10. Di Cristofano, A., et al., *Pten is essential for embryonic development and tumour suppression.* Nat Genet, 1998. **19**(4): p. 348-55.
11. Suzuki, A., et al., *High cancer susceptibility and embryonic lethality associated with mutation of the PTEN tumor suppressor gene in mice.* Curr Biol, 1998. **8**(21): p. 1169-78.
12. Backman, S.A., et al., *Early onset of neoplasia in the prostate and skin of mice with tissue-specific deletion of Pten.* Proc Natl Acad Sci U S A, 2004. **101**(6): p. 1725-30.
13. Ma, X., et al., *Targeted biallelic inactivation of Pten in the mouse prostate leads to prostate cancer accompanied by increased epithelial cell proliferation but not by reduced apoptosis.* Cancer Res, 2005. **65**(13): p. 5730-9.
14. Trotman, L.C., et al., *Pten dose dictates cancer progression in the prostate.* PLoS Biol, 2003. **1**(3): p. E59.
15. Wang, S., et al., *Prostate-specific deletion of the murine Pten tumor suppressor gene leads to metastatic prostate cancer.* Cancer Cell, 2003. **4**(3): p. 209-21.
16. Rossi, D.J., C.H. Jamieson, and I.L. Weissman, *Stems cells and the pathways to aging and cancer.* Cell, 2008. **132**(4): p. 681-96.
17. Orkin, S.H. and L.I. Zon, *Hematopoiesis: an evolving paradigm for stem cell biology.* Cell, 2008. **132**(4): p. 631-44.
18. Wang, J.C. and J.E. Dick, *Cancer stem cells: lessons from leukemia.* Trends Cell Biol, 2005. **15**(9): p. 494-501.
19. Ailles, L.E. and I.L. Weissman, *Cancer stem cells in solid tumors.* Curr Opin Biotechnol, 2007. **18**(5): p. 460-6.
20. Reya, T., et al., *Stem cells, cancer, and cancer stem cells.* Nature, 2001. **414**(6859): p. 105-11.
21. Lam, J.S. and R.E. Reiter, *Stem cells in prostate and prostate cancer development.* Urol Oncol, 2006. **24**(2): p. 131-40.
22. Campbell, L.L. and K. Polyak, *Breast tumor heterogeneity: cancer stem cells or clonal evolution?* Cell Cycle, 2007. **6**(19): p. 2332-8.
23. Adams, J.M. and A. Strasser, *Is tumor growth sustained by rare cancer stem cells or dominant clones?* Cancer Res, 2008. **68**(11): p. 4018-21.
24. Visvader, J.E. and G.J. Lindeman, *Cancer stem cells in solid tumours: accumulating evidence and unresolved questions.* Nat Rev Cancer, 2008. **8**(10): p. 755-68.
25. English, H.F., R.J. Santen, and J.T. Isaacs, *Response of glandular versus basal rat ventral prostatic epithelial cells to androgen withdrawal and replacement.* Prostate, 1987. **11**(3): p. 229-42.

26. Collins, A.T. and N.J. Maitland, *Prostate cancer stem cells.* Eur J Cancer, 2006. **42**(9): p. 1213-8.
27. Lawson, D.A. and O.N. Witte, *Stem cells in prostate cancer initiation and progression.* J Clin Invest, 2007. **117**(8): p. 2044-50.
28. Burger, P.E., et al., *Sca-1 expression identifies stem cells in the proximal region of prostatic ducts with high capacity to reconstitute prostatic tissue.* Proc Natl Acad Sci U S A, 2005. **102**(20): p. 7180-5.
29. Tsujimura, A., et al., *Proximal location of mouse prostate epithelial stem cells: a model of prostatic homeostasis.* J Cell Biol, 2002. **157**(7): p. 1257-65.
30. Leong, K.G., et al., *Generation of a prostate from a single adult stem cell.* Nature, 2008. **456**(7223): p. 804-8.
31. Wang, S., et al., *Pten deletion leads to the expansion of a prostatic stem/progenitor cell subpopulation and tumor initiation.* Proc Natl Acad Sci U S A, 2006. **103**(5): p. 1480-5.
32. Zhou, Z., A. Flesken-Nikitin, and A.Y. Nikitin, *Prostate cancer associated with p53 and Rb deficiency arises from the stem/progenitor cell-enriched proximal region of prostatic ducts.* Cancer Res, 2007. **6**7(12): p. 5683-90.
33. Hudson, D.L., et al., *Epithelial cell differentiation pathways in the human prostate: identification of intermediate phenotypes by keratin expression.* J Histochem Cytochem, 2001. **49**(2): p. 271-8.
34. Wang, Y., et al., *Cell differentiation lineage in the prostate.* Differentiation, 2001. **68**(4-5): p. 270-9.
35. Fornaro, M., et al., *Cloning of the gene encoding Trop-2, a cell-surface glycoprotein expressed by human carcinomas.* Int J Cancer, 1995. **62**(5): p. 610-8.
36. Goldstein, A.S., et al., *Trop2 identifies a subpopulation of murine and human prostate basal cells with stem cell characteristics.* Proc Natl Acad Sci U S A, 2008. **105**(52): p. 20882-7.
37. Backman, S., V. Stambolic, and T. Mak, *PTEN function in mammalian cell size regulation.* Curr Opin Neurobiol, 2002. **12**(5): p. 516-22.
38. Ellwood-Yen, K., et al., *Myc-driven murine prostate cancer shares molecular features with human prostate tumors.* Cancer Cell, 2003. **4**(3): p. 223-38.
39. Greenberg, N.M., et al., *Prostate cancer in a transgenic mouse.* Proc Natl Acad Sci U S A, 1995. **92**(8): p. 3439-43.
40. Han, G., et al., *Mutation of the androgen receptor causes oncogenic transformation of the prostate.* Proc Natl Acad Sci U S A, 2005. **102**(4): p. 1151-6.
41. Kim, M.J., et al., *Nkx3.1 mutant mice recapitulate early stages of prostate carcinogenesis.* Cancer Res, 2002. **62**(11): p. 2999-3004.
42. Maddison, L.A., et al., *Conditional deletion of Rb causes early stage prostate cancer.* Cancer Res, 2004. **64**(17): p. 6018-25.
43. Acevedo, V.D., et al., *Inducible FGFR-1 activation leads to irreversible prostate adenocarcinoma and an epithelial-to-mesenchymal transition.* Cancer Cell, 2007. **12**(6): p. 559-71.
44. Cleutjens, K.B., et al., *A 6-kb promoter fragment mimics in transgenic mice the prostate-specific and androgen-regulated expression of the endogenous prostate-specific antigen gene in humans.* Mol Endocrinol, 1997. **11**(9): p. 1256-65.
45. Groszer, M., et al., *PTEN negatively regulates neural stem cell self-renewal by modulating G0-G1 cell cycle entry.* Proc Natl Acad Sci U S A, 2006. **103**(1): p. 111-6.
46. Groszer, M., et al., *Negative regulation of neural stem/progenitor cell proliferation by the Pten tumor suppressor gene in vivo.* Science, 2001. **294**(5549): p. 2186-9.
47. Liu, X., et al., *Lifelong accumulation of bone in mice lacking Pten in osteoblasts.* Proc Natl Acad Sci U S A, 2007. **104**(7): p. 2259-64.
48. Modur, V., et al., *FOXO proteins regulate tumor necrosis factor-related apoptosis inducing ligand expression. Implications for PTEN mutation in prostate cancer.* J Biol Chem, 2002. **277**(49): p. 47928-37.
49. Rizzo, S., G. Attard, and D.L. Hudson, *Prostate epithelial stem cells.* Cell Prolif, 2005. **38**(6): p. 363-74.
50. Litvinov, I.V., A.M. De Marzo, and J.T. Isaacs, *Is the Achilles' heel for prostate cancer therapy a gain of function in androgen receptor signaling?* J Clin Endocrinol Metab, 2003. **88**(7): p. 2972-82.

51. Parsons, J.K., et al., *p63 protein expression is rare in prostate adenocarcinoma: implications for cancer diagnosis and carcinogenesis.* Urology, 2001. **58**(4): p. 619-24.
52. Xin, L., D.A. Lawson, and O.N. Witte, *The Sca-1 cell surface marker enriches for a prostate-regenerating cell subpopulation that can initiate prostate tumorigenesis.* Proc Natl Acad Sci U S A, 2005. **102**(19): p. 6942-7.
53. Xin, L., et al., *Self-renewal and multilineage differentiation in vitro from murine prostate stem cells.* Stem Cells, 2007. **25**(11): p. 2760-9.
54. Lawson, D.A., et al., *Isolation and functional characterization of murine prostate stem cells.* Proc Natl Acad Sci U S A, 2007. **104**(1): p. 181-6.
55. Collins, A.T., et al., *Prospective identification of tumorigenic prostate cancer stem cells.* Cancer Res, 2005. **65**(23): p. 10946-51.
56. Patrawala, L., et al., *Hierarchical organization of prostate cancer cells in xenograft tumors: the CD44+alpha2beta1+ cell population is enriched in tumor-initiating cells.* Cancer Res, 2007. **67**(14): p. 6796-805.
57. Richardson, G.D., et al., *CD133, a novel marker for human prostatic epithelial stem cells.* J Cell Sci, 2004. **117**(Pt 16): p. 3539-45.
58. Kumar-Sinha, C., S.A. Tomlins, and A.M. Chinnaiyan, *Recurrent gene fusions in prostate cancer.* Nat Rev Cancer, 2008. **8**(7): p. 497-511.
59. Hermans, K.G., et al., *Truncated ETV1, fused to novel tissue-specific genes, and full-length ETV1 in prostate cancer.* Cancer Res, 2008. **68**(18): p. 7541-9.
60. Hermans, K.G., et al., *Two unique novel prostate-specific and androgen-regulated fusion partners of ETV4 in prostate cancer.* Cancer Res, 2008. **68**(9): p. 3094-8.
61. Marino, S., et al., *PTEN is essential for cell migration but not for fate determination and tumourigenesis in the cerebellum.* Development, 2002. **129**(14): p. 3513-22.
62. Baugh, L.R., et al., *Quantitative analysis of mRNA amplification by in vitro transcription.* Nucleic Acids Res, 2001. **29**(5): p. E29.
63. Hendriksen, P.J., et al., *Evolution of the androgen receptor pathway during progression of prostate cancer.* Cancer Res, 2006. **66**(10): p. 5012-20.
64. Eisen, M.B., et al., *Cluster analysis and display of genome-wide expression patterns.* Proc Natl Acad Sci U S A, 1998. **95**(25): p. 14863-8.
65. Tusher, V.G., R. Tibshirani, and G. Chu, *Significance analysis of microarrays applied to the ionizing radiation response.* Proc Natl Acad Sci U S A, 2001. **98**(9): p. 5116-21.

Supplementary information

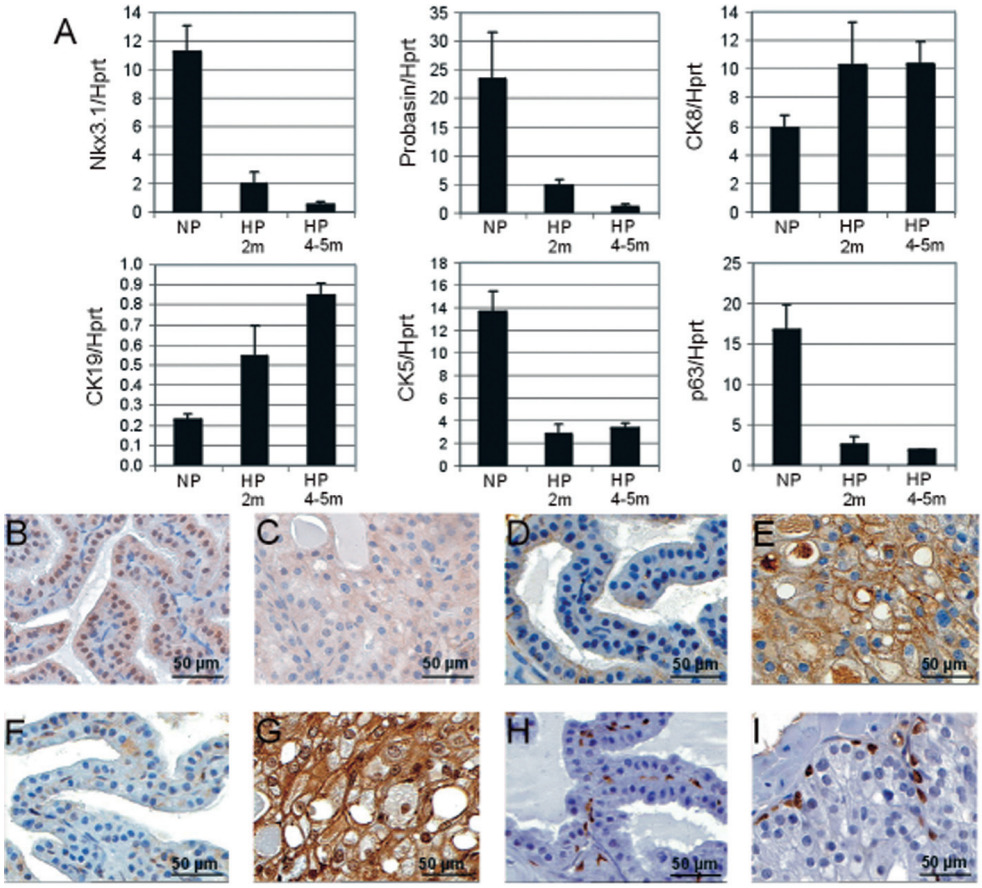

Figure S1. Hyperplastic prostate cells of *PSA-Cre;Pten-loxP/loxP* mice have an epithelial progenitor cell phenotype. (**A**) QPCR analysis of epithelial cell marker expression in hyperplastic prostates at 2m and 4-5m. Per group the gene expression in 5 prostate samples was measured. The expression levels are shown as average expression levels +/- SE relative to Hprt expression. NP: normal prostate, HP: hyperplastic prostate. (B-I) Immunohistochemical analysis of epithelial cell markers in the mouse anterior lobe of normal and hyperplastic prostates at 4-5m. (**B**) Nkx3.1 NP, (**C**) Nkx3.1 HP, (**D**) CK8 NP, (**E**) CK8 HP, (**F**) CK19 NP, (**G**) CK19 HP, (**H**) P63 NP and (**I**) P63 HP.

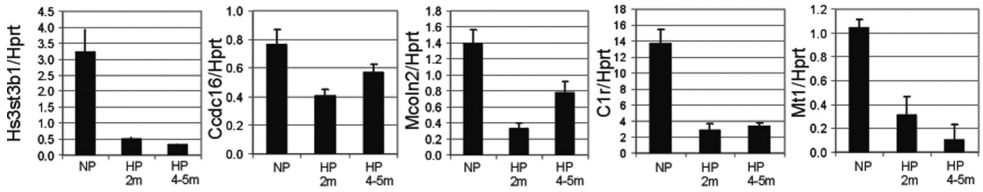

Figure S2. QPCR analysis of the five genes with the lowest expression in hyperplastic prostates (4-5m) as determined by calculation of the mean expression level difference (See Figure 1C). Each group was composed of five prostate samples. The expression levels in 2m and 4-5m old hyperplastic prostates are shown as average expression level +/- SE relative to *Hprt* expression.

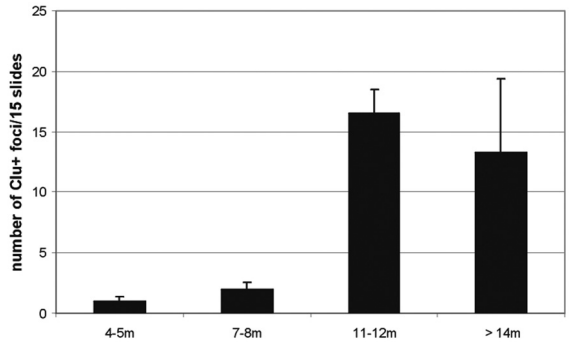

Figure S3. At older age (>11m) the number of Clu+ hyperplastic foci increased in prostates of *PSA-Cre;Pten-loxP/+* mice. Clu+ hyperplastic foci were counted in fifteen consecutive slides of a longitudinal embedded anterior prostate lobe. At each time point the prostates of three mice were analyzed.

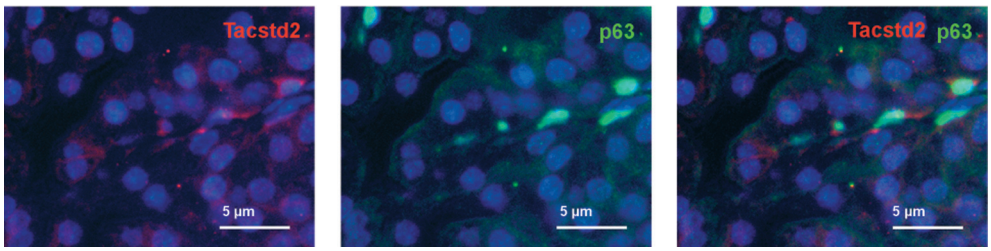

Figure S4. Rare Tacstd2+ cells in the P63+ basal epithelial cell layer of a normal mouse prostate (4-5w).

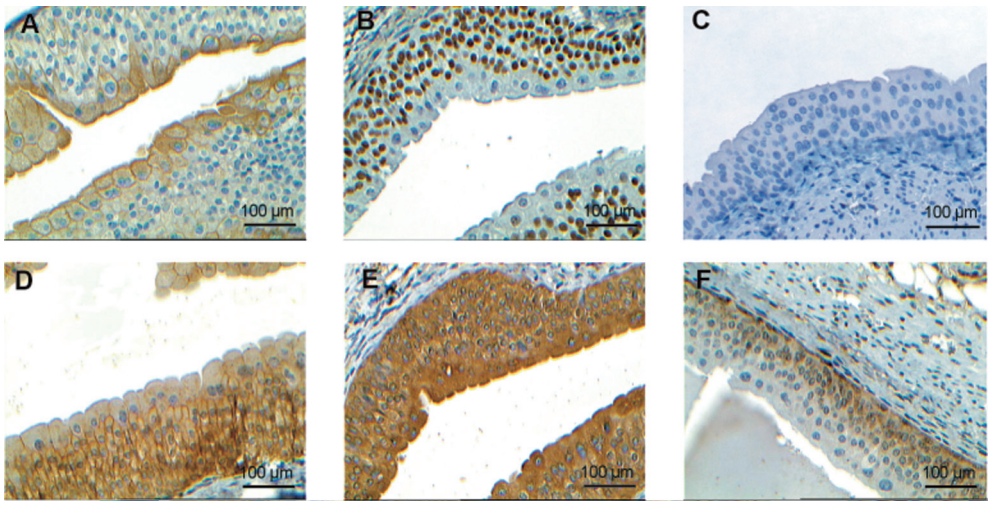

Supplement Figure 5. Immunohistochemical analysis of epithelial cell markers and hyperplastic cells markers in urethra of wild type mice. (**A**) CK8, (**B**) P63, (**C**) Ppp1r1b, (**D**) Tactsd2, (**E**) Clu and (**F**) Sca-1.

Table S1. Full names of genes overexpressed in hyperplastic prostates of *PSA-Cre;Pten-loxP/loxP* mice.

Abbreviation	Gene Name
Expi	Extracellular proteinase inhibitor
Wfdc2	WAP four-disulfide core domain 2
Tacstd2	Tumour-associated calcium signal transducer 2
Clu	Clusterin
Ppp1r1b	Protein phosphatase 1, regulatory (inhibitor) subunit 1B
Lcn2	Lipocalin 2
Slc39a4	Solute carrier family 39 (zinc transporter), member 4
Zfand2b	Zinc finger, AN1 type domain2B
Ckmt1	Creatine kinase, mitochondrial 1, ubiquitous
Anxa3	Annexin 3
Mlp	Marcks-like protein
Otud1	OUT domain containing 1
Klf5	Kruppel-like factor 5
Ly6a	Lymphocyte antigen 6 complex, locus A
Cbr2	Carbonyl reductase 2
Scotin	Scotin
Slc12a2	Solute carrier family 12, member 2
Pank3	Pantothenate kinase 3
Nupr1	Nuclear protein 1
Ptpn21	Protein tyrosine phosphatase, non-receptor type 21

Table S2. Significantly differentially expressed genes in hyperplastic prostates of *PSA-Cre;Pten-loxP/loxP* mice as assayed by SAM analysis.

Significant upregulated genes				
Accesion Code	**Unigene Number**	**Gene Name**	**Score(d)**	**Fold Change**
BG071358	Mm.1650	Expi	11.47	22,35956
BG071688	Mm.250165	Mamdc1	10.57	8,98338
BG066797	Mm.154045	Tacstd2	8.77	8,23533
BG072238	Mm.27289	Wfdc2	8.58	10,00670
BG065849	Mm.5574	Slc22a19	7.41	5,48686
BG071114	Mm.20675	Otud1	7.02	5,50665
BG070865	Mm.259645	Pank3	6.96	4,69510
BG072793	Mm.8180	Sca-1	6.91	5,19812
BG064167	Mm.2769	Mlp	6.46	5,54302
BG070413	Mm.7612	Ltf	6.41	3,49584
BG065106	Mm.2769	Mlp	6.38	5,46968
BG071309	Mm.28497	Ppp1r1b	6.25	8,09515
BG069030	Mm.4420	Ptpn21	6.23	4,40579
BG066823	Mm.970	Ckmt1	6.19	6,15851
BG064706	Mm.1012	CK19	6.15	3,65135
BG076188	Mm.29483	Slc39a4	6.00	6,18341
BG069863	Mm.154660	Plat	5.99	3,80224
BG065118	Mm.90587	Eno1	5.68	3,90298
BG070839	Mm.7214	Anxa3	5.45	5,33097
BG069367	Mm.32646	Zfand2b	5.25	6,17232
BG074576	Mm.4168	Slc12a2	5.12	4,41512
BG074344	Mm.17510	Msln	5.03	11,64736
BG065116	Mm.90587	Eno1	5.01	3,25239
BG071514	Mm.235090	Tcfcp2l1	4.97	3,20175
BG072403	Mm.250158	Rnf11	4.89	3,77734
BG067864	Mm.29587	LOC227616	4.87	3,63909
BG076074	Mm.18814	Baiap2l1	4.86	3,64365
BG071705	Mm.30262	Klf5	4.76	5,24630
BG074971	Mm.24510	Slc12a7	4.74	2,86031
BG068045	Mm.38441	Galnt3	4.66	2,78278
BG067918	Mm.903	Btg2	4.62	4,18896
BG067532	Mm.1662	Fxyd3	4.60	2,82506
BG064389	Mm.30010	Arpc1b	4.60	2,69594
BG074458	Mm.234242	Dhcr24	4.57	3,24006
BG064659	Mm.23575	Gprc5a	4.52	3,17411

Table S2. (*Continued)*

Significant upregulated genes				
Accesion Code	**Unigene Number**	**Gene Name**	**Score(d)**	**Fold Change**
BG067693	Mm.25613	Ier3	4.47	2,94791
BG075912	Mm.206505	Timp2	4.47	3,13271
BG071245	Mm.21454	Cbr2	4.38	4,97431
BG068068	Mm.27365	Fat1	4.37	2,34774
BG067727	Mm.28518	Tnfrsf12a	4.37	3,73157
BG073464	Mm.28986	Sqrdl	4.35	2,46512
BG075943	Mm.219635	Ptplad1	4.34	3,28708
BG063173	Mm.23961	Actn1	4.33	2,76328
BG067375	Mm.23939	Tpo1	4.21	2,30059
BG074770	Mm.195800	Rgnef	4.19	2,76110
BG071322	Mm.21454	Cbr2	4.18	3,85257
BG069628	Mm.12246	Ier5	4.14	3,10972
BG064378	Mm.24745	Bzw2	4.11	2,44005
BG072100	Mm.9772	Chdh	4.10	2,69430
BG071742	Mm.22547	Asah1	4.10	2,11695
BG075635	Mm.29619	Gga2	4.09	2,10064
BG070491	Mm.100144	S100a6	4.08	2,19837
BG069386	Mm.11662	Slco4c1	4.07	2,34379
BG069616	Mm.70573	Pde2a	4.04	2,29157
BG065926	Mm.35523	Adnp	4.03	2,64795
BG069516	Mm.41401	Slc6a8	4.02	2,24963
BG071387	Mm.30239	Slc39a8	4.01	4,46718
BG065159	Mm.200936	Sh2b3	3.98	2,38959
BG075302	Mm.135092	Slc4a7	3.96	3,04537
BG064186	Mm.28954	Arhu	3.95	2,44913
BG069782	Mm.4426	Cd63	3.94	2,10084
BG071171	Mm.282	Gsto1	3.93	3,45906
BG072122	Mm.18814	Baiap2l1	3.93	3,08255
BG072291	Mm.205601	Cttn	3.92	2,15382
BG064085	Mm.3963	Elf3	3.92	2,66938
BG063081	Mm.3532	Tmsb10	3.91	4,27950
BG072110	Mm.18742	Nupr1	3.90	3,96276
BG066817	Mm.154725	Ppapdc1	3.89	4,23496
BG065384	Mm.30017	Gabarapl2	3.88	2,36392
BG065470	Mm.101062	Ctnnb1	3.85	2,40472
BG063612	Mm.21203	Zfp265	3.84	2,52583
BG064050	Mm.6800	CK8	3.81	2,74686

Table S2. (*Continued)*

Significant upregulated genes				
Accesion Code	**Unigene Number**	**Gene Name**	**Score(d)**	**Fold Change**
BG065103	Mm.788	Sca-2	3.81	2,92747
BG063271	Mm.44552	Txnrd1	3.79	2,04798
BG073255	Mm.28484	Tspan3	3.79	2,31680
BG073025	Mm.222584	Pygb	3.77	2,47069
BG071200	Mm.95879	Jarid1a	3.76	2,31542
BG069505	Mm.4168	Slc12a2	3.75	3,93525
BG064087	Mm.25161	Sirt2	3.73	2,17960
BG068640	Mm.11935	Fbxo34	3.72	2,44193
BG064070	Mm.183102	Actr3	3.71	2,01388
BG070640	Mm.26223	Hace1	3.71	2,41787
BG070089	Mm.4259	Tacstd1	3.70	2,23965
BG066212	Mm.34497	Ltb4dh	3.69	2,94193
BG074931	Mm.4303	Ezh2	3.66	2,26496
BG071031	Mm.4825	Mmp7	3.66	2,67935
BG072281	Mm.7286	Ctbp1	3.65	2,84219
BG074474	Mm.31672	Cdk6	3.65	2,64506
BG064176	Mm.4554	Lgals3	3.63	2,58095
BG069726	Mm.4168	Slc12a2	3.63	3,16789
BG073116	Mm.29524	Clic2	3.62	2,69005
BG075859	Mm.73682	Tmepai	3.61	2,66887
BG072707	Mm.2734	Sat	3.61	2,84646
BG070245	Mm.4168	Slc12a2	3.61	3,58739
BG063000	Mm.30060	Avpi1	3.59	2,56568
BG074494	Mm.22119	Fcgr3	3.59	2,29876
BG075383	Mm.27790	Sfrs2ip	3.58	2,22605
BG072209	Mm.200608	Clu	3.57	5,76677
BG074542	Mm.196533	Scotin	3.55	5,28095
BG072254	Mm.1377	Tgfbr2	3.55	2,47781
BG072077	Mm.22248	Igfbp4	3.54	2,94279
BG063426	Mm.30142	CK7	3.54	2,26024
BG063109	Mm.21117	Itgb4	3.54	2,20503
BG075666	Mm.8155	Tgif	3.52	2,48134
BG063729	Mm.5289	Gapd	3.50	2,57073
BG070289	Mm.448	Cyba	3.50	4,07125
BG069415	Mm.1519	Ald	3.50	2,15556
BG069211	Mm.3204	Fdft1	3.49	2,03582
BG063090	Mm.30108	Actr2	3.49	2,17786

Table S2. (*Continued)*

Significant upregulated genes				
Accesion Code	**Unigene Number**	**Gene Name**	**Score(d)**	**Fold Change**
BG070902	Mm.18742	Nupr1	3.47	3,44853
BG074463	Mm.38450	Septin9	3.46	2,03440
BG072109	Mm.390590	Cntnap3	3.46	2,64455
BG070106	Mm.9537	Lcn2	3.45	6,09852
BG064639	Mm.259329	Cd2ap	3.45	2,31525
BG072676	Mm.24808	Fxyd6	3.43	2,86438
BG063567	Mm.14860	Anxa1	3.43	2,19141
BG069483	Mm.205010	Adipor1	3.43	2,27557
BG066697	Mm.1775	Hn1	3.41	2,44874
BG074171	Mm.133872	Stfa1	3.41	2,43656
BG074532	Mm.2159	Bnip3	3.39	2,22193
BG065385	Mm.22192	Slc31a1	3.38	2,49869
BG065686	Mm.1359	uPar	3.37	2,12928
BG067214	Mm.34268	Cdc42ep5	3.36	2,03345
BG068207	Mm.11827	Comtd1	3.36	2,26367
BG076240	Mm.28814	Casp6	3.34	2,16681
BG065049	Mm.2423	Col2a1	3.34	2,98133
BG073190	Mm.2662	Gsta4	3.33	3,34865
BG064907	Mm.35581	RIKEN cDNA 2310009O17 gene	3.31	2,49474
BG071601	Mm.26700	Tmem16a	3.30	2,07314
BG075211	Mm.381	Adfp	3.29	2,80754
BG067123	Mm.35605	Cdh1	3.27	2,79853
BG069891	Mm.231266	Sestd1	3.26	2,25431
BG074704	Mm.27764	Rnf128	3.26	2,01757
BG067911	Mm.7775	Gdpd1	3.26	2,47217
BG064165	Mm.1620	Anxa5	3.26	2,02078
BG067594	Mm.18718	Scml1	3.24	2,02643
BG071713	Mm.214958	Srebf1	3.22	2,05412
BG070656	Mm.18789	Sox4	3.21	2,04055
BG067160	Mm.2538	Pld2	3.19	2,38822
BG071672	Mm.18941	Chmp2b	3.18	2,03898
BG072807	Mm.156583	CARP	3.17	3,37532
BG070386	Mm.218846	Lbp	3.16	4,73538
BG067840	Mm.33819	Trpm7	3.16	2,71071
BG075881	Mm.260643	Ywhaz	3.15	2,08537
BG074954	Mm.197280	Nr2c2	3.15	2,04957
BG066006	Mm.25743	Tmprss2	3.14	2,33231

Table S2. (*Continued)*

Significant upregulated genes				
Accesion Code	**Unigene Number**	**Gene Name**	**Score(d)**	**Fold Change**
BG067543	Mm.258286	Sp100	3.13	2,01155
BG067807	Mm.29373	Mmp23	3.12	2,67757
BG070560	Mm.220901	Lpgat1	3.12	2,48754
BG075474	Mm.148155	Mod1	3.12	2,69955
BG076253	Mm.29823	Mgst3	3.11	2,48683
BG068718	Mm.1921	Fryl	3.10	2,08242
BG071707	Mm.259949	Slc6a8	3.10	2,74026
BG074067	Mm.28083	Cd164	3.08	2,05864
BG071644	Mm.3786	Slc34a2	3.07	2,23328
BG071673	Mm.26888	Camk1d	3.05	2,10487
BG074507	Mm.4394	Kit	3.03	2,03778
BG067642	Mm.24584	Tmem49	2.99	2,28150
BG064110	Mm.27764	Rnf128	2.99	2,10969
BG074800	Mm.173718	Gtl6	2.99	2,00323
BG070225	Mm.196382	Rsnl2	2.99	2,86828
BG073604	Mm.14796	Mgst1	2.96	2,15358
BG075145	Mm.183034	Stk38	2.95	2,00919
BG071101	Mm.27832	Ralb	2.91	2,05288
BG068674	Mm.26378	Tesc	2.91	3,22152
BG075016	Mm.30713	Socs6	2.90	2,25740
BG071728	Mm.12915	Nit1	2.89	2,57440
BG075920	Mm.126525	Dagk	2.88	2,02924
BG067012	Mm.1639	Mcl1	2.87	2,32342
BG072263	Mm.1639	Mcl1	2.86	2,32033
BG073809	Mm.2608	Bgn	2.85	2,33563
BG069187	Mm.6958	Capn2	2.84	2,14908
BG074814	Mm.370	C1qa	2.83	2,98528
BG074366	Mm.243085	Etv6	2.81	2,32457
BG071506	Mm.27917	Tanc1	2.79	2,03085
BG072227	Mm.21119	Litaf	2.78	2,16970
BG071169	Mm.439733	Camk2b	2.72	2,45339
BG075625	Mm.22179	Ergic2	2.71	2,00587
BG075073	Mm.142729	Tmsb4x	2.68	2,00811
BG064913	Mm.154286	Ralgps2	2.67	2,17799
BG071456	Mm.57225	Gpx2	2.65	3,19882
BG067321	Mm.28262	Rgs2	2.64	2,25183
BG074621	Mm.239470	Abca3	2.60	2,11436

Table S2. (*Continued)*

Significant upregulated genes				
Accesion Code	**Unigene Number**	**Gene Name**	**Score(d)**	**Fold Change**
BG071381	Mm.135621	Ncald	2.59	2,13839
BG070686	Mm.3863	Por	2.59	2,14565
BG073108	Mm.22506	G7e	2.57	6,43094
BG070117	Mm.43957	Bxdc1	2.55	2,93736
BG076077	Mm.41078	Wdr72	2.53	2,58964
BG069051	Mm.28034	Plcl2	2.50	2,01685
BG069421	Mm.29133	Bub1b	2.49	2,67433
BG067192	Mm.30217	Cib1	2.49	2,07899
BG074809	Mm.28099	Soat1	2.43	2,11402
BG071465	Mm.259998	Igf1	2.43	3,44328
BG075595	Mm.38387	Qk	2.43	2,01164
BG076042	Mm.182855	Cbara1	2.43	2,70131
BG070255	Mm.5034	Pde7a	2.42	2,04881
BG063978	Mm.18626	Capg	2.41	2,02424
BG076032	Mm.29254	Igfbp3	2.40	2,02024
BG069253	Mm.140761	Dnajc5	2.36	2,09158
BG067845	Mm.206775	Oas1c	2.34	2,00554
BG064710	Mm.22478	Smarcf1	2.31	2,49634
BG064661	Mm.29586	Basp1	2.28	2,56368
BG075814	Mm.25227	Klhl24	2.28	2,35980
BG074327	Mm.147387	Col3a1	2.27	2,18133
BG070107	Mm.25880	LOC218453	2.25	2,70188

Significant downregulated genes				
Accesion Code	**Unigene Number**	**Gene Name**	**Score(d)**	**Fold Change**
BG076333	Mm.443	Mthfd2	-6.66	0,20999
BG072212	Mm.17655	Hs3st3b1	-6.59	0,13937
BG064480	Mm.192991	Mt1	-6.31	0,19619
BG072125	Mm.173903	Sntb1	-6.01	0,22808
BG071962	Mm.29622	Ccdc16	-5.48	0,18301
BG064958	Mm.227925	Csrp2bp	-5.08	0,41595
BG067541	Mm.116862	Mcoln2	-5.03	0,17331
BG076017	Mm.2942	Asns	-4.98	0,27563
BG072041	Mm.78861	Nolc1	-4.85	0,27603
BG074372	Mm.17403	GlyRS	-4.53	0,35065
BG065320	Mm.196135	Gemin6	-4.43	0,36424
BG067706	Mm.200423	Gpt2	-4.41	0,28800

Table S2. (*Continued)*

Significant downregulated genes				
Accesion Code	**Unigene Number**	**Gene Name**	**Score(d)**	**Fold Change**
BG067809	Mm.27307	Gng3	-4.33	0,38194
BG076068	Mm.4952	Irs1	-4.16	0,35708
BG066832	Mm.172850	Abcc1	-4.06	0,43383
BG070042	Mm.104920	Sdh1	-4.02	0,35005
BG071862	Mm.56915	Csf3r	-4.02	0,41670
BG069760	Mm.206417	Cbs	-4.01	0,33962
BG074462	Mm.646	Tpm2	-4.00	0,33178
BG071147	Mm.200423	Gpt2	-4.00	0,29977
BG073164	Mm.258010	Pgm2l1	-3.98	0,26260
BG072435	Mm.32041	Pgm2l1	-3.96	0,28198
BG063880	Mm.255729	Slc30a2	-3.96	0,20991
BG064735	Mm.6587	Prdx5	-3.94	0,41365
BG069752	Mm.206417	Cbs	-3.94	0,29896
BG066347	Mm.172736	Wnk2	-3.88	0,48940
BG074541	Mm.24276	C1r	-3.82	0,21732
BG065084	Mm.4876	Rcn	-3.80	0,31595
BG071189	Mm.29902	Psat-pending	-3.79	0,45440
BG063304	Mm.30250	Aldh7a1	-3.76	0,48219
BG064323	Mm.7819	Pld1	-3.74	0,42185
BG074268	Mm.2011	Gstm1	-3.73	0,39590
BG069852	Mm.221029	Fastkd1	-3.67	0,46734
BG069444	Mm.24128	C1s	-3.66	0,31526
BG074546	Mm.182726	Dock9	-3.61	0,38908
BG075740	Mm.39038	Itpk1	-3.55	0,37387
BG067514	Mm.39038	Itpk1	-3.52	0,43114
BG070290	Mm.154307	Ift20	-3.52	0,45908
BG074397	Mm.2011	Gstm1	-3.48	0,41030
BG063736	Mm.9001	Nlk	-3.42	0,45846
BG065196	Mm.4419	Rpl5	-3.39	0,49496
BG065154	Mm.18737	Kntc1	-3.37	0,47502
BG067972	Mm.25530	Plekha4	-3.36	0,49303
BG066852	Mm.153315	Atf6	-3.34	0,42313
BG073197	Mm.27944	Acsl3	-3.33	0,38014
BG069966	Mm.203125	Pan3	-3.32	0,32431
BG073280	Mm.33650	Pycr1	-3.31	0,47403
BG066941	Mm.10	Srm	-3.24	0,38187
BG063119	Mm.16972	Chd7	-3.16	0,40761

Table S2. (*Continued)*

Significant downregulated genes				
Accesion Code	**Unigene Number**	**Gene Name**	**Score(d)**	**Fold Change**
BG070044	Mm.27680	Mylk	-3.14	0,34409
BG065409	Mm.155620	Pla2g6	-3.12	0,44252
BG071956	Mm.18652	Sms	-3.12	0,46322
BG072053	Mm.180553	Nr2e1	-3.04	0,38362
BG067357	Mm.4356	Cnn1	-2.88	0,42385
BG069668	Mm.104920	Sdh1	-2.87	0,43166
BG075348	Mm.24210	Bcat2	-2.80	0,37178
BG075019	Mm.143603	Sh3gl2	-2.75	0,49452
BG063438	Mm.28665	Edem2	-2.71	0,45748
BG065337	Mm.34388	Nudt16l1	-2.70	0,49022
BG074523	Mm.25848	Bckdha	-2.65	0,46688
BG071284	Mm.23352	Suox	-2.65	0,45828
BG069993	Mm.200423	Gpt2	-2.64	0,45515
BG063884	Mm.196080	Wdr42a	-2.60	0,47434
BG066444	Mm.38154	Bcas3	-2.59	0,46205
BG072362	Mm.42255	Atp2a2	-2.58	0,42757
BG066796	Mm.16898	Phgdh	-2.57	0,44819
BG072224	Mm.138100	Tssc8	-2.53	0,43942

Table S3. Primer sequences of genes analyzed by QPCR.

Gene name	Forward primer	Reverse primer
Hprt	5’-TCCCTGGTTAAGCAGTACAG-3’	5’-TTCCAGTTTCACTAATGACAC-3’
Nkx.3.1	5’-ACTGAACCCGAGTCTGATGC-3’	5’-CTTGGGTTTCGGTGAGTTTG-3’
Probasin	5’-ACAACTGTCCAAGCAAGATC-3’	5’-TGATGTTTCAGGTTCCAGGA-3’
CK8	5’-CTCCGGCAGATCCATGAAG-3’	5’-GGTACATGGTTTCAGCCTC-3’
CK19	5’-GGGCCTTGAGATTGAGCTGC-3’	5’-GGTTCTGGCGCTCTATGTCG-3’
CK5	5’-CAGGACATGGCCAGGCTG-3’	5’-CAACTCCTTCCCCACTCAGC-3’
p63	5’-CCCACAGACTGCAGCATTG-3’	5’-GAGATGAGGAGGTGAGGAGAAG-3’
Expi	5’-GGAGATGGATCGTGCTCTGG-3’	5’-GGCTAGCCATCAGTCCTGC-3’
Wfdc2	5’-TGTGACCAGGGAAGGCTTAGG-3’	5’-CTCCAGATGCACAGTCCGGC-3’
Tacstd2	5’-GACCTCTTCCTTCTCTCTCACC-3’	5’-CAAGTCCCTGGGAAACAAGTG-3’
Clu	5’-GTGAAGCTGTTTGACTCTGACC-3’	5’-GATTCCCTCCCAGACACTCC-3’
Ppp1r1b	5-CTGAGGACCAAGTGGAAGGC-3’	5’-CAGGGTACAAAGGAGGGTGG-3’
Sca-1	5’-GTCCCATTTGAGACTTCTTGCC-3’	5’-AGGAGGGCAGATGGGTAAGC-3’
Hs3st31b	5’-CCAGTCCCATCTCCAGCTTC-3’	5’-GGCATCAAGTCTCGGTACCAG-3’
Ccdc16	5’-TGCTCTGTAGTTTACTGTACTCC-3’	5’-GCAACTTACCTATCTTCCTGCC-3’
Mcoln2	5’-GGAGAGCGGAAGCAAAGATGG-3’	5’-ACCTCTGCATAAAGGGATCTGG-3’
C1r	5’-TGGAAGAATGAAGAGGAAGGAG-3’	5’-CGTGGGTAGTGGTGAAGGC-3’
Mt1	5’-CTCCAGCTTCACCAGATCTCG-3’	5’-CCTTTGCAGACACAGCCC-3’

Table S4. Information of antibodies used for immunohistochemistry and immunofluorescence.

Antibody	Company	Product number	Method	Dilution
CK8	Covance, Berkeley, CA	MMM-162P	IHC	1:1000
			IF	1:1000
CK19	Abcam, Cambridge, UK	ab15463	IHC	1:200
Nkx3.1	–	–	IHC	1:1000
p63	DAKO, Glostrup, Denmark	M7247	IHC	1:100
			IF	1:50
Tacstd2	R&D systems, Minneapolis, MN	AF1122	IHC	1:100
			IF	1:100
Clu	Santa Cruz, Santa Cruz, CA	SC-6420	IHC	1:800
			IF	1:400
Ppp1r1b	Cell Signaling Technology, Beverly, MA	2302	IHC	1:100
Sca-1	R&D systems, Minneapolis, MN	AF1226	IHC	1:100
pAkt	Cell Signaling Technology, Beverly, MA	4058	IHC	1:100
			IF	1:50
Goat Anti-Mouse-biotin	DAKO, Glostrup, Denmark	E0433	IHC	1:400
Swine Anti-Rabbit-biotin	DAKO, Glostrup, Denmark	E0431	IHC	1:400
Rabbit Anti-Goat-biotin	Santa Cruz, Santa Cruz, CA	SC-2774	IHC	1:400
			IF	1:400
Streptavidin-TRITC	Invitrogen, Carlsbad, CA	43-4314	IF	1:50
Rabbit Anti-Mouse-FITC	DAKO, Glostrup, Denmark	F0261	IF	1:40
Rabbit Anti-Mouse-TRITC	DAKO, Glostrup, Denmark	R0270	IF	1:100
Swine Anti-Rabbit-FITC	DAKO, Glostrup, Denmark	F0205	IF	1:100

IHC: Immunohistochemistry, IF: immunofluorescence

CHAPTER 3

Characterization of heterogeneous prostate tumors in targeted *Pten* knockout mice

Hanneke Korsten, Angelique Ziel-van der Made, Theo van der Kwast, Karin Hermans, Jan Trapman

Department of Pathology, Josephine Nefkens Institute, Erasmus Medical Center Rotterdam, The Netherlands

In preparation

ABSTRACT

Previously, we generated a mouse prostate tumor model based on PSA-Cre driven inactivation of *Pten*. In this model consecutive stages of hyperplasia and tumor development were clearly defined. A homogeneous population of Clu+Tacstd2+Sca-1+ luminal epithelial progenitor cells was identified as candidate tumor initiating cells. Tumors were derived from homogeneous hyperplastic cells. Here, we describe the molecular and histological characterization of the tumors and a model for tumor development is proposed.

In PSA-Cre targeted *Pten* knockout mice homogeneous hyperplastic prostates (4-5m) developed at older age (>10m) into heterogeneous tumors. In these tumors different histopathological growth patterns could be identified. We discriminated carcinomas, that included intraductal carcinoma (IDC), adenocarcinoma and undifferentiated carcinoma, which stained strongly positive for the epithelial cell marker Cytokeratin (CK) and carcinosarcomas, that were weakly positive or negative for CK. IDC was detected earlier than other growth patterns (7-8m), indicating that it could be a precursor stage. IDC and carcinosarcoma were the most frequent growth patterns. Gene expression profiling revealed increased expression of genes involved in the inflammatory response associated with prostate tumor development. Moreover, analysis of gene expression patterns of heterogeneous prostate tumors discriminated essentially two molecular types, denoted tumor class (TC) 1 and 2. The dominant histopathological growth pattern in TC1 was carcinoma, corresponding with high expression of epithelial markers, including *Msmb*, *Tff2*, *CK8*, and *E-cadherin*. TC2 tumors were mainly characterized by high expression of mesenchyme/stroma markers, like *Star*, *Adam12*, *Snail* and *Fibronectin.* Functional markers for senescence, proliferation, angiogenesis and apoptosis were higher expressed in all heterogeneous tumors compared to hyperplasia, but highest expression of proliferation and angiogensis markers was detected in TC2 tumors. Remarkably, *Trp53* and associated senescence/apoptosis markers showed not only increased expression in hyperplastic prostates, but expression in tumors was even higher. Finally, characterization of cell lines generated from prostate tumors indicated genomic homogeneity with frequent loss of chromosomes 4 and 12. However, again molecular analysis of tumor cell lines and *in vitro* and *in vivo* biological assays demonstrated heterogeneity.

Our data show that in the genetically homogeneous well-defined *PSA-Cre;Pten-loxP/loxP* prostate tumor model, histopathological, molecular and biological heterogeneity occur during later stages of tumor development.

INTRODUCTION

Prostate cancer is recognized as a clinical and genetic heterogeneous disease [1-3]. Heterogeneous prostate tumors can be classified by expression profiling into subtypes with a different prognosis [4-6]. However, little is known about mechanisms of development of heterogeneous tumors. Unraveling processes associated with tumor development is a prerequisite to elucidate the molecular and biological mechanisms of tumor heterogeneity.

It has been proposed that during multistep tumor development, prostate cells acquire malignant characteristics by the accumulation of genetic and epigenetic alterations [7-9]. Many biological processes, including inflammatory response, proliferative signaling, angiogenesis and apoptosis are involved in tumor development [7, 10, 11]. Different contributions of biological and molecular processes might lead to tumor heterogeneity. Moreover, tumor heterogeneity might be caused by differences in tumor initiating cells that can drive tumor growth and progression. Alternatively or complementary, clonal expansion of different dominant tumor cell populations has been proposed to contribute to tumor heterogeneity [12-15]. In a clinical setup, study of the dynamics of prostate tumor development is impossible and initial stages of tumor development are not available. Therefore, well-defined model systems are very helpful in unraveling mechanisms of tumor development including tumor heterogeneity.

PTEN inactivation is together with *ERG* overexpression the most frequent early genetic alteration in prostate cancer [16, 17]. Several genetically engineered mouse prostate tumor models (GEMMs) based on targeted bi-allelic deletion of the *Pten* tumor suppressor gene have been developed [18-21]. Additionally to the *Pten* models, models have been developed based on *c-Myc* or *Erg* overexpression [22-25]. None of the initial publications on mouse prostate tumor models based on *Pten* inactivation or other genetic alterations reported tumor heterogeneity [18-21], however, tumor heterogeneity, including epithelial mesenchymal transition (EMT), was reported in tumors that develop in *Pten/Trp53* double knockout mice and in mice with activation of Fibroblast Growth Factor Receptor-1 (FGFR1) in the prostate epithelium [26, 27].

Previously, we studied the development of a homogeneous hyperplasia in the early stages of tumor development in PSA-Cre targeted *Pten* knockout model and we identified Clu+Tacstd2+Sca-1+ luminal epithelial progenitor cells as candidate tumor initiating cells [28, 29]. Here, processes involved in the development of prostate tumors were analyzed. Increased expression of genes involved in the inflammatory response was associated with tumor development. Remarkably, *Trp53* and genes associated with senescence show the highest expressed in tumors. Tumors were histological heterogeneous, and composed of different carcinoma growth patterns and carcinosarcomas. Tumors could also be classified based on differential gene expression. Characterization of prostate cancer cell lines derived from the

tumors demonstrated frequent loss of chromosomes 4 and 12, heterogeneous gene expression patterns and different *in vitro* and *in vivo* biological properties.

MATERIAL AND METHODS

Generation of Prostate Targeted *Pten* Knockout Mice

PSA-Cre mice, mice carrying the *Pten-loxP* allele and *PSA-Cre;Pten-loxP/loxP* mice have been described previously [28, 30]. All *PSA-Cre;Pten-loxP/loxP* mice had a mixed 129/FVB background. Cre negative littermates were kept as controls. Mice were housed according to institutional guidelines, and procedures were carried out in compliance with the standards for use of laboratory animals.

DNA isolation, PCR analysis and array-CGH analysis

Protocols for DNA isolation were described earlier [31]. To check *Pten* recombination, a PCR analysis was performed with primers flanking a loxP site and with primer combinations showing recombination as described [28]. The whole-genome mouse BAC microarrays used for array-based comparative genomic hybridization (aCGH) analysis were kindly provided by Jos Jonkers (NKI, The Netherlands) and published previously [32]. Protocols for DNA labeling, hybridization and analysis of BAC microarrays was published previously [31]. Instead of human Cot-1 DNA, mouse Hybloc was used to inhibit nonspecific hybridization.

RNA extraction, cDNA preparation and QPCR analysis

RNA was isolated from snap frozen mouse prostates and cell lines using the Qiagen Easy RNA isolation Kit (Qiagen, Hilden, Germany) according to the manufacturer's guidelines, including an on column DNAseI digestion. RNA quality was assessed using the RNA 6000 Nano kit in a 2100 Bioanalyser (Agilent, Palo Alto, CA). For RNA extraction from normal, hyperplastic prostates and prostate tumors a pool of different prostate lobes of one mouse was used.

For reverse transcription 2 µg total RNA was incubated for 1 h at 37°C in buffer containing 50mM Tris-HCl pH 8.3, 75 mM KCl, 3mM $MgCl_2$, 10mM DTT and 1mM dNTPs, supplemented with 400 U M-MLV-reverse transcriptase (Invitrogen, Carlsbad, CA), 80 U RNAguard (Amersham Biosciences, Little Chalfont, UK) and 1 mg oligodT primer. The procedure for QPCR analysis was described earlier [29]. Primer sequences for both PCR as QPCR are provided in Table S1.

Probe preparation and hybridization, and analysis of Affymetrix gene expression arrays

Five ug total RNA was used to prepare antisense biotinylated RNA according to the manufacturer's one-cycle protocol (Affymetrix, Santa Clara, CA). Hybridization to Affymetrix Mouse Genome

430 2.0 GeneChips (>39000 transcripts), staining, washing and the scanning procedures were performed by ErasmusMC Center for Biomics according to the Affymetrix protocol. The Affymetrix gene expression data were normalized based on the average signal intensity. Before transforming expression array data to log2 values, low expression values (<4) were set at 4. For unsupervised hierarchical clustering and visualization of genes with the highest differential expression the programs Cluster and Treeview were used [33]. In addition, by performing Significance Analysis of Microarrays (SAM) [34] gene expression relative differences to the standard deviation of these expression levels within one group was calculated.

Cell culture, western blot analysis, soft agar assay and subcuteneous transplantation studies

To generate cell lines, prostate tissue was digested in Collagenase A solution (250U/ml, Roche, Mannheim, Germany) for ~1 hour. The culture medium used was described previously [35].

Western blot analysis was performed according to standard procedures. The primary antibodies used were rabbit polyclonal antibodies to Akt (Cell signaling technology), pAkt (Ser^{473}, Cell signaling technology) and Androgen Receptor (own production) and a mouse monoclonal β-actin antibody (Sigma, St. Louis, MO).

Procedures used in the soft agar assay and in subcuteneous transplantation studies were described earlier [36, 37]. Per cell line six mice were injected with $5*10^6$ cells.

Immunohistochemical analysis

Procedures for immunohistochemistry were described earlier [28, 29]. Detailed antibody information is provided in Table S2.

RESULTS

Prostate tumors of targeted *Pten* knockout mice are heterogeneous

Previously, we described prostate tumor development in *PSA-Cre;Pten-loxP/loxP* mice [28]. At 4-5 months (4-5m) prostates of targeted bi-allelic *Pten* knockout mice were completely filled with homogeneous, Cytokeratine (CK) positive hyperplastic epithelial cells lined by P63+ basal epithelial cells (Figure 1). Clu+Tacstd2+Sca-1+ luminal epithelial progenitor cells were identified as candidate tumor initiating cells [29]. Ultimately, all mice developed invasive prostate tumors at >10m. In the present study, the tumors are characterized and processes associated with tumor development are identified. Furthermore, cell lines derived from tumors of *PSA-Cre* targeted *Pten* knockout mice were generated and characterized.

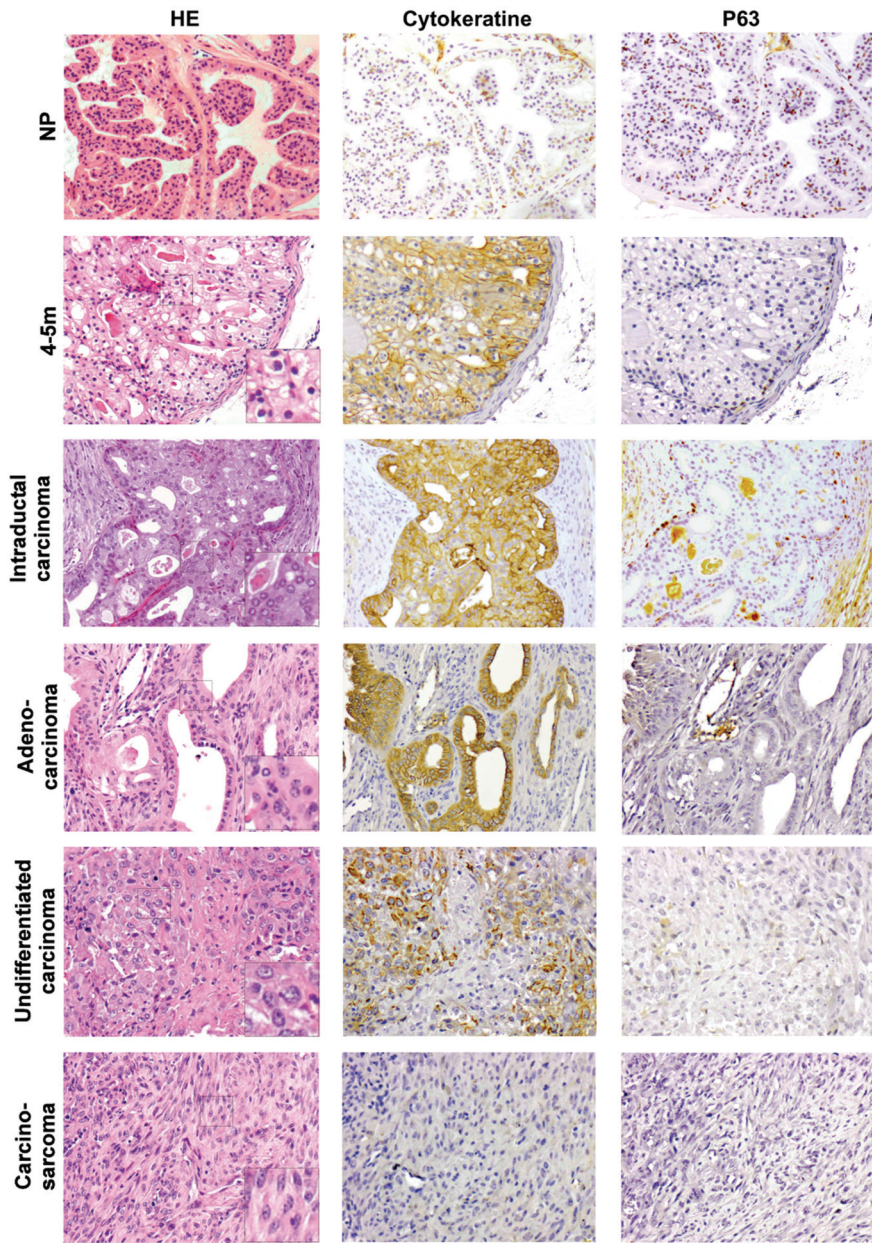

Figure 1. Characterization of hyperplastic prostates and prostate tumors of targeted *Pten* knockout mice. The prostate histology (HE staining) of hyperplastic prostates (4-5m) and different growth patterns in prostate tumors is shown (Intraductal carcinoma, adenocarcinoma, undifferentiated carcinoma and carcinosarcoma) (Magnification: 200x). Note that normal prostate (NP) is included as a reference. A detailed picture of the nuclear structure in these prostates is shown at higher magnifications. To characterize the prostates a consecutive slide stained for P63 and CK is included.

Although hyperplastic prostates (HP) were histological very homogeneous, the tumors were not. In contrast to the regular nucleï of hyperplastic cells at 4-5m, tumor cells showed nuclear atypia with prominent nucleoli (Figure 1). HP developed into heterogeneous tumors containing areas showing many different histopathologic growth patterns. At 7-8m foci of cells with atypical nuclei, which we named intraductal carcinoma (IDC), because of the histologic resemblance to human IDC, could be detected (Figure S1). Prostates with characteristics of IDC contained dysplastic cells that showed a cribriform growth pattern surrounded by an interrupted P63+ basal epithelial cell layer (Figure 1, Figure S1).

In all older mice (>10m) heterogeneous prostate tumors were detected with different cell types and tissue growth patterns that we distinguished as carcinoma. Three carcinoma growth patterns were defined: IDC, adenocarcinoma and undifferentiated carcinoma. The undifferentiated carcinosarcoma was composed of spindle form cells. Tumor cells in IDC, adenocarcinoma and undifferentiated carcinoma showed strong CK staining. Carcinosarcoma cells were weakly positive or negative for CK staining. IDC and carcinosarcoma were the dominating growth patterns. Because foci of IDC were already detected at 7-8 months, it might represent a precursor stage of other tumor types. However, transitions from one growth pattern to another were not very clear.

Prostate tumors are associated with increased expression of genes associated with an inflammatory response. To investigate differences in gene expression profiles between HP and tumors, global gene expression profiling of RNA of three HP samples and thirteen prostate tumors was undertaken. Unsupervised hierarchical clustering separated two clusters (Figure 2A). Surprisingly, one cluster contained eight tumors (indicated in red), and the second cluster was composed of the three HP and the remaining five tumors (indicated in blue).

Although part of the tumor samples showed overlap in gene expression profile with HP, we first carried out SAM to identify genes differentially expressed in all prostate tumor as compared to HP (Figure 2B, Table S3, S4). In Figure 2B the 20 genes with the highest expression in prostate tumors as compared to HP are visualized. Remarkably, six out of the top 20 genes, *Cpn1*, *Tnfrsf9, Gzmf, Zap70, Il18rap* and *Gzmd*, were identified as genes involved in the inflammatory response [38-43]. Expression of *Cpn1*, *Tnfrsf9* and *Zap70* in individual HP samples and tumor samples are shown as examples (Figure 2C). Strong differential expression of genes involved in the inflammatory response between tumor and HP samples was supported by Ingenuity analysis (Figure 2D). Here, inflammatory response was by far the top process associated with the prostate tumors.

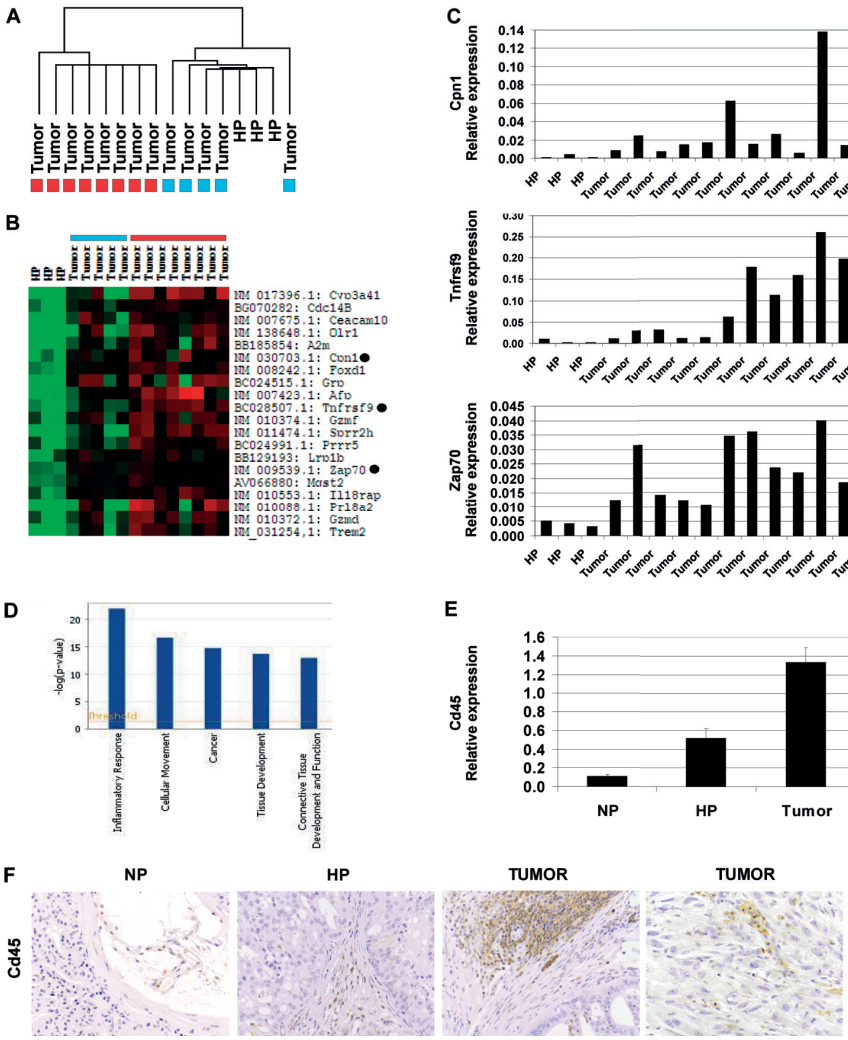

Figure 2. Increased expression of markers associated with inflammatory response in prostate tumors of targeted *Pten* knockout mice. (**A**) Unsupervised hierarchical clustering of hyperplastic prostates and prostate tumors. Blue and red boxes indicate tumors with differences in expression profiles. (**B**) Top20 of genes high expressed in prostate tumors as compared to HP identified by SAM. A blue and red bar indicate the tumors as in Figure 2A. Green indicates lower gene expression and red indicates higher expression. The expression levels of the genes indicated by a black dot (*Cpn1*, *Tnfrsf9* and *Zap70*) in individual HP samples and prostate tumors are shown in (**C**). (**D**) Top5 of processes annotated by Ingenuity analysis based on genes differentially expressed between HP and prostate tumors. (**E**) Relative expression analysis for CD45 in NP, HP and prostate tumors. (**F**) CD45 staining of immune cells in NP, HP and prostate tumors (Magnification: 125x). In (**C**) and (**E**) the gene expression was plotted relative to the housekeeping gene *Hypoxanthine guanine phosphoribosyl transferase 1* (*Hprt*).

As shown in Figure 2A part of the tumor samples co-clustered with HP. We compared the expression profiles of these five tumor samples to the three HP samples present in this cluster by SAM to obtain patterns of the most specific expressed genes in these tumors. Interestingly, again here genes associated with immune response were differentially expressed. Members of the immunoglobulin family (*Igh-6*, *Igh-4* and *IgVH*) were among the top ten genes high expressed in tumor samples as compared to HP (Figure S2A). The expression of *Igh-6* and *IgVH* in individual HP samples and prostate tumor samples are shown (Figure S2B). These markers were also higher, but more variable expressed in the eight tumor samples in the second tumor cluster indicated by red in Figure 2A (data not shown).

Further studies showed that RNA expression of the common leukocyte marker CD45 was already higher in HP as compared to normal prostate (NP), however the expression of this marker was the highest in prostate tumor samples (Figure 2E). Immunohistochemical staining of prostates for CD45 confirmed that both HP and prostate tumors were infiltrated by immune cells that stained positive for the common leukocyte marker (Figure 2F).

Based on expression profiling two subclasses of prostate tumors in PSA-Cre targeted *Pten* knockout mice were discriminated: TC1 and TC2

To extend the analyses of gene expression patterns in all heterogeneous tumor samples, unsupervised clustering of the thirteen tumor samples analyzed in Figure 2A was undertaken, but now leaving out the HP samples. As expected from Figure 2A, based on gene expression profiling again two clusters could be discriminated: red and blue samples in Figure 2A were again separated in two clusters (data not shown). To address the question whether differences in expression profiles were associated with prostate tumor histology, these thirteen tumors were independently scored for the presence of different tumor growth patterns by two pathologists. As mentioned above, all prostate tumors were heterogeneous, however some differences could be detected. In three tumors the predominating growth pattern (>70%) was carcinoma (IDC, adenocarcinoma and undifferentiated carcinoma), whereas six prostate tumors contained large areas (>70%) of carcinosarcomas. Four tumors contained such a complex mixture of carcinoma and carcinosarcoma that a predominating growth pattern could not be determined. These four samples were excluded in further analyses. The three samples in the carcinoma group co-clustered with HP in Figure 2A, whereas the carcinosarcomas clustered in the separate cluster (Figure 2A). The carcinoma group was denoted tumor class (TC) 1 and tumor class (TC) 2 was characteristic for carcinosarcomas.

Next, a third SAM experiment was done, now to identify genes differentially expressed between TC1 and TC2 (Figure 3A, B). Among the genes with the highest expression in TC1 were genes known to be higher expressed in epithelial cells, including *Msmb*, *Tff2* and *Agr2*, whereas genes higher expressed in TC2, like *Star*, *Adam12* and *Gja1*, were known to be expressed in stromal/mesenchymal cells [44-50]. Full names of the top twenty differentially genes are listed in

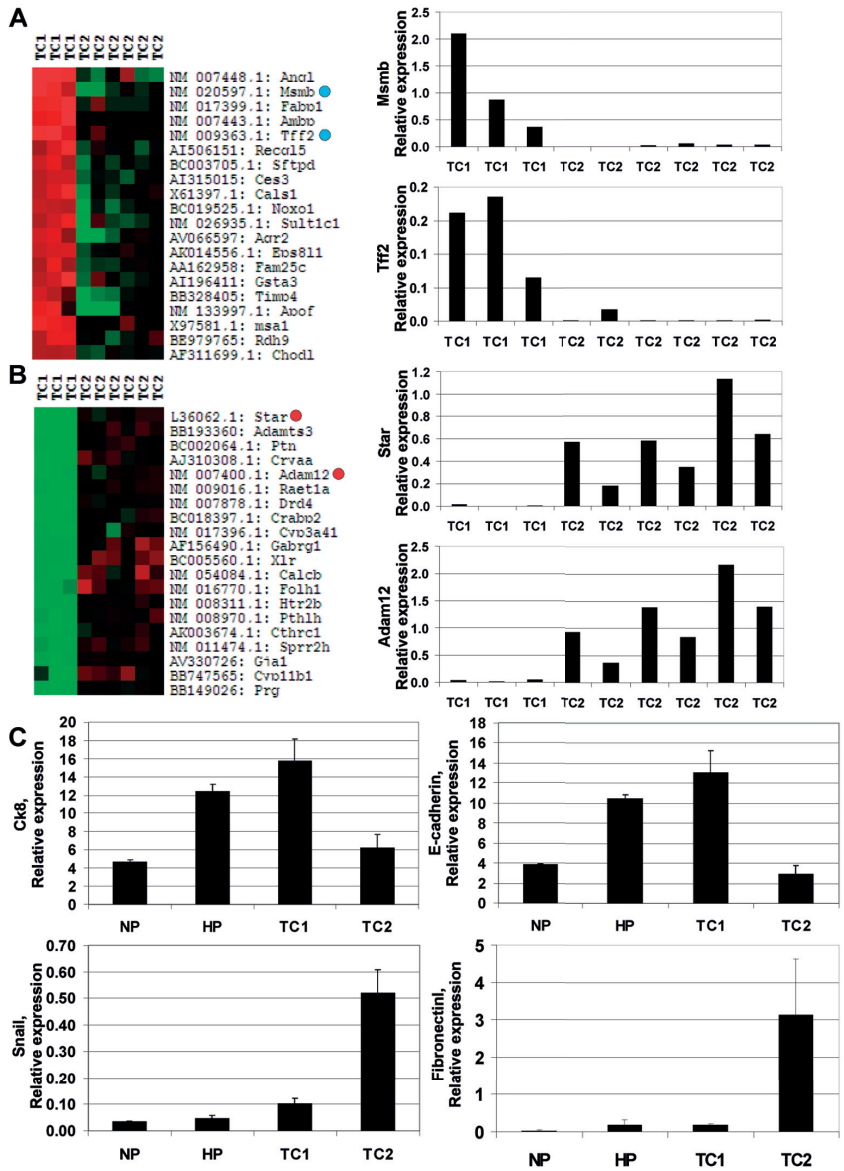

Figure 3. Markers expressed in epithelial and mesenchymal cells are differentially expressed in TC1 and TC2 tumors. (**A**) Top20 of genes high expressed in TC1 as compared to TC2 as identified by SAM. Green indicates lower gene expression and red indicates higher expression. The relative expression of *Msmb* and *Tff2* (indicated by blue dots) are show as examples. (**B**) Top20 of genes high expressed in TC2 as compared to TC1 as identified by SAM. Green indicates lower gene expression and red indicates higher expression. The relative expression of *Star* and *Adam12* (indicated by red dots) are shown as examples. (**C**) The relative expression levels of CK8, E-cadherin, Snail and Fibronectin in NP, HP, TC1 and TC2 expressed as mean +/- SE. In (**A**), (**B**) and (**C**) the gene expression was plotted relative to the housekeeping gene *Hprt*.

Tables S5 and S6. The expression of *Msmb*, *Tff2*, *Star* and *Adam12* in individual prostate tumors are shown as examples (Figure 3A,B). So, although strongly hampered by the heterogeneity of the samples, a separation of (selected) tumor samples in TC1 and TC2, based on gene expression and histology can be accomplished.

Further comparison of expression of individual genes in TC1 and TC2 with HP and NP (Figure S3) showed that the relative expression of the basal epithelial cell marker *P63* was lower in HP and prostate tumors. The *androgen receptor (AR)* expression was increased in prostates of targeted *Pten* knockout mice as compared to NP, in contrast to markers for differentiated luminal epithelial cells like *Nkx3.1* and *Probasin*. Analysis of expression profiles of known markers for epithelial (*CK8* and *E-cadherin*) and mesenchymal (*Snail* and *Fibronectin*) cells confirmed differential expression of genes associated with epithelial cells and mesenchymal cells in TC1 and TC2, respectively (Figure 3C). These data are in line with the immunohistochemical data for CK expression as observed in Figure 1.

During prostate tumor development in PSA-Cre *Pten* knockout mice differential expression of markers of senescence, proliferation, angiogenesis and apoptosis was observed

To explore biological processes that can be associated with tumor development, RNA expression of markers associated with these processes was analyzed. Previously, Chen *et al*. reported an increased expression of genes involved in the *Trp53* dependent cellular senescence response in early hyperplasia stages of tumor development in the related Probasin (PB)-Cre targeted *Pten* knockout mouse model [51]. We also observed higher expression of *Trp53, Trp53*-regulated and *Trp53*-independent senescence markers, including *Cdkn2a* (encoding P16), *Cdkn1a* (encoding p21) and *Dec1* in HP as compared to NP (Figure 4A). Surprisingly, even a higher expression level for these markers was observed in TC1 and TC2 tumors (Figure 4A), indicating that diminished senescence is not a factor involved in tumor development from hyperplasia.

Two other hallmark biological processes associated with tumor development are proliferation and angiogenesis. In prostates of targeted *Pten* knockout mice an increase in the proliferation rate was detected, as demonstrated by an elevated expression level of *Ki67* and *Pcna* and the presence of more Bromodeoxyuridine (BrdU) positive cells (Figure 4B). These data confirm and extend previous observations [28] that the proliferation rate is increased in HP and TC1 tumors as compared to NP, however TC2 tumors show the highest proliferation rate (Figure 4B). Furthermore, analysis of gene expression showed a slightly higher expression of the endothelium markers *CD31* and *Tie2* in HP and TC1 tumors, and the highest expression of these markers in TC2 tumors (Figure 4C), indicating that angiogenesis is mostly stimulated in the TC2 tumors.

Previously, we published an increased number of cells that stained for active Caspase3 in prostate hyperplasia and tumor in *PSA-Cre;Pten-loxP/loxP* mice [28]. Although less convincing, in line with these data the pro-apoptotic markers *Bax* and *Bak1* were higher expressed in HP, and in TC1 and TC2 (Figure 4D).

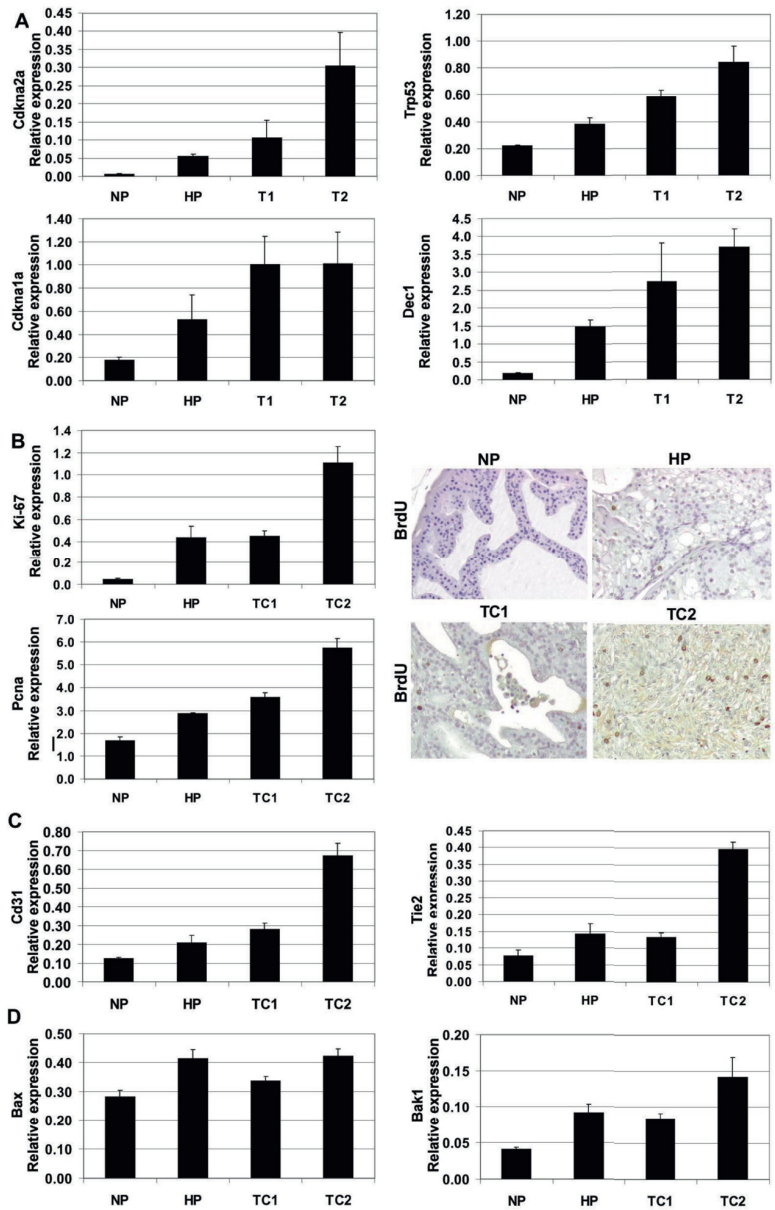

Figure 4. Differential expression of markers involved in cellular senescence, cellular proliferation, angiogenesis and apoptosis during prostate tumorigenesis in targeted *Pten* knockout mice. (**A**) Relative expression levels of cellular senescence markers *Cdkna1a*, *Trp53*, *Cdkna2a* and *Dec1* in NP, HP, TC1 and TC2. (**B**) Relative expression levels of *Ki67* and *Pcna* and examples of a representative picture of BrdU+ cells in NP, HP, TC1 and TC2 (Magnification: 200x). (**C**) Relative expression of angiogenesis markers *CD31* and *Tie2* in NP, HP, TC1 and TC2. (**D**) Relative expression of pro-apoptotic markers *Bax* and *Bak1* in NP, HP, TC1 and TC2. In (**A**), (**B**), (**C**) and (**D**) the gene expression was plotted relative to the housekeeping *Hprt*.

Characterization of prostate tumor cell lines derived from prostate tumors of targeted *Pten* knockout mice

To obtain additional information on properties of prostate tumor cells, cell lines derived from the prostate tumors were generated and characterized. In total 4 cell lines, C1, C4, C7 and C9, were generated and studied. C1, C4 and C9 were derived from very heterogeneous tumors and C7 originated from a TC2 tumor. PCR analysis of DNA of these cell lines confirmed that they were all completely *Pten* negative (Figure 5A).

Tumor cells accumulate genomic alterations during tumor development and progression. Analysis of the genomic alterations in the *Pten* negative cancer cell lines showed loss of part or complete chromosome 4 in all cell lines (Figure 5B). Loss of chromosome 12 was observed in all cell lines, except C4. In addition to these common alterations in cell lines derived from prostate tumors of PSA-Cre targeted *Pten* knockout mice, C1 had loss of chromosome 8 and C7 was the only cell line where we found gain of chromosome 19.

Remarkably, expression of the Pten downstream target phospho-Akt (pAkt) was variable. C1 and C7 expressed high levels pAkt, but a faint band for pAkt was observed in C4 and C9 was pAkt negative (Figure 5C). In cell line C4 by far the highest androgen receptor (AR) protein levels was observed as compared to the low expression in C1 and C7 (Figure 5C). No AR protein expression was detected in C9.

Next, QPCR was performed for cell type specific markers (Figure 5D). The epithelial cell marker *E-cadherin* was highest expressed in C4, C7 and C9. C1 showed highest expression of the mesenchymal marker *Snail*. Expression of *Nkx3.1*, a marker for mature luminal epithelial cells was low in all cell lines. *Probasin* showed a similar expression pattern (data not shown).

We selected one cell line with relatively high expression of mesenchymal cell markers, C1, and a cell line with higher expression of epithelial cell markers, C4 for biological assays. No difference in *in vitro* migratory capacity could be detected (data not shown), and in a soft agar assay the differences between C1 and C4 were small (Figure 5E). However, *in vivo* subcutaneous transplantation of C1 in nude mice resulted in tumor formation after 20 days, in contrast to C4 (Figure 5F). Summarizing, these data showed that cell lines derived from targeted *Pten* knockout mice can differ in their molecular and biological properties, but the properties of these cell lines seem not to be determined by the predominating growth pattern of the tumor from which they are derived.

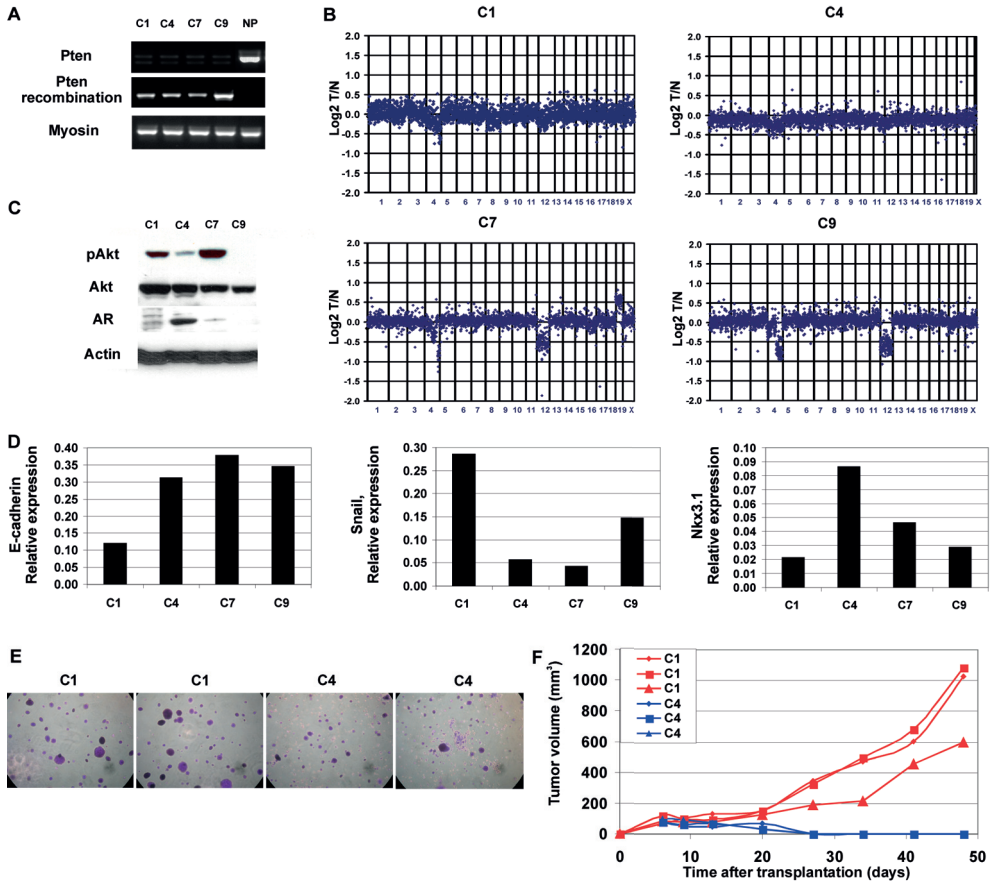

Figure 5. Heterogeneity between cell lines derived from prostate tumors of targeted *Pten* knockout mice. (**A**) PCR analysis showing complete Pten recombination in C1, C4, C7 and C9. Myosin was used as a loading control. (**B**) Array-CGH analysis of C1, C4, C7 and C9 plotted as log2 T/N ratio per chromosome. (**C**) Western blot analysis of pAkt, Akt and AR expression in C1, C4, C7 and C9. Actin was used as a loading control. (**D**) QPCR analysis of E-cadherin, Snail and Nkx3.1 in C1, C4, C7 and C9. (**E**) Examples of colony formation in a Soft agar assay for C1 and C4. (**F**) Tumor growth after subcutaneous transplantation of C1 and C4 in nude mice plotted as tumor volume (mm^3) against time after transplantation (days). Note that at day 20 C1 starts to form a tumor in contrast to C4.

DISCUSSION

The present study mainly focuses on two aspects of tumor development in the *PSA-Cre;Pten-loxP/loxP* mouse prostate cancer model [28]: characterization of tumor heterogeneity, and identification of biological and molecular processes associated with tumor development.

Previously we showed that the initial stages of tumor development in our model were well defined and very homogeneous: (1) The process starts with targeted bi-allelic inactivation of *Pten* in the prostate (2) The tumor initiating cells are Clu+Tacstd2+Sca-1+ luminal epithelial progenitor cells [29] (3) At 4-5m a homogeneous prostate hyperplasia has developed [28, 29]. Later steps in tumor development are less well defined. In the present study we showed that at 7-8m foci of dysplastic cells, designated IDC, had developed. At >10m all targeted mice developed heterogeneous tumors, with mixed growth patterns characteristic of carcinomas and carcinosarcomas.

Carcinoma in *PSA-Cre;Pten-loxP/loxP* prostate tumors was subdivided in three growth patterns: IDC, adenocarcinoma and undifferentiated carcinoma, with IDC as major component. Additionally, we recognized carcinosarcoma as a predominating growth pattern. This heterogeneous growth complicated detailed characterization of the tumors. Remarkably, in previous investigations of prostate targeted *Pten* knockout mice, tumor heterogeneity has not been studied in detail [18-21]. In many of the previous studies pre-maligant prostate intra-epithelial neoplasia (PIN) lesions were defined, which showed morphological resemblance to IDC. Because the mouse IDC growth pattern is very similar to human IDC and different from human PIN we prefer IDC as terminology. Recently, several studies provided evidence that IDC in human prostate cancers is predictive for the development of high-grade invasive cancer with advanced stage disease [52, 53]. It was even proposed that IDC predicted the development of lymph node metastases [54]. Complete inactivation of *PTEN* is also demonstrated in late stage aggressive clinical prostate cancer. Therefore, although metastases are very rare in the mouse model, it would be interesting to compare the properties of the mouse model and human IDC in order to find out whether there are more similarities additional to the histological growth pattern.

It might be argued that tumor heterogeneity in the mouse model is due to differences in genetic background between mice in the mixed 129/FVB mice. Indeed, it is known that genetic background can be a determinant in *Pten* knockout mice [55-57] (VanDuijn, unpublished). However, tumor heterogeneity was detected in every mouse. Moreover, recently we generated *PSA-Cre;Pten-loxP/loxP* mice in a homogeneous FVB background, but again prostate tumors were heterogeneous (data not shown).

We were unable to find a clear transition of one tumor growth patterns to another. Because IDC was already detected at 7-8m, it is tempting to speculate that prostate tumors at older age developed from IDC. However, we have no direct evidence for this hypothesis. As described here for *Pten* knockout mice, in GEMMs induced by different genetic alterations prostate tumor heterogeneity was also described [26, 27, 58, 59]. In mouse models induced by targeted overexpression of activated *FGFR1*, in mice overexpressing *FGF8b* or targeted inactivation of both *Pten* and *Trp53* or *Rb,* growth patterns characteristic for adenocarcinomas, carcinosarcomas or sarcomas were described. In *PB-FGFR1* mice and the *PB-Cre;Pten/Trp53* double knockout mouse model it was suggested that carcinomas progressed into (carcino)sarcomas by EMT

[26, 27]. Although an attractive hypothesis, so far, we have no direct evidence for EMT in the *PSA-Cre;Pten-loxP/loxP* model. A further aspect that remains to be investigated is a role of (reactive) stroma in tumor development. However, because of the heterogeneity of the tumors identification of reactive stromal cells that were clearly different from carcinosarcoma cells was so far not reliable.

This is the first study describing gene expression profiling in heterogeneous prostate tumors of targeted *Pten* knockout mice. Based on gene expression profiling the heterogeneous tumors could be separated in TC1 and TC2 tumors with differential expression of genes in carcinoma and carcinosarcoma, respectively. Previously, Wang and coworkers [18] compared expression profiles of four prostate tumors of PB-Cre targeted *Pten* knockout mice, with normal prostate. Unfortunately, this number of samples is too small to detect heterogeneity. In this study, among the genes higher expressed in prostate tumors were genes also higher expressed in the tumor samples described in our study. Examples are *Sppr2h*, *Igk-V28*, *Igh-6* and *Pgr* (Figure 2, 3 and S2). However, by comparison we observed that many genes reported as higher expressed in prostate tumors of PB-Cre mice were also overexpressed in HP. So, it seemed that the tumor samples analyzed were mixtures of HP and TC1, as defined in our study. Comparison with other GEMMs indicated that genes overexpressed in TC2 tumors showed some overlap with the integrated SV40 T/t-antigen cancer signature observed in TRAMP mice [60]. This signature was predictive for aggressive human breast and lung tumors with a poor prognosis. Prostate tumors of PB-FGFR1 and PB-Myc mice were also subjected to expression profiling, however, again the number of tumors analyzed was very small, making comparison with the data from the present study unreliable [22, 26].

To collect initial information about biological processes associated with tumor development in the *PSA-Cre;PtenloxP/loxP* model, we studied the RNA expression of markers for inflammation, proliferation, apoptosis, senescence and angiogenesis. Confirming and extending data from our previous study [28] we found that cellular proliferation was increased in tumors, but the highest proliferation rate was detected in TC2 samples. Similarly, endothelial cell markers showed higher expression in TC2 samples, indicative of increased angiogenesis. Expression of apoptosis markers was slightly higher in both HP and tumors. These data suggested that TC2 contained most aggressive tumors, which would be in accordance with their histopathologic phenotype.

Based on gene expression profiles and supported by Ingenuity data and Immunohistochemistry (IHC), a large difference between HP and tumor samples was found for genes associated with an inflammatory response. It is increasingly becoming clear that interaction of tumor cells with inflammatory cells occurs frequently, and can even play a role in tumor development. Also in the mouse prostate infiltration of immune cells has been documented [61-64]. In the present study we did not only observe frequent infiltration in prostate tumors but also in HP. There seemed to be a preferency for infiltration of antibody producing cells in TC1 tumors. However, the number

of tumors analyzed should be expended before final conclusions can be drawn. The function of the infiltrating cells in our prostate tumor model is unknown as yet. Potentially these cells and their products might stimulate tumor development and can also be involved in removal of degradation products.

Remarkably, genes involved in the *Trp53* pathway, including senescence markers were the highest expressed in tumors. Previously, it was postulated that senescence regulated by *Trp53* overexpression functioned as a barrier for progression from hyperplasia and PIN to tumor in targeted *Pten* knockout mice [51]. However, the even higher expression of *Trp53* and senescence markers in tumor than in HP, as observed in the present study indicates a more complicated role of these markers in tumor development. It is evident that downregulation of the *Trp53* response seems not a prerequisite for tumor development.

We generated and characterized cell lines derived from tumors to have access to materials that were possibly less heterogeneous and more easy to manipulate in follow up experiments. In all experiments we used early passages of the cell lines to ensure that *in vitro* induced secondary changes were as limited as possible. A drawback of this approach was that probably cell lines were not completely homogeneous. As described in the Results sections, the properties of the cell lines did not reflect these of the predominating growth pattern in the tumor (carcinoma or carcinosarcoma). No doubt, during establishment of the cell lines selection occurred, at least partly due to the composition of the growth medium that selected for epithelial cells. Importantly, genomic analysis showed substantial homogeneity. This offers the opportunity to use genomic DNA or RNA in recently established sequencing methods for identification of additional genomic alterations that might contribute to different steps in tumor development in the mouse model. The heterogeneity of the tumors makes such an approach for *in vivo* collected material less fruitful. Cell lines differed in gene expression, in activation of pAKT and in *in vitro* and *in vivo* biological properties. Previously, cell lines were derived from the TRAMP model, and from the PB-c-Myc model [65, 66]. In contrast to cell lines from *Pten* knockout mice [67, 68], those derived from the TRAMP and PB-c-Myc models were positive for neuroendocrine markers [65, 66]. Cell lines developed from PB-Cre targeted *Pten* knockout mice were resistant to anti-androgens. They formed tumors after subcutaneous transplantation in severe combined immunodeficiency (SCID) mice, just like C1 in our study [67]. Recently, a cell line established from prostate tumors of *PB-Cre;Pten/Trp53* knockout was orthotopically transplanted and showed the capacity to undergo EMT but also to differentiate into cells with either basal or luminal epithelial characteristics [27].

Combined with our data, all findings indicate heterogeneous properties of cell lines, which up to now are difficult to correlate with *in vivo* tumor growth. This might also be true for human prostate cancer cell lines. Extended study of the mouse cell lines will allow further comparison on *in vitro* and *in vivo* growing prostate tumors.

REFERENCES

1. Liu, A.Y., M.P. Roudier, and L.D. True, *Heterogeneity in primary and metastatic prostate cancer as defined by cell surface CD profile.* Am J Pathol, 2004. **165**(5): p. 1543-56.
2. Roudier, M.P., et al., *Phenotypic heterogeneity of end-stage prostate carcinoma metastatic to bone.* Hum Pathol, 2003. **34**(7): p. 646-53.
3. Squire, J.A., et al., *Prostate cancer as a model system for genetic diversity in tumors.* Adv Cancer Res, 2011. **112**: p. 183-216.
4. Markert, E.K., et al., *Molecular classification of prostate cancer using curated expression signatures.* Proc Natl Acad Sci U S A, 2011. **108**(52): p. 21276-81.
5. Lapointe, J., et al., *Gene expression profiling identifies clinically relevant subtypes of prostate cancer.* Proc Natl Acad Sci U S A, 2004. **101**(3): p. 811-6.
6. Tomlins, S.A., et al., *Integrative molecular concept modeling of prostate cancer progression.* Nat Genet, 2007. **39**(1): p. 41-51.
7. Diaz-Cano, S.J., *Tumor heterogeneity: mechanisms and bases for a reliable application of molecular marker design.* Int J Mol Sci, 2012. **13**(2): p. 1951-2011.
8. Taylor, B.S., et al., *Integrative genomic profiling of human prostate cancer.* Cancer Cell, 2010. **18**(1): p. 11-22.
9. Jeronimo, C., et al., *Epigenetics in prostate cancer: biologic and clinical relevance.* Eur Urol, 2011. **60**(4): p. 753-66.
10. Hanahan, D. and R.A. Weinberg, *Hallmarks of cancer: the next generation.* Cell, 2011. **144**(5): p. 646-74.
11. Allen, M. and J. Louise Jones, *Jekyll and Hyde: the role of the microenvironment on the progression of cancer.* J Pathol, 2011. **223**(2): p. 162-76.
12. Shackleton, M., et al., *Heterogeneity in cancer: cancer stem cells versus clonal evolution.* Cell, 2009. **138**(5): p. 822-9.
13. Adams, J.M. and A. Strasser, *Is tumor growth sustained by rare cancer stem cells or dominant clones?* Cancer Res, 2008. **68**(11): p. 4018-21.
14. Kelly, P.N., et al., *Tumor growth need not be driven by rare cancer stem cells.* Science, 2007. **317**(5836): p. 337.
15. Visvader, J.E. and G.J. Lindeman, *Cancer stem cells in solid tumours: accumulating evidence and unresolved questions.* Nat Rev Cancer, 2008. **8**(10): p. 755-68.
16. Yoshimoto, M., et al., *Interphase FISH analysis of PTEN in histologic sections shows genomic deletions in 68% of primary prostate cancer and 23% of high-grade prostatic intra-epithelial neoplasias.* Cancer Genet Cytogenet, 2006. **169**(2): p. 128-37.
17. Zhang, S., et al., *Detection of TMPRSS2 gene deletions and translocations in carcinoma, intraepithelial neoplasia, and normal epithelium of the prostate by direct fluorescence in situ hybridization.* Diagn Mol Pathol, 2010. **19**(3): p. 151-6.
18. Wang, S., et al., *Prostate-specific deletion of the murine Pten tumor suppressor gene leads to metastatic prostate cancer.* Cancer Cell, 2003. **4**(3): p. 209-21.
19. Trotman, L.C., et al., *Pten dose dictates cancer progression in the prostate.* PLoS Biol, 2003. **1**(3): p. E59.
20. Luchman, H.A., et al., *The pace of prostatic intraepithelial neoplasia development is determined by the timing of Pten tumor suppressor gene excision.* PLoS One, 2008. **3**(12): p. e3940.
21. Ratnacaram, C.K., et al., *Temporally controlled ablation of PTEN in adult mouse prostate epithelium generates a model of invasive prostatic adenocarcinoma.* Proc Natl Acad Sci U S A, 2008. **105**(7): p. 2521-6.
22. Ellwood-Yen, K., et al., *Myc-driven murine prostate cancer shares molecular features with human prostate tumors.* Cancer Cell, 2003. **4**(3): p. 223-38.
23. King, J.C., et al., *Cooperativity of TMPRSS2-ERG with PI3-kinase pathway activation in prostate oncogenesis.* Nat Genet, 2009. **41**(5): p. 524-6.

24. Klezovitch, O., et al., *A causal role for ERG in neoplastic transformation of prostate epithelium.* Proc Natl Acad Sci U S A, 2008. **105**(6): p. 2105-10.
25. Tomlins, S.A., et al., *Role of the TMPRSS2-ERG gene fusion in prostate cancer.* Neoplasia, 2008. **10**(2): p. 177-88.
26. Acevedo, V.D., et al., *Inducible FGFR-1 activation leads to irreversible prostate adenocarcinoma and an epithelial-to-mesenchymal transition.* Cancer Cell, 2007. **12**(6): p. 559-71.
27. Martin, P., et al., *Prostate epithelial Pten/TP53 loss leads to transformation of multipotential progenitors and epithelial to mesenchymal transition.* Am J Pathol, 2011. **179**(1): p. 422-35.
28. Ma, X., et al., *Targeted biallelic inactivation of Pten in the mouse prostate leads to prostate cancer accompanied by increased epithelial cell proliferation but not by reduced apoptosis.* Cancer Res, 2005. **65**(13): p. 5730-9.
29. Korsten, H., et al., *Accumulating progenitor cells in the luminal epithelial cell layer are candidate tumor initiating cells in a Pten knockout mouse prostate cancer model.* PLoS One, 2009. **4**(5): p. e5662.
30. Marino, S., et al., *PTEN is essential for cell migration but not for fate determination and tumourigenesis in the cerebellum.* Development, 2002. **129**(14): p. 3513-22.
31. Hermans, K.G., et al., *TMPRSS2:ERG fusion by translocation or interstitial deletion is highly relevant in androgen-dependent prostate cancer, but is bypassed in late-stage androgen receptor-negative prostate cancer.* Cancer Res, 2006. **66**(22): p. 10658-63.
32. Chung, Y.J., et al., *A whole-genome mouse BAC microarray with 1-Mb resolution for analysis of DNA copy number changes by array comparative genomic hybridization.* Genome Res, 2004. **14**(1): p. 188-96.
33. Eisen, M.B., et al., *Cluster analysis and display of genome-wide expression patterns.* Proc Natl Acad Sci U S A, 1998. **95**(25): p. 14863-8.
34. Tusher, V.G., R. Tibshirani, and G. Chu, *Significance analysis of microarrays applied to the ionizing radiation response.* Proc Natl Acad Sci U S A, 2001. **98**(9): p. 5116-21.
35. Marques, R.B., et al., *Androgen receptor modifications in prostate cancer cells upon long-termandrogen ablation and antiandrogen treatment.* Int J Cancer, 2005. **117**(2): p. 221-9.
36. Hermans, K.G., et al., *Truncated ETV1, fused to novel tissue-specific genes, and full-length ETV1 in prostate cancer.* Cancer Res, 2008. **68**(18): p. 7541-9.
37. Rembrink, K., et al., *Orthotopic implantation of human prostate cancer cell lines: a clinically relevant animal model for metastatic prostate cancer.* Prostate, 1997. **31**(3): p. 168-74.
38. Hunt, K.A., et al., *Newly identified genetic risk variants for celiac disease related to the immune response.* Nat Genet, 2008. **40**(4): p. 395-402.
39. Matthews, K.W., S.L. Mueller-Ortiz, and R.A. Wetsel, *Carboxypeptidase N: a pleiotropic regulator of inflammation.* Mol Immunol, 2004. **40**(11): p. 785-93.
40. Park, S.J., et al., *Reverse signaling through the Co-Stimulatory Ligand, CD137L, as a critical mediator of sterile inflammation.* Mol Cells, 2012.
41. Fischer, A., et al., *ZAP70: a master regulator of adaptive immunity.* Semin Immunopathol, 2010. **32**(2): p. 107-16.
42. Shi, L., et al., *Granzyme F induces a novel death pathway characterized by Bid-independent cytochrome c release without caspase activation.* Cell Death Differ, 2009. **16**(12): p. 1694-706.
43. Wing, K., T. Yamaguchi, and S. Sakaguchi, *Cell-autonomous and -non-autonomous roles of CTLA-4 in immune regulation.* Trends Immunol, 2011. **32**(9): p. 428-33.
44. Han, Y., et al., *Connexin43 Expression Increases in the Epithelium and Stroma along the Colonic Neoplastic Progression Pathway: Implications for Its Oncogenic Role.* Gastroenterol Res Pract, 2011. 2011: p. 561719.
45. Jabara, S., et al., *Stromal cells of the human postmenopausal ovary display a distinctive biochemical and molecular phenotype.* J Clin Endocrinol Metab, 2003. **88**(1): p. 484-92.
46. Maresh, E.L., et al., *Differential expression of anterior gradient gene AGR2 in prostate cancer.* BMC Cancer, 2010. **10**: p. 680.

47. Thielen, J.L., et al., *Markers of prostate region-specific epithelial identity define anatomical locations in the mouse prostate that are molecularly similar to human prostate cancers.* Differentiation, 2007. **75**(1): p. 49-61.
48. Xia, H.H., et al., *Aberrant epithelial expression of trefoil family factor 2 and mucin 6 in Helicobacter pylori infected gastric antrum, incisura, and body and its association with antralisation.* J Clin Pathol, 2004. **57**(8): p. 861-6.
49. Jackerott, M., et al., *Trefoil factors are expressed in human and rat endocrine pancreas: differential regulation by growth hormone.* Endocrinology, 2006. **147**(12): p. 5752-9.
50. Peduto, L., et al., *ADAM12 is highly expressed in carcinoma-associated stroma and is required for mouse prostate tumor progression.* Oncogene, 2006. **25**(39): p. 5462-6.
51. Chen, Z., et al., *Crucial role of p53-dependent cellular senescence in suppression of Pten-deficient tumorigenesis.* Nature, 2005. **436**(7051): p. 725-30.
52. Robinson, B.D. and J.I. Epstein, *Intraductal carcinoma of the prostate without invasive carcinoma on needle biopsy: emphasis on radical prostatectomy findings.* J Urol, 2010. **184**(4): p. 1328-33.
53. Henry, P.C. and A.J. Evans, *Intraductal carcinoma of the prostate: a distinct histopathological entity with important prognostic implications.* J Clin Pathol, 2009. **62**(7): p. 579-83.
54. O'Brien, C., et al., *Histologic changes associated with neoadjuvant chemotherapy are predictive of nodal metastases in patients with high-risk prostate cancer.* Am J Clin Pathol, 2010. **133**(4): p. 654-61.
55. Freeman, D., et al., *Genetic background controls tumor development in PTEN-deficient mice.* Cancer Res, 2006. **66**(13): p. 6492-6.
56. Svensson, R.U., et al., *Slow disease progression in a C57BL/6 pten-deficient mouse model of prostate cancer.* Am J Pathol, 2011. **179**(1): p. 502-12.
57. Bianchi-Frias, D., et al., *Genetic background influences murine prostate gene expression: implications for cancer phenotypes.* Genome Biol, 2007. **8**(6): p. R117.
58. Hill, R., et al., *Heterogeneous tumor evolution initiated by loss of pRb function in a preclinical prostate cancer model.* Cancer Res, 2005. **65**(22): p. 10243-54.
59. Elo, T.D., et al., *Stromal activation associated with development of prostate cancer in prostate-targeted fibroblast growth factor 8b transgenic mice.* Neoplasia, 2010. **12**(11): p. 915-27.
60. Deeb, K.K., et al., *Identification of an integrated SV40 T/t-antigen cancer signature in aggressive human breast, prostate, and lung carcinomas with poor prognosis.* Cancer Res, 2007. **67**(17): p. 8065-80.
61. Birbach, A., et al., *Persistent inflammation leads to proliferative neoplasia and loss of smooth muscle cells in a prostate tumor model.* Neoplasia, 2011. **13**(8): p. 692-703.
62. Garlick, D.S., et al., *alpha(V)beta(6) integrin expression is induced in the POET and Pten(pc-/-) mouse models of prostatic inflammation and prostatic adenocarcinoma.* Am J Transl Res, 2012. **4**(2): p. 165-74.
63. Haverkamp, J.M., et al., *An inducible model of abacterial prostatitis induces antigen specific inflammatory and proliferative changes in the murine prostate.* Prostate, 2011. **71**(11): p. 1139-50.
64. Boehm, B.J., et al., *Acute bacterial inflammation of the mouse prostate.* Prostate, 2012. **72**(3): p. 307-17.
65. Watson, P.A., et al., *Context-dependent hormone-refractory progression revealed through characterization of a novel murine prostate cancer cell line.* Cancer Res, 2005. **65**(24): p. 11565-71.
66. Foster, B.A., et al., *Characterization of prostatic epithelial cell lines derived from transgenic adenocarcinoma of the mouse prostate (TRAMP) model.* Cancer Res, 1997. **57**(16): p. 3325-30.
67. Jiao, J., et al., *Murine cell lines derived from Pten null prostate cancer show the critical role of PTEN in hormone refractory prostate cancer development.* Cancer Res, 2007. **67**(13): p. 6083-91.
68. Liao, C.P., et al., *Mouse prostate cancer cell lines established from primary and postcastration recurrent tumors.* Horm Cancer, 2010. **1**(1): p. 44-54.

Supplementary data

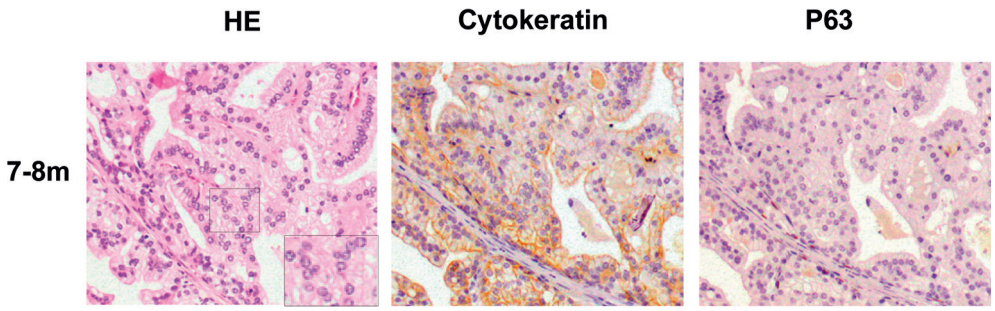

Figure S1. Intraductal carcinoma in prostates of targeted *Pten* knockout mice at 7-8m. An example of the typical histology (HE staining) of IDC in prostates of targeted *Pten* knockout mice at 7-8m is shown. Consecutive sections are stained for P63 and Cytokeratin. Magnification: 200x.

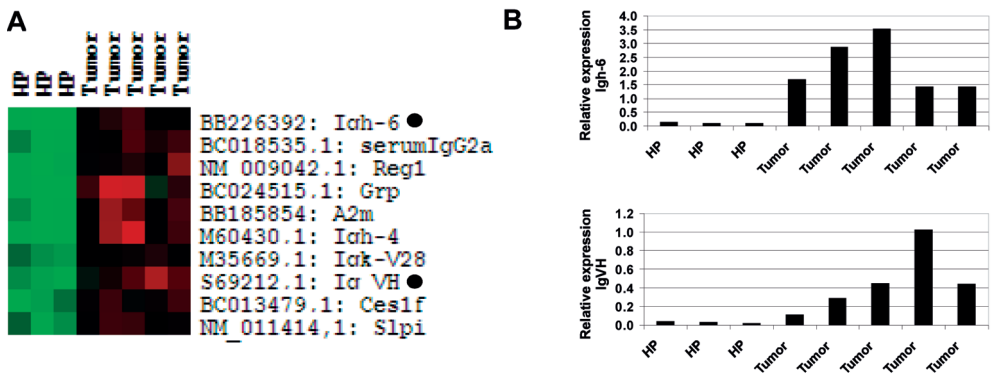

Figure S2. Increased expression of immunoglobulines in prostate tumors of PSA-Cre targeted *Pten* knockout mice. (**A**) Top10 of genes higher expressed in five prostate tumors as compared to HP as identified by SAM (q-value: 0). Black dots indicate *Igh-6* and *IgVH* of which the gene expression in individual samples is shown in (**B**). (**B**) Expression of *Igh-6* and *IgVH* in individual HP samples and prostate tumors. In (**B**) the gene expression was plotted relative to the housekeeping gene *Hprt*.

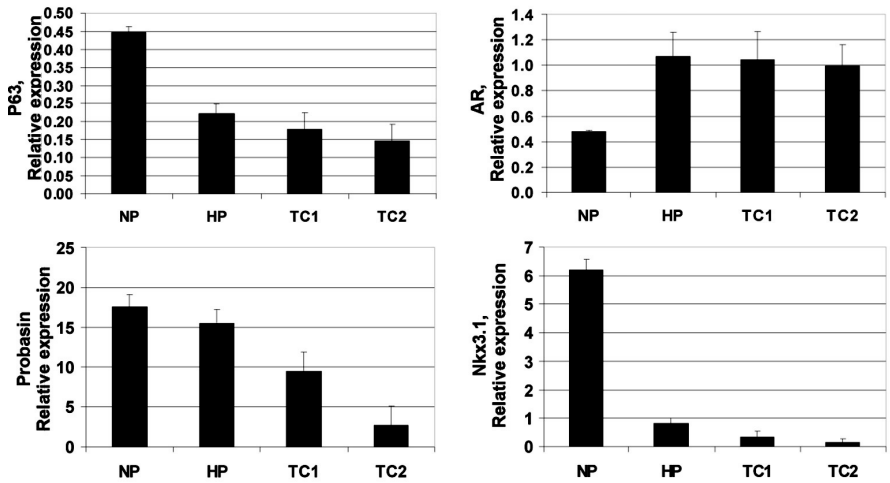

Figure S3. Characterization of TC1 and TC2 prostate tumors. Relative expression of *P63*, *AR*, *Nkx3.1* and *Probasin* in NP, HP, TC1 and TC2 tumors. The gene expression was plotted relative to the housekeeping gene *Hprt*.

Table S1. Primer sequences used for PCR and QPCR analysis.

Gene name	Forward primer	Reverse primer	Application
Pten (exon 5)	5'-TTCCTGAAAGTTAGGCTTCT-3'	5'-GGGAGAAAACCTGTTTCCCA-3'	PCR
Myosin	5'-TTACGTCCATCGTGGACAGC-3'	5'-TGGGCTGGGTGTTAGTCTTA-3'	PCR
Hprt	5'-TCCCTGGTTAAGCAGTACAG-3'	5'-TTCCAGTTTCACTAATGACAC-3'	QPCR
E-cadherin	5'-GGAGGTGGAGAAGAAGACCA-3'	5'-TCGCTGTCGGCTGCCTTCA-3'	QPCR
Snail	5'-CACACGCTGCCTTGTGTCT-3'	5'-TATCTCTTCACATCCGAGTG-3'	QPCR
Nkx3.1	5'-ACTGAACCCGAGTCTGATGC-3'	5'-CTTGGGTTTCGGTGAGTTTG-3'	QPCR

Table S2. Information of antibodies used for immunohistochemistry.

Antibody	Company	Product number	Dilution
BrdU	Biogenex	IIB5	1:150
CD45	DAKO, Glostrup, Denmark	M7019	1:200
CK	DAKO, Glostrup, Denmark	M0701	1:400
P63	DAKO, Glostrup, Denmark	M7247	1:100
Goat Anti-Mouse-biotin	DAKO, Glostrup, Denmark	E0433	1:400
Swine Anti-Rabbit-biotin	DAKO, Glostrup, Denmark	E0431	1:400

Table S3. Significantly differentially expressed genes in HP and prostate tumors of *PSA-Cre;Pten-loxP/loxP* mice as assayed by SAM analysis.

Genes higher expressed in prostate tumors as compared to HP (q-value(%) <7)				
Accession Code	**Gene Name**	**Score(d)**	**Fold Change**	**q-value(%)**
NM_017396,1	Cyp3a41	4.447108451	695.04619	0
BG96196	UNKNOWN	4.023867623	19.2868022	0
BB350820	UNKNOWN	3.914327885	15.8842405	0
BG070282	Cdc14B	3.590402662	14.9654763	0
NM_007675	Ceacam10	3.509129746	24.5517087	0
NM_138648	Olr1	3.495240026	87.657804	0
BB185854	A2m	3.492528038	40.6270629	0
NM_007675,1	Ceacam10	3.412031369	25.5987903	3.782632
NM_030703,1	Cpn1	3.301796273	18.0111988	3.782632
BB745211	UNKNOWN	3.178074122	25.8455542	3.782632
NM_008242,1	Foxd1	3.172342216	8.72977056	3.782632
BC024515,1	Grp	3.1341144	59.325864	3.782632
NM_007423,1	Afp	3.10673406	34.569803	3.782632
BC028507,1	Tnfrsf9	3.011659252	20.458914	3.782632
NM_010374,1	Gzmf	2.955652279	22.47305	3.782632
AI595721	UNKNOWN	2.938292338	64.3889737	6.416964
NM_011474,1	Sprr2h	2.922613888	45.8125846	6.416964
BC024991,1	Prrr5	2.911517428	18.6966944	6.416964
BB129193	Lrp1b	2.907925763	7.59088302	6.416964
BB787829	UNKNOWN	2.898868134	16.4595738	6.416964
NM_009539,1	Zap70	2.896221667	5.02988267	6.416964
AV066880	Mgst2	2.876928021	5.47444121	6.416964
NM_010553,1	Il18rap	2.875665884	7.32648171	6.416964
NM_010375,1	UNKNOWN	2.87008917	26.6601226	6.416964
NM_010088,1	Prl8a2	2.866259102	94.978354	6.416964
NM_010372,1	Gzmd	2.853342688	29.0615324	6.416964
NM_031254,1	Trem2	2.844917936	21.8716249	6.416964
AK016255,1	UNKNOWN	2.844733404	17.9142573	6.416964
BB233467	UNKNOWN	2.816908774	5.97195213	6.416964
NM_010373,1	Gzme	2.81201435	33.1412293	6.416964
NM_019779,1	Cyp11a	2.80141199	36.0757658	6.416964
NM_010373,1	Gzme	2.796870754	26.5781513	6.416964
L25890,1	Ephb2	2.778899073	8.54545775	6.416964
AI551889	UNKNOWN	2.777583556	28.7418368	6.416964
AJ310308,1	Cryaa	2.755483137	52.1469898	6.416964

Table S3. *(Continued)*

Genes higher expressed in prostate tumors as compared to HP (q-value(%) <7)				
Accession Code	**Gene Name**	**Score(d)**	**Fold Change**	**q-value(%)**
BC008152,1	Casp1	2.753533849	9.77033301	6.416964
NM_031198,1	Tcfec	2.733274253	13.839046	6.416964
BE947483	UNKNOWN	2.72038098	9.01485744	6.416964
BB149026	UNKNOWN	2.719421451	18.1854659	6.416964
NM_010372,1	Gzmd	2.712591938	21.0176402	6.416964
L36062,1	Star	2.702566559	69.2837018	6.416964
NM_009529,1	Xmr	2.702376231	88.7987542	6.416964
AW538452	UNKNOWN	2.70050021	6.51163865	6.416964
AI849139	UNKNOWN	2.693111197	8.77416089	6.416964
BB359887	UNKNOWN	2.678776728	17.4057153	6.416964
AV205680	UNKNOWN	2.663658713	11.1354448	6.416964
NM_029509,1	UNKNOWN	2.660232492	4.93686635	6.416964
BM250782	Tnfrsf9	2.651329233	10.3287714	6.416964

Genes higher expressed in HP as compared to prostate tumors (q-value(%) <7)				
Accession Code	**Gene Name**	**Score(d)**	**Fold Change**	**q-value(%)**
NM_008318,1	Ibsp	-3.388208524	0.02149951	5.133571
NM_008932,1	Prlr-rs1	-3.376695635	0.06625841	5.133571
BC024677,1	UNKNOWN	-3.335999223	0.01242106	5.133571
BB701723	UNKNOWN	-3.24783554	0.03826994	5.133571
C79967	UNKNOWN	-3.158494822	0.05739379	5.133571
AI836671	UNKNOWN	-3.145306991	0.04434046	5.133571
BC019528,1	UNKNOWN	-2.941631121	0.04094875	6.844762
AF441863,1	Uts2r	-2.896129324	0.09006397	6.844762
M22959,1	Prlr	-2.853141084	0.06543926	6.844762

Table S4. Full names of genes overexpressed in prostate tumors of *PSA-Cre;Pten-loxP/loxP* mice.

Abbreviation	Gene Name
Cyp3a41	Cytochrome P450, family 3, subfamily a, polypeptide 41A
Cdc14B	Cell division cycle 14 homolog B
Ceacam10	Carcinoembryonic antigen-related cell adhesion molecule 10
Olr1	Oxidized low density lipoprotein (lectin-like) receptor 1
A2m	Alpha-2-macroglobulin
Cpn1	Carboxypeptidase N, polypeptide 1
Foxd1	Forkhead box D1
Grp	Gastin-releasing peptide
Afp	Alpha fetoprotein
Tnfrsf9	Tumor necrosis factor receptor superfamily, member 9
Gzmf	Granzyme F
Sprr2h	Small proline-rich protein 2H
Prrr5	Proline rich 5
Lrp1b	Low density lipoprotein receptor-related protein 1B
Zap70	Zeta-chain (TCR) associated protein kinase 70kDa
Mgst2	Microsomal glutathione S-transferase 2
Il18rap	Interleukin 18 receptor accessory protein
Prl8a2	Prolactin family 8, subfamily a, member 2
Gzmd	Granzyme D
Trem2	Triggering receptor expressed on myeloid cells 2

Table S5. Full names of genes overexpressed in TC1 tumors of *PSA-Cre;Pten-loxP/loxP* mice.

Abbreviation	Gene Name
Angl	Angiogenin-like
Msmb	Beta-microseminoprotein
Fabp1	Fatty acid binding protein 1, liver
Ambp	Alpha 1 microglobulinbikunin
Tff2	Trefoil factor 2
Recgl5	RecQ protein-like 5
Sftpd	Surfactant associated protein D
Ces3	Carboxylesterase 3
Cals1	Carbonic anhydrase-related polypeptide
Noxo1	NADPH oxidase organizer 1
Sult1c1	Sulfotransferase family, cytosolic, 1C, member1
Agr2	Anterior gradient 2
Eps8l1	EPS8-like 1
Fam25C	Family with sequence similarity 25, member C
Gsta3	Glutathione S-transferase, alpha 3
Timp4	Tissue inhibitor of metalloproteinase 4
Apof	Apolipoprotein F
Msa1	Sall-3 like
Rdh9	Retinol dehydrogenase 9
Chod1	Chondrolectin

Table S6. Full names of genes overexpressed in TC2 tumors of *PSA-Cre;Pten-loxP/loxP* mice.

Abbreviation	Gene Name
Star	Steroidogenic acute regulatory protein
Adamts3	A disintegrin-like and metallopeptidase (reprolysin type) with thrombospondin type 1 motif, 3
Ptn	Pleiotrophin
Cryaa	Alpha-A-crystallin
Adam12	A disintegrin and metalloprotease domain 12
Raet1a	Retinoic acid early transcript 1, alpha
Drd4	Dopamine receptor 4
Carpb2	Cellular retinoic acid-bindingprotein 2
Cyp3a41	Cytochrome P450, steroid inducible 3a41
Gabrg1	Gamma-aminobutyric acid A receptor gamma 1subunit
Xlr	X-linked lymphocyte-regulated complex
Calcb	Calcitonin-related polypeptide, beta
Folh1	Folate hydrolase
Htr2b	5-hydroxytryptamine (serotonin) receptor 2B
Pth1h	Parathyroid hormone-like peptide
Cthrc1	Collagen triple helix repeat containing protein
Sprr2h	Small proline-rich protein 2H
Gja1	Gap junction membrane channel protein alpha 1
Cyp11b1	Cytochrome P450, family 11, subfamily b, polypeptide 1
Prg	Progesteron receptor

CHAPTER 4

Metastatic, chromosomal instable prostate cancer by *Trp53* inactivation in a targeted *Pten* knockout mouse prostate cancer model

Hanneke Korsten[1], Angelique Ziel-van der Made[1], Karin Hermans[1], Arno van Leenders[1], Theo van der Kwast[1], Xiaoqian Ma[1], Corrina de Ridder[2], Robert Kraaij[2], Alex Nigg[1], Jan Trapman[1]

Department of Pathology[1] and Urology[2], Josephine Nefkens Institute, Erasmus MC, Rotterdam, The Netherlands

In preparation

ABSTRACT

PTEN and *TP53* are frequently inactivated in clinical prostate cancer. We used genetically modified mouse models to study the role of *Trp53* inactivation in mouse prostate cancer induced by *Pten* inactivation. Previously, we showed that *PSA-Cre;Pten-loxP/loxP* mice developed prostate cancer in well defined progressive steps. Sole *Trp53* inactivation in *PSA-Cre;Trp53-loxP/loxP* mice induced in the prostate small foci of atypical cells at >11m that never progressed to cancer. These atypical cells expressed the same markers as luminal epithelial cells in the proximal region of the normal adult mouse prostate and as rare luminal epithelial progenitor cells in the more distal prostate. Targeted inactivation of one or two *Trp53* alleles in *PSA-Cre;Pten-loxP/loxP* mice accelerated development of a heterogeneous aggressive prostate cancer. In contrast to *PSA-Cre;Pten-loxP/+* mice, *PSA-Cre;Pten-loxP/+;Trp53-loxP/loxP* mice developed prostate cancer with or without inactivation of the second *Pten* allele. Compared to *Pten* knockout tumors, double *Pten*/*Trp53* knockout prostate tumors showed several important additional hallmarks of cancer. Most prominent is genomic instability, accompanied by overexpression of genes involved in cell cycle regulation. Importantly, in contrast to *Pten* knockout tumors, *Pten/Trp53* prostate tumors were metastatic. Cell lines derived from the tumors showed a high capacity to grow in soft agar, formed irregular colonies in 3D culture and *in vivo* tumors if orthotopically transplanted in immunocompetent mice. The cell lines derived from *Pten/Trp53* prostate tumors retained at least part of the gene expression profile of *in vivo* tumors, particularly high expression of genes induced by *Trp53* deletion. Genomic instability of the cell lines affected many different chromosomes but most frequently 4, 7 and 15. The combined *in vivo* and *in vitro* models are excellent tools to investigate the effect of *Trp53* inactivation in a well-defined tumor model. Moreover, they can function as preclinical models of late stage prostate cancer.

INTRODUCTION

PTEN and *TP53* are the most frequently inactivated genes in human tumors. Carriers of germ line mutations in *PTEN* or *TP53* develop the cancer susceptibility syndromes Cowden disease, and Li-Fraumeni syndrome, respectively [1-4]. *In vitro* and *in vivo* studies have shown that PTEN can modulate many cellular functions, including proliferation, apoptosis, DNA damage response, cell size, metabolism, senescence, polarity, migration, stem cell renewal and angiogenesis [2, 5-9]. The best characterized function of P53 is that of cell cycle regulator, including induction of senescence to allow DNA repair during mitosis, and induction of apoptosis to remove severely damaged cells [10-12]. Recently, there is a revival of the interest in the function of P53. It has been recognized that the function of P53 is even more complex than originally thought, and might also include stem cell regulation, development and metabolism [12-16].

Prostate cancer is a heterogeneous disease that, if metastasized cannot be cured. Improved characterization of late stage prostate cancer will contribute to development of more effective therapy. Frequent mono-allelic *PTEN* inactivation mostly by loss of a small genomic region on 10q has been reported in early stages of clinical prostate cancer [17-19]**.** Complete *PTEN* inactivation is found in late stage progressive disease [20-23]. Partial or complete inactivation of *TP53* is also associated with advanced disease [21, 24-26].

Several different *Pten* knockout mouse models of prostate cancer have been developed during the last decade. Conventional *Pten-/-* mice are embryonal lethal, but *Pten+/-* mice develop hyperplastic and dysplastic lesions in several tissues, including the prostate [27, 28]. Prostate-targeted models have been based on Cre expression driven by the prostate-specific PB, PSA and Nkx3.1 promoter [29-31]. In all models complete *Pten* inactivation leads to hyperplasia and prostate tumor development with absence of or low frequency of metastasis [29, 30, 32, 33]. Importantly, tumor initiating cells and dynamics of tumor development are different in the various models. In the PSA-Cre driven targeted *Pten* model prostate tumors developed from a luminal epithelial progenitor cell followed by well-defined stages of hyperplasia and tumor progression [29, 34] (Korsten, Chapter 3).

Conventional *Trp53* knockout mice develop almost normal but are more susceptible to develop spontaneous tumors, mainly lymphomas and soft tissue sarcomas [13, 35]. Conflicting data have been described of the effect of targeted *Trp53* inactivation on epithelium of the prostate, ranging from absence of histological abnormalities to dysplastic lesions with nuclear atypia [36, 37].

In targeted mouse prostate cancer models *Trp53* inactivation combined with *Rb1* and *Brca2* inactivation accelerates tumor development [36, 38]. Also, in *Pten* knockout models acceleration of prostate tumor development by *Trp53* inactivation has been described [37, 39-41]. However,

others reported that the effect of *Trp53* inactivation on prostate cancer development in *Pten* knockout mice is limited [39].

In the present study, we systematically characterized prostate tumors that developed by *PSA-Cre* driven targeted mono-allelic and bi-allelic *Trp53* and *Pten* inactivation in the mouse prostate. Moreover, we generated and investigated the properties of novel cell lines derived from the tumors. In this *Pten* kockout model model systems inactivation of *Trp53* not only accelerated prostate cancer development but also induced metastatic disease. Although heterogeneous, most double knockout tumors showed altered expression of genes involved in many key processes of tumor development, including cell cycle regulation. Importantly, *Trp53* inactivation also induced prostate cancer in mono-allelic *Pten* knockout mice. Most prominent differences in the double knockout cell lines compared to *Pten* knockout cell lines are overexpression of mitotic checkpoint control genes and chromosomal instability, and *in vitro* and *in vivo* tumorigenic properties. The models developed and characterized in this study contribute to elucidation of the role of *Trp53* inactivation in the presence of *Pten* activation.

MATERIALS AND METHODS

Generation of targeted *Pten/Trp53* knockout mice

The generation of *PSA-Cre* mice (strain FVB), mice carrying *Pten-loxP* or *Trp53-loxP* alleles (strain 129Ola) and targeted *Pten* knockout mice have been described previously [29, 34, 42, 43]. To generate mice with targeted *Pten/Trp53* inactivation, *Pten-loxP/loxP;Trp53-loxP/loxP* mice were crossed with *PSA-Cre* mice. By subsequent breeding of *PSA-Cre;Pten-loxP/+Trp53-loxP/+* F1 offspring with *Pten-loxP/loxP;Trp53-loxP/loxP* mice, mice with different genotypes were generated. *Cre* negative littermates were kept as controls. Mice were housed according to institutional guidelines, and procedures were carried out in compliance with the standards for use of laboratory animals. Mice were sacrificed at 4-5m, 7-8m, 11-12m and >14m. An overview of the number of mice that we sacrificed or found dead per genotype per time point is given in Table S1. The animal experiments performed in this study have been approved by the animal experimental committee of Erasmus Medical Centre (DEC-consult Erasmus MC project 106-03-02).

Genomic DNA analyses

Procedures for genotyping and DNA recombination PCR were described previously [29]. Detection of allelic loss in genomic DNA of tumor cell lines was done by standard PCR. DNA sequencing was described previously [44]. The sequences of the primers used for DNA recombination PCR, detection of allelic and sequencing are given in Table S2.

RNA extraction, QPCR analysis and cDNA microarray analysis

Procedures for RNA isolation, cDNA preparation and QPCR analysis were as described [34, 45]. Primer sequences are given in Table S2. Methods used for transcription profiling on mouse cDNA microarrays (NKI, Amsterdam, The Netherlands) were described previously [34, 46]. For unsupervised hierarchical clustering the programs Cluster and Treeview were used [47]. Criteria for clustering analyses were 100% signal and at least 2 observations of log2 |1|. By SAM (Significance Analysis of Microarrays) differentially expressed genes with a q-value of 0% were ordered [48].

Histology, immunohistochemistry and analysis of proliferation and apoptotic rate

Procedures for immunohistochemistry were as described [34]. Detailed antibody information is given in Table S3. Procedures measuring the *in vivo* cell proliferation and the apoptotic index were also described earlier [29]. The percentages BrdU positive cells and Caspase-3 positive cells were counted for 500 and 1000 luminal epithelial cells, respectively.

Cell culture, arrayCGH analysis, *in vitro* biological assays and orthotopic transplantation studies

To generate cell cultures minced prostate tissue was incubated for 1h in Collagenase A solution (250U/ml, Roche, Mannheim, Germany). Single cells were isolated and cultured under standard conditions. The composition of the culture medium was described previously [49].

The whole-genome mouse BAC microarrays used for array-based comparative genomic hybridization (arrayCGH) analysis were described previously [50]. Protocols for DNA isolation, DNA labeling, hybridization and analysis of microarrays were published previously [44]. Mouse Hybloc was used to block unspecific hybridization.

The procedure for the soft agar assay was described earlier [51]. The soft agar data were analyzed using the KS-400 image analysis package (Carl Zeiss Microimaging, Inc.). For three dimentional cell culture 10^4 cells were suspended in 0.4 ml matrigel (354234, BD Biosciences, Franklin lakes, NJ) and poured on top of a thin layer of matrigel. After two hours at 37ºC, culture medium was added and cells were incubated at 37ºC.

The procedures for orthotopic growth of prostate cancer cell line on mice with a mixed genetic background (129Ola/FVB) were essentially as described previously [52]. In each prostate 10^6 cells were injected.

Statistics

The Mann-Whitney U test was applied for statistical analyses.

RESULTS

Prostate-specific *Pten* and *Trp53* inactivation

In Supplementary Figure S1A the strategy for inactivation of both *Pten* and *Trp53* is schematically illustrated [29, 43]. Using Cre expression driven by the PSA promoter/enhancer and LoxP recombination, *Pten* exon 5 was deleted. Similarly, *Trp53* recombination deletes exons 2-10. Targeted *Pten* and *Trp53* inactivation in the prostate was very efficient in all mice (Figure S1B). In a proportion of the *Pten* and *Pten/Trp53* negative mice *Pten* and *Trp53* recombination in the adrenal gland was noticed. In *Pten/Trp53* double knockout mice also rare recombination of both genes in the salivary gland and the skin was detected (data not shown).

Targeted *Trp53* inactivation resulted in foci of atypical Clu^{+}Tacstd2^{+}Sca-1^{+} luminal epithelial cells

Sole targeted *Trp53* inactivation did not affect the overall morphology or weight of the prostate. However, at older age (>11m) in prostates of *PSA-Cre;Trp53-loxP/loxP* and *PSA-Cre;Trp53-loxP/+* mice foci of compact atypical luminal epithelial cells were observed and cells with enlarged atypical nuclei were detected (Figure 1A and data not shown). These lesions were also occasionally seen in old control mice although at a much lower frequency. None of the *PSA-Cre* targeted *Trp53* knockout mice developed prostate cancer.

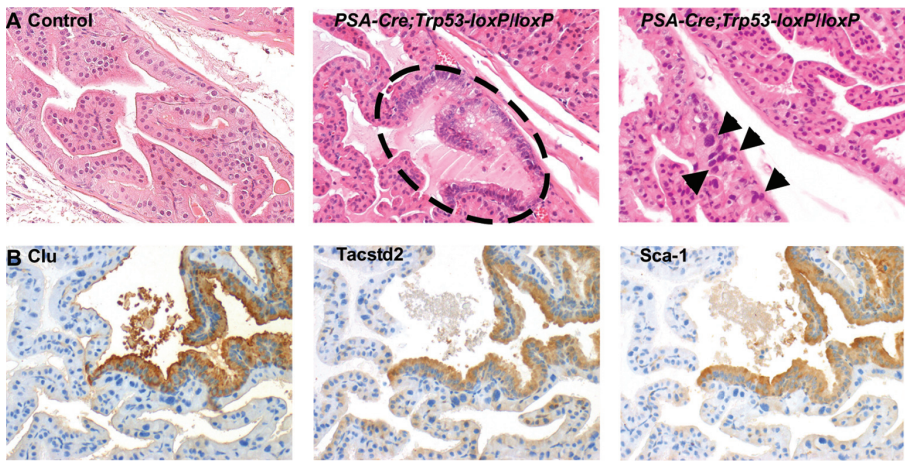

Figure 1. The characterization of dysplastic foci in prostates of *PSA-Cre* targeted *Trp53* knockout mice at older age (>11m). (**A**) Prostate histology of control mice, *PSA-Cre;Trp53-loxP/loxP* and *PSA-Cre;Trp53-loxP/+* mice at >11m. Examples of atypical foci are shown, such as a focus of compact dysplastic cells in a *PSA-Cre;Trp53-loxP/loxP* mouse (indicated by a dashed line) and dysplastic cells with atypical nuclei (indicated by arrowheads) in a *PSA-Cre;Trp53-loxP/+* mouse of >11m. (**B**) Expression of luminal epithelial progenitor cell markers Clusterin (Clu), Tacstd2 and Sca-1 in dysplastic foci in prostates of aged *PSA-Cre* targeted *Trp53* knockout mice.

Previously, we showed that targeted *Pten* inactivation leads to accumulation of hyperplastic $Clu^+Tacstd2^+Sca\text{-}1^+$ luminal epithelial progenitor cells in the distal prostate [34]. Luminal epithelial cells with a similar marker expression were also present in the proximal region of the normal prostate. Interestingly, immunohistochemical analysis of foci of compact atypical cells in prostates of *Trp53* knockout mice showed that these cells expressed the same markers, indicative of an association between these different cell types (Figure 1B). Staining of tissue sections for expression of the luminal epithelial progenitor cell markers Clu, Sca-1 and Tacstd2 even more clearly revealed the atypical foci in prostates of *Trp53* knockout mice. In essentially all prostates of *PSA-Cre;Trp53-loxP/loxP* mice these $Clu^+Tacstd2^+Sca\text{-}1^+$ foci were detected at >11m, and these foci were observed in ~50% of the prostates of *PSA-Cre;Trp53-loxP/+* mice at this age. In ~15% of the prostates from control mice similar but considerably smaller atypical foci were observed (data not shown).

Targeted *Trp53* inactivation in *PSA-Cre;Pten-loxP/loxP* mice accelerates prostate tumor development

Next, the effect of targeted *Trp53* inactivation on prostate tumor development in bi-allelic *Pten* knockout mice was studied. As described previously, at 4-5m prostate lobes of *PSA-Cre;Pten-loxP/loxP* mice were filled with a homogeneous population of hyperplastic cells [29, 34]. These hyperplastic prostate lesions progressed to lesions resembling human intraductal carcinoma (IDC). At 10m or older, morphologically heterogeneous invasive prostate tumors developed in all *PSA-Cre;Pten-loxP/loxP* [29] (Korsten et al., in preparation). These tumors can be subdivided in carcinoma (IDC, adenocarcinoma and undifferentiated carcinoma) and carcinosarcoma.

Complete *Trp53* inactivation in targeted bi-allelic *Pten* knockout mice resulted in a marked acceleration of prostate tumor development. Although at 4-5m no significant differences in prostate weights were detected between *PSA-Cre;Pten-loxP/loxP* and *PSA-Cre;Pten-loxP/loxP;Trp53-loxP/loxP* mice, in prostates of bi-allelic double knockout mice, cells with atypical nuclei and foci of cells resembling human IDC were identified (Figure 2A,C). At 7-8m, complete *Trp53* inactivation in *PSA-Cre;Pten-loxP/loxP* mice resulted in invasive prostate tumors in all mice, accompanied by a significant increase in prostate weight ($P<0.01$) (Figure 2A,C). Like in bi-allelic *Pten* knockout mice at 10m or older (Korsten, in preparation), prostate tumors in the double knockout mice were heterogeneous and had characteristics of differentiated and undifferentiated carcinoma and of carcinosarcoma. Because of accelerated formation of aggressive tumors lead to rapid animal death, double knockout mice were all sacrificed at 7-8 m.

Similar to complete *Trp53* inactivation, inactivation of one *Trp53* allele in *PSA-Cre;Pten-loxP/loxP* mice accelerated prostate tumor development, although the effect was less pronounced (Figure 2A-C). Four out of 13 *PSA-Cre;Pten-loxP/loxP;Trp53-loxP/+* mice developed invasive

prostate tumors at 7-8m. At older age (>11m) invasive prostate tumors were observed in all *PSA-Cre;Pten-loxP/loxP;Trp53-loxP/+* mice (n=20).

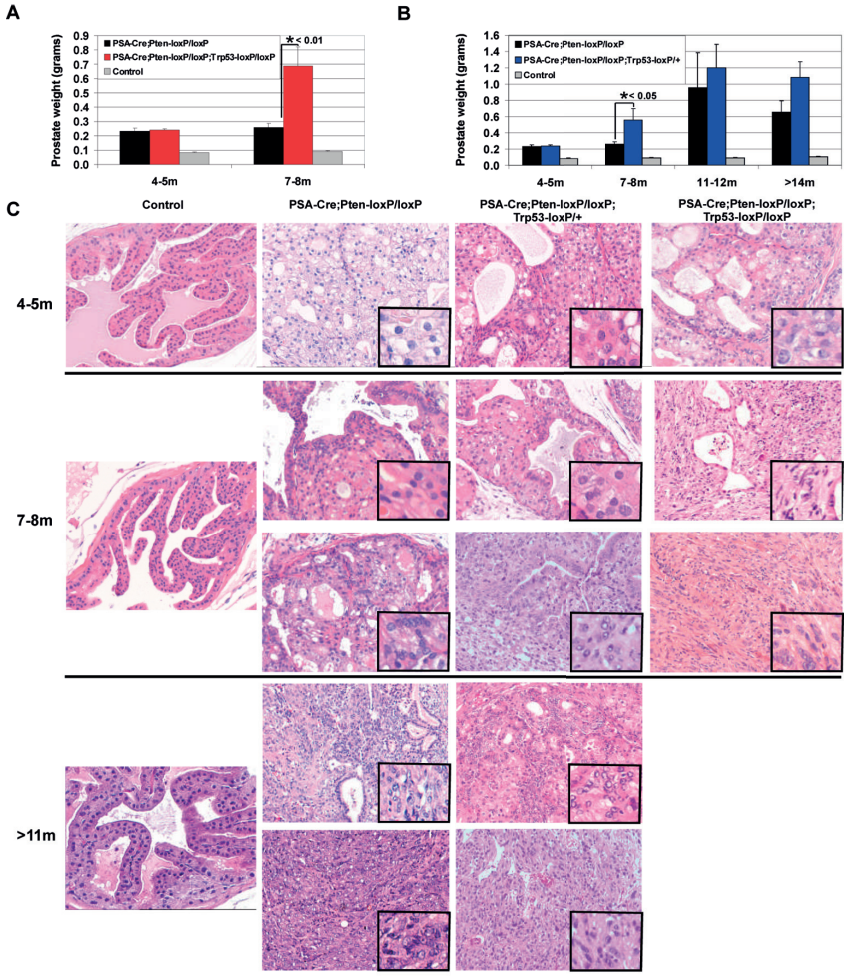

Figure 2. *Trp53* inactivation in *PSA-Cre;Pten-loxP/loxP* mice accelerates prostate tumor development. (**A**) Prostate weights of control mice, *PSA-Cre;Pten-loxP/loxP* and *PSA-Cre;Pten-loxP/loxP;Trp53-loxP/loxP* mice at 4-5m and 7-8m. Note that a statistically significant difference in prostate weight ($p<0.01$) was measured at 7-8m between *PSA-Cre;Pten-loxP/loxP* and *PSA-Cre;Pten-loxP/loxP;Trp53-loxP/loxP* mice. (**B**) Prostate weights of control mice, *PSA-Cre;Pten-loxP/loxP* and *PSA-Cre;Pten-loxP/loxP;Trp53-loxP/+* mice at 4-5m, 7-8m, 11-12m and >15m. Here the prostate weights of *PSA-Cre;Pten-loxP/loxP* and *PSA-Cre;Pten-loxP/loxP;Trp53-loxP/+* mice were statistically significant different at 7-8m ($p<0.05$). (**C**) Representative examples of the prostate histology of control mice, *PSA-Cre;Pten-loxP/loxP*, *PSA-Cre;Pten-loxP/loxP;Trp53-loxP/+* and *PSA-Cre;Pten-loxP/loxP;Trp53-loxP/loxP* mice at 4-5m, 7-8m and >11m. Enlarged pictures show that nuclei in prostates of *PSA-Cre;Pten-loxP/loxP*, *PSA-Cre;Pten-loxP/loxP;Trp53-loxP/+* and *PSA-Cre;Pten-loxP/loxP;Trp53-loxP/loxP* mice become atypical with prominent micronuclei during tumorigenesis.

The acceleration of prostate tumor development by inactivated *Trp53* was accompanied by a slightly higher proliferation rate, as assessed by BrdU incorporation (Figure S2, 7-8m), but the apoptotic rate, as determined by active Caspase 3 staining, was not significantly affected (Figure S2, 7-8m). As shown in Figure S2 and previously published [29] sole *Pten* inactivation strongly stimulated the proliferation and apoptotic rates of cells in hyperplastic prostates and in prostate tumors as compared to normal prostates. Although prostate tumors in targeted *Pten/Trp53* mice developed earlier, after tumor development *Trp53* inactivation had no additional effect on the proliferation and apoptotic rate in prostate tumors. In summary, our data showed that *Trp53* inactivation accelerated prostate tumorigenesis in bi-allelic *Pten* knockout mice. This process depends on the number of *Trp53* gene copies inactivated.

Bi-allelic *Trp53* inactivation in mono-allelic *Pten* knockout mice can induce prostate cancer

Previously, we showed that *PSA-Cre;Pten-loxP/+* mice developed small hyperplastic foci at old age [29, 34]. The effect of inactivation of one *Trp53* allele in prostates of these mono-allelic *Pten* knockout mice was small. In prostates from mice of this genotype a mixture of hyperplastic cells and dysplastic cells with atypical nuclei could be detected. The prostate weight was not increased. In contrast, bi-allelic prostate-specific *Trp53* inactivation in *PSA-Cre;Pten-loxP/+* mice induced prostate tumor development in two out of five mice at >14m (mouse 4 and 5, Figure 3A). Tumor 5 was a large undifferentiated carcinosarcoma and tumor 4 had characteristics of a more differentiated carcinoma including IDC (Figure 3A,B). The other three mice at this age showed less prominent histological abnormalities of the prostate, including hyperpastic and dysplastic foci, but not cancer (Figure 3A, mouse 3). The weights of prostates 4 and 5 was strongly increased, moreover, prostate cells showed a higher proliferation and apoptotic rates as compared to the other three prostates (Figure 3B).

From tumors 4 and 5 *in vitro* growing cell lines were generated. PCR analysis of DNA isolated from these cell lines showed that in the tumor cell line derived from tumor 5 not only the floxed *Pten* allele but also the wild type *Pten* allele was deleted (Figure 3C). In line with this finding, *Pten* expression was at a similar low level as in tumors from *PSA-Cre;Pten-loxP/loxP* control bi-allelic knock-out mice (Figure 3D). In tumor 4, the wild type *Pten* allele was retained and *Pten* mRNA expression level was clearly higher than in complete *Pten* knockout mice, and approximately half of the expression in a normal control prostate (Figure 3D). Sequencing of the *Pten* open reading frame in the cell line derived from tumor 4 did not show any mutations. Together these data indicate that complete *Pten* inactivation can occur, but is not a prerequisite for tumor development in *PSA-Cre;Pten-loxP/+;Trp53-loxP/loxP* mice.

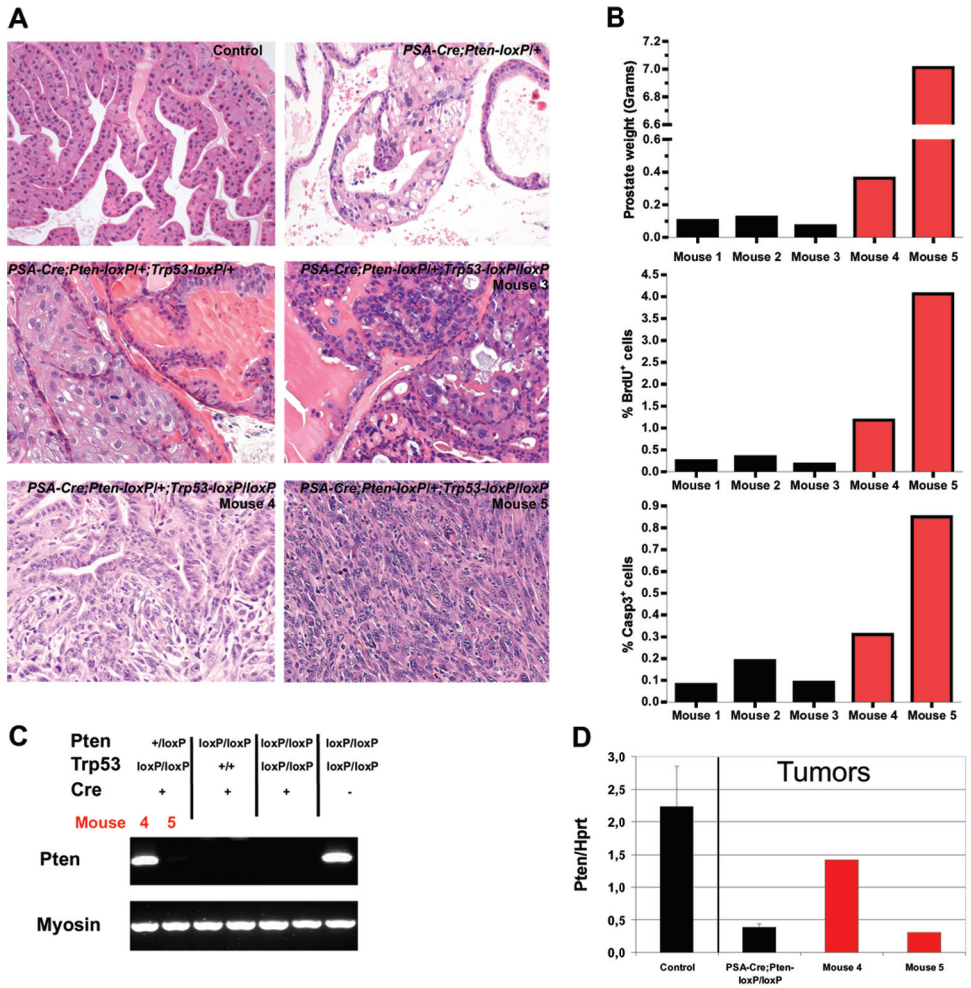

Figure 3. Complete *Trp53* inactivation in *PSA-Cre;Pten-loxP/+* mice can result in prostate tumor development. (**A**) Prostate histology of control mice, *PSA-Cre;Pten-loxP/+*, *PSA-Cre;Pten-loxP/+;Trp53-loxP/+* and *PSA-Cre;Pten-loxP/+;Trp53-loxP/loxP* mice at >14m. Note that prostate lesions observed in prostates of *PSA-Cre;Pten-loxP/+;Trp53-loxP/loxP* mice vary from dysplastic foci to invasive prostate cancer. (**B**) The prostate weights, proliferation rates (% BrdU+ cells) and apoptotic rates (% Active Caspase-3+ cells) of prostates of five *PSA-Cre;Pten-loxP/+;Trp53-loxP/loxP* mice at >14m. Mouse 4 and 5, indicated by red bars, developed prostate tumors. (**C**) PCR analysis of DNA isolated from cell lines generated from the prostate tumors of mouse 4 and 5 (*PSA-Cre;Pten-loxP/+;Trp53-loxP/loxP* mice), *PSA-Cre;Pten-loxP/loxP* and *PSA-Cre;Pten-loxP/loxP;Trp53-loxP/loxP* mice. As a control a wild type cell line was included. Note that in tumor cells of mouse 5 the wild type *Pten* allele was lost. (**D**) *Pten* expression in prostates of control mice and prostate tumors of *PSA-Cre;Pten-loxP/loxP* mice, mouse 4 and mouse 5.

Trp53 inactivation in targeted *Pten* knockout mice promoted the development of prostate cancer metastases

As reported previously, *PSA-Cre;Pten-loxP/loxP* mice rarely developed metastases [29]. However, in the present study prostate cancer metastases were readily detected in a proportion of *PSA-Cre;Pten-loxP/loxP;Trp53-loxP/+*, *PSA-Cre;Pten-loxP/loxP;Trp53-loxP/loxP* and *PSA-Cre;Pten-loxP/+;Trp53-loxP/loxP* mice (Figure 4A). The percentage of metastases in the mice of different genotypes varied considerably, possibly due to the differences of the ages at which the mice were sacrificed. An overview of all metastases detected is given in Table S4. Note that *PSA-Cre;Pten-loxP/loxP;Trp53-loxP/loxP* mice were always sacrificed at 7-8 months, and other genotypes at older ages. Most metastases were found in the abdominal cavity. In three mice, regional lymph node metastases were detected. Two mice developed lung metastases and in one *PSA-Cre;Pten-loxP/loxP;Trp53-loxP/loxP* mouse metastasized prostate cancer cells were found in the liver (Table S4). The morphology of distant metastases resembled the corresponding primary tumor. In all cases tumors and metastases presented as undifferentiated carcinoma or as carcinosarcoma (see Figure 4B). There was no correlation between the size of the primary tumor and the occurrence of metastases at the time of sacrificing (data not shown).

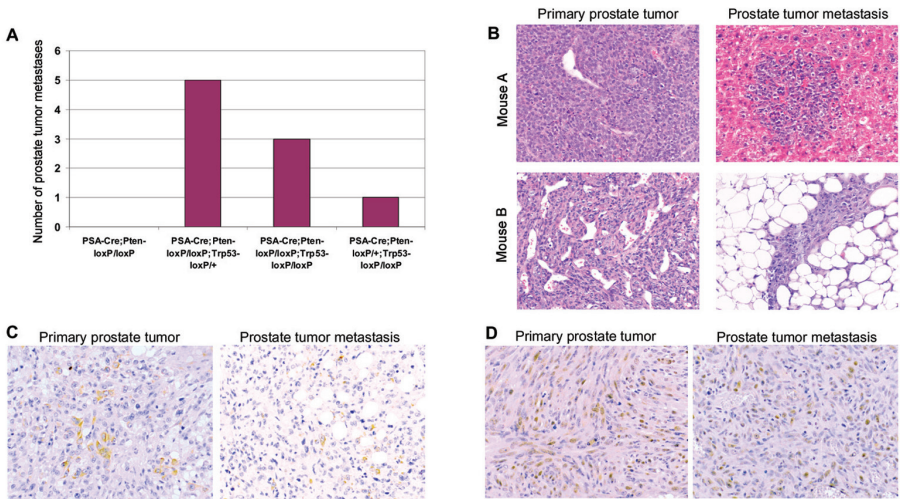

Figure 4. *Trp53* inactivation in targeted bi-allelic *Pten* knockout mice promotes the development of prostate cancer metastases. (**A**) The total number of prostate cancer metastases in *PSA-Cre;Pten-loxP/loxP*, *PSA-Cre;Pten-loxP/loxP;Trp53-loxP/+*, *PSA-Cre;Pten-loxP/loxP;Trp53-loxP/loxP* and *PSA-Cre;Pten-loxP/+;Trp53-loxP/loxP* mice. Note that prostate metastases were exclusively detected in mice with targeted inactivation of both *Pten* and *Trp53*. (**B**) Examples of the histology of the primary prostate tumors and its metastases. The prostate tumor of mouse A was metastasized to the liver, whereas the metastasis of the tumor in mouse B was found in the abdominal cavity. Cytokeratin (**C**) and Androgen Receptor (AR) (**D**) staining of a primary prostate tumor and its metastasis shows a similar staining pattern of both markers in these tumor samples.

To confirm that distant metastases were derived from prostate cancer, we performed immunohistochemical staining for the luminal epithelial cell marker Cytokeratin 8 (CK8) and for Androgen Receptor (AR). The primary tumors and metastases showed a similar heterogeneous expression pattern for these markers (Figure 4C,D). We were able to determine of the lymph node metastasis of one *PSA-Cre;Pten-loxP/loxP;Trp53-loxP/loxP* mouse the gene expression profile in cDNA expression arrays. A striking similarity in gene expression was observed between the primary prostate tumor and its metastasis (data not shown). Because adrenal gland tumors might develop in *PSA-Cre;Pten-loxP/loxP;Trp53-loxP/+* mice, we also stained the metastases for the adrenal markers synaptophysin (SYP) and Tyrosine Hydroxylase (TH) [53, 54]. However, although adrenal tumors were positive, the primary prostate tumors and the metastases were negative for these markers (data not shown).

Gene expression profiling of prostate tumors from *Pten/Trp53* knockout mice showed molecular heterogeneity

To study the molecular effects of *Trp53* inactivation in the *Pten* knockout mice, we compared the gene expression profiles in normal prostates, in hyperplastic prostates and in tumors from mice with the double knockout genotype. We added to the analyses the prostate tumors derived from the two *PSA-Cre;PtenloxP/+;Trp53loxP/loxP* mice.

Unsupervised hierarchical clustering of prostate gene expression profiles from 4-5m old mice with different genotypes separated into two clusters, one specific for prostates of control mice and *Trp53* knockout mice and a second cluster of genes expressed in prostates of *PSA-Cre;Pten-loxP/loxP* and *PSA-Cre;Pten-loxP/loxP;Trp53-loxP/loxP* mice (Figure S3A). As shown, at this age as compared to *Pten* inactivation, *Trp53* inactivation hardly affected the gene expression profile in prostates of *Pten* knockout mice, except for differential expression of *Trp53* and its direct target genes, like *Cdkn1a* and *Bax* (Figure S3B). An effect of sole *Trp53* inactivation on the gene expression profile in prostates was even less (data not shown). This was probably due to the lower number of *Trp53* negative cells in prostates of *PSA-Cre;Trp53-loxP/loxP* mice as compared to the much higher percentage of *Trp53* negative hyperplastic cells accumulating in prostates of *PSA-Cre;Pten-loxP/loxP;Trp53-loxP/loxP* mice.

Clustering of expression array data of prostate tumors from *Pten/Trp53* double knockout mice at 8m or older clearly showed tumor heterogeneity (Figure 5A). Two main clusters could be discriminated, indicated in red, orange and black for different subgroups in one cluster and yellow, in the second cluster, respectively. The different clusters did not separate according to genotype: *PSA-Cre;Pten-loxP/loxP;Trp53-loxP/loxP* mice and *PSA-Cre;Pten-loxP/loxP;Trp53-loxP/+* mice were present in both clusters. The two available tumors from *PSA-Cre;Pten-loxP/+;Trp53-loxP/loxP* mice were in the first cluster.

Adding array data from prostate tumors of *PSA-Cre;Pten-loxP/loxP* mice that were *Trp53* wild type showed a similar complex pattern (Figure 5B), although part of the original profile shown in Figure 5A remained intact. Now, three main clusters could be separated, denoted I, II and III. Cluster III was separated into the subgroups A and B. Although three *Pten* negative tumors without *Trp53* inactivation clustered with the *Pten/Trp53* negative tumors in I, most prostate tumors of *PSA-Cre;Pten-loxP/loxP* mice were in II. PCR analysis of genomic DNA of prostate cancer cell lines derived from prostate tumors of the three *PSA-Cre;Pten-loxP/loxP;Trp53-loxP/+* and *PSA-Cre;Pten-loxP/+;Trp53-loxP/loxP* mice in clusters IIIA and IIIB indicated loss of the wild type *Trp53* and *Pten* alleles, respectively (data not shown). So, all tumors in Cluster III ultimately were completely negative for both *Pten* and *Trp53.* Histological and immunohistochemical examination showed heterogeneity of all tumors. However, the Cluster I tumors were mainly composed of undifferentiated and more differentiated carcinomas with expression of luminal epithelial cell markers. The tumors in Cluster II were mainly carcinosarcomas. The tumors in Cluster III were mixtures of undifferentiated carcinomas and carcinosarcomas. So, it seemed that the heterogeneous gene expression profiles reflected at least partially the differences in morphology of the tumors. These observations were largely supported by QPCR mRNA expression data of epithelial markers *CK8* and *E-cadherin* and mesenchymal markers *Snail* and *Vimentin* (Figure 5C). Prostate tumors in cluster I showed the highest expression of *CK8* and *E-Cadherin*. Cluster II showed high expression of *Snail*, whereas cluster III was heterogeneous. In IIIA umors, *CK8* and *E-Cadherin* were highly expressed and in IIIB, *Snail* and *Vimentin.*

As described above, metastases (indicated by blue marks) were exclusively derived from tumors with inactivation of both *Pten* and *Trp53* and were absent in mice with sole *Pten* inactivation. Metastases were not exclusively present in cluster I or III, although there might be a preference for cancers in cluster III. In two out of seven *Pten/Trp53* negative tumors in cluster I metastases were detected, whereas in Cluster III three out of six tumors metastasized.

Because cluster III seemed to contain the most aggressive tumors we decided to perform SAM comparing genes differentially expressed in cluster III compared to I and II. A complete overview of the genes higher expressed in cluster III is given in Table S5. The top twenty genes with highest differential expression in III are shown in Figure 5D. Interestingly, the list contained many genes that might be associated with loss of TP53 function, including mitotic check point control (*Cenpa*, *Rfc3*) and components of DNA replication licensing complexes (*Ris2/Cdt1* and *Mdmd2*). As shown in Figure 5E,F highest expressions of these genes were observed in the two tumors in cluster IIIA.

We also checked expression of genes associated with cellular senescence/apoptosis (*Cdkn2a, Cdkn1a, and DEC*) in cluster III compared to I and II, but a clear differential expression was not observed (data not shown). However, if we compared expression of these genes for the different genotypes, independent of the clustering, downregulation of expression, associated with *Trp53* downregulation was obvious.

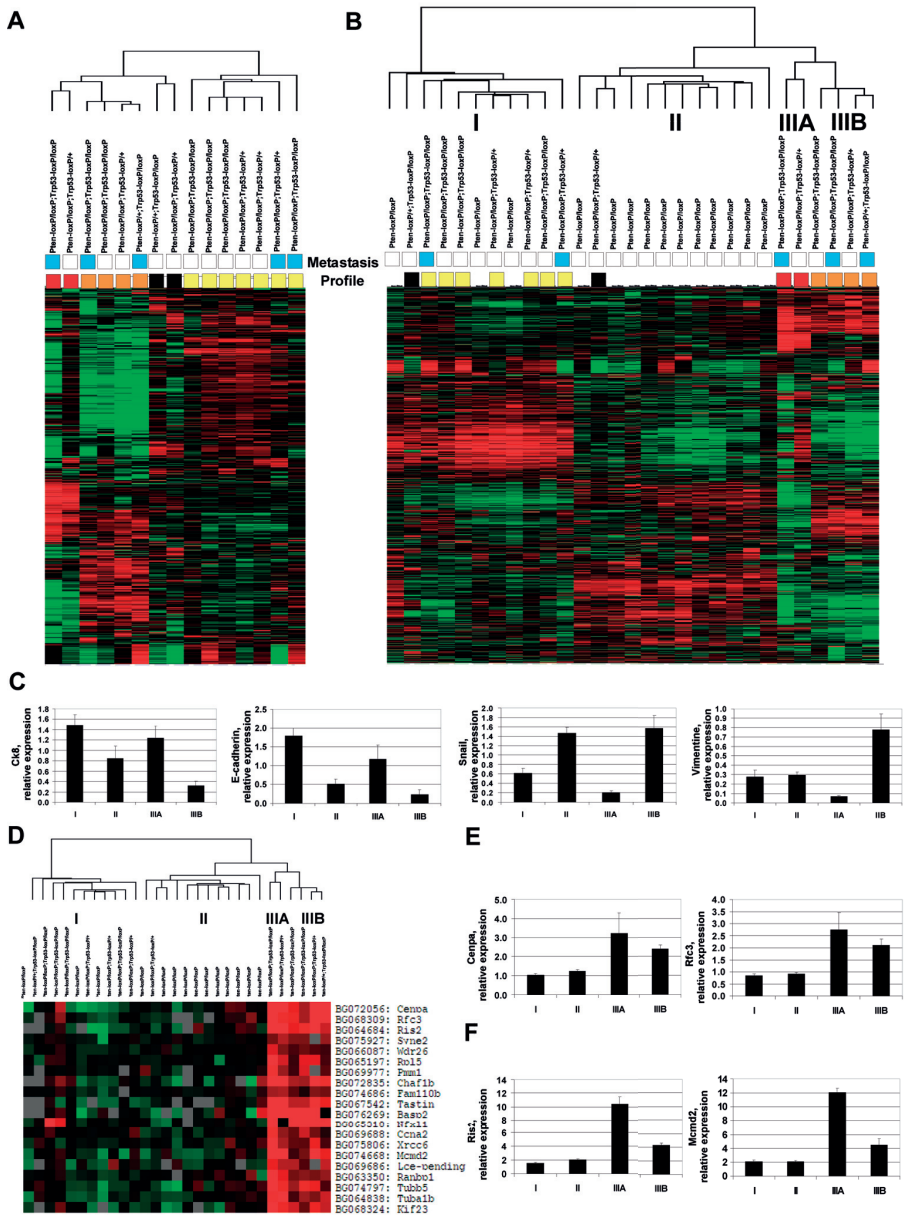

Figure 5. Gene expression profiling of prostate tumors from *Pten/Trp53* knockout mice showed molecular tumor heterogeneity. (**A**) Unsupervised hierarchical clustering of expression profiles of prostate tumors of *PSA-Cre;Pten-loxP/loxP;Trp53-loxP/+*, *PSA-Cre;Pten-loxP/loxP;Trp53-loxP/loxP* and *PSA-Cre;Pten-loxP/+;Trp53-loxP/loxP* mice. Tumors with prostate cancer metastases are indicated by blue squares (tumors without metastases are indicated by white squares). Tumors with identical expression profiles are indicated by coloured squares (red, orange, black and yellow). Green indicates lower gene expression and red indicates higher gene expression. (**B**) Unsupervised hierarchical

clustering of expression profiles of prostate tumors of *PSA-Cre;Pten-loxP/loxP, PSA-Cre;Pten-loxP/loxP;Trp53-loxP/+*, *PSA-Cre;Pten-loxP/loxP;Trp53-loxP/loxP* and *PSA-Cre;Pten-loxP/+;Trp53-loxP/loxP* mice. Note that four tumor clusters, I, II, IIIA and IIIB, can be discriminated. Green indicates lower gene expression and red indicates higher gene expression. (**C**) QPCR analysis of the *Ck8*, *E-Cadherin*, *Snail* and *Vimentin* expression in prostate tumors in tumor clusters I, II, IIIA and IIIB as shown in B. (**D**) Top20 of annotated genes with specific high expression in tumor cluster III (A and B) as determined by SAM. Green indicates lower gene expression and red indicates higher gene expression. (**E**) Relative expression of *Cenpa* and *Rfc3*, genes associated with mitotic check point control, high expressed in cluster III (as determined by SAM shown in D) in tumor cluster I, II, IIIA and IIIB. (**F**) Relative expression of *Ris2* and *Mcmd2*, genes associated with formation of the pre-replication complex, high expressed in cluster III (as determined by SAM shown in D) in cluster I, II, IIIA and IIIB.

Cell lines derived from prostate tumors of *Pten/Trp53* knockout mice have characteristics of aggressive tumor cells, including genomic instability

To investigate further differences between cells derived from prostate tumors of *PSA-Cre;Pten-loxP/loxP* and *PSA-Cre;Pten-loxP/loxP* mice with inactivation of one or two *Trp53* alleles, tumor cell lines were generated and characterized. First we performed genome-wide array CGH analyses on DNA from eight *PSA-Cre;Pten-loxP/loxP*, three *PSA-Cre;Pten-loxP/loxP;Trp53-loxP/+* and four *PSA-Cre;Pten-loxP/loxP;Trp53-loxP/loxP* cell lines (summarized in Figure 6A). Cell lines derived from prostates of *PSA-Cre;Pten-loxP/loxP* mice showed complete or partial loss of chromosome 4 (particularly distal part 4qD3-4qE2) and complete loss of chromosome 12 (see as an example cell line C9 in Figure 6B). Prostate tumor cell lines derived from *PSA-Cre;Pten-loxP/loxP;Trp53-loxP/+* and *PSA-Cre;Pten-loxP/loxP;Trp53-loxP/loxP* mice (*Pten/Trp53* negative cells) contained many more chromosomal alterations. In part, but not all, of the double knockout cell lines also loss of chromosomes 4 and 12 was found. Additionally, we observed trisomy 15 in all *Pten/Trp53* negative cell lines analyzed. Gains of chromosomes 3, 5, 8, 11, 17 and 19 and losses of chromosomes 1, 7, 10, and 14 were observed in varying combinations (see as an example C11 in Figure 6B). Further, as described above, in two out of three *PSA-Cre;Pten-loxP/loxP;Trp53-loxP/+* cell lines the wild type *Trp53* allele was lost.

Next, we addressed the question whether *Pten* and *Pten/Trp53* negative tumor cells showed different biological properties. First of all, the *Pten/Trp53* negative cell lines showed a higher proliferation rate than *Pten-/Trp53+* cells (data not shown). Two cell lines (C1 and C9) derived from *PSA-Cre;Pten-loxP/loxP* prostate tumors, and two cell lines (C11 and C19) from *PSA-Cre;Pten-loxP/loxP;Trp53-loxP/loxP* tumors were compared for anchorage independent growth in a soft agar colony assay. As shown in Figure 6C, in contrast to C1 and C9, both *Pten/Trp53* negative cell lines were able to grow in soft agar. Further, we compared C1 and C11 cells in 3D culture. The *Pten/Trp53* negative cell line C11 formed irregular colonies, whereas colonies of C1 cells were

regularly shaped. Moreover, orthotopic transplantation of C11 in syngenic mice resulted in the growth of prostate tumors, in contrast to C1 cells that could not be maintained *in vivo* (Figure 6E). All of these biological properties indicated that *Trp53* inactivation induced a more aggressive behavior in the cell lines.

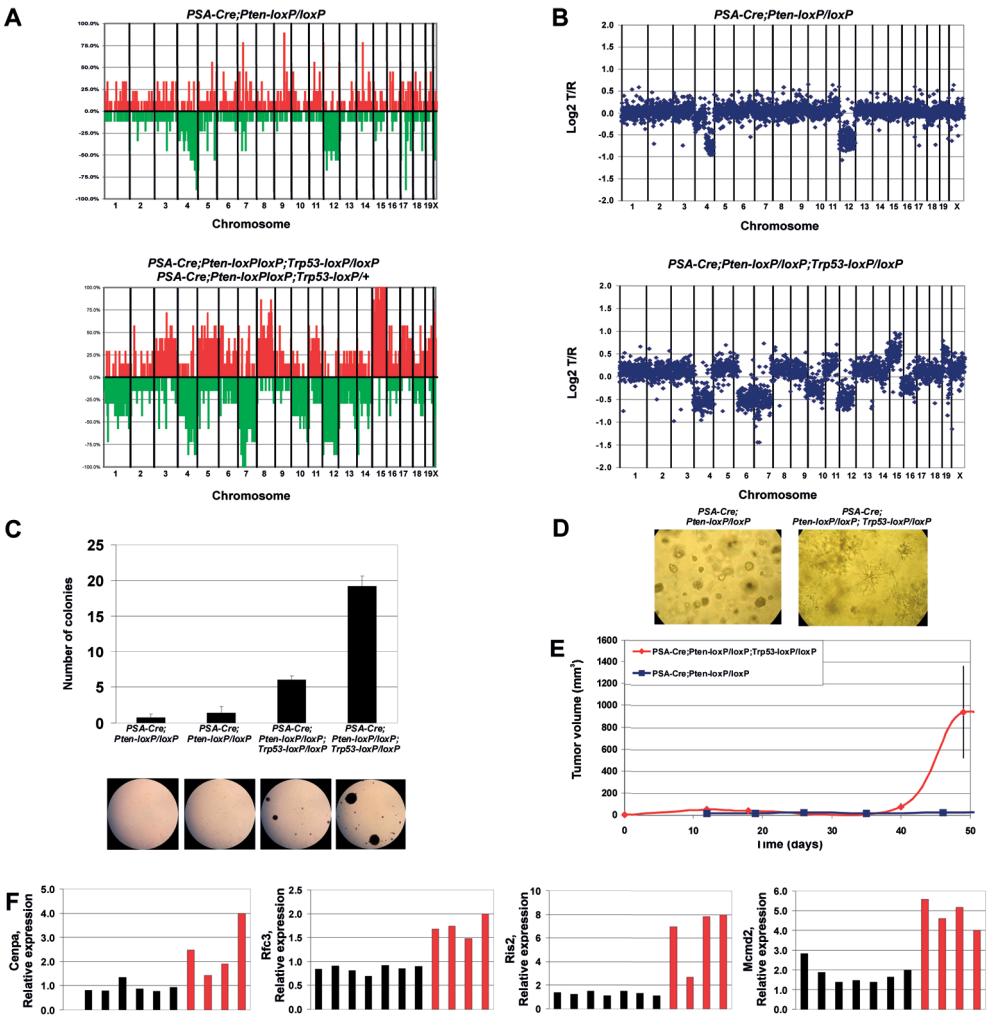

Figure 6. Prostate cancer cell lines derived from prostate tumors of *Pten/Trp53* knockout mice have characteristics of aggressive tumor cells, including genetic instability. (**A**) Overview of array CGH data of cell lines derived from eight *PSA-Cre;Pten-loxP/loxP* mice and seven targeted *Pten/Trp53* knockout mice. The results are plotted as percentage gain (red) and loss (green) per chromosome. (**B**) Examples of array CGH data of a cell line derived from a *PSA-Cre;Pten-loxP/loxP* mouse and a *PSA-Cre;Pten-loxP/loxP;Trp53-loxP/loxP* mouse. The data are plotted as log2 T/R ratio per chromosome. (**C**) Soft agar analysis of two *Pten* knockout cell lines and two cell lines derived from tumors of *PSA-Cre;Pten-*

loxP/loxP;Trp53-loxP/loxP mice plotted as number of colonies per cell line. Pictures of examples of colonies are shown. (**D**) Pictures of colonies grown in 3D culture after plating prostate tumor cell lines derived from either a *PSA-Cre;Pten-loxP/loxP* mouse or a *PSA-Cre;Pten-loxP/loxP;Trp53-loxP/loxP* mouse. (**E**) Graph of the tumor growth (expressed as tumor volume in mm3) in time after orthotopic transplantation of a *Pten* and a *Pten/Trp53* negative prostate cancer cell line. (**F**) Relative expression of genes high expressed in tumor cluster III, *Cenpa*, *Rfc3* and *Ris2*. Black bars represent the tumor cell lines of *PSA-Cre;Pten-loxP/loxP* mice, whereas the red bars represent tumor cell lines of *PSA-Cre;Pten-loxP/loxP;Trp53-loxP/loxP* mice.

Finally, we tested seven *Pten* knockout and four *Pten/Trp53* negative cell lines for expression of genes overexpressed in Cluster III tumors (Figure 5D-F). *Cenpa*, *Rfc3, Ris2* and *Mcmd2* were all overexpressed in *Pten/Trp53* double knockout cell lines (Figure 6F).

In conclusion, essentially all molecular, genetic and biological assays performed showed much more aggressive properties of prostate tumors and tumor cell lines with loss of one or two copies of *Trp53* in *Pten* negative mice. The findings support an important role of *Trp53* inactivation in progressive tumor growth, although sole *Trp53* inactivation had no substantial effect in the mouse prostate.

DISCUSSION

In this study we performed a systematic analysis of the effect of mono-allelic and bi-allelic inactivation of *Trp53* in a targeted *Pten* mouse prostate cancer model. One or two copies of the floxed *Trp53* gene and/or *Pten* gene were inactivated by Cre expression driven by the prostate-specific PSA promoter. Previously, we showed in *PSA-Cre;Pten-loxP/loxP* mice development of a homogeneous hyperplasia followed by development of a heterogeneous tumor. Luminal epithelial progenitor cells that express AR and CK8 but not the basal cell marker P63 were proposed as the tumor initiating cells [29, 34] (Korsten in preparation).

Oncogenic activation or other stress situations can trigger the activation of the p53 response pathway, blocking cell cycle in mitosis and inducing apoptosis and senescence for protection [12, 13, 55]. Therefore, it is not surprising that *Trp53* inactivation leads to uncontrolled cell cycle progression and accelerates tumor development. However, because of the very complex p53 signaling, that affects many cellular functions, the most important molecular and biological effects of p53 pathway inactivation on tumor progression are not well understood. In fact, the cell type and primary genetic event in tumor initiation in individual tumors might determine loss of which specific p53 activity is most relevant for tumor progression. Moreover, it has been postulated that inactivation of one or two copies of the *Trp*53 gene, and p53 gain of function

mutations can have different effects on tumor development/progression. The latter supposed to be involved in more aggressive tumors, including metastasis.

As expected, we and others [37, 56] observed in targeted *Pten* knockout prostate tumors that *Trp53* inactivation by deletion accelerated the oncogenic process. We found that not only inactivation of both *Trp53* alleles but also inactivation of one allele had this effect. Importantly, we demonstrated that this could lead to the development of more aggressive, metastatic tumors. Moreover, *Trp53* inactivation induced tumor formation in *PSA-Cre;Pten-loxP/+* mice that in the absence of *Trp53* inactivation had minimal phenotypical changes. The findings summarized above formed the basis of further characterization of the tumors.

Our data showed that sole *Trp53* inactivation in the mouse prostate induced small foci of hyperplastic and dysplastic cells in the prostate. This observation confirmed and extended previous findings in non-prostatic tissues that inactivation of *Trp53* by itself does not lead to tumor formation [13, 55]. Using different systems, all based on *Pb-Cre;Trp53* inactivation in the prostate, so far conflicting data have been reported of the effect of *Trp53* inactivation, ranging from absence of a phenotype to the presence of dysplastic cells, as reported here [36, 37, 39, 56]. It is remarkable that individual cells in the foci expressed the same markers as found in cells in the proximal prostate and in rare luminal epithelial cells in the distal adult prostate [34]. In our opinion this indicates that these cells are related to less differentiated luminal epithelial cells. This observation would support a role of *Trp53* inactivation in cellular reprogramming by dedifferentiation or by aberrant differentiation. A similar function was observed for *Pten* inactivation in the prostate, but the inhibition of differentiation by *Pten* inactivation was by far more dramatic [34].

The targeted *Pten* knockout model is the most frequently studied mouse prostate cancer model [30, 33, 57, 58]. As described above, in the majority of studies a (modified) Pb promoter has been applied to express Cre for inactivation of floxed *Pten* genes [30, 33, 39]. Different from the PSA-Cre driven model, in the Pb-Cre model multipotent P63+Sca-1+Bcl2+ progenitor epithelial cells are proposed as tumor initiating cells [59]. The tumors that develop are composed of mixtures of CK5/P63 positive cells and CK8 positive cells [56, 59]. In the Pb-Cre model, tumor development is much faster than in the PSA-Cre driven model and different stages of tumor development cannot be separated. Moreover, limited information is available about the morphological and molecular heterogeneity of the tumors. So direct comparison between the two models is difficult.

Comparison between for PSA-Cre driven and Pb-Cre driven mouse *Pten/Trp53* double knockout prostate cancers is also complicated, although it has been reported that, like shown here for PSA-Cre based *Pten* knockout mice, growth of Pb-Cre based *Pten* knockout mice is accelerated by *Trp53* deletion [37, 56]. Chen et al. [37] showed that *Pten* inactivation in the mouse prostate induced a p53 response associated with cellular senescence. It was suggested that accelerated tumor growth by *Trp53* inactivation was due to decreased senescence. Because a broader investigation of p53 function was lacking it was impossible to judge the relative

significance of this observation. Martin et al. [56] described morphological heterogeneity of the double knockout tumors. However, morphology of these tumors was not compared with that of *Pten* knockout tumors. As we showed (Korsten et al, in preparation) histopathologic heterogeneity is already present in *Pten* knockout tumors in the absence of *Trp53* inactivation, so most heterogeneity is not a function of *Trp53* inactivation.

Like *Pten* knockout prostate tumors, tumors from *Pten/Trp53* double knockout mice were composed of complex mixtures of carcinoma and carcinosarcoma subtypes, complicating accurate study of the effect of *Trp53* inactivation on tumor progression. Tumors were also molecularly heterogeneous. However, gene expression studies indicated that *Trp53* inactivation in aggressive tumors was associated with increased expression of cell cycle control genes, particularly components of the mitotic checkpoint complex and of the DNA pre-replication complex. Aberrant control of chromosome duplication and segregation resulting in chromosomal instability was observed as a prominent effect of *Trp53* inactivation. We did not find a strong effect of *Trp53* inactivation on overall stimulation of cell proliferation or a decrease of apoptosis, both processes that were strongly upregulated by *Pten* inactivation. The downregulation of p53-associated genes that were upregulated in prostate cancer induced by *Pten* inactivation, and supposed to be involved in senescence was limited. In *Pten* knockout prostate tumors an increased expression of inflammation markers and angiogenesis markers was detected (Korsten, in preparation). However, we did not observe a clear effect of *Trp53* inactivation on expression of marker genes for these processes (data not shown).

In the *Pten/Trp53* double knockout mice described here metastases were frequently detected. Although most metastases were small we could show that they were histological and immunohistochemical related to the primary prostate tumor. Most metastases were found in the abdominal cavity, but also lymph node, liver and lung metastases were observed. In contrast, in over 50 *Pten* knockout mice that we generated in our laboratory during the last years only one metastasis was identified [29] (Korsten in preparation). So, metastases were clearly associated with *Trp53* inactivation. Unfortunately, we were unable to generate a gene expression profile that corresponded to a metastatic phenotype. Sufficient RNA could only be detected from one lymph node metastasis (see Results section). Metastases seemed to be derived from different types of tumors, present in Clusters IIIA, IIIB and I. Possibly, the properties of a metastatic component of an individual heterogeneous tumor were not clearly reflected in the overall gene expression profile. Also in other model systems a direct or indirect role of induction of metastases by *Trp53* inactivation is not well explained. The PSA-Cre driven *Pten/Trp53* double knockout model seems a good opportunity to investigate this p53 function further. However, a considerably larger group of heterogeneous tumors and metastases needs to be collected to address this question. Metastases seemed to be absent in *Pten/Trp53* knockout mice based on Pb-Cre expression [39, 56]. It is possible that the follow up time in the experiments was too short or, alternatively, that mice carrying the more aggressive tumors died prior to development of metastases. Also a different

genetic background can play a role in this regard. Although metastases of primary tumors were not found, Martin et al. [56] described the metastatic capacity of an undifferentiated cell line derived from one *Pten/Trp53* double knockout mouse. Recently, metastases have been described in prostate targeted *Pten/Smad4* double knockout mice, but metastases were not observed in *Pten/Trp53* double knockout mice [39]. We checked *Smad4* expression in our metastatic tumors. However, downregulation of *Smad4* was not observed, indicated a different metastatic pathway in both models.

In the present study we detected for the first time prostate tumor development in two *PSA-Cre;Pten-loxP/+;Trp53-loxP/loxP* mice. In analyses done so far, these tumors seemed to be related to tumors in bi-allelic *Pten/Trp53* knockout mice. One tumor was a carcinosarcoma, the other a differentiated carcinoma. The former tumor showed loss of the wild type *Pten* allele, the latter retained the wild type allele. So, the genetic background of tumor development in these mice is different. Collection of a larger group of tumors will be of utmost importance to extend this observation. It is tempting to speculate that in an individual tumor different genetic or epigenetic events can contribute to tumor development in this model. Currently available deep sequencing technology will allow to investigate if different genetic alterations contribute to tumor development.

Aberrant chromosome duplication and segregation leading to aneuploidy is a hallmark of cancer that is frequently observed in late stage prostate cancer. Aberrant chromosome duplication is due to overexpression of mitotic checkpoint genes. We observed a strong upregulation of expression of several mitotic checkpoint genes by *Trp53* inactivation, as shown in Figure 5, but this was also true for other components of the mitotic checkpoint complex like *Bub1a* and *Mad2* (data not shown). We also observed a strong overexpression of genes of the minichromosome maintenance (MCM) complex that contributes to regulation of timely and accurate copying of the genome. Recently, evidence has been provided that the MCM complex also binds to the centrosome, suggesting that DNA replication and segregation are interdependent [60]. The genetic analysis of cell lines showed that the less coordinated function of the mitotic checkpoint by *Trp53* inactivation had a strong effect on genomic stability. The high overexpression of many genes involved in these processes is by far the most predominant contribution of *Trp53* inactivation on the development of more aggressive, metastatic prostate tumors.

Inactivation of *Trp53* resulted also in more tumorigenic cell lines derived from the double knockout tumors. This is reflected in the *in vitro* and *in vivo* biological properties of the cell lines (Figure 6). The cell lines are an important source to study metastasis due to *Trp53* inactivation. The cell lines will also be instrumental as models of late stage aggressive clinical prostate cancer. In fact, preliminary data indicated that overexpression of checkpoint genes and MCM complex genes in primary human prostate tumors is associated with progressive disease (Boormans, Korsten unpublished results).

REFERENCES

1. Birch, J.M., *The Li-Fraumeni cancer family syndrome.* J Pathol, 1990. **161**(1): p. 1-2.
2. Sansal, I. and W.R. Sellers, *The biology and clinical relevance of the PTEN tumor suppressor pathway.* J Clin Oncol, 2004. **22**(14): p. 2954-63.
3. Gustafson, S., et al., *Cowden syndrome.* Semin Oncol, 2007. **34**(5): p. 428-34.
4. Malkin, D., et al., *Germ line p53 mutations in a familial syndrome of breast cancer, sarcomas, and other neoplasms.* Science, 1990. **250**(4985): p. 1233-8.
5. Stiles, B., et al., *PTENless means more.* Dev Biol, 2004. **273**(2): p. 175-84.
6. Salmena, L., A. Carracedo, and P.P. Pandolfi, *Tenets of PTEN tumor suppression.* Cell, 2008. **133**(3): p. 403-14.
7. Chow, L.M. and S.J. Baker, *PTEN function in normal and neoplastic growth.* Cancer Lett, 2006. **241**(2): p. 184-96.
8. Carnero, A., *The PKB/AKT pathway in cancer.* Curr Pharm Des, 2010. **16**(1): p. 34-44.
9. Restuccia, D.F. and B.A. Hemmings, *From man to mouse and back again: advances in defining tumor AKTivities in vivo.* Dis Model Mech, 2010. **3**(11-12): p. 705-20.
10. Harris, S.L. and A.J. Levine, *The p53 pathway: positive and negative feedback loops.* Oncogene, 2005. **24**(17): p. 2899-908.
11. Vogelstein, B., D. Lane, and A.J. Levine, *Surfing the p53 network.* Nature, 2000. **408**(6810): p. 307-10.
12. Vousden, K.H. and C. Prives, *Blinded by the Light: The Growing Complexity of p53.* Cell, 2009. **137**(3): p. 413-31.
13. Donehower, L.A. and G. Lozano, *20 years studying p53 functions in genetically engineered mice.* Nat Rev Cancer, 2009. **9**(11): p. 831-41.
14. Aylon, Y. and M. Oren, *New plays in the p53 theater.* Curr Opin Genet Dev, 2010. **21**(1): p. 86-92.
15. Feng, Z., M. Lin, and R. Wu, *The Regulation of Aging and Longevity: A New and Complex Role of p53.* Genes Cancer, 2011. **2**(4): p. 443-52.
16. Bohlig, L. and K. Rother, *One function--multiple mechanisms: the manifold activities of p53 as a transcriptional repressor.* J Biomed Biotechnol, 2011. **2011**: p. 464916.
17. Hermans, K.G., et al., *Loss of a small region around the PTEN locus is a major chromosome 10 alteration in prostate cancer xenografts and cell lines.* Genes Chromosomes Cancer, 2004. **39**(3): p. 171-84.
18. Lotan, T., et al., *PTEN Protein Loss by Immunostaining: Analytic Validation and Prognostic Indicator for a High Risk Surgical Cohort of Prostate Cancer Patients.* Clin Cancer Res, 2011.
19. Berger, A.H. and P.P. Pandolfi, *Haplo-insufficiency: a driving force in cancer.* J Pathol, 2011. **223**(2): p. 137-46.
20. Majumder, P.K. and W.R. Sellers, *Akt-regulated pathways in prostate cancer.* Oncogene, 2005. **24**(50): p. 7465-74.
21. Dong, J.T., *Prevalent mutations in prostate cancer.* J Cell Biochem, 2006. **97**(3): p. 433-47.
22. Vlietstra, R.J., et al., *Frequent inactivation of PTEN in prostate cancer cell lines and xenografts.* Cancer Res, 1998. **58**(13): p. 2720-3.
23. Verhagen, P.C., et al., *The PTEN gene in locally progressive prostate cancer is preferentially inactivated by bi-allelic gene deletion.* J Pathol, 2006. **208**(5): p. 699-707.
24. MacGrogan, D. and R. Bookstein, *Tumour suppressor genes in prostate cancer.* Semin Cancer Biol, 1997. **8**(1): p. 11-9.
25. Macoska, J.A., et al., *Loss of the 17p chromosomal region in a metastatic carcinoma of the prostate.* J Urol, 1992. **147**(4): p. 1142-6.
26. Taylor, B.S., et al., *Integrative genomic profiling of human prostate cancer.* Cancer Cell, 2010. **18**(1): p. 11-22.

27. Di Cristofano, A., et al., *Pten is essential for embryonic development and tumour suppression.* Nat Genet, 1998. **19**(4): p. 348-55.
28. Stambolic, V., et al., *Negative regulation of PKB/Akt-dependent cell survival by the tumor suppressor PTEN.* Cell, 1998. **95**(1): p. 29-39.
29. Ma, X., et al., *Targeted biallelic inactivation of Pten in the mouse prostate leads to prostate cancer accompanied by increased epithelial cell proliferation but not by reduced apoptosis.* Cancer Res, 2005. **65**(13): p. 5730-9.
30. Wang, S., et al., *Prostate-specific deletion of the murine Pten tumor suppressor gene leads to metastatic prostate cancer.* Cancer Cell, 2003. **4**(3): p. 209-21.
31. Wang, X., et al., *A luminal epithelial stem cell that is a cell of origin for prostate cancer.* Nature, 2009. **461**(7263): p. 495-500.
32. Backman, S.A., et al., *Early onset of neoplasia in the prostate and skin of mice with tissue-specific deletion of Pten.* Proc Natl Acad Sci U S A, 2004. **101**(6): p. 1725-30.
33. Trotman, L.C., et al., *Pten dose dictates cancer progression in the prostate.* PLoS Biol, 2003. **1**(3): p. E59.
34. Korsten, H., et al., *Accumulating progenitor cells in the luminal epithelial cell layer are candidate tumor initiating cells in a pten knockout mouse prostate cancer model.* PLoS ONE, 2009. **4**(5): p. e5662.
35. Donehower, L.A., *The p53-deficient mouse: a model for basic and applied cancer studies.* Semin Cancer Biol, 1996. **7**(5): p. 269-78.
36. Zhou, Z., et al., *Synergy of p53 and Rb Deficiency in a Conditional Mouse Model for Metastatic Prostate Cancer.* Cancer Res, 2006. **66**(16): p. 7889-98.
37. Chen, Z., et al., *Crucial role of p53-dependent cellular senescence in suppression of Pten-deficient tumorigenesis.* Nature, 2005. **436**(7051): p. 725-30.
38. Francis, J.C., et al., *Brca2 and Trp53 deficiency cooperate in the progression of mouse prostate tumourigenesis.* PLoS Genet, 2010. **6**(6): p. e1000995.
39. Ding, Z., et al., *SMAD4-dependent barrier constrains prostate cancer growth and metastatic progression.* Nature, 2011. **470**(7333): p. 269-73.
40. Abou-Kheir, W.G., et al., *Characterizing the contribution of stem/progenitor cells to tumorigenesis in the Pten-/-TP53-/- prostate cancer model.* Stem Cells, 2010. **28**(12): p. 2129-40.
41. Couto, S.S., et al., *Simultaneous haploinsufficiency of Pten and Trp53 tumor suppressor genes accelerates tumorigenesis in a mouse model of prostate cancer.* Differentiation, 2009. **77**(1): p. 103-11.
42. Marino, S., et al., *PTEN is essential for cell migration but not for fate determination and tumourigenesis in the cerebellum.* Development, 2002. **129**(14): p. 3513-22.
43. Jonkers, J., et al., *Synergistic tumor suppressor activity of BRCA2 and p53 in a conditional mouse model for breast cancer.* Nat Genet, 2001. **29**(4): p. 418-25.
44. Hermans, K.G., et al., *TMPRSS2:ERG fusion by translocation or interstitial deletion is highly relevant in androgen-dependent prostate cancer, but is bypassed in late-stage androgen receptor-negative prostate cancer.* Cancer Res, 2006. **66**(22): p. 10658-63.
45. Hermans, K.G., et al., *Two unique novel prostate-specific and androgen-regulated fusion partners of ETV4 in prostate cancer.* Cancer Res, 2008. **68**(9): p. 3094-8.
46. Hendriksen, P.J., et al., *Evolution of the androgen receptor pathway during progression of prostate cancer.* Cancer Res, 2006. **66**(10): p. 5012-20.
47. Eisen, M.B., et al., *Cluster analysis and display of genome-wide expression patterns.* Proc Natl Acad Sci U S A, 1998. **95**(25): p. 14863-8.
48. Tusher, V.G., R. Tibshirani, and G. Chu, *Significance analysis of microarrays applied to the ionizing radiation response.* Proc Natl Acad Sci U S A, 2001. **98**(9): p. 5116-21.
49. Marques, R.B., et al., *Androgen receptor modifications in prostate cancer cells upon long-termandrogen ablation and antiandrogen treatment.* Int J Cancer, 2005. **117**(2): p. 221-9.
50. Chung, Y.J., et al., *A whole-genome mouse BAC microarray with 1-Mb resolution for analysis of DNA copy number changes by array comparative genomic hybridization.* Genome Res, 2004. **14**(1): p. 188-96.

51. Hermans, K.G., et al., *Truncated ETV1, fused to novel tissue-specific genes, and full-length ETV1 in prostate cancer.* Cancer Res, 2008. **68**(18): p. 7541-9.
52. Kraaij, R., et al., *Validation of transrectal ultrasonographic volumetry for orthotopic prostate tumours in mice.* Lab Anim, 2002. **36**(2): p. 165-72.
53. Lin, B.T., et al., *Oncocytic adrenocortical neoplasms: a report of seven cases and review of the literature.* Am J Surg Pathol, 1998. **22**(5): p. 603-14.
54. Pace, V., E. Perentes, and P.G. Germann, *Pheochromocytomas and ganglioneuromas in the aging rats: morphological and immunohistochemical characterization.* Toxicol Pathol, 2002. **30**(4): p. 492-500.
55. Junttila, M.R. and G.I. Evan, *p53--a Jack of all trades but master of none.* Nat Rev Cancer, 2009. **9**(11): p. 821-9.
56. Martin, P., et al., *Prostate epithelial Pten/TP53 loss leads to transformation of multipotential progenitors and epithelial to mesenchymal transition.* Am J Pathol, 2011. **179**(1): p. 422-35.
57. Luchman, H.A., et al., *The pace of prostatic intraepithelial neoplasia development is determined by the timing of Pten tumor suppressor gene excision.* PLoS ONE, 2008. **3**(12): p. e3940.
58. Ratnacaram, C.K., et al., *Temporally controlled ablation of PTEN in adult mouse prostate epithelium generates a model of invasive prostatic adenocarcinoma.* Proc Natl Acad Sci U S A, 2008. **105**(7): p. 2521-6.
59. Wang, S., et al., *Pten deletion leads to the expansion of a prostatic stem/progenitor cell subpopulation and tumor initiation.* Proc Natl Acad Sci U S A, 2006. **103**(5): p. 1480-5.
60. Knockleby, J. and H. Lee, *Same partners, different dance: involvement of DNA replication proteins in centrosome regulation.* Cell Cycle, 2010. **9**(22): p. 4487-91.

Supplementary data

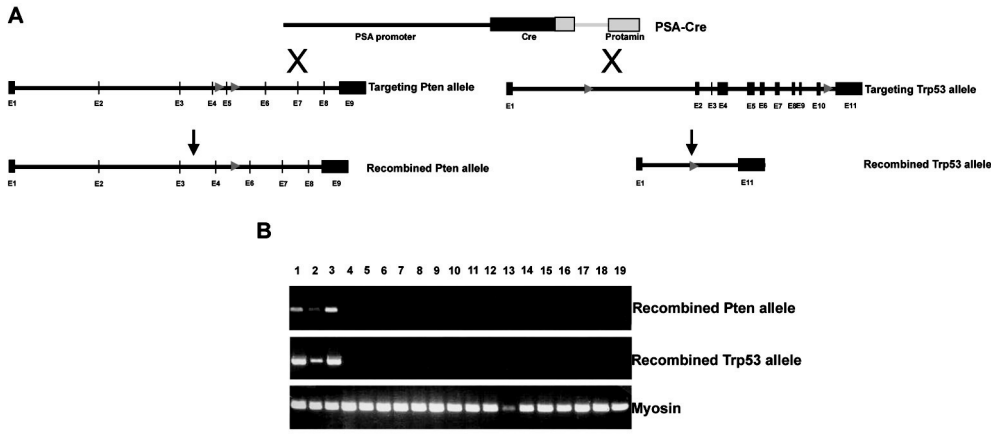

Figure S1. Prostate specific recombination of *Pten* and *Trp53* in targeted *Pten/Trp53* mice. (**A**) The strategy of the generation of prostate-specific *Pten/Trp53* knockout mice. The exon 5 targeting fragment contains loxP sites in intron 4 and 5 of the *Pten* allele. Cre expression driven by the PSA promoter resulted in prostate specific androgen dependent *Pten* inactivation by deletion of exon 5. To inactivate *Trp53*, loxP sites in intron 1 and 10 were introduced and by crossing of mice containing the targeted *Trp53* allele and the *PSA-Cre* fragment *Trp53* was inactivated. (**B**) Prostate specific recombination of *Pten* and *Trp53* in *Pten/Trp53* knockout mice (4m). Recombination specific PCR fragments were detected in mouse prostate lobes. 1: anterior prostate, 2: ventral prostate, 3: dorsolateral prostate, 4: seminal vesicle, 5: vas deferens, 6: epididymus, 7: testis, 8: bladder, 9: lymph node, 10: kidney, 11: adrenal gland, 12: salivary gland, 13: parotis, 14: spleen, 15: liver, 16: stomach, 17: small intestine, 18: large intestine, 19: pancreas.

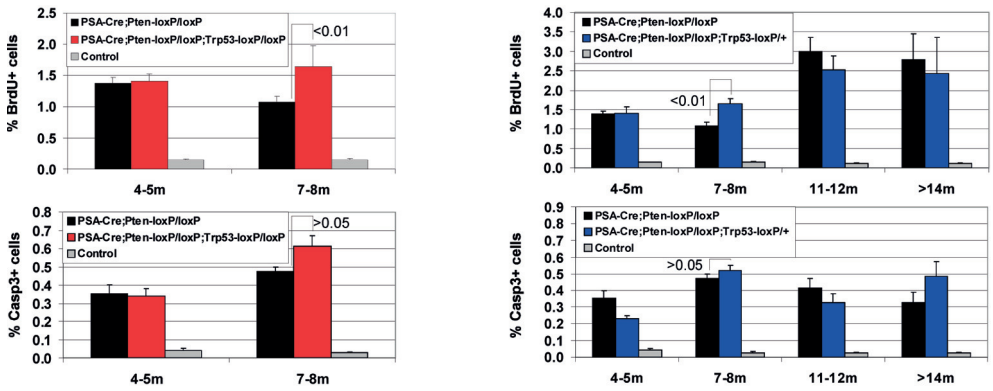

Figure S2. *Trp53* inactivation in targeted *Pten* knockout mice had no effect on the proliferation rate and apoptotic rate in tumors. The proliferation rate and apoptotic rate in control mice, *PSA-Cre;Pten-loxP/loxP* and *PSA-Cre;Pten-loxP/loxP;Trp53-loxP/loxP* mice were compared at 4-5m and 7-8m. The effect of mono-allelic *Trp53* inactivation in *PSA-Cre;Pten-loxP/loxP* mice was determined at 4-5m, 7-8m, 11-12m and >15m. Both the proliferation rate and apoptotic rate are expressed as percentage BrdU or active Caspase-3 positive cells, respectively.

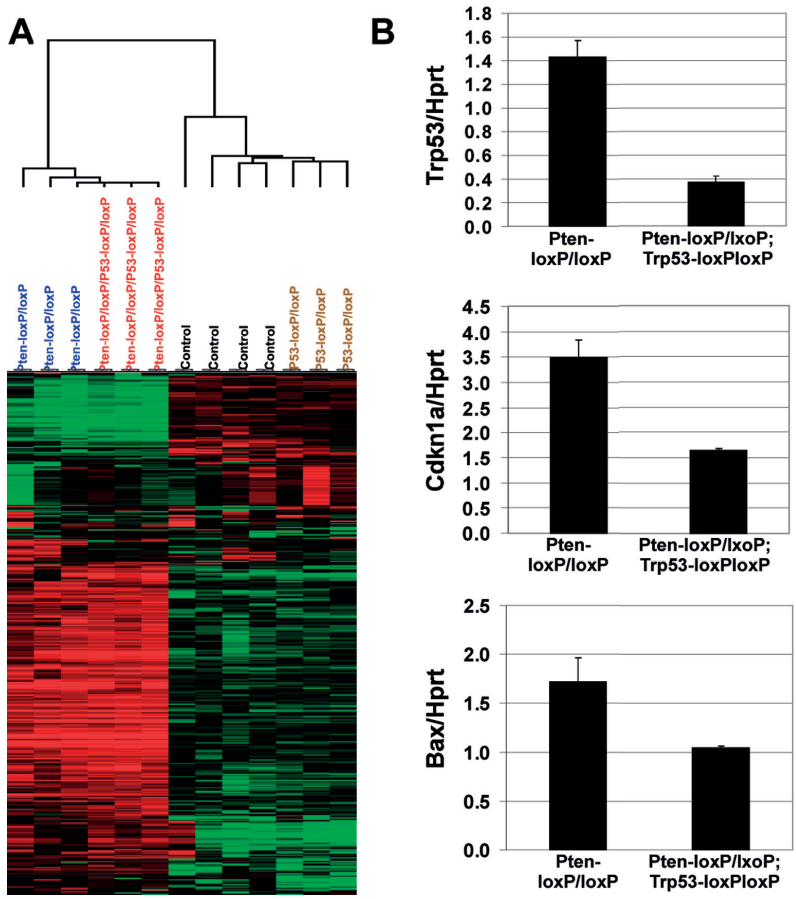

Figure S3. *Trp53* inactivation at 4-5m only affected the expression of direct *Trp53* target genes. (**A**) Unsupervised hierarchical clustering of expression profiles of prostates of control mice, *PSA-Cre;Trp53-loxP/loxP*, *PSA-Cre;Pten-loxP/loxP* and *PSA-Cre;Pten-loxP/loxP;Trp53-loxP/loxP* mice at 4-5m. Green indicates lower gene expression and red indicates higher gene expression. (**B**) Relative expression of *Trp53*, *Cdkn1a* (encoding p21) and *Bax* in prostates of *PSA-Cre;Pten-loxP/loxP* and *PSA-Cre;Pten-loxP/loxP;Trp53-loxP/loxP* mice at 4-5m.

Table S1. Overview of the number of mice analyzed and the number of dead mice at different time points per genotype and per age. The time points analyzed are 4-5 m, 7-8m, 11-12m and >14m. Note that *PSA-Cre;Pten-loxP/loxP;Trp53-loxP/loxP* mice were only analyzed at 4-5m and 7-8m.

Genotype	Age	Number of mice	Number of dead mice
PSA-Cre;Pten-loxP/loxP	4-5m	10	0
	7-8m	9	0
	11-12m	10	0
	>14m	7	1
PSA-Cre;Pten-loxP/+	4-5m	11	0
	7-8m	10	0
	11-12m	8	0
	>14m	9	1
PSA-Cre;Trp53-loxP/loxP	4-5m	12	0
	7-8m	10	0
	11-12m	8	0
	>14m	5	0
PSA-Cre;Trp53-loxP/+	4-5m	11	0
	7-8m	10	0
	11-12m	8	0
	>14m	8	0
PSA-Cre;Pten-loxP/loxP; Trp53-loxP/+	4-5m	10	0
	7-8m	13	3
	11-12m	12	3
	>14m	8	4
PSA-Cre;Pten-loxP/loxP; Trp53-loxP/loxP	4-5m	10	0
	7-8m	32	2
PSA-Cre;Pten-loxP/+; Trp53-loxP/+	4-5m	7	0
	7-8m	5	0
	11-12m	6	1
	>14m	6	0
PSA-Cre;Pten-loxP/+; Trp53-loxP/loxP	4-5m	10	0
	7-8m	9	0
	11-12m	9	2
	>14m	6	1
Controls	4-5m	30	0
	7-8m	30	0
	11-12m	28	0
	>14m	21	0

Table S2. Sequences of primers used for PCR, DNA recombination PCR, sequencing and QPCR analysis.

Primer name	Sequence forward primer	Sequence reverse primer	Application
Pten (exon 5)	5′-TTCCTGAAAGTTAGGCTTCT-3′	5′-GGGAGAAAACCTGTTTCCCA-3′	PCR
Myosin	5′-TTACGTCCATCGTGGACAGC-3′	5′-TGGGCTGGGTGTTAGTCTTA-3′	PCR
Pten-recombination	5′-TGGCATAAGTTAGGAAAGATG-3′	5′-GGCAAAGAATCTTGGTGTTAC-3′	Recombination PCR
Trp53-recombination	5′-CACAAAAACTTAAACCCAG-3′	5′-GAAGACAGAAAAGGGGAGGGT-3′	Recombination PCR
Hprt	5′-TCCCTGGTTAAGCAGTACAG-3′	5′-TTCCAGTTTCACTAATGACAC-3′	QPCR
Bax	5′-TTGCCCTCTTCTACTTTGCT-3′	5′-TTCTTCCAGATGGTGAGCGA-3′	QPCR
Bub1b	5′-GAACTCTACAGCTATGGGAC-3′	5′-AATGATTTCGCAGCTGTGGAC-3′	QPCR
Cdkn1a	5′-AGGGCAACTTCGTCTGGGA-3′	5′-GGCACTTCAGGGTTTTCTCT-3′	QPCR
Cdkn2a	5′-CGGGCATAGCTTCAGCTCA-3′	5′-TAAGAAGAAAAAGGCGGGCT-3′	QPCR
DEC	5′-AAGGATCTCCTACCCGAACA-3′	5′-CTGGAAACCTGAGCAGAACA-3′	QPCR
E-cadherin	5′-GGAGGTGGAGAAGAAGACCA-3′	5′-TCGCTGTCGGCTGCCTTCA-3′	QPCR
Ki67	5′-CTGGGAACCAAGAAAGATGC-3′	5′-ACAGTTCATCTTTACACTGG-3′	QPCR
Pten	5′-CCAACCGATACTTCTCTCCA-3′	5′-GATCAGAGTCAGTGGTGTCA-3′	QPCR
Snail	5′-CACACGCTGCCTTGTGTCT-3′	5′-TATCTCTTCACATCCGAGTG-3′	QPCR
Trp53	5′-GCCAAGTCTGTTATGTGCAC-3′	5′-TCATGTGCTGTGACTTCTTC-3′	QPCR
Primer name	**Primer sequence**		**Application**
mpten ex1forC	AGTTGCTCTCTCCCCTTCT		Sequencing
mpten in2revC	GAACAGCCCGCAGAAATGGAT		Sequencing
mpten in2for	ACAGCTAGCGTGGGAAAAGC		Sequencing
mpten in3rev	CTCATCCAGTGACGCATCCA		Sequencing
mpten in3for	CTGTTTTAGTCCTGTGCAGC		Sequencing
mpten ex3AS	GAGACCCAACAACTCTCTCT		Sequencing
mpten ex4S	GGTATGATAGAAAGGGTGGA		Sequencing
mpten ex4AS	GATAATTATCACCAGGCAGT		Sequencing
mpten ex5S	TTCCTGAAAGTTAGGCTTCT		Sequencing
mpten ex5AS	GGGAGAAAACCTGTTTCCCA		Sequencing
mpten ex6S	GGGATAACCCAGTTATAGCA		Sequencing
mpten ex6AS	GGGTTAGCTTTCTTAACCCA		Sequencing
mpten ex7S	AAGTCCTTACATGGGTTGGT		Sequencing
mpten ex7AS	GCAAAAGGTCTGTGGTTACT		Sequencing
mpten ex8S	ACAAGGTGTTTGCCTTCACT		Sequencing
mpten ex8AS	GCAACCACTCGGGAATGTTA		Sequencing
mpten ex9S	GAAAAGCATGCCCTTCAGA		Sequencing
mpten ex9AS	TGGTATTTTATCCCTCTTGA		Sequencing

Table S3. Information of antibodies used for immunohistochemistry.

Antibody	Company	Product number	Dilution
AR	--	SP197	1:1500
BrdU	Biogenex	IIB5	1:150
Caspase-3	R&D systems, Minneapolis, MN	AF835	1:1000
CK8	Covance, Berkeley, CA	MMM-162P	1:1000
Clu	Santa Cruz, CA	SC-6420	1:800
Sca-1	R&D systems, Minneapolis, MN	AF1226	1:100
Tacstd2	R&D systems, Minneapolis, MN	AF1122	1:100
Goat Anti-Mouse-biotin	DAKO	E0433	1:400
Swine Anti-Rabbit-biotin	DAKO	E0431	1:400
Rabbit Anti-Goat-biotin	Santa Cruz, CA	SC-2774	1:400

Table S4. Characteristics of mice with prostate cancer metastases and the sites of metastases. LN, lymph node.

Genotype	Age (Months)	Prostate weight (Grams)	Site of metastasis
PSA-Pten-loxP/loxP;Trp53-loxP/loxP	6.5	0.84	Abdominal cavity
	7	1.91	LN, abdominal cavity
	8	3.33	LN, lung,liver
PSA-Pten-loxP/+;Trp53-loxP/loxP	14.5	7.01	LN, abdominal cavity
PSA-Pten-loxP/loxP;Trp53-loxP/+	8.5	1.83	Abdominal cavity
	8.5	0.67	Abdominal cavity, lung
	12	3.88	Abdominal cavity
	12	1.35	Abdominal cavity
	13.5	1.09	Abdominal cavity

Table S5. Significantly differentially expressed genes in cluster III as assayed by SAM analysis.

176 genes significant high expressed in cluster III (q-value 0).					
Accession code	**Unigene**	**Gene Name**	**Score(d)**	**Fold Change**	**q-value (%)**
BG072056	Mm.6579	Mus musculus centromere autoantigen A (Cenpa). mRNA	9.935427369	2.32E+48	0
BG068309	Mm.12553	Mus musculus similar to Activator 1 38 kDa subunit (Replication factor C 38 kDa subunit) (A1 38 kDa subunit) (RF-C 38 kDa subunit) (RFC3) (LOC209575). mRNA	8.490407269	2.81E+39	0
BG069637	Mm.173431	UNKNOWN	8.373947114	6.26E+37	0
BG069969	Mm.25966	UNKNOWN	8.149052695	2.65E+35	0
BG064684	Mm.21873	Mus musculus retroviral integration site 1 (Ris2). mRNA	7.959940511	1.22E+51	0
BG075927	Mm.182840	Syne2	7.956844558	1.33E+22	0
BG066087	Mm.21126	Wdr26	7.932621384	6.72145E+18	0
BG065197	Mm.4419	Mus musculus ribosomal protein L5 (Rpl5). mRNA	7.717928791	4.56E+28	0
BG069977	Mm.18939	Mus musculus phosphomannomutase 1 (Pmm1). MRNA	7.611549473	4.50E+24	0
BG072835	Mm.5458	Chaf1b	7.522840829	1.93E+52	0
BG073790	Mm.259293	UNKNOWN	7.396858983	3.02E+45	0
UNKNOWN	UNKNOWN	UNKNOWN	7.118283336	3.17E+34	0
UNKNOWN	UNKNOWN	UNKNOWN	7.096954008	1.24E+38	0
BG074686	Mm.103079	Fam110b	7.026626265	4.09E+19	0
BG067542	Mm.124905	Mus musculus similar to trophinin associated protein (tastin) [Homo sapiens] (LOC223890). mRNA	6.947707348	8.77E+35	0
BG076269	Mm.1222	Mus musculus brain abundant. membrane attached signal protein 2 (Basp2). mRNA	6.902461893	9.42E+58	0
BG065318	Mm.27827	Nfxl1	6.665678581	2.54E+54	0
BG069688	Mm.4189	Mus musculus cyclin A2 (Ccna2). mRNA	6.658475436	4.74E+22	0
BG075806	Mm.16147	Xrcc6	6.65638759	4.93E+24	0
BG074668	Mm.16711	Mus musculus mini chromosome maintenance deficient 2 (S. cerevisiae) (Mcmd2). mRNA	6.635745812	2.65E+49	0
UNKNOWN	UNKNOWN	UNKNOWN	6.61761847	2.60E+28	0

Table S5. *(Continued)*

176 genes significant high expressed in cluster III (q-value 0).					
Accession code	**Unigene**	**Gene Name**	**Score(d)**	**Fold Change**	**q-value (%)**
BG069686	Mm.26171	Mus musculus long chain fatty acyl elongase (Lce-pending). mRNA	6.606823901	3.45E+24	0
BG063350	Mm.3752	Mus musculus RAN binding protein 1 (Ranbp1). mRNA	6.536909664	9.11E+24	0
BG074797	Mm.1703	Mus musculus tubulin. beta 5 (Tubb5). mRNA	6.520147923	4.21E+35	0
BG068397	Mm.250057	UNKNOWN	6.507976504	4.74E+23	0
BG063487	Mm.32150	UNKNOWN	6.474817757	3.70517E+17	0
UNKNOWN	UNKNOWN	UNKNOWN	6.437055461	7.12E+36	0
BG064838	Mm.197515	Tuba1b	6.432437001	9.45E+35	0
BG068324	Mm.77342	Kif23	6.415878354	5.30E+32	0
BG067511	Mm.28955	Mus musculus RIKEN cDNA 4930570C03 gene (4930570C03Rik). mRNA	6.335313943	1.80E+32	0
BG075025	Mm.138404	UNKNOWN	6.244511337	1.20703E+13	0
BG067576	Mm.2186	Mus musculus RNA polymerase II 3 (Rpo2-3). mRNA	6.229874598	6.17134E+18	0
BG064835	Mm.29304	UNKNOWN	6.182448317	7.24742E+18	0
BG073208	UNKNOWN	UNKNOWN	6.174239763	1.39538E+18	0
BG064451	Mm.28465	Mus musculus. Similar to DKFZP564C1940 protein. clone MGC	6.02171028	1.95128E+17	0
BG076003	Mm.29253	Mus musculus RIKEN cDNA 2310032N20 gene (2310032N20Rik). mRNA	6.019903447	2.78E+30	0
BG064725	Mm.3797	UNKNOWN	6.012339317	7.10E+27	0
BG071028	Mm.11333	Mus musculus similar to helicase-like protein NHL. isoform c; tumor necrosis factor receptor superfamily. member 6b precursor; decoy receptor 3 [Homo sapiens] (LOC263882). mRNA	6.00953739	2.91E+25	0
BG065235	Mm.19170	Mus musculus methionine aminopeptidase 2 (Metap2). mRNA	6.006409572	3.78284E+12	0
BG063560	Mm.30034	Mus musculus translocase of inner mitochondrial membrane 8 homolog a (yeast) (Timm8a). mRNA	5.957064941	1.73E+30	0
BG071069	Mm.47870	Mus musculus. clone MGC	5.940794092	1.58E+33	0
BG072534	Mm.27927	Mus musculus heterogeneous nuclear ribonucleoprotein A1 (Hnrpa1). mRNA	5.898543911	1.32604E+16	0

Table S5. *(Continued)*

176 genes significant high expressed in cluster III (q-value 0).					
Accession code	**Unigene**	**Gene Name**	**Score(d)**	**Fold Change**	**q-value (%)**
BG071683	Mm.181792	Mus musculus centromere autoantigen H (Cenph). mRNA	5.895125883	1.98E+22	0
BG074981	Mm.9244	Mus musculus suppressor of variegation 3-9 homolog 1 (Drosophila) (Suv39h1). mRNA	5.89073671	7.03E+47	0
UNKNOWN	UNKNOWN	UNKNOWN	5.871022594	7.10E+37	0
BG064046	Mm.145488	Mus musculus expressed sequence AL024047 (AL024047). mRNA	5.860224964	2.12245E+18	0
BG071084	Mm.3797	Mus musculus nucleosome assembly protein 1-like 1 (Nap1l1). mRNA	5.858253044	5.39E+29	0
BG063054	Mm.78861	Mus musculus similar to Nucleolar phosphoprotein p130 (Nucleolar 130 kDa protein) (140 kDa nucleolar phosphoprotein) (Nopp140) (Nucleolar and coiled-body phosphoprotein 1) (Nolc1). mRNA	5.849147978	1.37E+23	0
BG074533	Mm.25610	Homo sapiens KIAA0144 gene product (KIAA0144). mRNA	5.832910224	1.62578E+17	0
BG074962	Mm.12155	Mus musculus similar to p47 protein [Rattus norvegicus] (LOC228764). mRNA	5.801106646	1.31376E+18	0
BG063247	Mm.4071	UNKNOWN	5.770180183	6.63019E+15	0
BG073072	Mm.182931	Mus musculus phosphoribosylaminoimidazole carboxylase. phosphoribosylaminoribosylaminoimidazole. succinocarboxamide synthetase (Paics). mRNA	5.764393498	1.79E+22	0
BG066394	Mm.172746	UNKNOWN	5.755002561	3.77476E+13	0
BG067492	Mm.101264	Mus musculus RIKEN cDNA 2810473M14 gene (2810473M14Rik). mRNA	5.737225348	1.3862E+16	0
BG067873	Mm.3170	Mus musculus poly (A) polymerase alpha (Papola). mRNA	5.708595971	2.91E+30	0
BG073876	Mm.1886	Mus musculus RNA and export factor binding protein 1 (Refbp1). mRNA	5.700204586	5.12E+27	0
BG074721	Mm.18923	Mus musculus mini chromosome maintenance deficient 7 (S. cerevisiae) (Mcmd7). mRNA	5.693192635	2.52E+30	0
BG076165	Mm.29460	Mus musculus. adenylate kinase 2. clone MGC	5.692207522	1.56E+27	0
BG064804	Mm.89830	Mus musculus ubiquitin-conjugating enzyme E2C (Ube2c). mRNA	5.690365629	2.51E+28	0
BG076333	Mm.443	Mus musculus methylenetetrahydrofolate dehydrogenase (NAD+ dependent). methenyltetrahydrofolate cyclohydrolase (Mthfd2). mRNA	5.659945239	3.07E+44	0
BG076204	Mm.197305	UNKNOWN	5.640441096	2.97E+21	0

Table S5. *(Continued)*

176 genes significant high expressed in cluster III (q-value 0).					
Accession code	**Unigene**	**Gene Name**	**Score(d)**	**Fold Change**	**q-value (%)**
BG074867	Mm.174176	UNKNOWN	5.611464907	9.78186E+14	0
BG065112	Mm.29123	UNKNOWN	5.602858423	5.40E+24	0
BG064884	Mm.20315	UNKNOWN	5.591651019	1.25E+24	0
BG063530	Mm.41801	Mus musculus RIKEN cDNA 2610511E03 gene (2610511E03Rik). mRNA	5.563772544	9.96656E+18	0
BG072376	Mm.158086	Mus musculus. Similar to leucine-rich and death domain containing. clone IMAGE	5.537355381	2.57E+23	0
BG064975	Mm.89515	UNKNOWN	5.534005432	4.02407E+13	0
BG070309	Mm.25920	UNKNOWN	5.532787604	7.97245E+11	0
BG076273	Mm.164114	UNKNOWN	5.530941901	3.2374E+12	0
BG070554	Mm.153891	Mus musculus. protein tyrosine phosphatase 4a3. clone MGC	5.514981623	6.54E+26	0
BG069751	Mm.27871	Mus musculus RIKEN cDNA 2610012O22 gene (2610012O22Rik). mRNA	5.501043472	4.40E+24	0
UNKNOWN	UNKNOWN	UNKNOWN	5.469265446	1.15E+22	0
BG064776	Mm.232232	Mus musculus similar to proteolipid protein 2 [Mus musculus] (LOC218482). mRNA	5.464895489	1.93E+21	0
BG075062	Mm.29144	Mus musculus DNA segment. Chr 15. Wayne State University 59. expressed (D15Wsu59e). mRNA	5.462117357	2.54951E+18	0
BG073103	Mm.195392	UNKNOWN	5.428091621	3.36667E+16	0
BG063283	Mm.45312	Mus musculus anaphase-promoting complex subunit 5 (Anapc5). mRNA	5.42254732	5.52162E+16	0
BG069714	Mm.143167	Mus musculus RIKEN cDNA 0610010J20 gene (0610010J20Rik). mRNA	5.417003748	1.73E+20	0
BG067148	Mm.197520	Mus musculus f-box only protein 5 (Fbxo5). mRNA	5.413675135	6.40E+27	0
BG069256	Mm.41803	Mus musculus developmentally regulated GTP binding protein 2 (Drg2). mRNA	5.411901529	5.38868E+18	0
BG066321	Mm.46722	Mus musculus PDZ domain containing 1 (Pdzk1). mRNA	5.399190618	1.34265E+13	0
BG070495	Mm.173273	UNKNOWN	5.388287148	5.11233E+16	0

Table S5. *(Continued)*

176 genes significant high expressed in cluster III (q-value 0).					
Accession code	**Unigene**	**Gene Name**	**Score(d)**	**Fold Change**	**q-value (%)**
BG068799	Mm.23526	Mus musculus RIKEN cDNA 2610036L13 gene (2610036L13Rik). mRNA	5.383284535	7.09E+31	0
BG068936	Mm.28762	UNKNOWN	5.360006745	3.00E+23	0
BG067953	Mm.10665	Mus musculus testis expressed gene 292 (Tex292). mRNA	5.3435218	1.97E+21	0
BG063655	Mm.180763	Mus musculus Rap1. GTPase-activating protein 1 (Rap1ga1). mRNA	5.341174875	9.17E+23	0
BG071029	Mm.26079	UNKNOWN	5.338705117	217381236	0
BG063032	Mm.29627	UNKNOWN	5.330527179	4.39517E+17	0
UNKNOWN	UNKNOWN	UNKNOWN	5.322954372	1.89E+21	0
BG073402	Mm.29780	Mus musculus LOC232679 (LOC232679). mRNA	5.314496081	1.73E+20	0
BG069477	Mm.121973	UNKNOWN	5.296986628	5.87E+20	0
BG073557	Mm.201371	Mus musculus. eukaryotic translation initiation factor 5A. clone MGC	5.29327431	7.99E+24	0
BG067860	Mm.43444	UNKNOWN	5.276357792	8.43E+31	0
BG075357	Mm.4933	Mus musculus mini chromosome maintenance deficient 6 (S. cerevisiae) (Mcmd6). mRNA	5.275742669	2.01E+28	0
BG072821	Mm.4071	Mus musculus laminin receptor 1 (67kD. ribosomal protein SA) (Lamr1). mRNA	5.268976696	4.35E+26	0
BG076020	Mm.30020	Mus musculus RIKEN cDNA 1110006I15 gene (1110006I15Rik). mRNA	5.259762293	2.38E+23	0
BG064434	Mm.260633	UNKNOWN	5.252792826	2.70E+31	0
UNKNOWN	UNKNOWN	UNKNOWN	5.248712366	1.43644E+19	0
BG071956	Mm.18652	UNKNOWN	5.239850816	4.00838E+13	0
BG075625	Mm.22179	Mus musculus RIKEN cDNA 1200009B18 gene (1200009B18Rik). mRNA	5.228020771	6.85E+28	0
BG063774	Mm.52356	Mus musculus similar to hypothetical protein DKFZp761J139 (LOC218437). mRNA	5.220170026	2.20393E+18	0
BG064523	Mm.9550	Mus musculus RIKEN cDNA 2310081H14 gene (2310081H14Rik). mRNA	5.21918538	1.45882E+16	0
BG064049	Mm.33853	Mus musculus. Similar to hypothetical protein MGC29271. clone IMAGE	5.180666007	12709756956	0
BG069524	Mm.3797	Mus musculus similar to Nucleosome assembly protein 1-like 1 (NAP-1 related protein) (Brain protein DN38) (LOC215265). mRNA	5.14537711	3.67E+24	0

Table S5. *(Continued)*

176 genes significant high expressed in cluster III (q-value 0).					
Accession code	**Unigene**	**Gene Name**	**Score(d)**	**Fold Change**	**q-value (%)**
UNKNOWN	UNKNOWN	Mus musculus RIKEN cDNA 2700029C06 gene (2700029C06Rik). mRNA	5.139913639	3.54E+25	0
BG073331	Mm.1951	Mus musculus ribonucleic acid binding protein S1 (Rnps1). mRNA	5.1392714	3.62878E+15	0
BG068759	Mm.27836	Mus musculus transforming. acidic coiled-coil containing protein 3 (Tacc3). mRNA	5.1352766	7.69E+35	0
UNKNOWN	UNKNOWN	UNKNOWN	5.131056211	1.62E+39	0
BG070433	Mm.239575	UNKNOWN	5.128741347	6.99E+30	0
BG065141	Mm.201917	Mus musculus RIKEN cDNA 2610318G08 gene (2610318G08Rik). mRNA	5.122823218	1.17E+26	0
BG074396	Mm.53435	Mus musculus hypothetical protein. clone 2-24 (AB030190). mRNA	5.119119894	2.75491E+17	0
BG074075	Mm.27142	Mus musculus. RIKEN cDNA 2610306D21 gene. clone IMAGE	5.106798081	7.92731E+16	0
BG069450	Mm.4071	Mus musculus laminin receptor 1 (67kD. ribosomal protein SA) (Lamr1). mRNA	5.08321687	1.39733E+15	0
BG065508	Mm.253156	UNKNOWN	5.079337594	1.46469E+16	0
BG069700	Mm.27424	Mus musculus similar to H4-K20-specific histone methyltransferase SET7 (LOC209316). mRNA	5.078252823	5.13E+20	0
BG071144	Mm.21578	Mus musculus ceroid-lipofuscinosis. neuronal 8 (Cln8). mRNA	5.041321185	9.55593E+16	0
UNKNOWN	UNKNOWN	UNKNOWN	4.985655173	4.50E+27	0
BG063615	Mm.35492	Mus musculus RIKEN cDNA 2600013N14 gene (2600013N14Rik). mRNA	4.980658602	9.26982E+18	0
BG076358	Mm.33840	Mus musculus hypothetical gene supported by BC026398; BC026398 (LOC263410). mRNA	4.956188745	9.94E+40	0
BG073419	Mm.196624	Mus musculus similar to putative oral cancer suppressor [Mesocricetus auratus] (LOC231728). mRNA	4.952172058	2.26E+23	0
BG069421	Mm.29133	Mus musculus budding uninhibited by benzimidazoles 1 homolog. beta (S. cerevisiae) (Bub1b). mRNA	4.947971738	3.65E+41	0
BG068707	Mm.192448	Mus musculus RIKEN cDNA 2700088M22 gene (2700088M22Rik). mRNA	4.944604419	4.0471E+18	0
BG075056	UNKNOWN	Mus musculus telomerase associated protein 1 (Tep1). mRNA	4.931564446	7.07231E+13	0
BG076017	Mm.2942	Mus musculus. Similar to asparagine synthetase. clone MGC	4.906234323	1.98E+37	0
BG064976	Mm.29546	Mus musculus BRG1/brm-associated factor 53A (Baf53a-pending). mRNA	4.893577493	1.68271E+15	0

Table S5. *(Continued)*

176 genes significant high expressed in cluster III (q-value 0).					
Accession code	**Unigene**	**Gene Name**	**Score(d)**	**Fold Change**	**q-value (%)**
BG063145	UNKNOWN	Mus musculus LOC236591 (LOC236591). mRNA	4.887305102	6.76368E+13	0
BG064461	Mm.220982	UNKNOWN	4.885972074	9.22941E+13	0
BG069655	Mm.4347	Mus musculus X-ray repair complementing defective repair in Chinese hamster cells 1 (Xrcc1). mRNA	4.866152526	4.12E+21	0
BG063508	Mm.147946	Mus musculus MYB binding protein (P160) 1a (Mybbp1a). mRNA	4.844867189	1.88614E+18	0
BG063841	Mm.28688	Mus musculus seryl-aminoacyl-tRNA synthetase 1 (Sars1). mRNA	4.822973401	1.36185E+19	0
UNKNOWN	UNKNOWN	UNKNOWN	4.818701889	1.78E+20	0
BG076131	Mm.103389	UNKNOWN	4.816408139	2.57079E+17	0
UNKNOWN	UNKNOWN	UNKNOWN	4.815197425	4.54E+21	0
UNKNOWN	UNKNOWN	UNKNOWN	4.812977707	1.22E+22	0
BG065906	Mm.1013	Mus musculus ligase I. DNA. ATP-dependent (Lig1). mRNA	4.799973666	4.17E+22	0
BG072944	Mm.873	Mus musculus. Similar to U5 snRNP-specific protein. 116 kD. clone IMAGE	4.782231182	7.20576E+16	0
BG074102	Mm.1141	Mus musculus hepatoma-derived growth factor (Hdgf). mRNA	4.780645045	6.06155E+17	0
BG074979	Mm.16323	Mus musculus similar to KIAA0690 protein [Homo sapiens] (LOC226120). mRNA	4.769046185	3.22446E+17	0
BG074412	Mm.3941	Mus musculus eukaryotic translation initiation factor 4E (Eif4e). mRNA	4.74510737	1.24755E+14	0
BG066941	Mm.10	Mus musculus spermidine synthase (Srm). mRNA	4.733483603	1.34E+30	0
BG068004	Mm.29894	Mus musculus. Similar to hypothetical protein FLJ22693. clone IMAGE	4.714917008	1.37349E+16	0
BG065117	Mm.90587	Mus musculus enolase 1. alpha non-neuron (Eno1). mRNA	4.711119637	5.05E+27	0
BG064948	Mm.218278	UNKNOWN	4.704916243	1.85927E+18	0
BG068615	Mm.173619	UNKNOWN	4.696735276	1.06925E+18	0
BG065249	Mm.4587	Mus musculus peptidylprolyl isomerase C (Ppic). mRNA	4.691540518	2.00893E+12	0
BG075192	Mm.57223	Mus musculus helicase. lymphoid specific (Hells). mRNA	4.687538547	3.86E+38	0
BG070214	Mm.6856	UNKNOWN	4.680513862	1.95E+38	0

Table S5. *(Continued)*

176 genes significant high expressed in cluster III (q-value 0).					
Accession code	**Unigene**	**Gene Name**	**Score(d)**	**Fold Change**	**q-value (%)**
BG064522	Mm.24789	Mus musculus RIKEN cDNA 5930415H02 gene (5930415H02Rik). mRNA	4.674586875	2.90924E+15	0
BG063998	Mm.29105	Mus musculus transcription factor IIIA mRNA. partial cds	4.670260598	4.24E+27	0
BG070559	Mm.22731	UNKNOWN	4.662807077	1.17E+26	0
BG067502	Mm.28470	Mus musculus RIKEN cDNA 0910001B06 gene (0910001B06Rik). mRNA	4.6607417	8.57869E+19	0
BG075069	Mm.24997	Mus musculus phosphatidylserine receptor (Ptdsr). mRNA	4.655378442	8.0709E+17	0
BG064439	Mm.182580	UNKNOWN	4.655269622	2.37E+21	0
BG063400	Mm.21586	Mus musculus Src activating and signaling molecule (Srcasm). mRNA	4.635398784	1.95688E+13	0
UNKNOWN	UNKNOWN	UNKNOWN	4.629683752	6.71822E+14	0
BG064846	Mm.4761	Mus musculus cell division cycle 2 homolog A (S. pombe) (Cdc2a). mRNA	4.616880067	4.14E+29	0
BG065812	Mm.28726	Mus musculus similar to putative nucleotide binding protein. estradiol-induced [Homo sapiens] (LOC218871). mRNA	4.606629911	7.32E+20	0
BG070759	Mm.24529	Mus musculus RIKEN cDNA 1100001F19 gene (1100001F19Rik). mRNA	4.601293794	4.85E+27	0
BG069489	Mm.2390	Mus musculus Cbp/p300-interacting transactivator with Glu/Asp-rich carboxy-terminal domain 1 (Cited1). mRNA	4.593103562	4.77439E+15	0
UNKNOWN	UNKNOWN	UNKNOWN	4.582308403	2.01E+35	0
BG071896	Mm.3752	Mus musculus RAN binding protein 1 (Ranbp1). mRNA	4.571947745	7.09799E+16	0
BG068084	Mm.28808	UNKNOWN	4.571670417	1.36077E+18	0
BG075959	Mm.29707	Mus musculus poly(rC) binding protein 4 (Pcbp4). mRNA	4.566764823	9.45E+26	0
BG071892	Mm.182628	Mus musculus RAD21 homolog (S. pombe) (Rad21). mRNA	4.559834887	1.21371E+14	0
BG064821	Mm.101931	Mus musculus. Similar to oxidative-stress responsive 1. clone IMAGE	4.545478355	1.75669E+18	0
BG072952	Mm.105040	UNKNOWN	4.544205971	6.68719E+11	0
UNKNOWN	UNKNOWN	UNKNOWN	4.542436222	3.80272E+18	0
BG073373	Mm.4595	UNKNOWN	4.540353304	2.29259E+16	0

Table S5. *(Continued)*

176 genes significant high expressed in cluster III (q-value 0).					
Accession code	**Unigene**	**Gene Name**	**Score(d)**	**Fold Change**	**q-value (%)**
BG063591	Mm.142380	Mus musculus ribosomal protein L27a (Rpl27a). mRNA	4.534424766	4.57837E+12	0
BG064473	Mm.3797	M.musculus mRNA for clone DN38	4.530057079	7.91736E+16	0
BG073422	Mm.69	Mus musculus nuclear distribution gene C homolog (Aspergillus) (Nudc). mRNA	4.524929403	2.09148E+19	0
BG069118	Mm.203747	UNKNOWN	4.509434405	2.68E+28	0
BG070381	Mm.30017	Mus musculus GABA(A) receptor-associated protein like 2 (Gabarapl2). mRNA	4.509167164	5.88764E+13	0
BG070990	Mm.259358	Mus musculus casein kinase II. alpha 2. polypeptide (Csnk2a2). mRNA	4.503413055	48267670983	0
BG073965	Mm.35511	Mus musculus RIKEN cDNA 2900019C14 gene (2900019C14Rik). mRNA	4.497970934	4.03E+21	0
BG070129	Mm.37820	UNKNOWN	4.491079989	523555818.4	0
BG063083	Mm.196198	UNKNOWN	4.489712413	9.62925E+19	0

Table S5. *(Continued)*

40 genes significant low expressed in cluster III (q-value 0)					
Accession code	**Unigene**	**Gene Name**	**Score(d)**	**Fold Change**	**q-value (%)**
BG076229	Mm.27897	UNKNOWN	-8.115113549	2.07E-17	0
BG071976	Mm.42927	Mus musculus LIM motif-containing protein kinase 2 (Limk2). mRNA	-7.006992286	3.76E-39	0
BG075828	Mm.1075	Mus musculus RIKEN cDNA 2010004M01 gene (2010004M01Rik). mRNA	-6.805737467	1.16E-21	0
BG073939	Mm.4514	Mus musculus aldehyde dehydrogenase family 1. subfamily A1 (Aldh1a1). mRNA	-6.64473151	6.97E-60	0
BG071504	Mm.143527	Mus musculus RIKEN cDNA 2500002L14 gene (2500002L14Rik). mRNA	-6.612819885	1.01E-23	0
BG071284	Mm.23352	Mus musculus similar to sulfite oxidase [Rattus norvegicus] (LOC211389). mRNA	-6.541627802	1.05E-37	0
BG068548	Mm.196080	Mus musculus similar to H326 [Homo sapiens] (LOC226666). mRNA	-6.429259892	1.07E-19	0
BG071521	Mm.25552	Mus musculus grainyhead like 1 (Drosophila) (Grhl1-pending). mRNA	-6.365329511	9.16E-47	0
BG075482	Mm.37835	Mus musculus ribosomal protein L7 (Rpl7). mRNA	-6.091737555	1.09E-16	0
BG069254	Mm.253329	Mus musculus similar to hypothetical protein MBC3205 [Homo sapiens] (LOC235043). mRNA	-5.890957751	1.51E-39	0
BG075466	Mm.41767	Mus musculus RIKEN cDNA 3110023E09 gene (3110023E09Rik). mRNA	-5.728246009	1.28E-16	0
BG075679	Mm.46653	UNKNOWN	-5.704436111	1.25E-45	0
UNKNOWN	UNKNOWN	UNKNOWN	-5.640097944	3.70E-15	0
BG076024	Mm.5027	Mus musculus enhancer of zeste homolog 1 (Drosophila) (Ezh1). mRNA	-5.552825135	1.49E-22	0
BG064004	Mm.9239	Mus musculus. clone IMAGE	-5.533991514	2.03E-24	0
UNKNOWN	UNKNOWN	Mus musculus RIKEN cDNA 2500002L14 gene (2500002L14Rik). mRNA	-5.499819328	2.54E-18	0
BG075054	Mm.12616	UNKNOWN	-5.46621666	2.40E-27	0
BG074999	Mm.27664	Mus musculus Unc-51 like kinase 2 (C. elegans) (Ulk2). mRNA	-5.443038926	8.96E-13	0
BG063234	Mm.171800	UNKNOWN	-5.42726693	4.65E-35	0
BG069754	Mm.3960	Mus musculus interferon regulatory factor 3 (Irf3). mRNA	-5.333208341	3.20E-18	0
BG066195	Mm.155523	UNKNOWN	-5.280711927	2.46E-21	0
BG075058	Mm.28537	Mus musculus. secretory carrier membrane protein 2. clone MGC	-5.248394103	2.02E-18	0
BG075763	Mm.20903	Mus musculus similar to Junctional adhesion molecule 1 precursor (JAM) (LOC226655). mRNA	-5.239936847	8.22E-34	0

Table S5. *(Continued)*

40 genes significant low expressed in cluster III (q-value 0)					
Accession code	**Unigene**	**Gene Name**	**Score(d)**	**Fold Change**	**q-value (%)**
BG066624	UNKNOWN	UNKNOWN	-5.23796135	7.15E-25	0
BG074538	Mm.233161	Mus musculus LOC212371 (LOC212371). mRNA	-5.192359244	1.80E-35	0
BG063148	Mm.27585	UNKNOWN	-5.177728833	7.91E-25	0
BG075429	Mm.16340	UNKNOWN	-5.149986904	9.52E-43	0
BG068743	Mm.30731	UNKNOWN	-5.135626018	4.83E-24	0
BG075840	Mm.27477	Mus musculus RIKEN cDNA 2010100O12 gene (2010100O12Rik). mRNA	-5.121491667	5.71E-16	0
BG063153	Mm.444	UNKNOWN	-5.112333242	9.27E-36	0
BG074499	Mm.18688	Mus musculus RIKEN cDNA 1110014C03 gene (1110014C03Rik). mRNA	-5.106127426	1.91E-23	0
BG066151	Mm.201128	UNKNOWN	-5.096962963	2.03E-21	0
UNKNOWN	UNKNOWN	UNKNOWN	-5.069345005	3.32E-16	0
UNKNOWN	UNKNOWN	UNKNOWN	-5.021753318	2.80E-17	0
BG063044	Mm.21739	Mus musculus fusion 1 (Fus1-pending). mRNA	-5.020606015	1.31E-15	0
BG070643	Mm.170167	UNKNOWN	-5.018975389	1.67E-14	0
UNKNOWN	UNKNOWN	UNKNOWN	-5.005662934	2.41E-19	0
BG064392	Mm.128834	Mus musculus vacuolar protein sorting 4b (yeast) (Vps4b). mRNA	-5.002711781	2.91E-18	0
BG075729	Mm.27432	Mus musculus DnaJ (Hsp40) homolog. subfamily B. member 9 (Dnajb9). mRNA	-4.98953621	2.34E-21	0
BG071495	Mm.21591	Mus musculus RIKEN cDNA 4932702F08 gene (4932702F08Rik). mRNA	-4.970046041	2.05E-17	0

CHAPTER 5

Identification of *TDRD1* as a direct target gene of *ERG* in primary prostate cancer

Joost L Boormans[1]*, Hanneke Korsten[2]*, Angelique CJ Ziel-van der Made[2], Geert JLH van Leenders[2], Carola V de Vos[2], Guido Jenster[1], and Jan Trapman[2]

[1] Department of Urology Erasmus Medical Centre, Rotterdam, the Netherlands
[2] Department of Pathology, Josephine Nefkens Institute, Erasmus University Medical Center, Rotterdam, the Netherlands.
* Equal contribution

Submitted

ABSTRACT

Genomic rearrangements involving fusion of the androgen-regulated gene *TMPRSS2* to the oncogene *ERG*, are frequent in prostate cancer. The function of this gene fusion, however, is still largely unknown. We used genome-wide gene expression arrays and quantitative reverse transcription-PCR (Q-RT-PCR) to identify genes that were co-expressed with *ERG* overexpression in different stages of prostate cancer. In a cohort of primary prostate tumors (n=48, cohort A), the expression of the gene Tudor domain containing 1 (*TDRD1*) showed by far the strongest correlation with *ERG* overexpression. This observation was confirmed by Q-RT-PCR for both cohort A and for an independent cohort of primary prostate tumors (n=31). Analysis of expression array data of a cohort of primary prostate tumors from a different institute (n=128) showed a large overlap in genes that were positively correlated with *ERG* overexpression in cohort A, including *TDRD1*. In late-stage prostate cancer, *TDRD1* was also co-expressed with *ERG* overexpression, although a proportion of *ERG*-negative late-stage samples also expressed *TDRD1*. *TDRD1* expression was not associated with the expression of other ETS family members and even seemed to be an inverse-correlation with *ETV1* overexpression. *Tdrd1* expression showed similar kinetics as *Erg* during mouse prostate development. In the prostate cancer cell line VCaP, downregulation of ERG by shRNA lead to a lower expression level of TDRD1. Moreover, downregulation of ERG in VCaP cells resulted in a decreased activity of the *TDRD1* promoter. By mutation analysis we identified a functional *ERG* binding site in the *TDRD1* promoter. In conclusion, our findings show *TDRD1* as the first identified upregulated direct ERG target gene that is strongly associated with *ERG* overexpression in primary prostate cancer.

INTRODUCTION

Erythroblast transformation-specific (ETS) transcription factors regulate the expression of genes that are important in cancer-related processes like cell growth, differentiation, and transformation [1]. It is well known that deregulated expression of ETS family members and chimeric ETS proteins caused by gene fusions are associated with leukemia and Ewing's sarcoma [1-3]. In prostate cancer, gene fusions involving ETS transcription factors, including fusions of the v-ets erythroblastosis virus E26 oncogene homolog (avian), *ERG*, and the ETS variant gene 1, *ETV1*, have recently been detected [4]. Fusion of the androgen-regulated and prostate-specific gene transmembrane protease, serine 2, *TMPRSS2* and *ERG* is the most frequent genomic rearrangement in prostate cancer with a reported frequency of 40-70%, whereas fusions involving *ETV1* are present in 5-10% of prostate cancers [5, 6].

The significance of fusion genes involving ETS family members in the development and progression of prostate cancer is still largely unknown. It has been demonstrated that transgenic mice with targeted, prostate-specific overexpression of *ERG* developed mouse prostate intra-epithelial neoplasia (PIN) [7, 8], although this has been questioned by others [9]. Progression to invasive cancer involving *ERG* overexpression was described in mice with a phosphatase and tensin homologue (*Pten*) haploinsufficient genetic background [10, 11]. Like observed in *ERG* transgenic mice, mice with targeted, prostate-specific overexpression of *ETV1* developed PIN-like lesions, but invasive prostate cancer was not observed [12, 13]. These data indicate that overexpression of *ERG* or *ETV1* is insufficient for prostate cancer development and that additional molecular events are necessary for neoplastic transformation.

To increase our knowledge of the function of *ERG* overexpression in prostate cancer, we analyzed RNA expression profiles of primary prostate tumors to identify genes that were strictly co-expressed with *ERG* overexpression. In these analysis, Tudor domain containing 1 (*TDRD1*) showed by far the strongest association with *ERG* overexpression. Coexpression of *TDRD1* and *ERG* was validated in a completely independent large patient cohort from a different institute. Further, we observed that during mouse prostate development, *Erg* and *Tdrd1* were coregulated. Promoter studies indicated that *TDRD1* expression was directly regulated by *ERG*. In late-stage prostate cancer samples and in prostate cancer cell lines and xenografts, *TDRD1* was not only expressed in *ERG*-positive, but also in a proportion of *ERG*-negative tumor samples. *TDRD1* expression was not correlated with *ETV1* overexpression. Because *TDRD1* expression was very low in normal prostatic tissue, it is an excellent diagnostic marker for a large proportion of prostate cancers.

MATERIAL AND METHODS

Clinical samples

Primary prostate tumors were obtained by radical prostatectomy (patients whose initial treatment was not a radical prostatectomy were not included), late-stage tumors by transurethral resection of the prostate (TURP), and lymph node metastases by pelvic lymphadenectomy. Expression data were obtained from 48 primary prostate tumors, 11 lymph node metastases, and nine TURP samples. Furthermore, normal adjacent prostatic tissue (NAP) from radical prostatectomy, NAP from TURP specimens, and from benign lymph nodes were included (n=12, n=2, and n=3, respectively). In addition, a cohort of 31 primary prostate tumors (initial treatment was a radical prostatectomy in all cases) and a cohort of 17 NAP tissue samples was analyzed by quantitative reverse transcription-PCR (Q-RT-PCR) for validation purposes. Hematoxilin/eosin stained tissue sections were histologically evaluated by two uropathologists (T.H. van der Kwast; G.J.L.H. van Leenders). All tumor samples contained at least 70% tumor. Tissues were snap-frozen and stored in liquid nitrogen. Use of the samples for research purposes was approved by the Erasmus MC Medical Ethics Committee according to the Medical Research Involving Human Subjects Act (MEC-2004-261).

Human prostate cancer cell lines and xenografts, and mouse tissue samples

Prostate cancer cell lines LNCaP, VCaP, PC346C, LAPC4, 22Rv1, and MDAPCa2B were grown in RPMI-1640 or D-MEM supplemented with 5% fetal calf serum and antibiotics. Prostate cancer xenografts PCEW, PC82, PC295, PC310, PC329, PC346B, PC374, PC133, PC135, PC324, and PC339, were propagated by serial transplantation on male nude mice, as described [14, 15]. *Balb/c* mouse prostate tissues were collected at different developmental stages (16.5 and 18.5 embryonal days and postnatal days 3, 9, 15, and 50).

RNA isolation

RNA from snap-frozen sections of clinical prostate cancer samples was isolated using RNA-Bee (Campro Scientific, Berlin, Germany). The RNeasy RNA extraction kit (Qiagen, Valencia, CA, USA) was used to isolate RNA from human prostate cancer cell lines and mouse prostates of different developmental stages. Xenograft RNA was isolated according to the LiCl protocol.

Hybridization and analysis of exon arrays

Expression profiles were determined using GeneChip Human Exon 1.0 ST array (Affymetrix, Santa Clara, CA, USA) at the Center for Biomics, Erasmus MC, Rotterdam, the Netherlands and at ServiceXS, Leiden, the Netherlands, according to the manufacturer's instructions. Microarray data were processed and RMA quantile normalized using Partek Genomics Suite (St. Louis, MO,

USA). To study the expression of genes differentially expressed between prostate tumors with and without *ERG* rearrangement, the expression values of the different probe sets of a transcript were processed by Partek on gene level. By significance analysis of microarrays (SAM), genes coexpressed with *ERG* were identified [16]. The q-value (false discovery rate) for genes identified by SAM was set to zero. The programs Cluster and Treeview were used to visualize genes with the highest differential expression according to SAM [17].

Quantitative RT-PCR (Q-RT-PCR)

Total RNA was reverse transcribed using M-MLV reverse transcriptase (Invitrogen, Carlsbad, CA, USA) and an oligo dT12 primer. Q-RT-PCR was performed using Power SYBR Green PCR Master Mix (25 µl), containing 0.33 µM forward and reverse primer in an ABI Prism 7700 Sequence Detection System (Applied Biosystems, Foster City, CA, USA). Amplified products were quantified relative to Hydroxymethylbilane synthase (*HMBS*, formerly *PBGD*; human RNAs), or Hypoxanthine guanine phosphoribosyl transferase 1 (*Hprt*; mouse RNAs) by the Standard curve method (Applied Biosystems). Primer sequences are shown in Supplementary Table S1.

***TDRD1* promoter analyses**

In VCaP cells that overexpress ERG, ERG expression was downregulated by incubation with specific siRNA (SiGenome smartpool, m-003886-01-0005, Thermo scientific) or by infection with lentivirus expressing *ERG* shRNA (Erasmus MC Rotterdam). ERG and TDRD1 expression were assayed by standard Western blotting, using ERG antibody NBPI-40794 (Novus Biologicals, Littleton, CO, USA) or TDRD1 antibody HPA037730 (Sigma Aldrich, St. Louis, MO, USA), respectively. Specificity of the TDRD1 antibody was demonstrated in HEK293 cells, transfected with a TDRD1 expression vector. Protein bands were visualized by chemoluminescence (Pierce, Rockford, IL, USA). For promoter activity studies, appropriate fragments of the *TDRD1* promoter were amplified by PCR on genomic DNA, sequenced and cloned in front of the LUC reporter in the promoterless vector pLUC. Candidate ERG binding sites CGGAA/T and the opposite reverse sequence T/ATCCG were identified. Inactivating mutations in ERG binding sites were introduced by the QuikChange method (200516-5, Stratagene, San Diego, CA, USA). VCaP cells transfected by the various LUC reporter constructs were harvested after 24h and luciferase activity was measured in cell lysates in a LUMAC 2500 Biocounter (Lumac, Landgraaf, The Netherlands).

Statistical analysis

A Perl implementation of Pearson's correlation (correlation factors >0.5 or ≤0.5) was used to identify genes that were most closely coexpressed with *ERG*. Associations between clinico-pathological variables and the expression of different transcripts were evaluated by the Pearson's χ^2 test or the Mann-Whitney U (MWU) test, where appropriate. Linear regression analysis was

used to model the relationship between the expression of *ERG* and that of other genes. Statistical analyses were done using the Statistical Package for Social Sciences, version 17.0 (SPSS) with a significance level of 0.05 (two-tailed probability).

RESULTS

Strong association of *TDRD1* and *ERG* expression in primary prostate cancers

A cohort of 48 primary prostate tumors (cohort A) was analyzed for genes that were coexpressed with *ERG* overexpression using the GeneChip Human Exon 1.0 ST array. The clinicopathological characteristics of this cohort are summarized in Supplementary Table S2. Thirty-three out of the 48 tumor samples (69%) showed *ERG* overexpression caused by gene fusion. SAM identified 206 genes that were significantly differentially expressed between *ERG*-positive and *ERG*-negative tumor samples (see Supplementary Table S3). One hundred ninety-seven genes were positively correlated with *ERG* overexpression, whereas the expression of nine genes was inverse correlated with *ERG* overexpression. *TDRD1* showed by far the strongest association with *ERG* overexpression (Score(d)=10.3 and Fold Change=8.55) (Figure 1A,B and Supplementary Table S3). Figure 1B shows a heat map of the 20 genes with the most significant positive correlation with *ERG* overexpression. The function of these genes is variable but several genes, like *NKAIN1, CACNA1D* and *KCNH8* are involved in ion-transporting pathways (see for gene abbreviations, full gene names and accession numbers Supplementary Table S4). One tumor (G275) had low *ERG* and high *TDRD1* expression. *PLA2G7, GPR110, CRISP3* and *PIGR* showed a variable d-score but a high fold change value, indicating a strong association with a subgroup of cancers with *ERG* overexpression.

For validation purposes, Q-RT-PCR of *TDRD1* and *ERG* was carried out. The results were consistent with the expression array data with two exceptions (G165 and G124; Figure 1C). The median level of expression of *TDRD1* in tumors with *ERG* overexpression was significantly higher than in tumors that did not overexpress *ERG* ($p < 0.001$, MWU test; Supplementary Figure S1).

Next, the expression of *ERG* and *TDRD1* was analyzed in an independent set of 31 primary prostate tumors (cohort B) (see for the clinicopathological characteristics of this validation set Supplementary Table S2). Q-RT-PCR data showed that 13 out of the 31 samples (42%) overexpressed *ERG*. In this cohort, *TDRD1* expression was also strongly correlated with *ERG* overexpression (Figure 1D) and again the median expression level of *TDRD1* was significantly higher in *ERG*-positive than in *ERG*-negative samples ($p<0.001$, MWU test, data not shown). Linear regression analysis confirmed the significant correlation between *TDRD1* and *ERG* expression for both cohort A and B ($p<0.001$ and $p<0.001$, Supplemental Figure S2). The unique specificity of the association of *TDRD1* and *ERG* overexpression in primary prostate cancers was supported

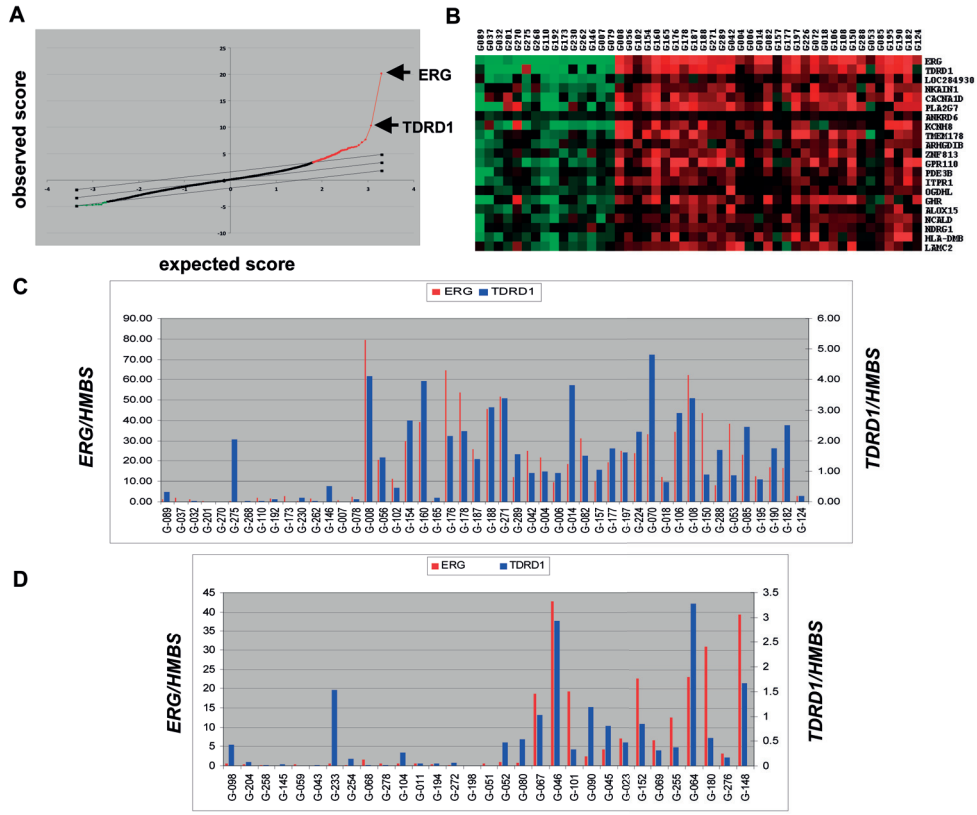

Figure 1. Identification of genes coexpressed with *ERG* in a cohort of 48 primary prostate tumours (cohort A) and in a validation set of 31 primary prostate tumors (cohort B). (**A**) Scatter plot of the expected relative difference score (*X*-axis) versus the observed relative difference score (*Y*-axis) from the comparison of primary prostate tumors that overexpress *ERG* (N=33) versus tumours without *ERG* overexpression (N=15) by SAM. Significantly upregulated genes are shown in red, whereas significantly downregulated genes are shown in green. *ERG* and *TDRD1* are indicated. (**B**) Heat map showing the 20 genes strongest correlated with *ERG* overexpression. Each cell in the image shows the $\log^2$ expression ratio for the particular gene divided by the median expression of that gene in all the samples. *Red*, expression above the median; *green*, expression below the median. (**C**) Q-RT-PCR analysis of *TDRD1* and *ERG* expression in primary prostate tumors of cohort A (N=48). *ERG* and *TDRD1* expression relative to *HMBS* are shown. The relative expression of *ERG* is depicted on the primary *Y*-axis, whereas the relative expression of *TDRD1* is depicted on the secondary *Y*-axis. (**D**) Q-RT-PCR analysis of *TDRD1* and *ERG* expression in a validation cohort of primary prostate tumours (N=31). *ERG* and *TDRD1* expression relative to *HMBS* are shown. The relative expression of *ERG* is depicted on the primary *Y*-axis, whereas the relative expression of *TDRD1* is depicted on the secondary *Y*-axis.

by comparison with Q-RT-PCR analyses of two other randomly selected genes that correlated with *ERG* overexpression: *NKAIN1* and *CACNA1D* (see Figure 1B). In cohort A and B, the median expression level of *NKAIN1* was significantly higher in *ERG*-positive than in *ERG*-negative tumors ($p<0.001$ and $p=0.04$, respectively), but with lower statistical significance than for *TDRD1*. *CACNA1D* was only significantly differentially expressed in cohort A ($p=0.011$; cohort B, $p=0.34$) (data not shown). Linear regression analysis confirmed the correlation between *NKAIN1* and *ERG*, and between *CACNA1D* and *ERG* expression in cohort A but not in the validation cohort B (Supplementary Figure S3).

Identification of genes coexpressed with *ERG* overexpression in a cohort of primary prostate tumors from a different institute

To further validate our findings of genes that were coexpressed with *ERG* overexpression in primary prostate cancer, we analyzed expression array data (GeneChip Human Exon 1.0 ST array) of a large cohort of primary prostate tumors from Memorial Sloan Kettering Center (MSKCC) [18]. The data of this study are available at http://cbio.mskcc.org/prostate-portal. We excluded from the analysis patients whose initial treatment was not a radical prostatectomy leaving 128 patients eligible for analysis. We identified 53 *ERG*-positive and 75 *ERG*-negative primary prostate tumors. By SAM, it was shown that 639 genes were significantly differentially expressed between *ERG*-positive and *ERG*-negative tumor samples; 559 were positively correlated with *ERG* overexpression, whereas the expression of 80 genes was inverse correlated with *ERG* overexpression.

We found a large overlap of genes that were positively correlated with *ERG* overexpression with our series (Figure 2A). One hundred and ten out of 197 genes (56%) that we found to be coexpressed with *ERG* overexpression were also present among the coexpressed genes of the MSKCC data set (Figure 2A). Importantly, out of the top 20 genes with *ERG* overexpression from our series (Supplementary Table S4), all but two (*LOC284930* and *ZNF813*), were also identified in the MSKCC cohort. In the MSKCC cohort, *TDRD1* was also strongly associated with *ERG* overexpression (Score(d)=7.38 and Fold Change=2.73), although it was not the strongest correlated gene. This probably was due to the observation that, unlike in our cohort, a proportion of the *ERG*-negative primary tumors harbored *TDRD1* expression (Figure 2B) but in this cohort too all tumors with *ERG* overexpression showed overexpression of *TDRD1*. Two out of nine genes that were inverse correlated with *ERG* overexpression in our array data set were also downregulated in the MSKCC cohort: Hydroxyprostaglandin dehydrogenase 15-(NAD) (*HPGD*) and Trefoil factor 3 (*TFF3*).

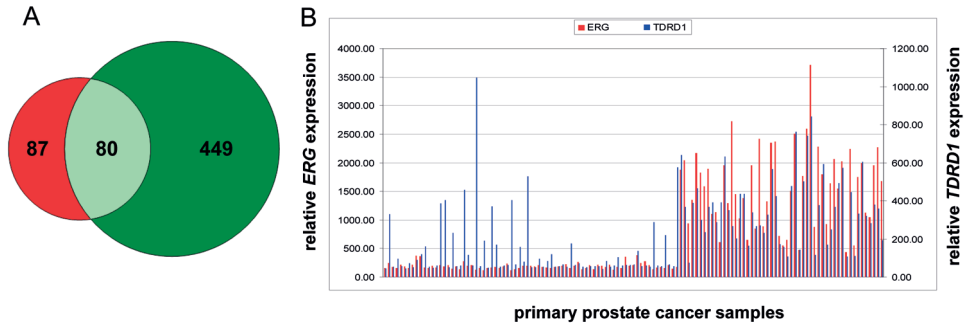

Figure 2. Genes coexpressed with *ERG* overexpression as analyzed by expression array data of 128 primary prostate tumors from MSKCC [18]. (**A**) Venn-diagram showing the overlap in genes that were positively correlated with *ERG* overexpression between the present series (red) and the series of MSKCC (green). *TDRD1* is among the 80 genes that were coexpressed with *ERG* overexpression in both series. (**B**) Bar chart showing expression levels of *ERG* (red bars) and *TDRD1* (blue bars) according to the analysis of genome-wide expression array data (GeneChip Human Exon 1.0 ST array) of 128 primary prostate tumors of MSKCC. The relative expression of *ERG* is depicted on the primary *Y*-axis, whereas the relative expression of *TDRD1* is depicted on the secondary *Y*-axis. Note that part of *ERG*-negative samples harbored *TDRD1* expression.

Expression of *TDRD1* and *ERG* in late-stage prostate cancer

Expression array data of a small set of nine late-stage prostate tumors (three *ERG*-positive and six *ERG*-negative tumors) indicated that *TDRD1* was not only expressed in *ERG*-positive but also in several *ERG*-negative tumors (data not shown). This preliminary finding was extended by Q-RT-PCR in a cohort of 51 late-stage prostate tumors and 11 prostate cancer lymph node metastases. Like observed in primary tumors, *TDRD1* was coexpressed with *ERG*, however, not only *ERG*-positive tumors but also a proportion of *ERG*-negative, late-stage tumor samples and metastases showed expression of *TDRD1* (Figure 3A). In addition, in the samples with *TDRD1* overexpression, the median expression level of *TDRD1* in primary tumors (N=48) was significantly lower than in the group of late-stage tumors and lymph node metastases (N=32 and N=9, respectively) (p=0.005, MWU test) (Figure 3B), although in the samples that overexpressed *ERG* (45 primary tumors versus 41 late-stage tumors and metastases (N=31 and N=10, respectively), the median expression level of *ERG* in the primaries was comparable with the median expression level in the group of late-stage tumors and metastases (p=0.73, MWU test). High *TDRD1* expression was also observed in the prostate cancer cell line VCaP that overexpresses *ERG* and in the xenografts with *ERG* overexpression, but here too several *ERG*-negative samples showed *TDRD1* expression (PC346C, PC133, PC324, and PC346B, Supplementary Figure S4).

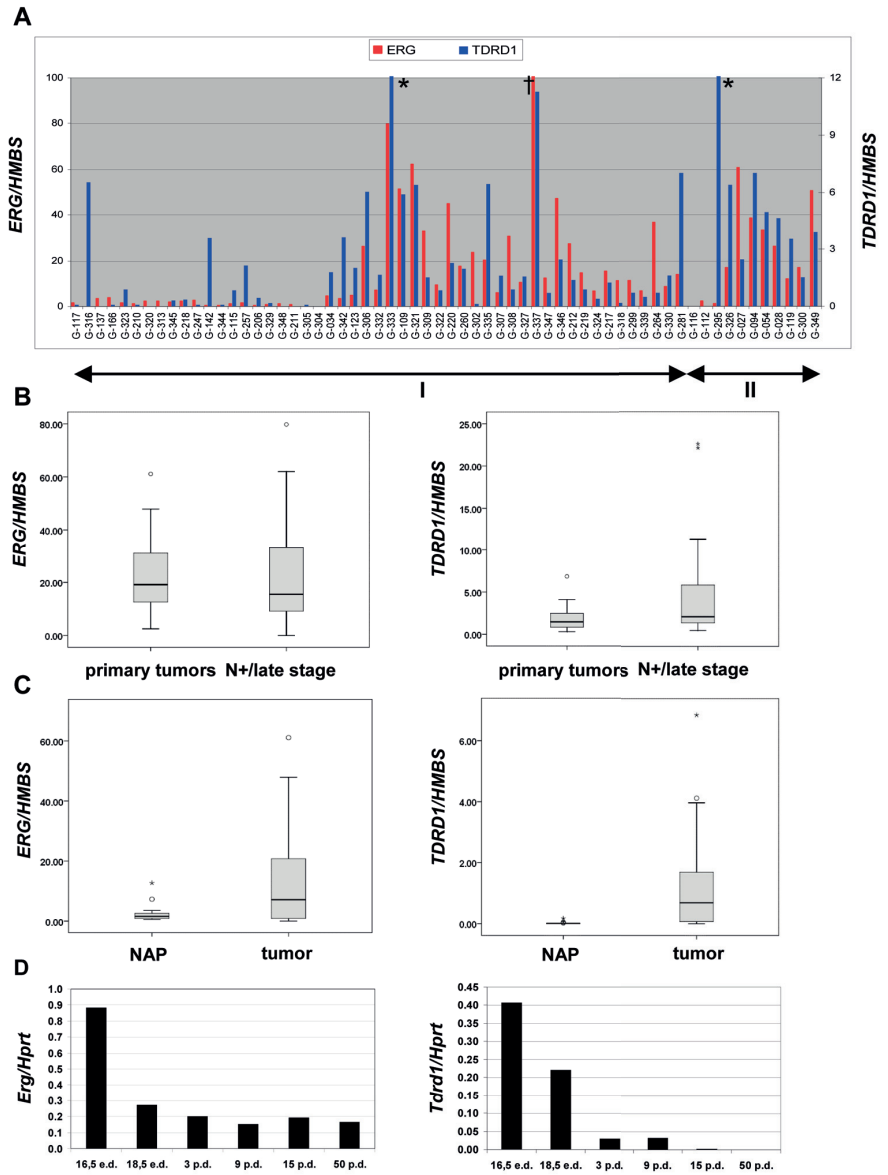

Figure 3. Expression of *ERG* and *TDRD1* in late-stage prostate cancer. (A) Q-RT-PCR analysis of *ERG* and *TDRD1* transcripts in a cohort of late-stage prostate tumors and prostate cancer lymph node metastases. Late-stage tumour samples are indicated by I (N=51), whereas the lymph node metastases are indicated by II (N=11). *ERG* (red bars) and *TDRD1* (blue bars) expression relative to *HMBS* are shown. The relative expression of *ERG* is depicted on the primary *Y*-axis, whereas the relative expression of *TDRD1* is depicted on the secondary *Y*-axis.* The relative expression of *TDRD1* in samples G333 and G295 is 22.6 and 22.1, respectively.† The relative expression of *ERG* in G337 is 266.8. (**B**) Box plot showing median expression of *ERG* (left panel) and *TDRD1* (right panel) relative

to *HMBS*, as detected by Q-RT-PCR, in primary versus late-stage prostate tumors and prostate cancer lymph node metastases. Only samples with *ERG* (left panel) or *TDRD1* (right panel) overexpression were included in the analysis. Outliers are depicted by an open circle (°) and extremes are depicted by an asterisk (*). For readability of the figure, in the left panel, the late-stage sample G-337 is not shown (relative expression of *ERG* = 266.8). (**C**) Box plots show the median expression of *ERG* (left panel) and *TDRD1* (right panel) relative to *HMBS*, as detected by Q-RT-PCR, in 17 normal adjacent prostatic (NAP) tissue samples versus 81 primary prostate tumors. Outliers are depicted by an open circle (°) and extremes are depicted by an asterisk (*). (**D**) The expression of *Erg* and *Tdrd1* during mouse prostate development as determined by Q-RT-PCR. The expression of *Erg* (left panel) and *Tdrd1* (right panel) relative to *Hprt* expression is presented on the *Y*-axis. Time points of RNA isolation are indicated on the *X*-axis. E.d. = embryonal day; p.d. = postnatal day.

Expression of *TDRD1* and *ERG* in normal prostatic tissue

Next, we investigated *ERG* and *TDRD1* expression in non-cancerous prostate tissues. The relative expression of both *ERG* and *TDRD1* was very low in the NAP (normal adjacent to cancer) tissue samples compared with primary tumors ($p=0.052$ and $p<0.001$, MWU test, respectively) (Figure 3C). Additionally, we investigated *Erg* and *Tdrd1* expression in prostate development in mice. *Tdrd1* showed similar kinetics as *Erg* during mouse prostate development. Q-RT-PCR analysis found that *Erg* is overexpressed in the urogenital sinus at the time point that prostate development starts at embryonal day 16.5 (16.5 e.d.) (Figure 3D). During later stages of mouse prostate development, *Erg* was expressed at a much lower level. *Tdrd1* expression was also high during the early stages of mouse prostate development, whereas in the adult mouse prostate (50 postnatal days, 50 p.d.), *Tdrd1* expression was very low.

Expression of *TDRD1* and *ETV1* in primary prostate tumors

Next, we analyzed the expression of *TDRD1* and of the *ERG*-related ETS transcription factors *ETV1*, *ETV4*, and *ETV5*. *ETV1* is overexpressed in 5-10% of prostate cancer gene fusions. *ETV4* and *ETV5* overexpression is rare (less than 1%) [5, 6]. The expression array data showed five out of 48 primary prostate tumors to harbor *ETV1* overexpression, whereas *ETV4* or *ETV5* overexpression was absent. None of the five tumor samples overexpressing *ETV1* showed *TDRD1* overexpression (Figure 4A). The array data were validated and extended by Q-RT-PCR for *ETV1* and *TDRD1* in a larger cohort of primary prostate tumors, which were all without treatment at the time of radical prostatectomy (N=79). Nine tumors (11%) showed *ETV1* overexpression. Three out of nine samples with *ETV1* overexpression showed *TDRD1* expression at very low levels, whereas in six samples *TDRD1* expression could not be detected (Figure 4B). These data indicated that, in contrast to the strong positive correlation with *ERG* overexpression, *TDRD1* expression is inversely correlated with *ETV1* overexpression in primary prostate cancer.

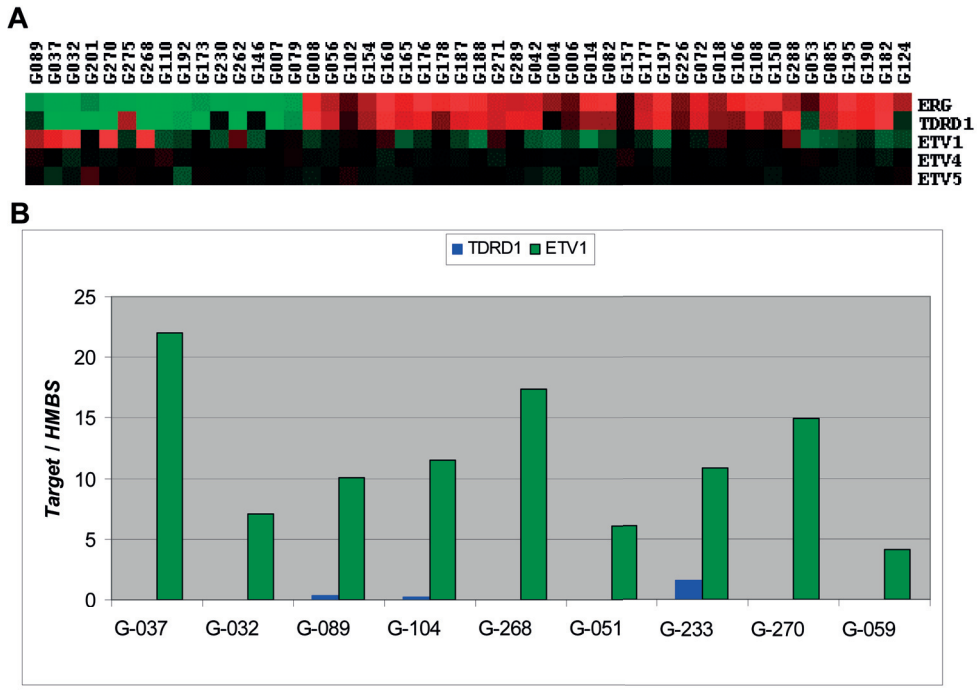

Figure 4. Expression of *TDRD1* and *ETV1* in primary prostate tumors. (**A**) Heat map showing the correlation between the expression of ETS family members *ETV1*, *ETV4*, and *ETV5*, and the expression of *ERG* and *TDRD1* in primary prostate tumors of cohort A. Each cell in the image shows the $\log^2$ expression ratio for the particular gene divided by the median expression of that gene in all the samples. *Red*, expression above the median; *green*, expression below the median. (**B**) Bar chart showing expression levels of *TDRD1* and *ETV1* relative to *HMBS* for nine primary prostate tumours with *ETV1* overexpression as determined by Q-RT-PCR.

ERG directly regulates *TDRD1* expression

Because of the strong association between *TDRD1* and *ERG* expression, we analyzed TDRD1 protein expression in the VCaP cell line that expresses both *ERG* and *TDRD1*. Western blot analysis of a lysate of HEK293T cells transfected with a TDRD1 expression plasmid showed a specific TDRD1 protein band at 132 kD, and a slightly smaller non-specific band (Figure 5A). The specific TDRD1 protein band was also clearly detectable in a lysate of VCaP cells (Figure 5A). To investigate whether ERG can regulate TDRD1 expression, ERG was downregulated in VCaP cell by infection with lentivirus expressing a specific shRNA (Figure 5B). The downregulation of ERG lead to a substantial lower expression level of the TDRD1 protein, which indicated that ERG can regulate TDRD1 expression. TDRD1 shRNA did not downregulate ERG expression (data not shown).

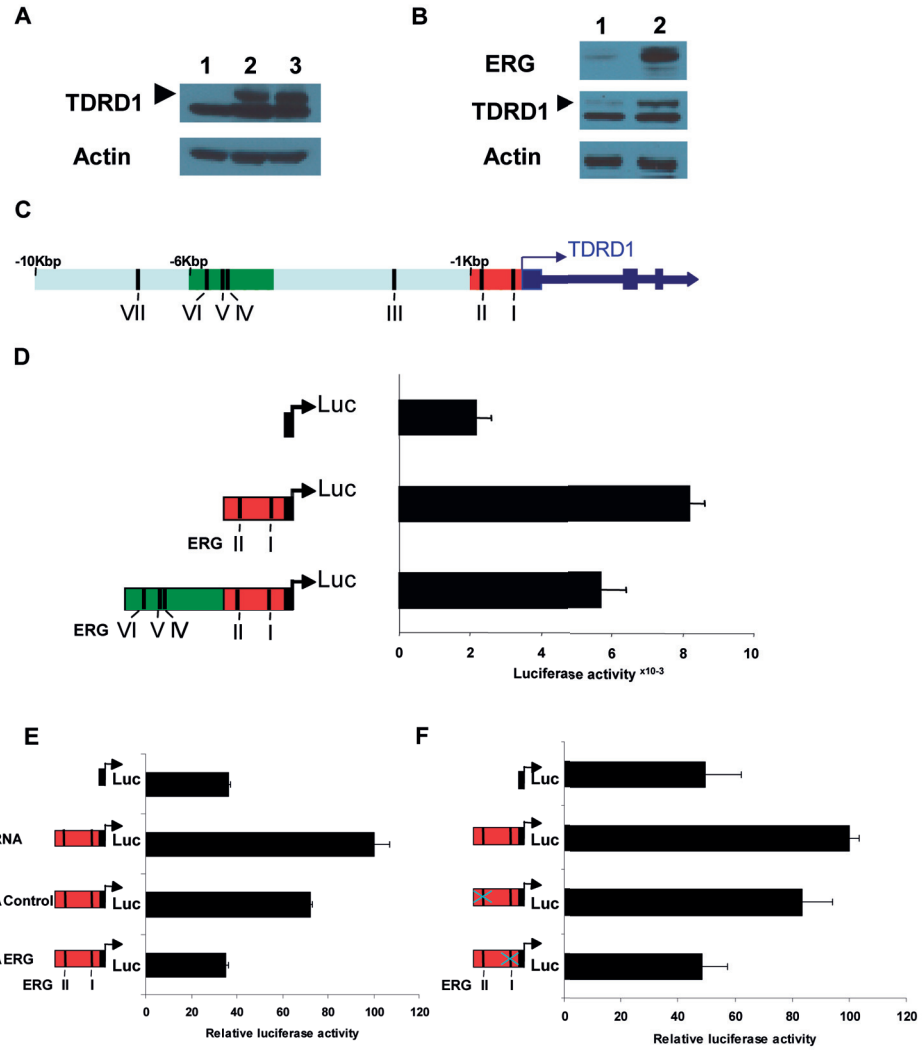

Figure 5. ERG directly regulates *TDRD1* promoter activity. (**A**) Western blot analysis of TDRD1 expression in HEK293 cells transfected with a TDRD1 expression plasmid and in VCaP cells. Lane 1: control HEK293 cells; lane 2: transfected HEK293 cells; Lan 3: endogenous TDRD1 expression in VCaP cells. Note that the antibody recognises TDRD1 and a slightly smaller unidentified protein. (**B**) Western blot analysis of ERG and TDRD1 expression in VCaP cells incubated with *ERG* shRNA lentivirus. Lane 1: ERG shRNA; Lane 2: control. (**C**) Schematical representation of a 10kbp *TDRD1* promoter fragment. Positions of seven candidate ERG binding sites and promoter fragments used in reporter gene assays are indicated. (**D**) *TDRD1* promoter activity in transiently transfected VCaP cells as determined by Luciferase activity. (**E**) Effect of *ERG* siRNA on *TDRD1* promoter activity as determined by Luciferase assay in transiently transfected VCaP cells. (**F**) Effect of inactivation of candidate ERG binding sites I and II on *TDRD1* promoter activity in transiently transfected VCaP cells.

To unravel the mechanisms of TDRD1 expression regulation by ERG, candidate ERG binding sites CGGA(A/T) or (T/A)TCCG were determined in a 10 Kbp genomic region upstream of *TDRD1* (Figure 5C). In total, seven candidate ERG binding sites were detected. Based on the locations of these sequences, two regions (Figure 5C and 5D) were selected for further analysis. Luciferase (Luc) reporter gene constructs driven by, either the promoter region that contains two candidate ERG binding sites, or the promoter region plus an upstream region that contains three potential ERG binding sites (Figure 5D) were generated and transfected into VCaP cells. The Luc data showed that the promoter region was active but that the upstream region did not increase activity (Figure 5D). To investigate whether *TDRD1* promoter region activity was regulated by ERG, the activity was determined in the presence of *ERG* siRNA. Downregulation of ERG resulted in decreased activity of the *TDRD1* promoter (Figure 5E). To determine whether one of the two predicted ERG binding sites in the promoter was important for the promoter activation, both binding site I and II were inactivated by mutation. A clear decrease in Luc activity upon mutation of the ERG binding site I, but not of candidate binding site II was observed (Figure 5F), indicating that ERG site I was essential for direct regulation of *TDRD1* expression by ERG.

DISCUSSION

Fusion of the androgen-regulated and prostate-specific gene *TMPRSS2* and the oncogene *ERG* is by far the most frequent gene fusion in prostate cancer, indicating a prominent role in cancer development. *TMPRSS2-ERG* fusion leading to ERG overexpression is an early event in prostate cancer development because it is already present in PIN lesions [19-21]. Although first described more than five years ago, the role of *TMPRSS2-ERG* in prostate cancer is still largely unknown. Recently, we and others showed that overexpression of *ERG* by gene fusion does not predict the clinical course of the disease [22-25]. In contrast, it has also been published that *ERG* fusion has a poor [26-28] or good prognosis [29, 30]. Moreover, we observed that expression of *TMPRSS2-ERG* from an alternative, more upstream promoter correlated with a favorable prognosis [24, 31]. So, it seems that regulation of *TMPRSS2-ERG* expression is a complex process.

To increase our knowledge of *TMPRSS2-ERG* function in prostate cancer, we analyzed well-defined cohorts of primary tumors from patients with a long clinical follow up, using both genome-wide expression arrays and Q-RT-PCR to identify genes that were coexpressed with *ERG* overexpression. In our experiments, expression of *TDRD1* was by far the strongest associated gene with *ERG* overexpression. Analysis of publically available expression array data of a cohort of 128 primary prostate tumors from MSKCC confirmed coexpression of *TDRD1* with *ERG* overexpression in primary prostate cancer. Like *ERG*, *TDRD1* was hardly expressed in normal adult prostatic tissue. During mouse prostate development, *Tdrd1* showed similar kinetics as

Erg. Remarkably, in late-stage prostate cancer, *TDRD1* was not only expressed in *ERG*-positive prostate cancers but also in a proportion of *ERG*-negative tumors. Finally, *TDRD1* expression was not associated with the expression of other ETS family members in primary prostate cancer and there even seemed to be an inverse correlation with *ETV1* overexpression.

In vitro studies in the prostate cancer cell line VCaP that overexpresses *ERG* and in prostate cells with forced *ERG* overexpression, suggested genes differentially expressed in *ERG*-rearranged prostate cancer [7, 32]. Tomlins *et al.* found that overexpression of *ERG* in immortalized, non-tumor prostate cells induced the expression of genes in the plasminogen pathway, which were involved in invasion [7]. Downregulation of *ERG* expression in VCaP cells inhibited the invasive capacity of the cells and induced the expression of genes expressed in differentiated luminal epithelial cells, including androgen-regulated genes NK3 homeobox 1 (*NKX3.1*), Prostate specific antigen (*PSA*), Solute carrier family 45 member 3 (*SLC45A3*), and *TMPRSS2*, suggesting that *ERG* overexpression may keep prostate (tumor) cells in a less-differentiated state. In agreement with these observations, Sun *et al.* showed that downregulation of *ERG* in VCaP decreased the expression of the proto-oncogene *c-MYC* [33].

So far, studies addressing gene expression profiles in clinical prostate tumors that take into account *ERG* overexpression have been hampered by the use of small patient cohorts and limited number of genes studied [34-39]. It was published that genes involved in the WNT pathway and Histone deacetylase 1 (*HDAC1*) were overexpressed in *ERG*-rearranged advanced prostate cancer, whereas expression of Tumor necrosis factor (*TNF*) and genes involved in cell death pathways were downregulated in these tumors [34]. Setlur *et al.* analyzed expression of 6100 genes and defined an 87-gene signature in *TMPRSS2-ERG*-positive prostate cancer in a patient cohort from Sweden [35]. This signature included Rho GDP dissociation inhibitor, beta (*ARHGDIB*), *CACNA1D*, Growth hormone receptor (*GHR*), and Phospholipase A2, Group VII (*PLA2G7*), which were also present in the top-20 genes overexpressed in our *ERG*-positive cohort (Figure 1B). Barwick *et al.* combined the Swedish patient cohort with a cohort from Canada and identified 51 out of 502 genes to be differentially expressed, including *HDAC1* [36]. We analyzed genome-wide gene expression in a set of 48 well-defined primary prostate tumors and confirmed and validated the expression array data by Q-RT-PCR. Comparison of genes that coexpressed with *ERG* overexpression between data of the Rotterdam patients and the MSKCC data (18) revealed an extensive overlap (Figure 2A and Supplementary Figure S5).

Although highly ranked, in the MSKCC cohort, *TDRD1* was not the strongest correlated gene with *ERG* overexpression. This might be due to *TDRD1* expression in some *ERG*-negative primary tumors. Alternatively, it might be caused by the composition of the tumor cohort. In the Rotterdam cohort, five out of 15 *ERG*-negative samples harbored *ETV1* overexpression, whereas in the MSKCC cohort five out of 75 were *ETV1* positive. Because *TDRD1* expression seemed inverse-correlated with *ETV1* overexpression, the higher percentage of *ETV1*-positive samples

in our cohort might be an explanation for the discrepancies between the two cohorts regarding *TDRD1* expression.

Jhavar and co-workers performed a transcriptome-wide search of 28 primary prostate cancers to find genes coexpressed with *ERG* [37, 38]. In this cohort, fourteen tumors overexpressed *ERG*, and *TDRD1* ranked highest of the genes that were coexpressed with *ERG*. Although the number of *ERG*-positive patients was small in this study, a considerable overlap in genes that were positively correlated with *ERG* overexpression was seen between the Rotterdam series, the MSKCC data, and that of Jhavar *et al.* (Supplemental Table S5 and Venn diagram in Supplemental Figure S5). Out of the 30 genes that were coexpressed with *ERG* overexpression in all three cohorts, 11 genes, including *TDRD1* were present in the top 20 genes that correlated with *ERG* overexpression in the Rotterdam series. (Supplementary Table S4). In a recent expression array study by Brase *et al. TDRD1* ranked also highest among differentially expressed genes between *ERG*-positive and *ERG*-negative prostate tumors [39]. By Q-RT-PCR, it was validated that *TDRD1* expression was significantly higher in *ERG*-positive than in *ERG*-negative and normal prostate tissue samples.

Out of the nine genes that showed inverse-correlation with *ERG* overexpression in the Rotterdam set of primary prostate tumors, *HPGD* and *TFF3* have previously been described; Mohamed *et al.* [40] showed that downregulation of ERG in the prostate cancer cell line VCaP resulted in *HPGD* overexpression that was regulated by the binding of ERG to its promoter. Like *HPGD* expression, expression of *TFF3*, a gene earlier described to be overexpressed in prostate cancer [41], was inversely correlated with *ERG*-positive primary prostate tumors. Rickman *et al.* [42] who showed that in hormone-naïve prostate cancer, *TFF3* expression was low in *ERG*-rearranged tumors and described that ERG was able to bind to the *TFF3* promoter. However, the authors stated that *TFF3* was expressed at high levels in *ERG*-rearranged prostate cancer in the castration-resistant stage of the disease. In agreement with the abovementioned observations, we found in the MSKCC cohort, both *TFF3* and *HPGD* to be inverse correlated with *ERG* overexpression (Score(d) -6.13 and -4.53, respectively).

Although different, the regulation of *TDRD1* expression seemed to be similarly complex as *TFF3* expression. We observed in functional studies that *TDRD1* was directly upregulated by ERG. However, in a proportion of *ERG*-negative late-stage tumor samples *TDRD1* was also overexpressed. We propose that other pathways that regulate *TDRD1* expression become activated in late-stage cancers. Moreover, the effect of endocrine therapy in late-stage prostate cancer should be taken into account.

TDRD1 belongs to a large family of Tudor domain containing proteins. The observed correlation between *ERG* and *TDRD1* expression, however, was specific for *TDRD1* as the expression of other Tudor family members did not associate with *ERG* overexpression (Supplementary Figure S6). Our results suggest that only TDRD1 plays a role in *ERG*-rearranged prostate cancer. So

far, the function of TDRD1 in prostate cancer is unknown. Tudor domain containing proteins, including TDRD1, were previously identified as binding partners of Piwi family proteins [33]. Piwi family proteins interact with a specific class of noncoding RNAs (piRNAs) that are involved in post-transcriptional gene regulation. The formation of Piwi-TDRD1 complexes is critical for the subcellular localization of these proteins, which on its turn is essential for spermatogenesis [43]. Sterility in mice, as a result of mutant *TDRD1*, further stressed the importance of *TDRD1* in normal spermatogenesis [44]. Recently, it has been published that loss of *TDRD1* activates transposons [45]. Further functional studies, including forced *TDRD1* overexpression and specific *TDRD1* downregulation in cell lines will be instrumental in clarifying the role of TDRD1 in prostate cancer.

In contrast to high expression of *TDRD1* in *ERG*-positive tumors, *TDRD1* was not or very low expressed in primary tumors with *ETV1* overexpression. Expression of *TDRD1* even seemed inverse correlated with *ETV1* overexpression. These observations argue in favor of a different concept of *ERG*- versus *ETV1*-rearranged prostate cancer. In concordance, differences in cell growth, proliferation and migration were previously described for both types of rearranged prostate cancers [8, 47]. Small differences in DNA-binding preferences can contribute to *in vivo* targeting specificities [48]. So far, gene expression profiling in a larger cohort of prostate cancers to identify genes coexpressed with *ETV1* overexpression have not been reported, although *in vitro* studies suggested matrix metalloproteinases and integrins as potential targets of *ETV1* [47, 49].

In summary, the data presented here on the one hand add to the complex nature of prostate cancer and the apparent different role of ETS fusion genes in the disease. On the other hand, however, knowledge of gene expression profiles and of direct *ERG* target genes are important steps in elucidation of the molecular pathways in *ERG*-positive tumor development.

ACKNOWLEDGEMENTS

We thank Wilfred van IJcken from the Center for Biomics, Erasmus MC and ServiceXS, Leiden, the Netherlands for technical support and providing microarray data, Wytske van Weerden for xenograft tissues, and Natasja Dits for cDNA synthesis of clinical prostate tumors. The work was supported by the Foundation for Scientific Urological Research (SUWO), the Netherlands.

REFERENCES

1. Oikawa T, Yamada T. *Molecular biology of the Ets family of transcription factors*. Gene 2003;**303**:11-34.
2. Sorensen PH, Lessnick SL, Lopez-Terrada D, Liu XF, Triche TJ, Denny CT. *A second Ewing's sarcoma translocation, t(21;22), fuses the EWS gene to another ETS-family transcription factor, ERG*. Nat Genet 1994;**6**:146-51.
3. Mitelman F, Johansson B, Mertens F. *The impact of translocations and gene fusions on cancer causation*. Nat Rev Cancer 2007;**7**:233-45.
4. Tomlins SA, Rhodes DR, Perner S, et al. *Recurrent fusion of TMPRSS2 and ETS transcription factor genes in prostate cancer.* Science 2005;**310**:644-8.
5. Clark JP, Cooper CS. *ETS gene fusions in prostate cancer.* Nat Rev Urol 2009;**6**:429-39.
6. Kumar-Sinha C, Tomlins SA, Chinnaiyan AM. *Recurrent gene fusions in prostate cancer.* Nat Rev Cancer 2008;**8**:497-511.
7. Tomlins SA, Laxman B, Varambally S, et al. *Role of the TMPRSS2-ERG gene fusion in prostate cancer.* Neoplasia 2008;**10**:177-88.
8. Klezovitch O, Risk M, Coleman I, et al. *A causal role for ERG in neoplastic transformation of prostate epithelium.* Proc Natl Acad Sci USA 2008;**105**:2105-10.
9. Carver BS, Tran J, Chen Z, et al. *ETS rearrangements and prostate cancer initiation.* Nature 2009;**457**:E1; discussion E2-3.
10. Carver BS, Tran J, Gopalan A, et al. *Aberrant ERG expression cooperates with loss of PTEN to promote cancer progression in the prostate.* Nat Genet 2009;**41**:619-24.
11. King JC, Xu J, Wongvipat J, et al. *Cooperativity of TMPRSS2-ERG with PI3-kinase pathway activation in prostate oncogenesis.* Nat Genet 2009;**41**:524-6.
12. Tomlins SA, Laxman B, Dhanasekaran SM, et al. *Distinct classes of chromosomal rearrangements create oncogenic ETS gene fusions in prostate cancer.* Nature 2007;**448**:595-9.
13. Shin S, Kim TD, Jin F, et al. *Induction of prostatic intraepithelial neoplasia and modulation of androgen receptor by ETS variant 1/ETS-related protein 81.* Cancer Res 2009;**69**:8102-10.
14. van Weerden WM, de Ridder CM, Verdaasdonk CL, et al. *Development of seven new human prostate tumor xenograft models and their histopathological characterization.* Am J Pathol 1996;**149**:1055-62.
15. Hermans KG, van Marion R, van Dekken H, Jenster G, van Weerden WM, Trapman J. *TMPRSS2:ERG fusion by translocation or interstitial deletion is highly relevant in androgen-dependent prostate cancer, but is bypassed in late-stage androgen receptor-negative prostate cancer.* Cancer Res 2006;**66**:10658-63.
16. Tusher VG, Tibshirani R, Chu G. *Significance analysis of microarrays applied to the ionizing radiation response.* Proc Natl Acad Sci USA 2001;**98**:5116-21.
17. Eisen MB, Spellman PT, Brown PO, Botstein D. *Cluster analysis and display of genome-wide expression patterns.* Proc Natl Acad Sci USA 1998;**95**:14863-8.
18. Taylor BS, Schultz N, Hieronymus H, Gopalan A, et al. *Integrative genomic profiling of human prostate cancer.* Cancer Cell 2010;**18**:1-12.
19. Furusato B, Gao CL, Ravindranath L, et al. *Mapping of TMPRSS2-ERG fusions in the context of multi-focal prostate cancer.* Mod Pathol 2008;**21**:67-75.
20. Mosquera JM, Perner S, Genega EM, et al. *Characterization of TMPRSS2-ERG fusion high-grade prostatic intraepithelial neoplasia and potential clinical implications.* Clin Cancer Res 2008;**14**:3380-5.
21. Perner S, Mosquera JM, Demichelis F, et al. *TMPRSS2-ERG fusion prostate cancer: an early molecular event associated with invasion.* Am J Surg Pathol 2007;**31**:882-8.
22. Fitzgerald LM, Agalliu I, Johnson K, et al. *Association of TMPRSS2-ERG gene fusion with clinical characteristics and outcomes: Results from a population-based study of prostate cancer.* BMC Cancer 2008;**8**:230.
23. Gopalan A, Leversha MA, Satagopan JM, et al. *TMPRSS2-ERG gene fusion is not associated with outcome in patients treated by prostatectomy.* Cancer Res 2009;**69**:1400-6.

24. Hermans KG, Boormans JL, Gasi D, et al. *Overexpression of prostate-specific TMPRSS2(exon 0)-ERG fusion transcripts corresponds with favorable prognosis of prostate cancer.* Clin Cancer Res 2009;**15**:6398-403.
25. Hoogland AM, Jenster G van Weerden WM et al. *ERG immunohistochemistry is not prededictive for PSA recureence, local recurrence, or overall survival after radical prostatectomy for prostate cancer.* Mod Pathol 2012;**25**:471-9.
26. Attard G, Clark J, Ambroisine L, et al. *Duplication of the fusion of TMPRSS2 to ERG sequences identifies fatal human prostate cancer.* Oncogene 2008;**27**:253-63.
27. Demichelis F, Fall K, Perner S, et al. *TMPRSS2:ERG gene fusion associated with lethal prostate cancer in a watchful waiting cohort.* Oncogene 2007;**26**:4596-9.
28. Nam RK, Sugar L, Yang W, et al. *Expression of the TMPRSS2:ERG fusion gene predicts cancer recurrence after surgery for localised prostate cancer.* Br J Cancer 2007;**97**:1690-5.
29. Petrovics G, Liu A, Shaheduzzaman S, et al. *Frequent overexpression of ETS-related gene-1 (ERG1) in prostate cancer transcriptome.* Oncogene 2005;**24**:3847-52.
30. Saramaki OR, Harjula AE, Martikainen PM, Vessella RL, Tammela TL, Visakorpi T. *TMPRSS2:ERG Fusion Identifies a Subgroup of Prostate Cancers with a Favorable Prognosis.* Clin Cancer Res 2008;**14**:3395-400.
31. Boormans JL, Porkka K, Visakorpi T, Trapman J. *Confirmation of the association of TMPRSS2(exon 0)-ERG expression and a favourable prognosis of primary prostate cancer.* Eur Urol 2011;**60**:183-4.
32. Tomlins SA, Mehra R, Rhodes DR, et al. *Integrative molecular concept modeling of prostate cancer progression.* Nat Genet 2007;**39**:41-51.
33. Sun C, Dobi A, Mohamed A, et al. *TMPRSS2-ERG fusion, a common genomic alteration in prostate cancer activates C-MYC and abrogates prostate epithelial differentiation.* Oncogene 2008;**27**:5348-53.
34. Iljin K, Wolf M, Edgren H, et al. *TMPRSS2 fusions with oncogenic ETS factors in prostate cancer involve unbalanced genomic rearrangements and are associated with HDAC1 and epigenetic reprogramming.* Cancer Res 2006;**66**:10242-6.
35. Setlur SR, Mertz KD, Hoshida Y, et al. *Estrogen-dependent signaling in a molecularly distinct subclass of aggressive prostate cancer.* J Natl Cancer Inst 2008;**100**:815-25.
36. Barwick BG, Abramovitz M, Kodani M, et al. *Prostate cancer genes associated with TMPRSS2-ERG gene fusion and prognostic of biochemical recurrence in multiple cohorts.* Br J Cancer 2010;**102**:570-6.
37. Jhavar S, Brewer D, Edwards S, et al. *Integration of ERG gene mapping and gene-expression profiling identifies distinct categories of human prostate cancer.* BJU Int 2009;**103**:1256-69.
38. Jhavar S, Reid A, Clark J, et al. *Detection of TMPRSS2-ERG translocations in human prostate cancer by expression profiling using GeneChip Human Exon 1.0 ST arrays.* J Mol Diagn 2008;**10**:50-7.
39. Brase JC, Johannes M, Mannsperger H et al. *TMPRSS2-ERG-specific transcriptional modulation is associated with prostate cancer biomarkers and TGF-β signaling.* BMC Cancer 2011;**11**:507.
40. Mohamed AA, Tan SH, Sun C, et al. *ERG oncogene modulates prostaglandin signaling in prostate cancer cells.* Cancer Biol Ther 2011;**11**:410-7.
41. Vestergaard EM, Nexo E, Torring N, Borre M, Orntoft TF, Sorensen KD. *Promoter hypomethylation and upregulation of trefoil factors in prostate cancer.* Int J Cancer 2010;**127**:1857-65.
42. Rickman DS, Chen YB, Banerjee S, et al. *ERG cooperates with androgen receptor in regulating trefoil factor 3 in prostate cancer disease progression.* Neoplasia 2010;**12**:1031-40.
43. Chen C, Jin J, James DA, et al. *Mouse Piwi interactome identifies binding mechanism of Tdrkh Tudor domain to arginine methylated Miwi.* Proc Natl Acad Sci USA 2009;**106**:20336-41.
44. Kojima K, Kuramochi-Miyagawa S, Chuma S, et al. *Associations between PIWI proteins and TDRD1/MTR-1 are critical for integrated subcellular localization in murine male germ cells.* Genes Cells 2009;**14**:1155-65.
45. Chuma S, Hosokawa M, Kitamura K, et al. *Tdrd1/Mtr-1, a tudor-related gene, is essential for male germ-cell differentiation and nuage/germinal granule formation in mice.* Proc Natl Acad Sci USA 2006;**103**:15894-9.
46. Reuter M, Chuma S, Tanaka T, Franz T, Stark A, Pillai RS. *Loss of the Mili-interacting Tudor domain-containing protein-1 activates transposons and alters the Mili-associated small RNA profile.* Nat Struct Mol Biol 2009;**16**:639-46.

47. Hermans KG, van der Korput HA, van Marion R, et al. *Truncated ETV1, fused to novel tissue-specific genes, and full-length ETV1 in prostate cancer.* Cancer Res 2008;**68**:7541-9.

48. Wei GH, Badis G, Berger MF, et al. *Genome-wide analysis of ETS-family DNA-binding in vitro and in vivo.* EMBO J 2010;**29**:2147-60.

49. Cai C, Hsieh CL, Omwancha J, et al. *ETV1 is a novel androgen receptor-regulated gene that mediates prostate cancer cell invasion.* Mol Endocrinol 2007;**21**:1835-46.

Supplementary data

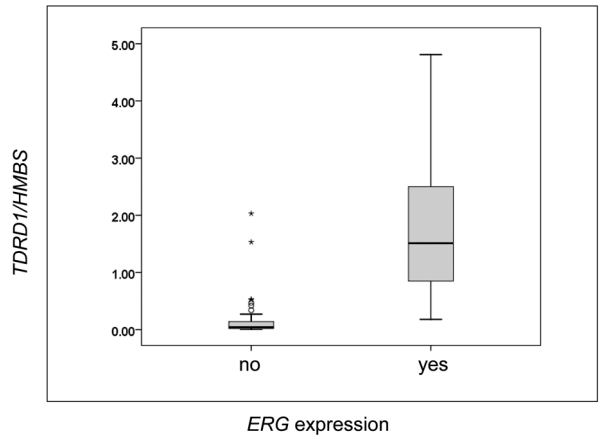

Supplemental Figure S1. Box plot showing median expression of *TDRD1* relative to *HMBS*, as detected by Q-RT-PCR, in 48 primary prostate tumors, of which 33 overexpressed *ERG* and 15 did not overexpress *ERG*, p<0.001 (MWU test). Outliers are depicted by an open circle (°) and extremes are depicted by an asterisk (*).

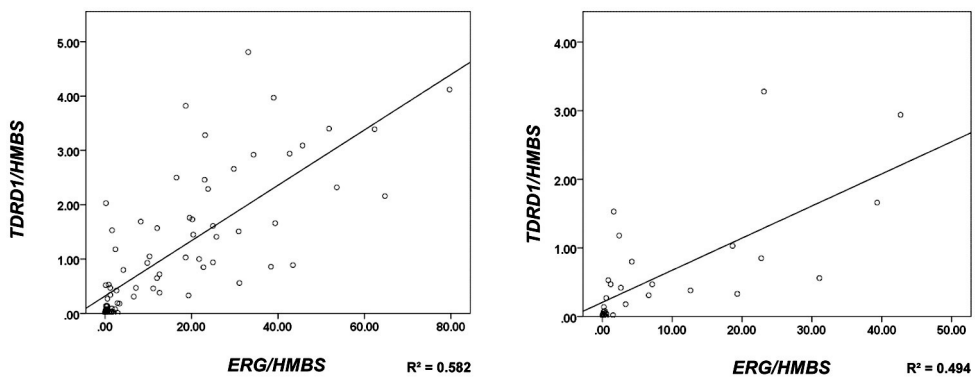

Supplemental Figure S2. Correlation plot showing coexpression of *ERG* and *TDRD1* in the primary prostate cancer samples of both cohort A (N=48, left panel) and cohort B (validation cohort, N=31, right panel). *ERG* and *TDRD1* expression relative to *HMBS*, as detected by Q-RT-PCR, is shown. The trend line and *R* squared change (R^2) are indicated.

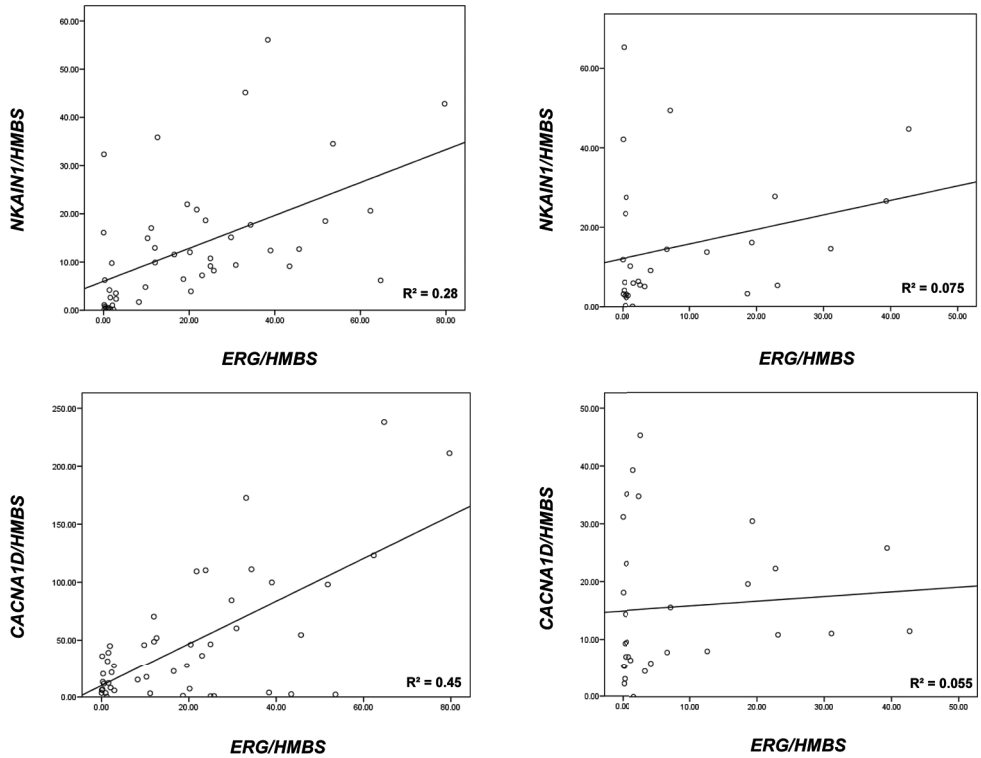

Supplemental Figure S3. Correlation plots showing coexpression of *ERG* and *NKAIN1*, and of *ERG* and *CACNA1D* in primary prostate tumors of both cohort A (N=48, left panels) and cohort B (validation cohort, N=31, right panels). Expression of *ERG, NKAIN1*, and *CACNA1D* relative to *HMBS*, as detected by Q-RT-PCR, are shown. The trend lines and *R* squared changes (R^2) are indicated. Respective p-values for cohort A: p<0.001 (*NKAIN1*) and p<0.001 (*CACNA1D*), and for cohort B: p=0.14 (*NKAIN1*) and p=0.67 (*CACNA1D*).

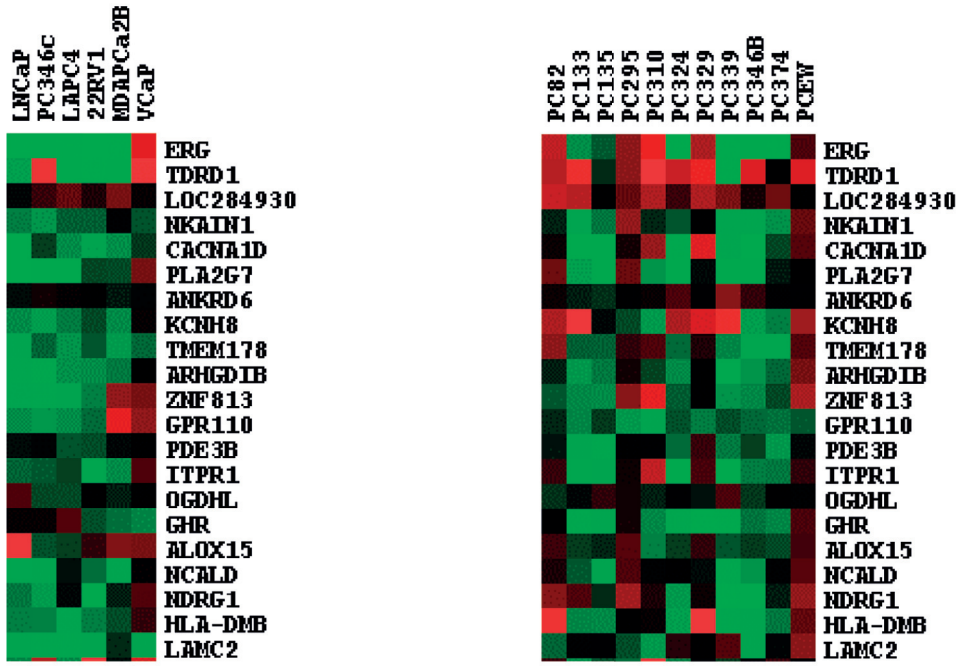

Supplemental Figure S4. Heat maps showing the correlation of the expression of the 20 genes, which were most significantly co-expressed with *ERG* overexpression in primary prostate tumors as assayed by SAM, in six prostate cancer cell lines (left panel) and 11 prostate cancer xenografts (right panel). Each cell in the image shows the $\log^2$ expression ratio for the particular gene divided by the median expression of that gene in all the samples. *Red*, expression above the median; *green*, expression below the median.

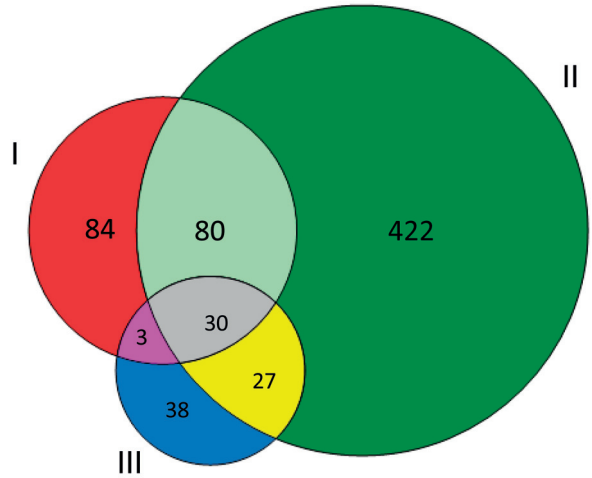

Supplemental Figure S5. Venn-diagram showing the overlap in genes that were positively correlated with *ERG* overexpression between the present series (circle I), the series of MSKCC (circle II), and the series of Jhavar *et al.* (circle III). *TDRD1* is among the 30 genes that were coexpressed with *ERG* overexpression in all three series.

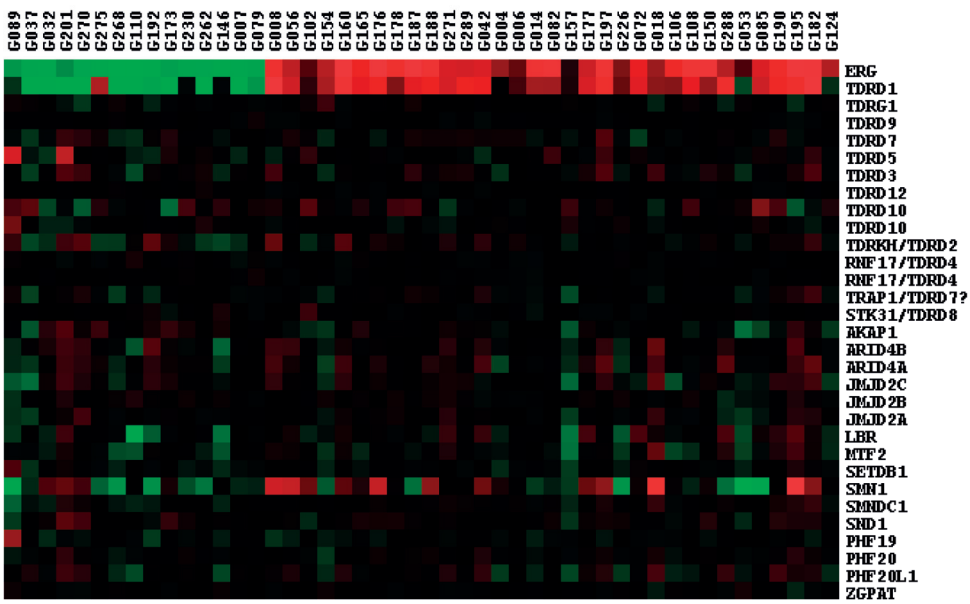

Supplemental Figure S6. Heat map showing the correlation of the expression of Tudor family members with *ERG* expression. Each cell in the image shows the $\log^2$ expression ratio for the particular gene divided by the median expression of that gene in all the samples. *Red*, expression above the median; *green*, expression below the median.

Supplemental Table S1. Sequences of primers used for Q-RT-PCR analysis.

Target	Forward 5'->3'	Reverse 5'->3'
HMBS	catgtctggtaacggcaatg	gtacgaggctttcaatgttg
CACNA1D	ggactttcacaccagccagc	cacaggcatcagagatttcg
ERG	tgctcaaccatctccttcca	tgggtttgctcttccgctct
Erg	tgctcaaccatctccttcca	tgggtttgctcttccgctct
ETV1	cataccaacggcgaggatca	tggagaaaagggcttctgga
Hprt	tccctggttaagcagtacag	ttccagtttcactaatgacac
NKAIN1	ggcagaggctaccccgac	cttcgtgttcgcctgctac
TDRD1	accaccctatagaccaagaat	tttcaatgtttccatagtctgca
Tdrd1	gagaagctgtgtgtgttag	tccgacgtttccagaacaatg
TMPRSS2-ERG	gagctaagcaggaggcgga	catcaggagagttccttgag

Supplemental Table S2. Clinicopathological characteristics of two cohorts of primary prostate cancer patients; cohort A and the validation cohort (cohort B)**.**

Characteristic	**Cohort A (N=48)**	**Cohort B (N=31)**	**p-value**
Mean age (± SD)	61.8 ± 5.9 years	63.1 ± 5.1 years	p=0.30*
Mean PSA (± SD)	16.6 ± 25.5 ng/ml	15.9 ± 14.0 ng/ml	p=0.56**
pT-stage			
≤ pT2c	16 (33.3%)	8 (28.6%)	p=0.57***
≥ pT3a	32 (66.7%)	20 (71.4%)	
Surgical margins			
positive	24 (50.0%)	13 (48.1%)	p=0.67***
negative	24 (50.0%)	14 (51.9%)	
Gleason score			
< 7	23 (47.9%)	22 (73.3%)	p=0.028***
≥ 7	25 (52.1%)	8 (26.7%)	
Occult metastases at RP			
Yes	4 (8.7%)	5 (21.7%)	p=0.24***
No	42 (91.3%)	23 (78.3%)	

Abbreviations: SD, standard deviation; PSA, prostate-specific antigen; pT-stage, pathological T-stage; RP, radical prostatectomy

** Student's T-test*

*** Mann-Whitney U test*

**** Pearson's χ^2 test*

Patients with unknown values were not included in the analysis.

Supplemental Table S3. Significantly differentially expressed genes between primary prostate tumors with *ERG* rearrangement versus those lacking *ERG* rearrangement as assayed by SAM.

Significantly upregulated genes			
Affymetrix ID	**Score(d)**	**Fold Change**	**Gene Name**
3931765	20.11815351	12.56928284	*ERG*
3265175	10.31880671	8.548930766	*TDRD1*
3949431	7.654239186	2.75881225	*LOC284930*
2404344	7.083695342	2.916805869	*NKAIN1*
2624385	6.562973646	3.515014739	*CACNA1D*
2955827	6.284218276	5.094809046	*PLA2G7*
2916825	6.239813812	1.510350802	*ANKRD6*
2613293	6.190598291	3.364139375	*KCNH8*
2478269	6.159897026	3.345057544	*TMEM178*
3445786	6.048628694	2.090047161	*ARHGDIB*
3840883	6.033349426	2.43219119	*ZNF813*
2955999	5.967458475	4.380334029	*GPR110*
3321512	5.798619393	2.137256133	*PDE3B*
2608469	5.725527815	2.30793309	*ITPR1*
3288803	5.701459382	1.804776118	*OGDHL*
2807949	5.699595264	3.139162528	*GHR*
3742212	5.652896818	2.040232386	*ALOX15*
3147173	5.626123781	2.088663486	*NCALD*
3154317	5.610370053	1.822068523	*NDRG1*
2950263	5.56894717	2.643441127	*HLA-DMB*
2371139	5.556637999	2.455049535	*LAMC2*
2710599	5.522741838	2.811994064	*CLDN1*
2471384	5.376457822	1.679835213	*KCNS3*
2400027	5.326569239	3.691847969	*PLA2G2A*
3320169	5.2844448	1.657733612	*AMPD3*
3279154	5.188297225	1.62425659	*C10orf38*
3126504	5.100278577	2.246074912	*CSGALNACT1*
3160175	5.025259167	1.934213066	*VLDLR*
3200648	5.003535755	1.406835715	*ADFP*
2387606	4.998395716	2.760392738	*CHRM3*
3291281	4.952526048	2.986098026	*TMEM26*
2764192	4.884880425	1.919841897	*KIAA0746*
2793137	4.880417952	2.017299002	*SH3RF1*
3095313	4.820305763	2.808387509	*C8orf4*

Supplemental Table S3. *Continued*

Significantly upregulated genes			
Affymetrix ID	**Score(d)**	**Fold Change**	**Gene Name**
2658595	4.79828303	1.712748518	*HES1*
2920085	4.786303861	1.445044654	*SOBP*
2638077	4.780924706	2.669008213	*PLA1A*
2739308	4.739927836	1.876999137	*EGF*
2420642	4.717546409	1.637377438	*MCOLN2*
2443370	4.695895595	3.866672489	*F5*
2522094	4.686100955	1.460226116	*LOC26010*
2520138	4.679949915	1.529052135	*FLJ20160*
3898796	4.677369825	1.770275826	*KIF16B*
3502156	4.644714636	1.800081131	*ATP11A*
3735847	4.627355977	1.451229804	*Septin 9*
3840949	4.627111716	2.64826626	*ZNF765*
3179706	4.56713944	1.455687789	*WNK2*
3483468	4.547871607	1.399702817	*KIAA0774*
2748923	4.52922682	1.696402387	*GUCY1B3*
3081501	4.515340825	2.068810651	*LOC285889*
2397025	4.494232495	1.375398004	*DHRS3*
2970897	4.482979889	2.066092599	*FRK*
3986168	4.46409298	1.928715879	*MUM1L1*
2582124	4.446282167	1.708768373	*NR4A2*
3616894	4.406652066	1.994699698	*FMN1*
3863669	4.399789835	1.86038205	*CEACAM1*
3399678	4.382631111	1.463053387	*B3GAT1*
3792273	4.36321453	1.7373645	*CDH7*
3000342	4.360552372	1.521137276	*ADCY1*
3081511	4.352991478	1.879197713	*LOC100134747*
3943234	4.307140978	2.43918501	*SLC5A1*
3137120	4.29892628	1.583290823	*CA8*
2937144	4.287936637	1.854446861	*SMOC2*
2964231	4.285443353	1.660154612	*RRAGD*
2975741	4.283998041	1.496451081	*MAP7*
2956563	4.276122612	8.834620938	*CRISP3*
3775334	4.253594045	1.554865308	*ZNF750*
3060332	4.236117045	2.703018138	*STEAP4*
2694001	4.235766382	1.36425711	*MGLL*
2748830	4.217080423	1.986026953	*GUCY1A3*

Supplemental Table S3. *Continued*

Significantly upregulated genes			
Affymetrix ID	**Score(d)**	**Fold Change**	**Gene Name**
4054204	4.187278008	2.316394533	*APOD*
3577666	4.147469963	1.725208593	*SERPINA11*
3474372	4.125236881	1.30367961	*PXN*
3337516	4.124455486	1.360880436	*LRP5*
3717034	4.116761564	2.056348763	*LOC400590*
2828146	4.103578225	1.549152214	*CDC42SE2*
3285119	4.095545782	1.38600811	*FZD8*
3371114	4.089525239	1.66876887	*SYT13*
3189932	4.071245082	1.490306837	*STXBP1*
2916716	4.055421691	1.426159206	*PNRC1*
2967276	4.052242689	2.254050278	*POPDC3*
3352948	4.04866979	1.614764196	*SORL1*
2700365	4.042865344	1.874200124	*TM4SF1*
2467066	4.032138103	1.590334278	*PXDN*
2458513	4.018399386	1.521583341	*TMEM63A*
2453006	4.003630497	4.260013754	*PIGR*
2596763	4.002496831	1.826955077	*FZD5*
2474071	3.999224813	1.339510232	*MAPRE3*
3908149	3.994629098	1.547991608	*ZMYND8*
3802980	3.983226526	1.728043642	*DSC2*
3822723	3.982844451	1.374481371	*PKN1*
2991395	3.980750483	1.802373017	*HDAC9*
2420681	3.974350721	1.434130754	*MCOLN3*
3754797	3.964140209	1.729582229	*HNF1B*
3057370	3.960367175	1.515672812	*HIP1*
3971806	3.940405211	1.775739568	*SAT1*
3453120	3.932887602	1.290759991	*ZNF641*
3635776	3.930874745	1.444531761	*EFTUD1*
4035833	3.929207818	1.797029902	*CD24*
3751058	3.928555417	1.333999396	*C17orf63*
3790479	3.920415705	2.020758563	*SEC11C*
2796951	3.912745135	1.959066525	*PDLIM3*
2671728	3.902339079	1.615674209	*CDCP1*
3696317	3.900166063	1.457318566	*SMPD3*
2328868	3.899598663	1.375801232	*HDAC1*
2550175	3.898590786	1.875675153	*KCNG3*

Supplemental Table S3. *Continued*

Significantly upregulated genes			
Affymetrix ID	**Score(d)**	**Fold Change**	**Gene Name**
2656837	3.892646409	1.936854559	*ST6GAL1*
2353337	3.8505693	1.399889162	*SLC22A15*
3353441	3.846655707	1.297024844	*C11orf63*
2350489	3.841816602	2.16548607	*KIAA1324*
3835777	3.830684949	1.582777226	*BCAM*
3126625	3.81875319	1.79799529	*LOC100130604*
3781980	3.80492526	1.420933424	*C18orf17*
2976113	3.785671393	1.661191802	*IFNGR1*
3820443	3.782711948	1.623599342	*ICAM1*
3131741	3.78082806	1.451970357	*RAB11FIP1*
2468811	3.765167583	1.298364093	*DDEF2*
4010461	3.763385321	1.547059667	*SPIN4*
3980867	3.763240429	1.471490267	*GJB1*
2339995	3.745008365	1.541343736	*ROR1*
2443537	3.737885278	1.428894196	*SCYL3*
2903782	3.730675319	1.526479176	*ITPR3*
2899022	3.724634574	1.609330178	*TRIM38*
3614534	3.723644743	1.450647121	*GABRB3*
3723687	3.719107624	1.416058926	*MAPT*
3858852	3.713427579	1.579943843	*RHPN2*
2353396	3.713275166	1.360298159	*C1orf161*
2395177	3.704340292	1.64092129	*ERRFI1*
3365136	3.692520899	1.422734318	*SERGEF*
2412624	3.689483365	1.953094331	*RAB3B*
3864646	3.680145655	1.771210239	*KCNN4*
3444252	3.670669778	1.634248292	*CSDA*
2749011	3.657047123	2.977329188	*TDO2*
2777070	3.64431845	1.766456164	*HSD17B11*
3955357	3.635452093	1.24483905	*C22orf36*
2811145	3.635066984	1.671184886	*PART1*
2749611	3.632380478	1.688781496	*FNIP2*
3695867	3.624532481	1.283714077	*RANBP10*
3273870	3.621964145	1.911906512	*LOC642384*
2857204	3.619257703	1.915833592	*PPAP2A*
3445108	3.617308071	1.584433688	*GPRC5D*
2623662	3.612402949	1.18719986	*DNAH1*

Supplemental Table S3. *Continued*

Significantly upregulated genes			
Affymetrix ID	**Score(d)**	**Fold Change**	**Gene Name**
2824581	3.610276326	1.89574887	*KCNN2*
2867836	3.604394636	1.575296503	*GLRX*
3001479	3.600356851	1.375611397	*IKZF1*
2468622	3.593341965	1.288577329	*ID2*
3835751	3.581201134	1.291915074	*CBLC*
3907830	3.562971082	1.430525851	*ELMO2*
3209623	3.562020796	1.476760961	*ZFAND5*
3435192	3.552606731	1.373290392	*MLXIP*
2353477	3.551918339	1.40823953	*ATP1A1*
3464405	3.546554978	1.659432084	*RASSF9*
3464000	3.545001838	1.283685147	*CCDC59*
3628832	3.536542168	1.215934591	*DAPK2*
4021341	3.536169905	1.424082766	*ZDHHC9*
3587015	3.53526787	1.257521875	*KLF13*
2872848	3.527310093	1.711440292	*LOX*
3107342	3.520658739	1.480168231	*PPM2C*
3081205	3.515316576	1.391751666	*SHH*
3220846	3.509322522	1.323586639	*SUSD1*
2980290	3.50425814	1.56239401	*RGS17*
3747399	3.502795197	1.425098608	*KRT14*
2963313	3.499296777	1.45709902	*SNX14*
3869379	3.498439045	1.684610201	*ZNF614*
2327677	3.491184055	1.315659605	*EPB41*
3272736	3.484256312	1.386691951	*ZNF511*
3205659	3.478042927	1.234079329	*SHB*
2806091	3.476487583	1.538899582	*RAI14*
2955863	3.473740078	2.134974473	*GPR116*
3706439	3.466729369	1.454694181	*GARNL4*
3933863	3.454344062	2.275794469	*C21orf105*
2461531	3.452527119	1.405667821	*IRF2BP2*
2515471	3.445555967	1.310739192	*DLX1*
3567050	3.437908973	1.52212833	*RTN1*
3509473	3.43045929	1.516630856	*DCLK1*
2679406	3.422880112	1.731536325	*CADPS*
3400730	3.418955127	1.33544904	*CACNA1C*
3877265	3.410319797	1.236065017	*MACROD2*

Supplemental Table S3. *Continued*

Significantly upregulated genes			
Affymetrix ID	**Score(d)**	**Fold Change**	**Gene Name**
3473727	3.40181891	1.464717754	*WSB2*
2835300	3.39979255	1.610155759	*SLC26A2*
3844470	3.39901199	1.378599617	*PPAP2C*
2322389	3.396312919	1.289602636	*NECAP2*
3181240	3.378710688	1.38746325	*TMOD1*
2400518	3.373323472	1.443457902	*ECE1*
2921296	3.365389801	1.868899546	*AMD1*
3900091	3.364981704	1.594094208	*C20orf74*
2510713	3.364879555	1.41786028	*FMNL2*
2344464	3.360364928	1.347543626	*SAMD13*
2408681	3.349902322	1.192359105	*HIVEP3*
3384321	3.346401513	1.54282711	*RAB30*
3628432	3.343449591	1.565482856	*LOC100128979*
3493579	3.341394097	2.111674481	*NMD3*
2832423	3.340532568	1.690935206	*PCDHB10*
3363091	3.333025052	1.398984356	*GALNTL4*
3058991	3.330778902	1.76828498	*CACNA2D1*
3335952	3.327007836	1.310104224	*PACS1*
3590709	3.325950346	1.231756358	*LOC100137047-PLA2G4B*

Significantly downregulated genes			
Affymetrix ID	**Score(d)**	**Fold Change**	**Gene Name**
2794408	-4.86256937	0.331226614	*HPGD*
2907513	-4.833486317	0.527619446	*GNMT*
3916686	-4.746720159	0.583033121	*C21orf118*
2398287	-4.707438607	0.627350674	*NBPF16*
2632778	-4.6991188	0.396396476	*EPHA6*
3933536	-4.663890297	0.578068262	*TFF3*
2384401	-4.366122845	0.532071017	*RHOU*
3612739	-4.277834169	0.234330422	*CXADR*
3937943	-4.247219376	0.526048307	*FLJ42953*

Supplemental Table S4. Full names, abbreviations, and accession numbers of the 20 most correlated genes with *ERG* overexpression in primary prostate tumors as shown in Figure 1B.

Abbreviation	Full gene name	Accession number
ERG	V-ets erythoblastosis virus E26 oncogene homolog (avian)	NM182918 (isoform 1) NM004449 (isoform 2) NM001136154 (isoform 3) NM001136155 (isoform 4)
TDRD1	Tudor domain-containing protein 1	NM198895
LOC284930	--	AK093107 BC039485
NKAIN1	Na+/K+ transporting ATPase interacting 1	NM024522
CACNA1D	Calcium channel, voltage-dependent, L type, alpha unit 1D	NM000720 (isoform 1) NM001128840 (isoform 2) NM001128839 (isoform 3)
PLA2G7	Phospholipase A2, Group VII (platelet-activating factor acetylhydrolase, plasma)	NM005084 (isoform 1) NM001168357 (isoform 2)
ANKRD6	Ankyrin repeat domain 6	NM014942
KCNH8	Potassium voltage-gated channel, subfamiliy H (eag-related), member 8	NM144633
TMEM178	Transmembrane protein 178	NM152390 (isoform 1) NM001167959 (isoform 2)
ARHGDIB	Rho GDP dissociation inhibitor (GDI), beta	NM001175
ZNF813	Zinc finger protein 813	NM001004301
GPR110	G protein-coupled receptor 110	NM153840 (isoform 1) NM025048 (isoform 2)
PDE3B	Phosphodiesterase 3B, cGMP-inhibited	NM000922
ITPR1	Inositol 1,4,5-triphosphate receptor, type 1	NM001099952 (isoform 1) NM002222 (isoform 2) NM001168272 (isoform 3)
OGDHL	Oxyglutarate dehydrogenase-like	NM018245 (isoform 1) NM001143996 (isoform 2) NM001143997 (isoform 3)
GHR	Growth hormone receptor	NM000163
ALOX15	Arachidonate 15-lipoxygenase	NM001140
NCALD	Neurocalcin delta	NM001040624 (isoform 1) NM001040625 (isoform 2) NM001040626 (isoform 3) NM001040627 (isoform 4) NM001040628 (isoform 5) NM001040629 (isoform 6) NM001040630 (isoform 7) NM032041 (isoform 8)
NDRG1	N-myc downstream regulated 1	NM001135242 (isoform 1) NM006096 (isoform 2)
HLA-DMB	Major histocompatibility complex, class II, DM beta	NM002118
LAMC2	Laminin subunit gamma-2	NM005562 (isoform a) NM018891 (isoform b)

Supplemental Table S5. Genes that were positively correlated with *ERG* overexpression in primary prostate tumors of three different series according to the analysis of the GeneChip Human Exon 1.0 ST array. Genes that overlap with the present series are indicated in bold and highlighted in grey.

Boormans et al. **(n=197)**	**Taylor** et al. **(n=559)**	**Jhavar** et al. **(n=98)**
ADCY1	***ADCY1***	
ADFP		
ALOX15	***ALOX15***	***ALOX15***
AMD1	***AMD1***	***AMD1***
AMPD3	***AMPD3***	***AMPD3***
ANKRD6	***ANKRD6***	***ANKRD6***
APOD	***APOD***	
ARHGDIB	***ARHGDIB***	
ATP11A	***ATP11A***	
ATP1A1	***ATP1A1***	
B3GAT1		
BCAM	***BCAM***	
C10orf38		
C11orf63		
C17orf63	***C17orf63***	
C18orf17		
C1orf161		
C20orf74		
C21orf105		
C22orf36	***C22orf36***	
C8orf4	***C8orf4***	***C8orf4***
CA8	***CA8***	
CACNA1C		
CACNA1D	***CACNA1D***	***CACNA1D***
CACNA2D1		
CADPS		
CBLC	***CBLC***	***CBLC***
CCDC59		
CD24		
CDC42SE2		
CDCP1	***CDCP1***	
CDH7		
CEACAM1		
CHRM3		
CLDN1		

Supplemental Table S5. *Continued*

Boormans et al. **(n=197)**	**Taylor** et al. **(n=559)**	**Jhavar** et al. **(n=98)**
CRISP3	***CRISP3***	***CRISP3***
CSDA	***CSDA***	***CSDA***
CSGALNACT1	***CSGALNACT1***	
DAPK2		
DCLK1		
DDEF2		
DHRS3		
DLX1	***DLX1***	***DLX1***
DNAH1		
DSC2	***DSC2***	
ECE1	***ECE1***	
EFTUD1	***EFTUD1***	
EGF		
ELMO2	***ELMO2***	
EPB41		
ERG	***ERG***	***ERG***
ERRFI1		
F5	***F5***	
FLJ20160		
FMN1		
FMNL2	***FMNL2***	
FNIP2	***FNIP2***	
FRK	***FRK***	***FRK***
FZD5	***FZD5***	
FZD8		
GABRB3	***GABRB3***	
GALNTL4		
GARNL4		
GHR	***GHR***	***GHR***
GJB1	***GJB1***	
GLRX		
GPR110	***GPR110***	
GPR116		
GPRC5D	***GPRC5D***	
GUCY1A3	***GUCY1A3***	***GUCY1A3***
GUCY1B3	***GUCY1B3***	
HDAC1	***HDAC1***	***HDAC1***

Supplemental Table S5. *Continued*

Boormans et al. **(n=197)**	**Taylor** et al. **(n=559)**	**Jhavar** et al. **(n=98)**
HDAC9		
HES1	***HES1***	***HES1***
HIP1	***HIP1***	
HIVEP3		
HLA-DMB	***HLA-DMB***	***HLA-DMB***
HNF1B	***HNF1B***	
HSD17B11	***HSD17B11***	
ICAM1		
ID2		
IFNGR1	***IFNGR1***	
IKZF1	***IKZF1***	
IRF2BP2	***IRF2BP2***	
ITPR1	***ITPR1***	
ITPR3	***ITPR3***	***ITPR3***
KCNG3	***KCNG3***	***KCNG3***
KCNH8	***KCNH8***	***KCNH8***
KCNN2	***KCNN2***	
KCNN4	***KCNN4***	***KCNN4***
KCNS3	***KCNS3***	***KCNS3***
KIAA0746		
KIAA0774		
KIAA1324	***KIAA1324***	
KIF16B	***KIF16B***	
KLF13	***KLF13***	
KRT14		
LAMC2	***LAMC2***	
LOC100128979		
LOC100130604		
LOC100134747		
LOC100137047-PLA2G4B		
LOC26010		
LOC284930		
LOC285889		
LOC400590		
LOC642384		
LOX	***LOX***	
LRP5	***LRP5***	

Supplemental Table S5. *Continued*

Boormans et al. **(n=197)**	**Taylor** et al. **(n=559)**	**Jhavar** et al. **(n=98)**
MACROD2	***MACROD2***	
MAP7	***MAP7***	***MAP7***
MAPRE3	***MAPRE3***	
MAPT	***MAPT***	
MCOLN2	***MCOLN2***	
MCOLN3		
MGLL	***MGLL***	
MLXIP		
MUM1L1	***MUM1L1***	
NCALD	***NCALD***	***NCALD***
NDRG1	***NDRG1***	
NECAP2	***NECAP2***	
NKAIN1	***NKAIN1***	
NMD3		
NR4A2		***NR4A2***
OGDHL	***OGDHL***	
PACS1	***PACS1***	
PART1		***PART1***
PCDHB10	***PCDHB10***	
PDE3B	***PDE3B***	***PDE3B***
PDLIM3		
PIGR		
PKN1	***PKN1***	
PLA1A	***PLA1A***	
PLA2G2A		
PLA2G7	***PLA2G7***	***PLA2G7***
PNRC1		
POPDC3		
PPAP2A	***PPAP2A***	
PPAP2C	***PPAP2C***	
PPM2C		
PXDN	***PXDN***	
PXN	***PXN***	
RAB30	***RAB30***	
RAB3B	***RAB3B***	
RAB11FIP1		
RAI14		

Supplemental Table S5. *Continued*

Boormans et al. **(n=197)**	**Taylor** et al. **(n=559)**	**Jhavar** et al. **(n=98)**
RANBP10		
RASSF9		
RGS17	***RGS17***	
RHPN2	***RHPN2***	
ROR1		
RRAGD		
RTN1		
SAMD13	***SAMD13***	
SAT1		
SCYL3	***SCYL3***	
SEC11C		
Septin9	***Septin9***	
SERGEF	***SERGEF***	
SERPINA11		
SH3RF1	***SH3RF1***	
SHB		
SHH		
SLC22A15		
SLC26A2	***SLC26A2***	
SLC5A1		
SMOC2	***SMOC2***	
SMPD3	***SMPD3***	
SNX14		
SOBP		
SORL1	***SORL1***	***SORL1***
SPIN4	***SPIN4***	
ST6GAL1	***ST6GAL1***	
STEAP4	***STEAP4***	***STEAP4***
STXBP1	***STXBP1***	
SUSD1	***SUSD1***	
SYT13		
TDO2		
TDRD1	***TDRD1***	***TDRD1***
TM4SF1	***TM4SF1***	
TMEM178	***TMEM178***	
TMEM26	***TMEM26***	
TMEM63A	***TMEM63A***	

Supplemental Table S5. *Continued*

Boormans et al. **(n=197)**	**Taylor** et al. **(n=559)**	**Jhavar** et al. **(n=98)**
TMOD1		
TRIM38		
VLDLR	***VLDLR***	***VLDLR***
WNK2	***WNK2***	
WSB2	***WSB2***	
ZDHHC9	***ZDHHC9***	
ZFAND5		
ZMYND8		
ZNF511		
ZNF614	***ZNF614***	
ZNF641		
ZNF750		
ZNF765		
ZNF813		

CHAPTER 6

General discussion

Unraveling major mechanisms of prostate cancer development and progression and the role of genetic events in this process is important, because ultimately this will lead to improved therapies for patients. In this thesis the main focus was on deciphering mechanisms of prostate tumorigenesis in mouse models of prostate cancer. PTEN, the most frequently inactivated tumor suppressor gene in prostate cancer, was discovered ~15 years ago. More recently, overexpression of *ERG* caused by the *TMPRSS2-ERG* fusion gene was identified as the most frequent genomic alteration in prostate cancer. To investigate the role of *PTEN* and *TMPRSS2-ERG* in prostate cancer mouse models were generated. In addition to our PSA-Cre driven model described here, several other groups generated targeted *Pten* knockout mice [1-4]. In this thesis, the focus was on the analysis of *PSA-Cre;Pten-loxP/loxP* mouse model. In Chapter 4 the effect of *Trp53* inactivation, an event frequently observed in late stage prostate cancer, was assessed in this model. Recently, mouse models with prostate specific overexpression of *Erg* were also described [5-7]. In prostates of mice with PB-Cre targeted overexpression of *Erg*, Erg protein expression was detected, but these mice did not show a clear phenotype. Also in our laboratory, we generated *PSA-TMPRSS2-ERG* mice. In this model we observed low *Erg* mRNA expression, but Erg protein expression could not be detected and, obviously, no phenotype was observed. Later, experiments were performed indicating that that ERG can inhibit the activity of the PSA promoter, which at least partly can explain the low ERG protein expression. Although we were unsuccessful in generating the mouse model, we continued our research in human prostate cancer. Gene expression profiles of primary prostate tumors were analyzed to identify potential target genes of ERG (Chapter 5). Here, *TDRD1* was identified as a direct target gene regulated by ERG. So far, the function of *TMPRSS2-ERG* in prostate cancer is still not clear, but the new results described in Chapter 5 can aid to unravel the role of ERG overexpression in prostate tumors. In this General Discussion we will discuss selected aspects of the prostate tumor development in mouse models described in Chapters 2, 3 and 4, and discuss potential novel functions of *Pten in vivo*.

MOUSE MODELS OF PROSTATE CANCER

Many different models systems can be used in prostate cancer research. *In vitro* and *in vivo* systems can be complementary. For example, *in vivo* models, like mouse model of prostate cancer, can be used to validate results obtained in *in vitro* model systems. Furthermore, mouse models of prostate cancer are complementary to experiments using human prostate cancer cells.

Human prostate tumor cells can be characterized by different approaches. *In vitro* growing cell lines derived from human tumors are frequently used in prostate cancer research. Only a limited number of established human prostate cancer cell lines is available, because probably only aggressive cells with unique genetic traits can be propagated *in vitro* [8]. Another

disadvantage of the use of prostate cancer cell lines is that, using a single cell line, paracrine effects between different cell types cannot be analyzed. Further characterization of cell lines can be performed by studying the behaviour of cells in a three-dimensional environment, for example by growing cells in a matrix, like Matrigel. Paracrine effects between different cell populations can be investigated in co-cultivation studies or human prostate cancer cells can be transplanted onto immunodeficient mice, either as a cell line or as a piece of tumor. In these mouse model experiments the histology, the genetic alterations, the gene expression profile, the proliferation rate and the metastatic potential of an eventually resulting tumor on the mouse can be compared with the original tumor [9]. Recently, a new model was developed to study characteristics of tumor cells in a three-dimensional environment [10]. Here, thin tissue slices derived from human prostate tissue are grafted under the renal capsule of immunodeficient mice. The advantage of experiments with human tumor cells is that cells derived from tumors of patients are used and they should mimic the actual situation in the patient. Established tumor cells or pieces of tumors are used and the development of prostate tumors cannot be studied.

In addition to characterization of human prostate cancer cells as discussed above, tumors induced in mice are frequently used. As mentioned in Chapter 1, the number of mouse models, especially genetically engineered mouse models (GEMMs), of prostate cancer is still growing, just like the number of prostate cancer cell lines derived from these models (this thesis) [11-14]. Many experiments as described for human prostate cancer cells can also be performed with mouse prostate tumor cells. As compared to human models, the advantage of mouse models is that here the process of heterogeneous prostate tumor development can be studied from the initial stages. Furthermore, mouse models are most frequently induced by well-defined genetic events, so in addition, the role of this event in prostate cancer can be adequately studied.

Nowadays, some new techniques are used to generate novel mouse models of prostate cancer, like generating models with inducible mutations or entire human loci [15, 16]. Furthermore, in mouse models of breast and lung cancer virus infection was used to regulate more precisely the induction of a genetic alteration [17, 18]. So far, this technique was not used to generate a new GEMM of prostate cancer.

Mouse models also have some drawbacks as discussed in Chapter 1, like differences in prostate anatomy as compared to humans. Furthermore, the phenotype depends on the inducible genetic event and/or the promoter used [8]. The genetic background of the mouse strain can also determine the outcome of the study [19, 20]. The *PSA-C*re targeted *Pten* knockout mice described in this thesis had a mixed background of FVB/n and 129f. The tumor development in our mouse model on a C57BL/6 background was slower as compared to *Pten* knockout mice with a FVB/n background (Unpublished results) [21]. Prostate tumor development of *PSA-Cre* targeted *Pten* knockout mice on a pure FVB/n background seems comparable to results presented in this thesis (Unpublished results). Just like described for tumor cells of PSA-Cre targeted *Pten* knockout

mice on a mixed 129f/FVB/n background, also here heterogeneity of prostate tumor cells was detected. These variations in phenotype caused by the inducible genetic event, the promoter used and the genetic background can also be used to increase knowledge of prostate cancer development and growth and modifiers of prostate cancer can be identified.

An important question for all available model systems is to what extent they are a good representation of the human situation and whether experiments using these models can unravel mechanisms relevant for prostate cancer development and progression. Model systems, which mirror best the complex three-dimensional situation in humans, are models in which the interaction of different cell types can be assessed in a microenvironment resembling the human situation. Although GEMMs will never perfectly mimic the human situation, these model systems can be used as preclinical models to asses the potential of novel therapeutics for prostate cancer [9, 22].

TUMOR INITIATING CELLS OF PROSTATE CANCER

The initial stages of development of prostate cancer cannot be studied in humans, because at the time of diagnosis, the tumor is already established. Within tumors a small population of cells with stem/progenitor cell characteristics, the cancer stem cells or tumor initiating cells, can give rise to different tumor types [23, 24]. In leukemia, it was shown that tumors develop from modifications in stem cells or progenitor cells [25]. Also in prostate cancer research, the last ten years much effort was focused on the characterization of cells from which tumors can arise.

As described in Chapter 2, most studies on tumor initiating cells in the prostate focus on cells in the basal epithelial cell layer, because these cells have most regenerating capacity [26-28]. In our PSA-Cre *Pten* knockout mouse model we identified Clu+Tacstd2+Sca-1+ progenitor cells in the luminal epithelial cell layer as candidate tumor initiating cells [29]. Clu+Tacstd2+Sca-1+ cells were present at low frequency in the luminal epithelial cell layer of the normal adult prostate, whereas in the immature prostate the number of Clu+Tacstd2+Sca-1+ progenitor cells was higher. Upon *Pten* inactivation in our model, at 4-5 weeks of age the first small pAkt+ foci originated from these luminal epithelial progenitor cells were detected. Although *Pten* should be inactivated in all luminal epithelial cells in this model, at 4-5 weeks the pAkt+ hyperplastic foci were found in a patched pattern through the prostate lobe. At 4-5 months all luminal epithelial cells were hyperplastic. More immature progenitor cells in the luminal epithelial cell layer may have a higher capacity to form hyperplastic foci than fully mature luminal epithelial cells. This will partly explain the scattered development of pAkt+ hyperplastic foci at 4-5 weeks. In addition to the Clu+/Tacstd2+/Sca-1+ cells, recently, castrate resistant Nkx3.1-expressing cells (CARNs) in the luminal epithelial cell layer were identified as tumor initiating cells in Nkx3.1-Cre

targeted *Pten* knockout mice [30]. These cells do not express the basal epithelial cell marker P63 or the neuroendocrine marker Synaptophysin, but are positive for luminal epithelial markers and androgen receptor (AR), like Clu+Tacstd2+Sca-1+ cells in prostates of *PSA-Cre;Pten-loxP/loxP* mice. Whether these cells and Clu+Tacstd2+Sca-1+ cells compromise an identical luminal epithelial progenitor cell population remains to be determined. Furthermore, luminal epithelial progenitor cells can be isolated and transplanted in prostates of syngenic mice with or without manipulation, such as inactivation of *Pten*. By performing these experiments it can be tested whether these cell have indeed the capacity to induce prostate tumors upon the induction of an oncogenic event.

In our mouse models and in the study of Wang and colleagues, promoters strictly active in luminal epithelial cells were used to generate the models [29-31]. In the Probasin(PB)-Cre targeted *Pten* knockout model P63+Sca-1+Bcl2+ basal (multipotent) stem/progenitor cells were identified as tumor initiating cells [32]. Analysis of tumor development in *PB-Cre;RB1;Trp53* knockout mice suggests that tumors can develop from cells with stem-cell characteristics in the luminal epithelial cell layer of the proximal prostate, a proposed stem cell niche [33, 34]. The data so far show that, in contrast to the PSA and Nkx3.1 promoter, the PB promoter is not strictly active in the luminal epithelial cell layer in the distal prostate, but can also be active in the basal epithelial cell layer and in luminal epithelial cells in the proximal prostate.

As mentioned, in mouse models many different potential tumor initiating cell populations, mostly in the basal epithelial cell layer, have been postulated with stem/progenitor cell characteristics [26, 29, 30, 35-39]. Also in the human prostate different potential tumor initiating cell populations expressing stem/multipotent progenitor cell markers, including Sca-1+CD49f+ and Integrinα2/β1+CD133+ cells, are described [39-41]. As discussed in Chapter 2 some of these known stem/progenitor cell markers showed increased expression in prostates of *Pten* knockout mice, however whether Clu+Tacstd2+Sca-1+ cells co-express these markers needs to be investigated. Recently, in addition other stem/progenitor cell populations, a NKX3.1 positive cell population was identified in a prostate cancer xenograft, which survives castration and is capable of reinitiating tumor growth after androgen replacement [42]. This cell population resembling CARNs was strictly luminal and expresses the stem cell markers Nanog and Aldehyde dehydrogenase 1A1.

All data on potential tumor initiating cells of prostate cancer suggest that both stem and progenitor cells in either the basal or the luminal epithelial cell layer can give rise to a tumor (Figure 1). This demonstrates that cells with the highest regenerative capacity, as frequently found in the basal epithelial cell layer, are not necessarily the cells from which tumors arise. However, possibly, more immature cells can have a higher potential capacity to react upon an oncogenic event and initiate the formation of a tumor.

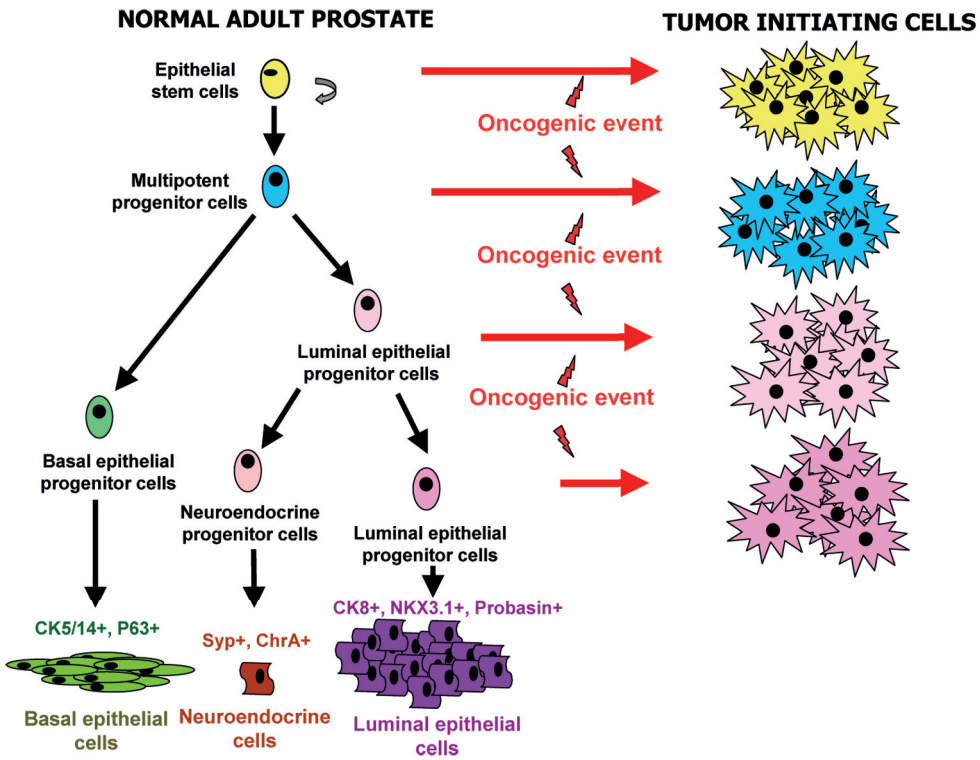

Figure 1. Hypothetical model for prostate tumor development from tumor initiating cells.

Depending on the characteristics of the tumor initiating cell and the type of oncogenic event, the properties of tumor cells might differ. After the initial oncogenic event prostate cancer develops and progresses by accumulation of epigenetic and genetic events, so in later stages of prostate tumorigenesis the characteristics of tumor cells change depending on the secondary events.

MECHANISMS OF PROSTATE TUMOR DEVELOPMENT

As discussed, *PTEN* is the most frequently inactivated tumor suppressor gene in prostate cancer. In Chapters 2 and 3 the prostate tumor development in a PSA-Cre driven mouse model was analyzed. The effect of *Trp53* inactivation in this mouse model was investigated in Chapter 4.

Tumor cells of PSA-Cre targeted *Pten* knockout mice showed frequent loss of chromosome 4 and 12. In tumor cells with inactivation of both *Pten* as *Trp53*, in addition to genomic alterations

observed in *Pten* negative cells, many additional chromosomal alterations were detected. This confirmed that *Trp53* inactivation affects the genetic stability in tumor cells [43]. So far, the function of these genomic alterations during tumor development is not established. The mouse tumor cell lines described in Chapters 3 and 4 were homogeneous at the genomic level. This will allow sequencing their DNA to discover new secondary events.

Epigenetic events are increasingly recognized as important for prostate cancer development [44, 45]. Some, but not all epigenetic events with a potential role in tumor growth and progression were investigated in the mouse models described in this thesis. Here, the expression levels of markers for hallmarks of cancer, like cellular senescence, inflammation, proliferation, apoptosis and angiogenesis were monitored.

Previously it was presumed that induction of cellular senescence was a barrier for tumor progression, also in targeted *Pten* knockout mice [46, 47]. However, we detected even higher expression levels of cellular senescence markers in prostate tumors as compared to pre-malignant HP lesions. We tested the prostates of our *Pten* knockout mice for positive senescence-associated ß-galactosidase activity, a well-established marker for cellular senescence. The prostates were completely negative for this marker. This may indicate that the increased expression of the cellular senescence markers points to a new mechanism important in prostate tumorigenesis. Induction of cellular senescence is a response to DNA damage [48]. In addition to the tumor suppressive function of cellular senescence, some reports suggest that senescent cells can also have positive effects on tumor growth [49, 50]. Senescent cells can secrete various molecules, like pro-inflammatory cytokines, chemokines and tissue-remodelling enzymes, which can reinforce the cellular senescence response and stimulate the malignant phenotypes of nearby tumor cells. It would be interesting to investigate the role of senescent cells not only during tumor development, but also during later stages of tumor progression. In contrast to the single *Pten* knockout model, in addition to many other effects of *Trp53* inactivation, lower expression of cellular senescence markers was detected in prostate tumors of PSA-Cre targeted *Pten/Trp53.*

Expression profiling of HP and prostate tumors in our *Pten* knockout model revealed higher expression of inflammation markers in prostate tumors (Chapter 3). Currently, much effort is focused on unraveling the promotive role of inflammation on epithelial changes in the mouse prostate [51-54]. Also in human prostate cancer, inflammation is increasingly recognized as a stimulus for prostate cancer development [55]. Whether the inflammatory response also stimulates tumor development in our *Pten* knockout mice is still unknown. To investigate this targeted *Pten* knockout mice can be treated with anti-inflammatory drugs.

The number of apoptotic cells and the proliferation rate were increased in prostates of *Pten* knockout mice, especially in tumors predominated by a carcinosarcoma growth pattern (TC2 tumors). Inactivation of *Trp53* had no strong effect on the number of BrdU and active Caspase-3 positive cells in prostate tumor cells. Interestingly, in Chapter 4 genes high expressed in a subset

of tumors *Pten/Trp53* negative mice (tumor Cluster III) were involved in the formation of the DNA pre-replication complex and the spindle checkpoint. We observed overexpression of genes like *Cenpa*, *Rfc3*, *Ris2* and *Mcmd2* that were associated with tumor progression in human prostate cancer (data not shown). Genes involved in the formation of the pre-replication complex regulate correct DNA replication during the cell cycle, however the exact function of high expression of spindle checkpoint genes, including *Cenpa*, in cluster III is unclear. In human cells it was reported that overexpression of CENPA can promote genetic instability [56]. It is tempting to speculate that the expression profiles of tumors in cluster III in Chapter 4 are characteristic for aggressive tumor cells. Remarkably, all cell lines derived from prostate tumors of PSA-Cre targeted *Pten/Trp53* knockout mice had characteristics of tumors in Cluster III, whereas not all tumors from which the cell lines were derived clustered in Cluster III. This suggests that cells with an expression profile characteristic for aggressive tumor cells are present in most prostate tumors of targeted *Pten/Trp53* mice. The tumors in cluster III are enriched for these cells.

In addition to regulation of mRNA expression, many pathways are regulated at the protein level. The activation of additional pathways by posttranslational modifications as secondary events in our GEMMs were not investigated. Knowledge on these alterations will also provide further insight into mechanisms involved in prostate tumor development and progression. It is possible to assess the activation of pathways by determination of kinase activation. Recently, it was shown that elevated tyrosine kinase signaling was detected in advanced prostate cancer [57]. Similar experiments can be performed to identify new pathways with a role in tumor growth and progression in our mouse models.

It is thought that within a tumor undifferentiated cancer cells, the cancer stem cells/tumor initiating cells, can give rise to heterogeneous prostate tumors. Expansion of different dominant clones of aggressive tumor cells is an alternative mechanism to cause tumor heterogeneity [24, 58-60]. During the initial stages of tumor development in *PSA-Cre;Pten-loxP/loxP* mice Clu+Tacstd2+Sca-1+ cells are the tumor initiating cells, however, so far, within prostate tumors we have not identified a cancer stem cell/tumor initiating cell population. The expression of cancer stem cell markers was variable in tumors and no enrichment of these markers was detected in a cancer cell population. Although we cannot exclude the possibility of the presence of cancer stem cells in prostate tumors of our PSA-Cre targeted mouse models, the data suggest clonal expansion of dominant clones. Histological analysis of prostate tumors in our *Pten* knockout mice showed that the characteristics of a tumor were determined by the predominating tumor growth pattern. Furthermore, in targeted *Pten/Trp53* knockout mice we concluded that cells with an expression profile of aggressive tumor cells are present in most tumors. An enrichment of these cells was detected in Cluster III.

The studies described in this thesis have gained insight into the process of prostate cancer development and progression. In the PSA-Cre *Pten* knockout model luminal epithelial progenitor

cells were identified as candidate tumor initiating cells during the initial stages of tumor development, the hyperplastic stages, in this model. IDC lesions were detected in prostates at 7-8m. These lesions progress to heterogeneous prostate tumors with different growth patterns (IDC, adenocarcinoma, undifferentiated carcinoma and carcinosarcoma) (Figure 2). So far, in our *PSA-Cre;Pten-loxP/loxP* mice we could not detect clear transitions between different tumor cell growth patterns, however we cannot exclude that they occur.

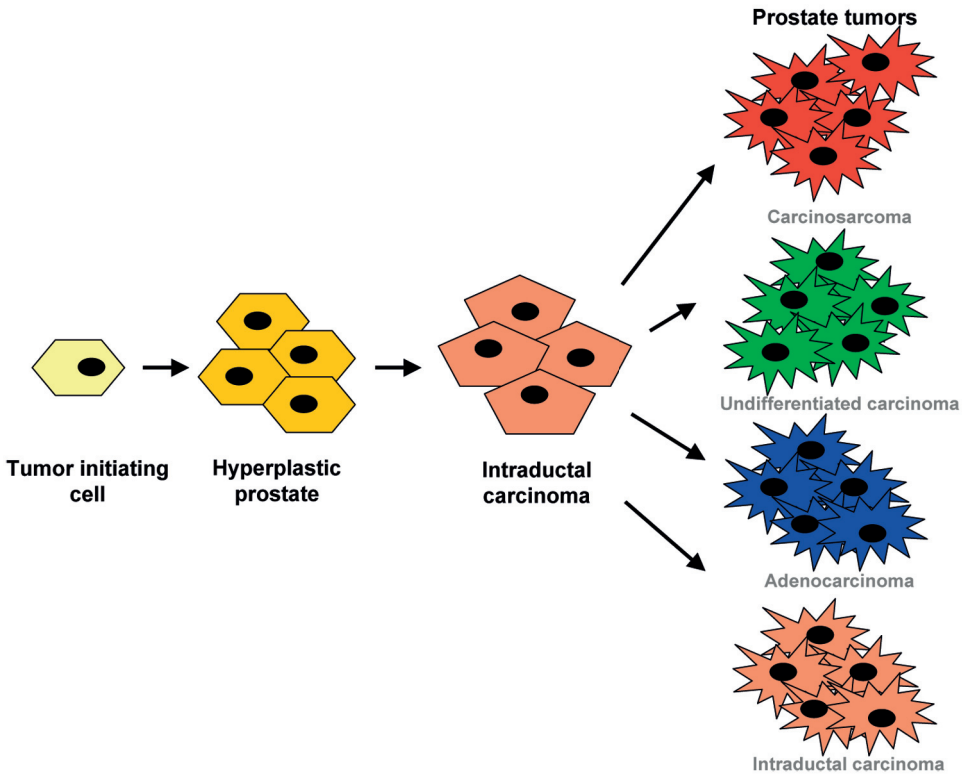

Figure 2. Hypothetical model for prostate cancer development and progression in *PSA-Cre;Pten-loxP/loxP* mice.

NEW FUNCTIONS OF PTEN AS IDENTIFIED IN THE *PSA-CRE;PTEN-LOXP/LOXP* MODEL

As mentioned in Chapter 1, PTEN inhibits the AKT pathway. Here also some new AKT-independent functions of PTEN were proposed. In this thesis the PSA-Cre targeted *Pten* knockout model was used to study the role of *Pten* during prostate tumor development and progression *in vivo*. As expected, during the early phases of prostate tumorigenesis in the targeted *Pten* knockout mice we detected high level expression of pAkt (Phospho-Akt) restricted to the membrane confirming activation of the AKT pathway. In prostate tumors the expression of pAkt was heterogeneous, suggesting that here other mechanisms sustain the tumor growth.

In contrast to the PB-Cre targeted *Pten* knockout mouse model [1], in PSA-Cre driven *Pten* knockout mice the process of prostate tumorigenesis is relatively slow and different stages of prostate cancer development can be clearly separated [29, 61]. An advantage is that the development of hyperplastic foci from luminal epithelial progenitor cells can be detected. In the normal prostate progenitor cells in the luminal epithelial cell layer can differentiate into mature luminal epithelial cells. Upon *Pten* inactivation we observed a block in this differentiation process. This was the first time that results clearly indicated that PTEN plays a role in the terminal differentiation of luminal epithelial cells of the prostate. Recently, loss of PTEN in renal proximal tubulus cells was associated with failed differentiation [62]. Interestingly, here the block in the differentiation by PTEN loss was accompanied by activation of the JNK pathway, which previously was reported as a new AKT-independent target of PTEN [63]. Apparently, PTEN and the JNK pathway can suppress each other, thereby identifying a new and possibly important feedback loop [64]. These data stress that AKT-independent functions of PTEN can play important roles in both normal tissues as in tumors. The role of the JNK pathway in our mouse model is not yet clear. The expression of major players, including Phospho-c-jun, in this pathway should be investigated in prostates of our *Pten* knockout mice.

As mentioned in Chapter 1, another newly proposed AKT-independent function of PTEN is maintenance of genomic stability by interaction with CENP-C and regulation of the transcription of RAD51 in the nucleus [65, 66]. By aCGH analysis of tumor cell lines derived from PSA-Cre *Pten* knockout mice in Chapter 3, mainly loss of chromosome 4 and 12 were detected. These data show that the genetic stability is affected, however the effect is small. A small increase in the expression of the cell cycle genes associated with aggressive tumors/genetic instability as overexpressed in cluster III (Chapter 4) was detected in prostate tumors of targeted *Pten* knockout mice, especially TC2 tumors. In addition to the AKT-dependent effects of *Pten* inactivation and the block in differentiation during the initial stages of tumor development in PSA-Cre targeted *Pten* knockout mice, a small increase in genetic instability was detected in this mouse model.

REFERENCES

1. Wang, S., et al., *Prostate-specific deletion of the murine Pten tumor suppressor gene leads to metastatic prostate cancer.* Cancer Cell, 2003. **4**(3): p. 209-21.
2. Trotman, L.C., et al., *Pten dose dictates cancer progression in the prostate.* PLoS Biol, 2003. **1**(3): p. E59.
3. Luchman, H.A., et al., *The pace of prostatic intraepithelial neoplasia development is determined by the timing of Pten tumor suppressor gene excision.* PLoS One, 2008. **3**(12): p. e3940.
4. Ratnacaram, C.K., et al., *Temporally controlled ablation of PTEN in adult mouse prostate epithelium generates a model of invasive prostatic adenocarcinoma.* Proc Natl Acad Sci U S A, 2008. **105**(7): p. 2521-6.
5. Klezovitch, O., et al., *A causal role for ERG in neoplastic transformation of prostate epithelium.* Proc Natl Acad Sci U S A, 2008. **105**(6): p. 2105-10.
6. Tomlins, S.A., et al., *Role of the TMPRSS2-ERG gene fusion in prostate cancer.* Neoplasia, 2008. **10**(2): p. 177-88.
7. King, J.C., et al., *Cooperativity of TMPRSS2-ERG with PI3-kinase pathway activation in prostate oncogenesis.* Nat Genet, 2009. **41**(5): p. 524-6.
8. Abate-Shen, C. and M.M. Shen, *Molecular genetics of prostate cancer.* Genes Dev, 2000. **14**(19): p. 2410-34.
9. Lopez-Barcons, L.A., *Serially heterotransplanted human prostate tumours as an experimental model.* J Cell Mol Med, 2009. **14**(6B): p. 1385-95.
10. Zhao, H., et al., *Tissue slice grafts: an in vivo model of human prostate androgen signaling.* Am J Pathol, 2010. **177**(1): p. 229-39.
11. Liao, C.P., et al., *Mouse prostate cancer cell lines established from primary and postcastration recurrent tumors.* Horm Cancer, 2010. **1**(1): p. 44-54.
12. Foster, B.A., et al., *Characterization of prostatic epithelial cell lines derived from transgenic adenocarcinoma of the mouse prostate (TRAMP) model.* Cancer Res, 1997. **57**(16): p. 3325-30.
13. Watson, P.A., et al., *Context-dependent hormone-refractory progression revealed through characterization of a novel murine prostate cancer cell line.* Cancer Res, 2005. **65**(24): p. 11565-71.
14. Jiao, J., et al., *Murine cell lines derived from Pten null prostate cancer show the critical role of PTEN in hormone refractory prostate cancer development.* Cancer Res, 2007. **67**(13): p. 6083-91.
15. Hensley, P.J. and N. Kyprianou, *Modeling prostate cancer in mice: limitations and opportunities.* J Androl, 2011. **33**(2): p. 133-44.
16. Devoy, A., et al., *Genomically humanized mice: technologies and promises.* Nat Rev Genet, 2011. **13**(1): p. 14-20.
17. Yiang, G.T., et al., *Immunotherapy for SV40 T/t antigen-induced breast cancer by recombinant adeno-associated virus serotype 2 carrying interleukin-15 in mice.* Int J Mol Med, 2012. **29**(5): p. 809-14.
18. Li, T., et al., *Transgenic mice for cre-inducible overexpression of the Cul4A gene.* Genesis, 2011. **49**(3): p. 134-41.
19. Freeman, D., et al., *Genetic background controls tumor development in PTEN-deficient mice.* Cancer Res, 2006. **66**(13): p. 6492-6.
20. Bianchi-Frias, D., et al., *Genetic background influences murine prostate gene expression: implications for cancer phenotypes.* Genome Biol, 2007. **8**(6): p. R117.
21. Svensson, R.U., et al., *Slow disease progression in a C57BL/6 pten-deficient mouse model of prostate cancer.* Am J Pathol, 2011. **179**(1): p. 502-12.
22. van Weerden, W.M., C. Bangma, and R. de Wit, *Human xenograft models as useful tools to assess the potential of novel therapeutics in prostate cancer.* Br J Cancer, 2009. **100**(1): p. 13-8.
23. Wang, F., *Modeling human prostate cancer in genetically engineered mice.* Prog Mol Biol Transl Sci, 2011. **100**: p. 1-49.

24. Visvader, J.E. and G.J. Lindeman, *Cancer stem cells in solid tumours: accumulating evidence and unresolved questions.* Nat Rev Cancer, 2008. **8**(10): p. 755-68.
25. Wang, J.C. and J.E. Dick, *Cancer stem cells: lessons from leukemia.* Trends Cell Biol, 2005. **15**(9): p. 494-501.
26. Goldstein, A.S., et al., *Trop2 identifies a subpopulation of murine and human prostate basal cells with stem cell characteristics.* Proc Natl Acad Sci U S A, 2008.
27. English, H.F., R.J. Santen, and J.T. Isaacs, *Response of glandular versus basal rat ventral prostatic epithelial cells to androgen withdrawal and replacement.* Prostate, 1987. **11**(3): p. 229-42.
28. Lawson, D.A. and O.N. Witte, *Stem cells in prostate cancer initiation and progression.* J Clin Invest, 2007. **117**(8): p. 2044-50.
29. Korsten, H., et al., *Accumulating progenitor cells in the luminal epithelial cell layer are candidate tumor initiating cells in a Pten knockout mouse prostate cancer model.* PLoS One, 2009. **4**(5): p. e5662.
30. Wang, X., et al., *A luminal epithelial stem cell that is a cell of origin for prostate cancer.* Nature, 2009. **461**(7263): p. 495-500.
31. Cleutjens, K.B., et al., *A 6-kb promoter fragment mimics in transgenic mice the prostate-specific and androgen-regulated expression of the endogenous prostate-specific antigen gene in humans.* Mol Endocrinol, 1997. **11**(9): p. 1256-65.
32. Wang, S., et al., *Pten deletion leads to the expansion of a prostatic stem/progenitor cell subpopulation and tumor initiation.* Proc Natl Acad Sci U S A, 2006. **103**(5): p. 1480-5.
33. Tsujimura, A., et al., *Proximal location of mouse prostate epithelial stem cells: a model of prostatic homeostasis.* J Cell Biol, 2002. **157**(7): p. 1257-65.
34. Zhou, Z., A. Flesken-Nikitin, and A.Y. Nikitin, *Prostate cancer associated with p53 and Rb deficiency arises from the stem/progenitor cell-enriched proximal region of prostatic ducts.* Cancer Res, 2007. **67**(12): p. 5683-90.
35. Xin, L., D.A. Lawson, and O.N. Witte, *The Sca-1 cell surface marker enriches for a prostate-regenerating cell subpopulation that can initiate prostate tumorigenesis.* Proc Natl Acad Sci U S A, 2005. **102**(19): p. 6942-7.
36. Xin, L., et al., *Self-renewal and multilineage differentiation in vitro from murine prostate stem cells.* Stem Cells, 2007. **25**(11): p. 2760-9.
37. Lawson, D.A., et al., *Isolation and functional characterization of murine prostate stem cells.* Proc Natl Acad Sci U S A, 2007. **104**(1): p. 181-6.
38. Leong, K.G., et al., *Generation of a prostate from a single adult stem cell.* Nature, 2008.
39. Wang, Z.A. and M.M. Shen, *Revisiting the concept of cancer stem cells in prostate cancer.* Oncogene, 2011. **30**(11): p. 1261-71.
40. Chen, S.Y., et al., *An overview of concepts for cancer stem cells.* Cell Transplant, 2011. **20**(1): p. 113-20.
41. Goldstein, A.S., T. Stoyanova, and O.N. Witte, *Primitive origins of prostate cancer: in vivo evidence for prostate-regenerating cells and prostate cancer-initiating cells.* Mol Oncol, 2010. **4**(5): p. 385-96.
42. Germann, M., et al., *Stem-like cells with luminal progenitor phenotype survive castration in human prostate cancer.* Stem Cells, 2012. **30**(6): p. 1076-86.
43. Talos, F. and U.M. Moll, *Role of the p53 family in stabilizing the genome and preventing polyploidization.* Adv Exp Med Biol, 2010. **676**: p. 73-91.
44. Jeronimo, C., et al., *Epigenetics in prostate cancer: biologic and clinical relevance.* Eur Urol, 2011. **60**(4): p. 753-66.
45. Nelson, W.G., A.M. De Marzo, and S. Yegnasubramanian, *Epigenetic alterations in human prostate cancers.* Endocrinology, 2009. **150**(9): p. 3991-4002.
46. Chen, Z., et al., *Crucial role of p53-dependent cellular senescence in suppression of Pten-deficient tumorigenesis.* Nature, 2005. **436**(7051): p. 725-30.
47. Campisi, J. and F. d'Adda di Fagagna, *Cellular senescence: when bad things happen to good cells.* Nat Rev Mol Cell Biol, 2007. **8**(9): p. 729-40.

48. d'Adda di Fagagna, F., *Living on a break: cellular senescence as a DNA-damage response.* Nat Rev Cancer, 2008. **8**(7): p. 512-22.
49. Kuilman, T. and D.S. Peeper, *Senescence-messaging secretome: SMS-ing cellular stress.* Nat Rev Cancer, 2009. **9**(2): p. 81-94.
50. Collado, M. and M. Serrano, *Senescence in tumours: evidence from mice and humans.* Nat Rev Cancer, 2010. **10**(1): p. 51-7.
51. Birbach, A., et al., *Persistent inflammation leads to proliferative neoplasia and loss of smooth muscle cells in a prostate tumor model.* Neoplasia, 2011. **13**(8): p. 692-703.
52. Garlick, D.S., et al., *alpha(V)beta(6) integrin expression is induced in the POET and Pten(pc-/-) mouse models of prostatic inflammation and prostatic adenocarcinoma.* Am J Transl Res, 2012. **4**(2): p. 165-74.
53. Haverkamp, J.M., et al., *An inducible model of abacterial prostatitis induces antigen specific inflammatory and proliferative changes in the murine prostate.* Prostate, 2011. **71**(11): p. 1139-50.
54. Boehm, B.J., et al., *Acute bacterial inflammation of the mouse prostate.* Prostate, 2012. **72**(3): p. 307-17.
55. Sfanos, K.S. and A.M. De Marzo, *Prostate cancer and inflammation: the evidence.* Histopathology, 2012. **60**(1): p. 199-215.
56. Amato, A., et al., *CENPA overexpression promotes genome instability in pRb-depleted human cells.* Mol Cancer, 2009. **8**: p. 119.
57. Drake, J.M., et al., *Oncogene-specific activation of tyrosine kinase networks during prostate cancer progression.* Proc Natl Acad Sci U S A, 2012. **109**(5): p. 1643-8.
58. Shackleton, M., et al., *Heterogeneity in cancer: cancer stem cells versus clonal evolution.* Cell, 2009. **138**(5): p. 822-9.
59. Adams, J.M. and A. Strasser, *Is tumor growth sustained by rare cancer stem cells or dominant clones?* Cancer Res, 2008. **68**(11): p. 4018-21.
60. Kelly, P.N., et al., *Tumor growth need not be driven by rare cancer stem cells.* Science, 2007. **317**(5836): p. 337.
61. Ma, X., et al., *Targeted biallelic inactivation of Pten in the mouse prostate leads to prostate cancer accompanied by increased epithelial cell proliferation but not by reduced apoptosis.* Cancer Res, 2005. **65**(13): p. 5730-9.
62. Lan, R., et al., *PTEN loss defines a TGF-beta-induced tubule phenotype of failed differentiation and JNK signaling during renal fibrosis.* Am J Physiol Renal Physiol, 2012. **302**(9): p. F1210-23.
63. Vivanco, I., et al., *Identification of the JNK signaling pathway as a functional target of the tumor suppressor PTEN.* Cancer Cell, 2007. **11**(6): p. 555-69.
64. Salmena, L., A. Carracedo, and P.P. Pandolfi, *Tenets of PTEN tumor suppression.* Cell, 2008. **133**(3): p. 403-14.
65. Yin, Y. and W.H. Shen, *PTEN: a new guardian of the genome.* Oncogene, 2008. **27**(41): p. 5443-53.
66. Shen, W.H., et al., *Essential role for nuclear PTEN in maintaining chromosomal integrity.* Cell, 2007. **128**(1): p. 157-70.

Summary

Prostate cancer is the most common malignancy in men in countries with a Western lifestyle. Increasing knowledge of the role of genetic alterations in prostate cancer and unraveling mechanisms of tumorigenesis will lead to improved therapies for prostate cancer patients. In this thesis genetically engineered mouse models were used to investigate the role of Pten during the process of prostate tumor development in the mouse. Furthermore, the effect of *Trp53* inactivation of the tumor development in targeted *Pten* knockout mice was investigated. The mouse models were also used to identify processes important during tumor development and progression. Although the main focus of this thesis was on mouse models of prostate cancer, in Chapter 5 by expression profiling of human primary prostate tumors, we attempted to identify genes directly regulated by ERG. These data can help to address the question what the function is *ERG* overexpression caused by the TMPRSS2-ERG fusion gene in prostate cancer.

Chapter 1 is a general introduction describing the genetics of prostate cancer and multiple aspects of mouse models of prostate cancer, like the generation of mouse models and different types of mouse models. Furthermore, an overview of conditional mouse models of prostate cancer is given.

In Chapters 2, 3 and 4 studies of the *PSA-Cre;Pten-loxP/loxP* mouse model were described. In Chapter 2 the initial stages of prostate tumor development, the hyperplastic stages, were characterized. Here, Clu+Tacstd2+Sca-1+ luminal epithelial progenitor cells were identified as candidate tumor initiaiting cells. We observed that at 4-5 weeks of age *PSA-Cre;Pten-loxP/loxP* mice develop small phospho-Akt+ hyperplastic foci in the distal prostate with increased expression of the luminal epithelial progenitor cell markers Clu, Tacstd2 and Sca-1. By inactivation of *Pten* the differentiation of progenitor cells into mature luminal epithelial cells was blocked. At 4-5m the lumen of prostates of *PSA-Cre;Pten-loxP/loxP* was completely filled with hyperplastic cells. The later stages of prostate tumor development in *PSA-Cre;Pten-loxP/loxP* mice were studied in Chapter 3. Heterogeneous prostate tumors are proposed to develop from intraductal carcinoma detected at 7-8 months. Prostate cancer development was associated with changes in various biological processes, including cellular senescence, proliferation, angiogenesis and apoptosis. Furthermore, an inflammatory response was detected during the development of prostate tumors. Molecular characterization of heterogeneous prostate tumors in *PSA-Cre;Pten-loxP/loxP* mice identified two main classes of prostate tumors, TC1 and TC2 tumors, with differential expression of epithelial and mesenchymal markers. Heterogeneity was also detected in cell lines derived from prostate tumors of the targeted *Pten* knockout mice. In addition to the analysis of prostate tumor development and progression in *PSA-Cre;Pten-loxP/loxP* mice, the effect of *Trp53* inactivation in PSA-Cre targeted *Pten* knockout mice was investigated (Chapter 4).

Sole targeted *Trp53* inactivation did result in small dysplastic prostate lesions at old age that never progressed to prostate cancer. In *Pten* knockout mice inactivation of *Trp53* promoted prostate cancer development and progression. Even *PSA-Cre;Pten-loxP/+;Trp53-loxP/loxP* mice developed prostate tumors. In contrast to sole *Pten* knockout mice, *Trp53* inactivation in *Pten* knockout mice resulted in the development prostate cancer metastases. Clustering of gene expression profiles of prostate tumors demonstrated that part of the tumors negative for *Pten* and *Trp53* expressed high levels of genes involved in spindle cell checkpoint and the formation of the DNA pre-replication complex. Characterization of cancer cell lines derived from tumors of *PSA-Cre;Pten;Trp53* knockout mice showed that *Trp53* inactivation in *Pten* negative cells stimulated genetic instability. In contrast to *Pten* negative cell lines, cell lines derived from *PSA-Cre;Pten;Trp53* knockout mice had the capacity to form tumors after orthotopic transplantation. Like in prostate tumors from *PSA-Cre;Pten-loxP/loxP;Trp53-loxP/loxP* mice cell lines derived from these mice showed higher expression of genes involved in cell cycle regulation.

In Chapter 5 expression profiles of human primary prostate tumors were analyzed to identify genes co-expressed with *ERG*. *TDRD1* was identified as a direct target gene regulated by ERG. Promoter studies showed that a specific region in the promoter of TDRD1 was regulated by ERG.

In Chapter 6 the data described in this thesis were discussed in more detail with the main focus on Chapter 2, 3 and 4. Moreover, mechanisms of development of prostate cancer in the mouse models and the role of PTEN in prostate cancer were discussed. Furthermore, future directions of research were suggested.

Samenvatting

Prostaatkanker is de meest voorkomende vorm van kanker bij mannen in landen met een Westerse leefstijl. Het vergroten van de kennis van de rol van genetische veranderingen in prostaatkanker en de mechanismen die een rol spelen bij het ontstaan en de progressie van prostaatkanker, zal leiden tot het ontwikkelen van betere therapiëen voor prostaatkankerpatiënten. In dit proefschrift werd de rol van Pten in prostaatkanker bestudeerd in genetisch gemodificeerde muismodellen. Verder werd onderzocht wat het effect is van *Trp53* inactivatie op de tumorontwikkeling in conditionele *Pten* knockout muizen. Tevens werden in genetisch gemodificeerde muismodellen processen geïdentificeerd die een belangrijke rol spelen tijdens het ontstaan en de progressie van prostaatkanker. De nadruk in dit proefschrift lag op muismodellen voor prostaatkanker, echter in hoofdstuk 5 hebben we genen die direkt gereguleerd worden door ERG proberen te identificeren met behulp van het analyseren van genexpressieprofielen van primaire prostaattumoren. Deze data kunnen helpen om de functie van overexpressie van *ERG* veroorzaakt door het TMPRSS2-ERG fusiegen in prostaatkanker te onrafelen.

Hoofdstuk 1 is een algemene introduktie over de genetica van prostaatkanker en verschillende aspecten van muismodellen voor prostaatkanker, zoals het genereren van genetisch gemodificeerde muismodellen en de eigenschappen van verschillende soorten muismodellen. Verder wordt er een volledig overzicht gegeven van de conditionele muismodellen voor prostaatkanker.

In de Hoofdstukken 2, 3 en 4 staan studies beschreven die uitgevoerd zijn met *PSA-Cre;Pten-loxP/loxP* muizen. In hoofdstuk 2 zijn de initiële stadia, de hyperplastische stadia, van de ontwikkeling van prostaatkanker in conditionele *Pten* knockout muizen gekarakteriseerd. Clu+Tacstd2+Sca-1+ luminale epitheliale voorlopercellen werden geïdentificeerd als potentiële tumor initiërende cellen. Op een leeftijd van 4-5 weken ontwikkelden *PSA-Cre;Pten-loxP/loxP* muizen kleine hyperplastische foci in de distale prostaat met verhoogde expressie van markers van luminale voorlopercellen, zoals Clu, Tacstd2 en Sca-1. Door het inactiveren van *Pten* wordt de differentiatie van voorlopercellen in rijpe luminale epitheliale cellen geblokkeerd. Het lumen van prostaten van 4-5 maanden oude *Pten* knockout muizen is volledig gevuld met hyperplastische cellen. De latere stadia van de ontwikkeling van prostaatkanker in *PSA-Cre;Pten-loxP/loxP* muizen staan beschreven in Hoofdstuk 3. De heterogene prostaattumoren worden verondersteld te ontstaan uit intraductale prostaattumoren op een leeftijd van 7-8 maanden. Tijdens de ontwikkeling van prostaattumoren zijn een aantal biologische processen veranderd, zoals “senescence”, proliferatie, angiogenese en apoptose. Verder gaat de ontwikkling van prostaattumoren in dit model gepaard met een ontstekingsreactie. Door het moleculair karakteriseren van heterogene prostaattumoren in *PSA-Cre;Pten-loxP/loxP* muizen werden er

twee klassen prostaattumoren geïdentificeerd, TC1 en TC2 tumoren, met differentiële expressie van epitheliale en mesenchymale markers. Heterogeniteit werd tevens gevonden tussen tumorcellijnen afkomstig van prostaattumoren van conditionele *Pten* knockout muizen. Naast de analyse van de ontwikkling en progressie van prostaatkanker in *PSA-Cre;Pten-loxP/loxP* muizen, werd het effect van *Trp53* inactivatie in conditionele *Pten* knockout muizen onderzocht (Hoofdstuk 4). Alleen conditionele inactivatie van *Trp53* resulteerde in kleine dysplastische lesies in de prostaat van oudere muizen die zich nooit verder ontwikkelden tot prostaattumoren. Inactivatie van *Trp53* in *Pten* knockout muizen stimuleerde de ontwikkeling en progressie van prostaatkanker. Zelfs *PSA-Cre;Pten-loxP/+;Trp53-loxP/loxP* muizen ontwikkelden prostaattumoren. In tegenstelling tot *Pten* knockout muizen, resulteerde *Trp53* inactivatie in *Pten* knockout muizen in de ontwikkeling van metastasen van prostaatkanker. Het clusteren van genexpressieprofielen van prostaattumoren toonde aan dat een gedeelte van de tumoren die negatief zijn voor zowel *Pten* als *Trp53* een verhoogde expressie heeft van genen die betrokken zijn bij de regulering van de celcyclus. Karakterisatie van cellijnen afkomstig van prostaattumoren van *PSA-Cre;Pten;Trp53* knockout muizen laat zien dat *Trp53* inactivatie in *Pten* negatieve cellen de genetische instabiliteit stimuleert. In tegenstelling tot cellijnen afkomstig van *Pten* knockout muizen vormen cellijnen die negatief zijn voor zowel *Pten* als *Trp53* tumoren na orthotope transplantatie. Bovendien, brengen deze cellijnen, net als in de tumoren, genen hoog tot expressie die een rol spelen bij de regulering van de celcyclus.

In Hoofdstuk 5 zijn expressieprofielen van primaire prostaattumoren geanalyseerd om genen te identificeren die co-expressie lieten zien met het oncogen *ERG*. TDRD1 werd geïdentificeerd als direct “targetgen” van ERG. Promoter-experimenten laten zien dat een specifiek deel van de TDRD1 promoter gereguleerd wordt door ERG.

In Hoofdstuk 6 werden de resultaten die beschreven zijn in dit proefschrift bediscussieerd met de nadruk op de Hoofdstukken 2, 3 en 4. Verder werden mechanismen voor de ontwikkeling van prostaatkanker in muismodellen en de rol van PTEN in prostaatkanker besproken. Tenslotte werden er suggesties voor toekomstig onderzoek gedaan.

Curriculum vitae

Hanneke Korsten werd geboren op 12 juli 1978 te Nijmegen. In 1996 behaalde ze haar VWO (Atheneum) diploma aan het College Sittard in Sittard. Aansluitend begon ze aan haar studie Biomedische gezondheidswetenschappen aan de Radboud Universiteit Nijmegen. Haar specialisatie was toxicologie met als bijvakken reproductie en geneesmiddelenonderzoek. De afstudeerstage werd uitgevoerd bij het Rijksinstituut voor Volksgezondheid en Milieu (RIVM) te Bilthoven, afdeling Carcinogenese, Mutagenese en Genetica, onder supervisie van Dr. Harry van Steeg. Van 2000 tot 2010 heeft Hanneke gewerkt aan verschillende onderzoeksprojecten op het laboratorium van Prof. Dr. Jan Trapman, afdeling Pathologie, Josephine Nefkens Instituut, ErasmusMC, Rotterdam. Gedurende deze periode heeft ze haar promotie-onderzoek afgerond binnen deze onderzoeksgroep. De resultaten van dit onderzoek staan beschreven in dit proefschrift. Tijdens haar promotietraject heeft ze een poster award op de pathologendagen en een travel award van de European Society for Urological Research (ESUR) ontvangen. Vanaf juni 2010 werkt Hanneke als regulatory affairs manager bij Interchemie werken De Adelaar B.V.. Daarnaast is ze sinds augustus 2011 back-up Qualified Person bij ditzelfde farmaceutisch bedrijf.

List of publications

Pepels PP, Pesman G, **Korsten H**, Wendelaar Bonga SE, Balm PH. Corticotropin-releasing hormone (CRH) in the teleost fish Oreochromis mossambicus (tilapia): in vitro release and brain distribution determined by a novel radioimmunoassay. *Peptides* 23 (**6**): 1053-62 (2002).

Mahabir AG, van Benthem J, **Korsten H**, Lynch AM, Bailey L, de Vries A, Hendriksen CF, van Steeg H. Detecting genotoxic effects of potential clastogens: an in vivo study using the transgenic lacZ plasmid and the MutaMouse model. *Mutat Res* 652 (**2**): 151-7 (2008).

Hermans KG, van der Korput HA, van Marion R, van de Wijngaart DJ, Ziel-van der Made A, Dits NF, Boormans JL, van der Kwast TH, van Dekken H, Bangma CH, **Korsten H**, Kraaij R, Jenster G, Trapman J. Truncated ETV1, fused to novel tissue-specific genes, and full-length ETV1 in prostate cancer. *Cancer Res* 68 (**18**): 7541-9 (2008).

Korpershoek E, Loonen AJ, Corvers S, van Nederveen FH, Jonkers J, Ma X, Ziel-van der Made A, **Korsten H**, Trapman J, Dinjens WN, de Krijger RR. Conditional *Pten* knock-out mice: a model for metastatic phaeochromocytoma. *J Pathol* 217 (**4**): 597-604 (2009).

Korsten H, Ziel-van der Made A, Ma X, van der Kwast TH, Trapman J. Accumulating progenitor cells in the luminal epithelial cell layer are candidate tumor initiating cells in a *Pten* knockout mouse prostate cancer model. *Plos One* 4 (**5**): e5662 (2009).

Boormans JL, **Korsten H**, Ziel-van der Made ACJ, van Leenders GJHL, Verhagen PCMS and Trapman J. E17K substitution in AKT1 in prostate cancer. *Br J Cancer* 102(**10**): 1491-4 (2010).

Korpershoek E, Kloosterhof NK, Ziel-van der Made A, **Korsten H**, Oudijk L, Trapman J, Dinjens WMN, de Krijger RR. Accelerated induction of malignant pheochromocytomas in *Pten/Trp53* KO mouse model. *Submitted*

Boormans JL, **Korsten H**, Ziel van der Made ACJ, van Leenders GJLH, Jenster G and Trapman J. Identification of *TDRD1* as a direct target gene of *ERG* in primary prostate cancer. *Submitted.*

Dankwoord

De laatste bladzijden van het proefschrift. Vele promovendi zijn blij als ze hier zijn aangekomen. Dat geldt ook voor mij. Een woord van dank voor mensen die op een of andere manier betrokken zijn geweest bij mijn promotieonderzoek.

In de eerste plaats wil ik mijn promoter Jan Trapman bedanken. Jan, ik wil je bedanken voor de mogelijkheden die je me geboden hebt om mijn proefschrift goed af te kunnen ronden. Als directe begeleider ben je altijd nauw betrokken geweest bij mijn onderzoek. We hebben zelfs regelmatig besprekingen en boeiende discussies gehad op zondag. Ik wil je bedanken voor je enthousiasme en tijd. Van je kritische blik op mijn werk heb ik veel geleerd.

Ik wil alle leden van de leescommissie en de grote commissie bedanken voor jullie interesse in mijn promotieonderzoek en al het advies en goede raad.

Verder wil ik een persoon, met wie in nauw heb mogen samenwerken, in het bijzonder bedanken, Angelique Ziel-van der Made. Angelique, samen hebben we heel wat muizenwerk verricht en dat heeft onder andere tot dit proefschrift geleid. Je bent een ervaren analist van wie ik veel heb kunnen leren. Daarnaast hebben we samen ook veel plezier gehad. Ook na mijn vertrek op het Trapman lab hielden we zo nu en dan contact en zo bleef ik toch een beetje op de hoogte van alle nieuwtjes van het lab. Er was dan ook geen twijfel over mogelijk dat ik jou als paranifm zou vragen. Leuk dat je dat je mijn paranimf wil zijn!

Ik wil ook mijn kamergenoten bedanken, Petra, Pascal, Martin, Dennis en Hetty, waar ik veel mee ben opgetrokken en die altijd weer zorgde voor de nodige gezelligheid. Petra, jij bent toch best enige tijd mijn buurvrouw geweest op de kamer. Het was altijd leuk om met jou te praten over vanalles en nog wat. Ook toen je enkele jaren elders werkte, hebben we contact gehouden. Nu ben je weer terug op het Trapman lab en werk je net als ik (toen ik er nog werkte) met muismodellen. Leuk! Het was logisch voor mij om ook jou als paranifm te vragen en gelukkig zei je ja. Dankjewel!

Uiteraard wil ik naast mijn kamergenoten ook andere collega's bedanken met wie ik samen op het lab gewerkt heb, Anke, Carola, Delila, Inez, Joost, Karin, Michel, Sonia, en nog vele anderen..... Jullie hebben er allemaal voor gezorgd dat ik jarenlang met plezier op het Trapman lab gewerkt heb. Bedankt voor de prettige samenwerking en alle gezellige momenten!

Ik wil alle mensen van andere afdelingen buiten het Trapman lab die me geholpen hebben met mijn onderzoek en met wie ik prettig contact heb gehad, heel erg hartelijk bedanken. In het bijzonder bedank ik Marcel Verweij voor het delen van al zijn kennis van muizen. Marcel, je was een echte expert op het gebied van muizen en ik heb altijd met plezier geluisterd naar je mooie verhalen en goede adviezen. Ook de collega's van het histolab beneden op de tweede verdieping waren altijd bereid mij te helpen met mijn onderzoek; coupes snijden, antilichamen lenen, etc.. Jullie verdienen dan ook een extra bedankje. Ik heb jullie magnetron maar al te vaak mogen gebruiken voor mijn immunohistochemie experimenten.

Vooral Chapter 5 en 6 van dit proefschrift zouden er anders uitgezien hebben zonder het waardevolle advies van pathologen Theo van der Kwast en Arno van Leenders. Het was een hele klus om de prostaatlesies die we vaststelde in onze muismodellen een naamkaartje te geven. Maar volgens mij zijn we er met jullie hulp uiteindelijk goed uitgekomen. Dank jullie wel!

Tijdens de laatste stadia van het afronden van dit proefshrift werkte ik bij het farmaceutisch bedrijf Interchemie werken De Adelaar B.V.. Mijn collega's bij dit bedrijf bedank ik voor hun interesse in het onderzoek.

Uiteraard wil ik ook mijn ouders, (schoon)familie en vrienden bedanken voor de steun en interesse in mijn onderzoek. Mama en papa, voor jullie even een speciale dank voor de onvoorwaardelijke steun, jullie begrip en interesse. Jullie hebben mij altijd gestimuleerd dit proefschrift af te ronden.

Last but absolutely not least wil ik jou bedanken, Jeroen, voor jouw steun, begrip en motivatie om dit proefschrift op een mooie manier af te ronden. Ook als ik even de kriebels kreeg van alles wat ik nog moest doen, wist jij het te relativeren. Jij kan mij altijd op de juiste manier stimuleren met je nuchterheid en optimisme. Gelukkig had je er begrip voor dat ik soms even geen tijd had om gezellige dingen samen te doen, maar.... ik beloof je, dat halen we in! Dankjewel, lief!

Dit waren dan zo ongeveer de laatste woorden van dit proefschrift. Nog voor de laatste keer: bedankt allemaal!

Liefs,

Hanneke

PhD portfolio summary

Name PhD student: Hanneke Korsten
ErasmusMC Department: Pathology
Research School: Erasmus Postgraduate School Molecular Medicine (Molmed)
Promoter(s): Prof. dr. J. Trapman
Supervisor: Prof. dr. J. Trapman

PHD TRAINING

Cources

The Nexus training course, ErasmusMC Rotterdam, 2009

Presentations

- Multiple presentations at different meetings at the ErasmusMC Rotterdam, 2006-2010
  7th World Basic Urological Research Congress, Dublin (Ireland), 2007
- Presentation: Progenitor cells in the luminal epithelial cell layer are tumor initiating cells in a conditional *Pten* knockout mouse prostate cancer model
- Dutch Cancer Institute, Amsterdam (The Netherlands), 2010
  Presentation: Prostate tumorigenesis in PSA-Cre targeted *Pten* knockout mice

(Inter)national conferences

- Pathologendagen, Ede (The Netherlands), 2006
  Poster: Tacstd2+/Clu+/Sca-1+ progenitor cells of luminal epithelial cells are targets in a conditional *Pten* knockout mouse prostate cancer model
- Mouse models of cancer, Boston (USA), 2006
  Poster: Tacstd2+/Clu+/Sca-1+ progenitor cells of luminal epithelial cells are targets in a conditional *Pten* knockout mouse prostate cancer model
- AACR Annual meeting, San Diego (USA), 2008
  Poster: Mechanisms of accelerated metastatic prostate cancer by *Trp53* inactivation in targeted *Pten* knockout mice
- Mouse model meeting, San Diego (USA), 2009
  Poster: Accumulating progenitor cells in the luminal epithelial cell layer are candidate tumor initiating cells in a *Pten* knockout mouse prostate cancer model

Seminars and workshops

- Department's "promovendi-avond", 2008-2010

Lecturing

- Research training medical students 2006-2009

Supervising Bachelor's theses

Ellen McLean, Hogeschool Rotterdam, 2008

Individual awards and fellowships

- April 2006, Poster award, "Pathologendagen", Ede (The Netherlands)
- Oct 2007, Travel award, 7th World Basis Urological Research Congress, Dublin (Ireland)